Regulation of KCNQ Genes as a Mechanism Underlying Epileptogenesis

Ruth Butler-Ryan

Submitted in accordance with the requirements for the degree of

Doctor of Philosophy

The University of Leeds

School of Biomedical Sciences

Faculty of Biological Sciences

September 2021

The candidate confirms that the work submitted is her own, except where work which has formed part of jointly authored publications has been included. The contribution of the candidate and the other authors to this work has been explicitly indicated below. The candidate confirms that appropriate credit has been given within the thesis where reference has been made to the work of others.

The work in Chapter 1 of the thesis has appeared in publication as follows:

The functions of repressor element 1-silencing transcription factor in models of epileptogenesis and post-ischemia, August 2021, Ruth Butler-Ryan and Ian C. Wood. Metabolic Brain Disease.

I was responsible for primary authorship.

The contribution of the other author were guidance and supervision, proof-reading and editing suggestions.

The work in Chapter 3 of the thesis has appeared in publication as follows:

Efficient infection of organotypic hippocampal slice cultures with adenovirus carrying the transgene REST/NRSF, May 2021, Ruth Butler-Ryan and Ian C. Wood. Journal of Neuroscience Methods.

I was responsible for primary authorship, experimental work, experimental design and analysis.

The contributions of the other author were guidance and supervision with experimental design and analysis, proof-reading and editing suggestions.

Acknowledgements

I would like to give my thanks to my supervisor Dr. Ian C. Wood for his continued support and guidance throughout my Ph.D., and for the opportunity to study in his laboratory. I would also like to thank my co-supervisor Prof. Nikita Gamper for additional support, materials and generous access to his electrophysiology laboratory. This thanks extends to the whole of the Gamper lab group for inclusion and feedback in weekly meetings, and more generally to colleagues from the Fillipi group and surrounding labs for companionship, advice and occasional reagents usage. Additional thanks to Sally and Ruth from the Bioimaging facility for assistance with imaging queries, and to the postgraduate administrative staff.

A special mention is made in memory of the late Dr. Mike Sharrard, most recently of The University of York, a dear friend of 13 years. His molecular biology advice throughout my career, including my Ph.D., has been invaluable for my development as a scientist, and his friendship will be deeply missed. Thanks also go to my always supportive parents and wonderful friends.

This Ph.D. was funded by the Emma and Leslie Reid scholarship from the University of Leeds.

Abstract

Epilepsy can develop in response to a brain insult, such as an initial seizure, stroke or traumatic brain injury. This insult induces a variety of cellular and molecular changes, observed in the clinic as a latent period, leading to a state of chronic spontaneous seizures. KCNQ/Kv7 channels are voltage-gated potassium channels which regulate neuronal excitability and protect against hyperexcitability through the Kv7 current. The transcriptional expression of KCNQ/Kv7 channels has previously been shown to be regulated by the transcription factors REST/NRSF, Sp1 and NFAT in peripheral neurons, but the presence of these mechanisms in the brain has not been examined. In this project, organotypic hippocampal slice cultures were used to investigate changes in *Kcnq*/Kv7 expression changes in epileptic conditions and in response to REST modulation. Adenovirus was used to deliver REST overexpression or a dominant negative REST to the slice cultures, with a novel delivery technique enabling up to 41% infection of total cells, including neurons and microglia, without observable toxicity. REST modulation had no effect on *Kcnq2/3* expression, but inhibition of HDACs, which are recruited by REST to repress its target genes, caused de-repression of *Kcnq2*, suggesting *Kcnq2* is regulated by HDACs. The chemoconvulsants kainate and 4-aminopyridine both caused a large upregulation of the epileptic marker BDNF. Kainate exposure caused a downregulation of *Kcnq2*, associated with a reduction of the Kv7.2 protein it encodes, specific to the CA1 hippocampal region. Expression patterns suggest that in contrast to REST's known direct repression of BDNF, it may indirectly contribute to *Bdnf* upregulation following seizure through its pro-epileptic effects. Furthermore, *Bdnf* levels were correlated with *Kcnq2* and *Kcnq3*, and *Bdnf* appears to help to maintain *Kcnq2/3* expression in epileptic conditions. The downregulation of *Kcnq2* after kainate exposure may contribute to epileptogenesis and could provide an area for therapeutic targeting.

Contents

List of Tables

List of Figures

Abbreviations

β-TrCP	β-Transducin
2DG	2-Deoxyglucose
4AP	4-aminopyridine
AAV	Adeno-associated virus
ACSF	Artificial cerebrospinal fluid
AIS	Axon initial segment
AKAP	A kinase anchoring protein
AMPA	α-amino-3-hydroxy-5-methyl-4-isoxazolepropionic acid
ANOVA	Analysis of variance
AV	Adenovirus
Bcl2	B-cell lymphoma 2
BDNF	Brain derived neurotrophic factor
BFNC	Benign familial neonatal convulsions
BHB	β-hydroxybutyric acid
BK	Bradykinin receptor
BRCA2	Breast cancer type 2 susceptibility protein
BRG1	Brahma-related gene-1
CA1	Cornu ammonis 1
CA2	Cornu ammonis 2
CA3	Cornu ammonis 3
CA4	Cornu ammonis 4
CAMKII	Calmodulin-dependent protein-kinase II
cAMP	Cyclic AMP
CDK4	Cyclin-dependent kinase 4
C/EBPα	CCAAT-enhancer binding proteins
CK1	Casein kinase 1
CMV	Cytomegalovirus

CNS	Central nervous system
Co-REST	REST corepressor 1 complex
CREB	cAMP response element binding protein
CRMP-2	Collapsing response mediator protein 2
CsA	Cyclosporin A
CtBP	C terminal-binding protein 1
CXCL10	C-X-C motif chemokine 10
CycA	Cyclophilin A
DAG	Diacylglycerol
DAPI	4′,6-diamidino-2-phenylindole
DEE	Developmental and epileptic encephalopathy
DIV	Days in vitro
DMEM	Dulbecco's Modified Eage Medium
DN	Dominant negative
DRG	Dorsal root ganglia
DTT	Dithiothreitol
EDTA	Ethylenediaminetetraacetic acid
EPSC	Excitatory postsynaptic current
ER	Endoplasmic reticulum
GABA	Gamma-amino-butyric acid
GFAP	Glial fibrillary acidic protein
GFP	Green fluorescent protein
GluR2	Glutamate receptor 2
GSK3β	Glycogen synthase kinase 3 β
HCN1	Hyperpolarization-activated cyclic nucleotide-gated channel 1
HDAC	Histone deacetylase
HEK-293	Human embryonic kidney
HEPES	4-(2-hydroxyethyl)-1-piperazineethanesulfonic acid
HRP	Horseradish peroxidase

HUC/D	HuA/B/C/D
IL-1β	Interkeukin-1β
IL-1R	Interkeukin-1 receptor
IL-6	Interkeukin-6
IP_3	Inositol triphosphate
IPSP	Inhibitory post-synaptic potential
JAK	Janus kinase
KCC2	Potassium-chloride transporter membrane 5
LSD1	Lysine-specific demethylase 1A
M1	Muscarinic receptor
MAP2	Microtubule associated protein 2
miR-124	MicroRNA-124
mRNA	Messenger ribonucleic acid
mTOR	Mechanistic target of rapamycin
MYD88	Myeloid differentiation primary response 88
NaII	Sodium channel type II
NAD+	Nicotinamide adenine dinucleotide
NADH	Nicotinamide adenine dinucleotide + hydrogen
NEM	N-ethylmaleimide
NFAT	Nuclear factor of activated T-cells
NF kappa B	Nuclear factor kappaB
NMDA	N-methyl-D-aspartate
NOS	Nitric oxide synthase
NRSF	Neuron-restrictive silencer factor
OHSC	Organotypic hippocampal slice culture
OSP	Oligodendrocyte-specific protein
P21	Cyclin-dependent kinase inhibitor 1
P2RX7	P2X purinoceptor 7
PBS	Phosphate-buffered saline

PBST	Phosphate-buffered saline with tween-20
PFA	Paraformaldehyde
PI	Propidium iodide
PIP_2	Phosphatidyinositol 4,5-bisphosphate
PKC	Protein kinase C
PLC	Phospholipase C
PP2	4-amino-5-(4-chlorophenyl)-7-(*t*-butyl)pyrazolo[3,4-d]pyrimidine
PTZ	Pentylenetetrazole
RE1	Repressor element-1
REST	Repressor element-1 silencing transcription factor
RFP	Red fluorescent protein
RNA	Ribonucleic acid
RT-PCR	Reverse-transcription polymerase chain reaction
SAHA	Suberanilohydroxamic acid
SCG10	Superior cervical ganglion 10
SCN2A	Sodium voltage-gated channel alpha subunit 2
Sdha	Succinate dehydrogenase
SDS-PAGE	Sodium dodecyl sulphate-polyacrylamide gel electrophoresis
SE	Status epilepticus
SEM	Standard error of the mean
shRNA	Short hairpin ribonucleic acid
siRNA	Small interfering ribonucleic acid
SKP2	S-phase kinase-associated protein 2
SLE	Seizure-like event
SNHG1	Small nucleolar RNA host gene 1
Sp1	Specificity protein 1
STAT	Signal transducer and activators of transcription
TEMED	Tetramethylethylenediamine
TGF-β	Transforming growth factor β

TLR4	Toll like receptor 4
TNF-α	Tumor necrosis factor α
TrkB	Tropomyosin receptor kinase B
YFP	Yellow fluorescent protein

Chapter 1

General Introduction

1.1 Epileptogenesis

Epilepsy is a chronic neurological condition characterised by recurrent spontaneous seizures, which are brief episodes of involuntary movement and loss of consciousness. Epilepsy affects at least 50 million people worldwide. Between 2007 and 2013, 50111 A&E admissions per year in England were due to seizures in adults, costing £88.2 million annually (Dickson et al., 2018). Epilepsy can effect people of all ages but is most common in children and the elderley. There are different types of epilepsy with temporal lobe epilepsy being the most common form. Epilepsy often has a detrimental effect on the patient's quality of life due to the seizures themselves, the often progressive nature of the condition, the restrictions such as being unable to drive, social stigma, and side effects of epilepsy medications. Epilepsy also has comorbidities such as depression, anxiety, migraine, and dementia (Keezer et al. 20162016). The risk of premature death is up to 3 times higher for epilepsy sufferers than for the general population. Currently the only treatments available are anti-seizure medications, which suppress seizures but do not alter long-term prognosis. No antiepileptogenic or disease-modifying drugs have been developed yet. Further to that, current seizure-suppressant medications are associated with a host of unpleasant side effects and around a third of patients are refractory to current medications. Surgery is highly effective in reducing or stopping seizures (Ontario, 2012; Wiebe et al., 2001), but is reserved for the most severe cases of those unresponsive to all medications, due to the invasiveness and associated risk.

Epileptogenesis is the process of a healthy brain undergoing cellular and structural changes to become hypersensitive to excitability following an initial brain insult. This insult could be a traumatic brain injury, infection, an initial seizure, stroke, hyperthermia or viral infection (Becker, 2018). For example, febrile seizures may occur during a high fever in young children and can lead to the development of epilepsy as adults (McNamara et al.2006). This cell damage induces structural, cellular and molecular level changes in the brain which makes the neurons vulnerable to hyperexcitability, eventually leading to repeated spontaneous seizures (Pitkänen et al., 2015). This is observed in the clinic as a 'latent period' where patients are symptom free for months or years after the initial insult, before episodes of spontaneous seizures develop. At this point the diagnosis of epilepsy is given. The insult leads to epilepsy

in some patients and model animals and not in others, which is believed to be due genetic and environmental factors (Kjeldsen et al., 2001).

A seizure occurs when neurons fire off bursts of uncontrolled action potentials which cause sudden changes in muscle control and consciousness. Types of seizures include absence seizures where consciousness is briefly absent, tonic-clonic seizures causing convulsions, atonic seizures involving sudden loss of muscle tone, tonic seizures causing muscle stiffness for around 20 seconds, or clonic (jerking) seizures. These can be focal or generalised. Focal seizures affect one side of the brain and are the most common type in people with temporal lobe epilepsy, when seizures begin in one of the temporal lobes. In contrast, generalised seizures affect both hemispheres of the brain.

1.1.1 Molecular pathways involved in epileptogenesis

Perhaps the most destructive physiological consequence of severe epilepsy is hippocampal sclerosis, which is a loss of cells in the hippocampus, particularly the CA1 and CA4 regions (Blümcke et al., 2013), and is likely to contribute greatly to the associated cognitive decline observed in some patients. In addition to cell death, the detrimental cascade of events triggered during epileptogenesis include blood brain barrier dysfunction, reactive astrocytosis, inflammation, aberrant sprouting of mossy fibers in the dentate gyrus, excitotoxicity and oxidative stress, and other molecular alterations within the neurons (Sloviter, 2017). While the details explaining and linking all of the physiological abnormalities of epilepsy have only partially been uncovered, the information obtained highlights key areas of interest for further research and therapeutic potential.

At the core of all the known pathological abnormalities found in epilepsy patients and animal models is the understanding that these disrupt the normal excitatory and inhibitory signalling between neurons and firing threshold within them. As the major inhibitory neurotransmitter, gamma-aminobutyric acid (GABA) and its receptors are critical for maintaining the balance in network excitation, and research suggests this control is disrupted in epileptic brains. $GABA_A$ receptors appear reorganised in hippocampal neurons of TLE patients with hippocampal sclerosis (Loup et al., 2000), and are downregulated in the CA1 and CA3 regions (Fritschy et al., 1999). Furthermore, epileptiform bursting during seizure causes internalisation of $GABA_A$

receptors, resulting in reduced inhibitory GABA signalling (Goodkin et al.2005). This downregulation of functional $GABA_A$ receptors in the hippocampus and consequential reduction in inhibitory GABAergic signalling is likely one of the greatest driving forces in epilepsy and epileptogenesis.

Inhibitory GABAergic signalling may also be reduced by activation of NMDA glutamate receptors during epilepsy. GABAergic inhibitory post-synaptic potentials (IPSPs) are reduced by kindling, most likely through activation of NMDA receptors (Stelzer et al. 1987). NMDA receptor activation is known to be critical for epileptogenesis in adults (Holmes et al., 1990; McNamara and Routtenberg, 1995; Sutula et al., 1996), by allowing a large Ca^{2+} influx which leads to excitotoxicity. In contrast, activation of AMPA glutamate receptors is proposed to be more important for hypoxic seizures in neonates; a time when there is a high proportion of AMPA receptors which are permeable to Ca^{2+} (McNamara et al., 2006)

As Ca^{2+} influx occurs through Ca^{2+} channels such as NMDA and AMPA receptors during seizure it can trigger the Ca^{2+}/calmodulin cascade. This leads to the NMDA-dependent reduction of Ca^{2+}/calmodulin-dependent protein-kinase II (CaMKII) in the cerebrum and hippocampus of post-seizure rats (Kochan et al., 2000). Furthermore, homozygous null mutants for CaMKII display seizures (Butler et al., 1995) and CaMKII knockdown results in epileptiform activity in cultured hippocampal neurons (Churn et al., 2000), suggesting the NMDA-dependent downregulation of CaMKII to be pivotal in the epileptogenic process. Also activated by the Ca^{2+} influx during seizure is the serine/threonine protein phosphatase calcineurin. Calcineurin is found to be upregulated in kindled rats. The calcineurin inhibitors cyclosporin A and FK506 prevented kindling and mossy fiber sprouting (Moia et al., 1994; Moriwaki et al., 1996), suggesting calcineurin upregulation is also essential for epileptogenesis.

Excitotoxicity and oxidative stress triggered by the excess glutamate and Ca^{2+} influx during seizure causes damage to the blood brain barrier, which likely mediates some of the longer-term effects observed in epileptogenesis. Blood brain barrier breakdown causes albumin to leak into the brain, activating the transforming growth factor β (TGF-β) pro-inflammatory pathway. TGF-β induces synaptogenesis of excitatory neurons, increasing overall excitability (Weissberg et al., 2015). TGF-β blockers inhibit epileptogenesis and downstream albumin-modulated transcriptional changes,

demonstrating its importance for the process (Cacheaux et al., 2009). Other inflammatory mediators are released in response to seizure, including the cytokines TNF-α, C-X-C motif chemokine 10 (CXCL10), IL-6, IL-1β and IL-1R (Rojas et al., 2014; Uludag et al., 2015). These also help to push neurons towards a more excitable state. TNF-α causes endocytosis of GABA receptors at the synapse whilst upregulating AMPA receptors (Stellwagen et al., 2005). IL-1β reduces inhibitory $GABA_A$ currents (Roseti et al., 2015), and upregulates NMDA receptor-mediated Ca^{2+} influx (Viviani et al., 2003). Activation of astrocytes and infiltration of leukocytes is also observed in epilepsy patients (Zattoni et al., 2011), contributing to inflammation levels and further increasing damage. The cAMP response element binding protein (CREB) is a transcription factor that activates in response to inflammatory signals and regulates cell proliferation and survival. CREB activation is increased in epilepsy patients (Rakhade et al., 2005) and CREB deficient mice have a suppressed seizure response following pilocarpine (Zhu et al., 2012), suggesting CREB to be pro-epileptogenic. Of all the genes that are differentially regulated in epilepsy, 74% have a cAMP response element and thus may potentially be regulated by CREB (Beaumont et al., 2012), suggesting its activation in epilepsy could mediate widespread effects.

The enzyme cyclooxygenase-2 is involved in inflammation. It is upregulated following status epilepticus (SE), and this causes the upregulation of brain-derived neurotrophic factor (Yu and Jiang, 2020). Brain-derived neurotrophic factor (BDNF) is a neurotrophic factor responsible for neuronal survival, differentiation and neurogenesis in the brain. BDNF levels are consistently increased following seizures in animal models (Ernfors et al., 1991) and human patients (Hou et al., 2010; Takahashi et al., 1999). Infusion of BDNF in rats led to spontaneous seizures (Scharfman et al., 2002) and kindling development is retarded in mice heterozygous for a *Bdnf* gene mutation (Kokaia et al., 1995), suggesting a pro-epileptic role of BDNF. The BDNF receptor Tropomyosin receptor kinase B (TrkB) is also shown to be important for facilitating the development of kindling in rats (Binder et al., 1999b). TrkB knockout mice showed complete resistance to kindling, whereas BDNF knockout mice showed only partial impairment of kindling-induced epileptogenesis, suggesting BDNF contributes to epileptogenesis while TrkB is essential (He et al., 2004). Activation of TrkB through BDNF seems to drive epileptogenesis through regulation of downstream pathways involving Janus kinase (JAK)/Signal Transducer

and Activators of Transcription (STAT), protein kinase C, and mitogen activated protein kinase. This leads to changes in $GABA_A$ receptor subunit expression, and hyperexcitability (Brooks-Kayal and Russek, 2012).

One of the most prominent structural alterations occurring during epileptogenesis is mossy fiber sprouting. This is when the axons of granule cells in the dentate gyrus of the hippocampus sprout mossy fibers which form aberrant synaptic connections to other granule cells, forming an excitatory loop. However, in addition to aberrant axonal sprouting, status epilepticus induces neurogenesis in the dentate gyrus, and this has been suggested to contribute to excitation in the hilus and inner molecular layer (Parent et al., 1997). The kinase mechanistic target of rapamycin (mTOR) promotes epileptogenesis through regulation of cell growth and proliferation, synaptic plasticity and protein synthesis. mTOR is implicated in the sprouting of mossy fibers in the dentate gyrus, causing aberrant granule cell-granule cell connections that form the hyperexcitable positive-feedback network. Inhibition of mTOR may be a key antiepileptogenic strategy due to its ability to prevent epileptogenesis in mouse models by prevention of mossy fiber sprouting (Buckmaster et al., 2009; Huang et al., 2010; Zeng et al., 2009)

Though key mechanistic pathways have been implicated in the various aspects of epileptogenesis, much is still unknown regarding the details of how they interact and induce long-term structural changes in the brain, and how accurately the findings from animal seizure models reflects epilepsy patients. Groups have identified hundreds of genes which are observed to change in expression levels following seizure, with the interest of highlighting potential disease biomarkers or targets for antiepileptogenic therapies. In 2015 Pitkanen and colleagues reported 47 drugs that had been observed to have some disease-modifying effects, but none of these have progressed to clinical use (Pitkänen et al., 2015). This may in part be due to the difficulty with designing clinical trials to assess antiepileptogenic effects in patients over a prolonged time scale. It may also be due to species differences, genetic differences, focussing on the wrong molecules, and incorrect timing in studies. It is important to define whether a molecular change is occurring at the acute seizure stage or is driving epileptogenesis, and these details can be challenging to distinguish. Furthermore, due to the heterogeneous nature of the condition, different epileptic disorders are likely to develop through different mechanisms (Kobow et al., 2012), Therefore different

therapies would be required for different epileptic conditions and may also depend on disease stage. The future could involve a selection of antiepileptogenic treatments, allowing patient specificity and higher efficacy in disease control than current generic treatments. Antiepileptogenic drugs may be used to help prevent epilepsy in vulnerable individuals such as those with a genetic susceptibility, a history of infantile seizures, or stroke and traumatic brain injury patients.

1.2 REST in epileptogenesis

Various models have been used to create epilepsy in rodents. While no single model recreates every aspect of all epilepsies, most replicate the majority of neuropathological traits with reasonable accuracy, and the type of model used per experiment is chosen specifically for each research question. The electrical kindling model was developed in 1967, and consists of repeated short, mild tetanic stimulations every 12 or 24 hours for weeks, leading to seizures of increasing severity. In the pentylenetetrazole (PTZ) kindling model, kindling is induced by an injection of a subconvulsive dose of the $GABA_A$ antagonist PTZ every 2 days for up to 43 days. Kindled rodents do not typically have spontaneous seizures, but they are very easily susceptible to triggered seizures. However, animals kindled for many months consisting of hundreds of trials can exhibit spontaneous seizures (Michalakis et al., 1998). In post status-epilepticus (SE) epilepsy models, SE can be induced by chemoconvulsants or a strong electrical stimulation. Most post-SE models use kainite, a glutamate analog. One large (18mg/kg) or a few smaller (5mg/kg) kainite injection(s) at 30 minute intervals induces SE within hours, followed by a latent period and then an epilepsy-like state where spontaneous seizures can reccur indefinitely. Post-SE models are favoured for investigations of epileptogenesis because this process occurs during the latent period in patients following an initial brain insult.

Epileptogenesis can affect the expression of many different genes. One example of a gene which is affected by seizure is the transcription factor Repressor Element 1-Silencing Transcription factor (*Rest*)/Neuron Restrictive Silencer Factor (*Nrsf*). REST represses the expression of its target genes by binding to a 21 bp Repressor Element 1 (RE1)/Neural Restrictive Silencer Element (NRSE) site through its zinc fingers (Chong et al., 1995). REST represses neuronal genes in non-neuronal tissues and is critical in regulating neuronal differentiation, but it also regulates gene expression in

the mature brain (Ballas et al., 2005; Ooi and Wood, 2007; Palm et al., 1998; Schoenherr et al., 1996). REST is shown to be present in all layers of the cerebral cortex, the pyramidal cells of the hippocampus and the dentate gyrus granule cells (Palm et al., 1998). Up to 1,892 potential RE1 sites have been identified in humans bioinformatically (Bruce et al., 2004; Johnson et al., 2006), and orthologues have been identified in 16 other species (Johnson et al., 2009). REST binding *in vivo* has been validated for most of these (Johnson et al., 2007). REST has N and C-terminal domains which recruit repressor protein complexes. mSin3 (Grimes et al., 2000) and histone deacetylases (HDACs) 1 and 2 are recruited by the N-terminal (Huang et al., 1999; Naruse et al., 1999; Roopra et al., 2000). REST corepressor 1 complex (Andrés et al., 1999) is recruited by the C-terminal of REST. Co-REST recruits BRG1 which stabilises REST binding to its target gene, as well as HDACs 1 and 2 (Ooi et al., 2006; Ooi and Wood, 2007). The H3K4 demethylase LSD1 and the H3K9 methylase G9a are also recruited by the C-terminal domain (Roopra et al., 2004; Shi et al., 2004).

Rest mRNA and REST protein have been found to be upregulated following status epilepticus in animal models by many different groups (Table 1). This is also reflected by upregulated REST in epilepsy patients, with REST protein level correlating with seizure frequency (Navarrete-Modesto et al., 2019). *Rest* mRNA levels are increased in response to kainate-induced status epilepticus in rat hippocampus and cortex (Palm et al., 1998; Spencer et al., 2006). REST protein and *Rest* mRNA is increased for 4-48 hours and REST target genes are downregulated in response to kainate-induced seizures (Brennan et al., 2016; McClelland et al., 2011), with REST protein levels highest after 24 hours (Carminati et al., 2019). Similarly, 24 hours after pilocarpine injection or kindling *Rest* mRNA and REST protein were observed to be upregulated by another group (Hu et al., 2011a). After kindling with 20 PTZ injections, REST protein was upregulated in rats resistant to kindling while REST remained at control levels in rats showing successful kindling (Chmielewska et al., 2020), suggesting REST increase may protect against seizures in the PTZ kindling model. Due to the upregulation of REST in epilepsy models, groups have attempted to understand the specific contribution of REST to epileptogenesis.

Model	Effect on REST	REST inhibition	Response	Role of REST	Reference
4AP	Increased mRNA & protein	shRNA knockout	High firing rate from 4AP remained high	Anti-epileptic	(Pozzi et al., 2013)
Kindling	Increased mRNA & protein	Cre-loxp knockout	Accelerated seizure progression	Anti-epileptic	(Hu et al., 2011a)
PTZ kindling	Increased protein in kindling-resistant rats	-	-	Anti-epileptic	(Chmielewska et al., 2020)
PTZ	-	Creloxp knockout	More PTZ required to initiate seizure	Pro-epileptic	(Liu et al., 2012)
Kainate	Increased mRNA	-	-	-	(Palm et al., 1998)
Kainate	Increased mRNA	-	-	-	(Spencer et al., 2006)
Kainate	Increased mRNA & protein	-	-	-	(Brennan et al., 2016)
Kainate	Increased protein	Decoy oligonucleotides	Prevented kainate-induced increase in firing rate	Pro-epileptic	(McClelland et al., 2011)

Kainate	Increased protein	Viral knockdown	Reduced & less severe seizures	Pro-epileptic	(Carminati et al., 2019)

Table 1.1. Animal epilepsy models involving REST. *Rest* mRNA and REST protein is upregulated in response to kainate (KA), PTZ and kindling. REST upregulation can be prevented by shRNA and siRNA knockdowns, decoy oligonucleotides or cre-loxp knockout. REST is shown to be anti-epileptic in kindling studies and pro-epileptic in SE epilepsy models.

1.2.1 REST in animal seizure models

Status epilepticus is induced in animal models by one or a few chemoconvulsant injections, or sometimes by a burst of electrical stimulation. SE is followed by a latent period when epileptogenic changes occur in the brain leading to a state of chronic epilepsy, observed as spontaneous seizures. Kainate is a glutamate analog which activates kainate receptors, and is the most commonly used convulsant *in vivo*. Kainate causes excitotoxicity, hippocampal sclerosis, deterioration of the blood brain barrier (Zucker et al., 1983) and sprouting of dentate gyrus mossy fibers (de Montigny and Tardif, 1981; Leite et al., 1996). The mechanism behind REST upregulation in SE animal models will now be discussed.

1.2.2 The upregulation of REST in seizure

The upregulation of REST in seizure was found to be dependent on a histone deacetylase called Sirt1 (Brennan et al., 2016). Sirt1 is responsive to NAD+, altering gene transcription levels through chromatin state, and is activated in epilepsy patients and animal models (Chen et al., 2013). Kainite-induced SE caused histone deacetylation by Sirt1 to downregulate microRNA-124 (miR-124). This led to an increase in C/EBPα, causing an upregulation of REST and a downregulation of REST target genes. The upregulation of REST was prevented by infusion of miR-124 agomirs, which also rescued expression of REST target genes. However, seizures were not prevented (Brennan et al., 2016). Another group also observed downregulation of miR-124 in response to pilocarpine and PTZ-induced seizure. Here, miR-124 infusion did prevent seizures. It also repressed the epileptogenesis regulator cAMP-response

element-binding protein 1 (CREB)(Wang et al., 2016), suggesting that CREB1 and miR-124 are involved in another pathway in epileptogenesis that does not involve REST. It has been proposed that miR-124 has two effects in post-SE epileptogenesis models. Firstly, it prevents the expression of REST, CREB, C/EBPα and Bcl2L13 which attenuates neuronal excitability and apoptosis, and increases the latency period (Brennan et al., 2016; Schouten et al., 2015; Wang et al., 2016). In contrast, miR-124 increases inflammation which drives seizures (Liu et al., 2019) independently of REST. The Sirt1 inhibitor EX-572 restored miR-124 levels after kainate-induced SE, but this had no effects on seizures, inflammation or cell loss (Hall et al., 2017), supporting this idea.

1.2.3 REST represses *Hcn1, GluR2* and *Kcnq2/3*

The upregulation of REST following SE can lead to repression of certain REST target genes involved in neuronal excitability, so these could be important in epileptogenesis. Firstly, REST represses potassium/sodium hyperpolarization-activated cyclic nucleotide-gated channel 1 (*Hcn1*) channels which help to regulate pyramidal neuron excitability at the dendrites in the hippocampus and entorhinal cortex (Santoro et al., 2010). REST protein was upregulated in response to kainate-induced SE, which was associated with increased binding of REST to *Hcn1* and increased seizure activity (McClelland et al., 2011). This suggests REST has a pro-epileptic role in the kainite model, by repressing expression of protective HCN1 channels.

GluR2 is repressed by REST, leading to cell death (Calderone et al., 2003). When the GluR2 subunit is incorporated into AMPA receptors it restricts Ca^{2+} flow, protecting against seizure. Conversely, knockdown of GluR2 increases AMPA permeability to Ca^{2+} and enhances seizure (Sanchez et al., 2001). SE also causes a downregulation of *GluR2* (Grooms et al., 2000). Ca^{2+} influx in interneurons, augmented by permeable AMPA receptors, may cause excitotoxic cell death, therefore reducing inhibitory GABA signalling and increasing overall network excitability (Rogawski and Donevan, 1999). REST was also found to repress the Kv7 channel subunits *Kcnq2* and *Kcnq3* during inflammation in dorsal root ganglia neurons, reducing the anti-excitatory Kv7 current (Mucha et al., 2010), but this will be discussed in more detail later.

Other groups have also found a pro-epileptic role for REST after SE. A virally-delivered genetic switch was used to inhibit REST in mouse hippocampal neurons. The REST inhibitor resulted in reduced kainate-induced seizure activity compared to control mice (Carminati et al., 2019). In addition, PTZ doses required for induction of tonic-clonic seizures or death were greater in mice with *Rest* knocked out compared to control, suggesting REST permits susceptibility to PTZ (Liu et al., 2012).

1.2.4 The role of REST in kindling epilepsy models

Kindling is a process of inducing seizures in animal models with either electrical or chemical repeated sub-convulsive stimulations. This makes the brain more sensitive to the stimulation and gradually increases overall excitability until full generalised seizures are achieved (Sato et al., 1990). Electrical kindling typically induces short seizures without cell death or astrogliosis, though mossy fiber sprouting has been reported (Sutula et al., 1988). Chemical kindling involves repeated application of chemoconvulsive drugs. For example, subthreshold doses of 20-50mg/kg PTZ can be injected into the peritoneum to induce a kindling effect (Yonekawa et al., 1980). PTZ is an antagonist of $GABA_A$ receptors, so when it reaches the brain it causes increasingly severe seizures through reduction of inhibitory signalling. These PTZ-induced seizures are associated with oxidative stress and astrogliosis, as well as permeabilisation of the blood brain barrier and BDNF upregulation (Uzüm et al., 2006; Zhu et al., 2015). Changes in neuronal morphology have been observed (Vasil'ev et al., 2013), but neuron death appears to vary (Tian et al., 2009; Zhu et al., 2015).

1.2.5 The downregulation of BDNF and TrkB by REST in epilepsy

REST is known to bind to the *Bdnf* promoter (Timmusk et al., 1999), and represses *Bdnf* in animal seizure models (Conforti et al., 2013). Furthermore, BDNF and its receptor TrkB are well understood to be upregulated in epilepsy models (Binder et al., 1999a; Dinocourt et al., 2006; Hu et al., 2011a; Isackson et al., 1991), and to contribute to epileptogenesis (Kang et al., 2015; Kokaia et al., 1995; Lähteinen et al., 2002).

Last year the interactions between REST and BDNF were investigated in a PTZ kindling model. Higher levels of REST protein but slightly reduced levels of *Rest* mRNA were observed in the rats that were resistant to kindling compared to the rats not resistant to kindling. This could suggest alterations in protein synthesis or degradation rates in kindling resistant rats. In addition, BDNF levels were increased

in rats resistant to kindling compared to kindled rats. Conversely, TrkB levels were higher in the kindled rats than the kindling-resistant rats (Chmielewska et al., 2020). This could suggest that the increased REST levels led to a prevention of TrkB upregulation, protecting the rats from kindling-induced seizures.

The BDNF TrkB pathway has been shown to activate phospholipase C gamma1 (PLCγ) in kindling and pilocarpine mouse models where it drives seizure (He et al., 2010). Post-SE epilepsy was prevented by uncoupling PLCγ from TrkB (Gu et al., 2015). TrkB recruits PLCγ to downregulate the K^+/Cl^- cotransporter KCC2, which causes increased neuronal excitability by reducing the Cl^- dependent hyperpolarizing postsynaptic current (Rivera et al., 2004). It is understood that the upregulation of TrkB following seizure drives epileptogenesis, and epileptogenesis is reduced by REST inhibiting TrkB activity through its repression of *Bdnf*.

1.2.6 REST may be involved in the anti-epileptic effects of the ketogenic diet

Drug-resistant epilepsy can be controlled by the ketogenic diet, which is high fat and low in carbohydrate. The mechanisms behind the control of seizures with the ketogenic diet have not been completely elucidated but are likely to involve a few different antiepileptogenic and antiseizure effects. During glycolytic inhibition, REST recruitment of its co-repressor C-terminal-Binding Protein 1 (CtBP) was increased. During glycolysis, increased NADH levels disrupted the REST-CtBP interaction. This suggests that reduced NADH during glycolytic inhibition facilitates REST CtBP binding which enhances repression of REST target genes (Garriga-Canut et al., 2006). REST was shown to be essential for the prevention of electrical kindling by 2DG, as the anti-seizure effects of 2DG did not work in REST knockout mice. In contrast, REST was shown to be non-essential to the effects of the ketogenic diet itself (Hu et al., 2011b). The ketogenic diet has several different mechanisms of action (Boison, 2017), but the evidence above suggests that repression of *Bdnf* by REST contributes to its effects.

1.2.7 The effects of REST in the 4AP model

Homeostatic plasticity can be either intrinsic excitability or synaptic scaling, and involves adjustments in responsive neuronal firing. REST has been shown to be involved in both intrinsic excitability and synaptic scaling in conditions of exposure

to the Kv1 voltage gated K^+ channel blocker and convulsant 4-aminopyridine (Pecoraro-Bisogni et al., 2018; Pozzi et al., 2013). *Rest* transfection downregulated voltage-gated sodium channels in cultured hippocampal neurons, enabling protection from 4AP through reduction of neuronal excitability. Cultured neurons showed increased excitability in response to 4AP which then reduced. However, in neurons with *Rest* knocked out this reduction did not occur, suggesting REST is necessary for the homeostatic attenuation of excitability (Pozzi et al., 2013). This group also demonstrated that 4AP-induced REST upregulation reduced presynaptic efficiciency through repression of presynaptic genes. These examples demonstrate how REST is involved in synaptic scaling and intrinsic excitability to protect against seizure in the 4AP model (Pecoraro-Bisogni et al., 2018)**.** *In vitro* 4AP seizure models share similarities with *in vivo* kindling models through the increase of network excitability without the excitotoxicity and cell death seen in the post-SE models. Similarly to kindling models, 4AP models demonstrate REST to protect against hyperexcitability and seizure.

1.2.8 The function of REST changes in different epilepsy models

Rest mRNA and REST protein is upregulated in all studies and models (Table 1.1). The regulation of REST target genes by REST can contribute anti-epileptic or pro-epileptic effects, depending on the type of animal model used (Figure 1.1). Individual variation in the balance of all of these effects is likely to govern susceptibility to seizure.

REST appears to be protective in preventing seizure in the kindling model while being pro-epileptic in models that involve status epilepticus (Table 1.1). The effect of REST could be governed by its own expression level. REST was found to be upregulated 1.3-fold in rats resistant to PTZ kindling while kindled rats had control levels of REST (Chmielewska et al., 2020). In comparison, REST protein is observed to increase 2-4 fold in 48 hours in response to kainate-induced SE (Brennan et al., 2016; Carminati et al., 2019; McClelland et al., 2011). A mild increase in REST may allow a small homeostatic reduction in induced excitability to control levels, while unchanged REST levels may allow the kindling process to occur. Greater REST upregulation might exacerbate epileptogenesis. A 96 hour 4AP exposure in cultured hippocampal neurons induced a 7-fold REST upregulation which had anti-epileptic effects (Pozzi et al.,

2013). REST may have been anti-epileptic in this *in vitro* system as it involved only a single cell type, and its pro-epileptic effects may depend on the presence of glial cells, for example. This suggests multiple factors govern the function of REST in epileptic conditions. The BDNF TrkB pathway is essential for kindling, with kindling effects being suppressed or completely prevented by the deletion of *Bdnf* or *TrkB*, respectively (Kokaia et al., 1995). TrkB is upregulated in kindled rats and is necessary for kindling, while TrkB remains at control levels in rats resistant to kindling (Binder et al., 1999b; Chmielewska et al., 2020). Furthermore, REST recruitment of CtBP at the BDNF promoter was increased in kindling-resistant mice (Potter et al., 2010). It is likely that in cases where excitability fluctuates within a controllable range, REST represses *Bdnf*, lowering activity through the BDNF TrkB pathway and homeostatically reducing excitability to normal levels. When kindling is successful, REST is mildly upregulated to a level that is insufficient to prevent *Bdnf* upregulation, so activation of TrkB occurs and enables kindling. REST has also been observed to be protective in other situations. During ageing REST levels are naturally upregulated which blocks oxidative stress and protects against Alzheimer's disease (Lu et al., 2014). Neuronal excitability increases with ageing and can have a negative effect on lifespan. REST protects from this by downregulating target genes that promote excitation in ageing (Zullo et al., 2019). Altogether it appears that REST increase in brains that are generally healthy leads to neuroprotection against oxidative stress and hyperexcitability, helping to increase lifespan.

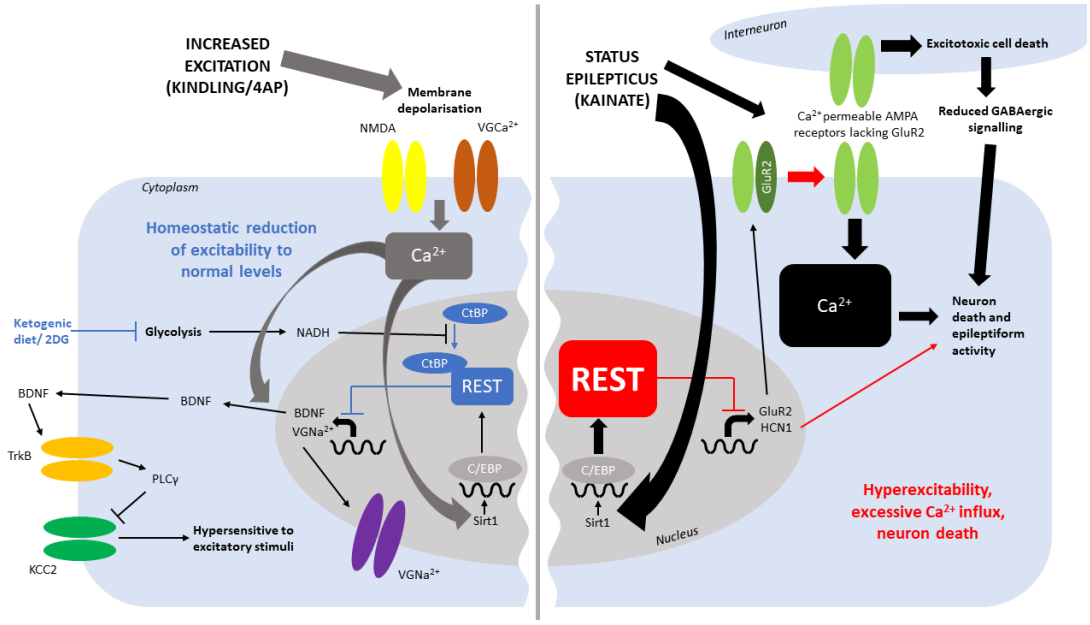

Figure 1.1. The opposing roles of REST in pyramidal neurons in different epilepsy models. REST can protect from (blue) or promote (red) seizure in the kindling and 4AP models (left), or status epilepticus models (right). Kindling or 4AP exposure induces an excitation within a controllable range, which causes an influx of Ca^{2+} through NMDA receptors and voltage gated Ca^{2+} channels. This Ca^{2+} leads to BDNF upregulation and activation of Sirt1, causing upregulation of the transcription factor C/EBP which enhances REST expression. REST then represses voltage gated Na^{+} channels and *Bdnf*. BDNF protein is released from the cell, and then binds to TrkB receptors, causing PLCγ activation. Recruitment of PLCγ by TrkB causes repression of KCC2 transporters, causing hypersensitivity to excitation. REST represses *Bdnf* expression which reduces the KCC2-mediated hyperexcitability. REST also represses voltage-gated Na^{+} channels, reducing action potential spiking. Therefore in this mechanism REST enables a homeostatic reduction of excitability to non-epileptic levels. In contrast, status epilepticus induced by chemoconvulsants induce a larger influx of Ca^{2+} to the cell, possibly associated with a larger REST upregulation. As well as the effects of REST in downregulating mild excitation (left of diagram), in response to status epilepticus REST also gains the function of targeting *Hcn1* and the AMPA receptor subunit *GluR2*. This GluR2 repression results in more AMPA receptors lacking GluR2 and therefore being more Ca^{2+} permeable. This means the Ca^{2+} influx induced by status epilepticus is greater. This enhanced Ca^{2+} influx in neighbouring interneurons causes excitotoxicity and cell death, reducing inhibitory GABAergic signalling to the pyramidal neuron. The reduced inhibitory signalling and large Ca^{2+}

Figure 1.1 *continued…* influx permits enhanced epileptiform activity in SE epilepsy models. REST also exacerbates seizure and neuron death through repression of *Hcn1*. Figure previously published (Butler-Ryan and Wood, 2021b).

REST seems to increase to a greater extent from SE than from kindling, which allows it to repress additional genes. A 40% reduction in the REST target gene *GluR2* occurs in pyramidal neurons of the CA1 and CA3 regions of the hippocampus at 24 hours following kainate-induced seizures, and this was implicated in neuron loss (Grooms et al., 2000). However, after kindling *GluR2* is reduced by 20-30% in the piriform cortex, amygdala and limbic forebrain but not in the hippocampus (Prince et al., 1995). This could mean that REST is upregulated and *GluR2* is downregulated in the hippocampus to a degree that is dependent on insult severity, and the piriform cortex, amygdala and limbic forebrain regions are affected prior to the hippocampus. REST is upregulated to a large degree after SE, which allows HDACs to downregulate *GluR2*. This leads to Ca^{2+} permeable AMPA receptors which increase neuronal excitotoxicity. AMPA receptors are activated by kainate and assist in inducing seizures. As the AMPA receptors lack GluR2 due to REST-mediated repression, they have increased Ca^{2+} permeability, so excitotoxicity and seizures induced by kainate are increased. Indeed, AMPA receptors that lack GluR2 have greater currents from kainate than AMPA receptors with GluR2 (Iihara et al., 2001). Therefore, in the kainate model REST drives epileptogenesis through its repression of GluR2, which makes the excitotoxic effects of kainate-mediated Ca^{2+} influx more severe (Figure 1.1). The excitotoxicity promoted by REST is expected to exacerbate epileptogenesis through cell death. Excitotoxicity from glutamate receptor activation causes death of pyramidal neurons in epilepsy through necrosis, apoptosis and autophagy. In addition, hyperactivation of glutamate receptors is caused by excitotoxicity, which also contributes to greater Ca^{2+} influx. This can lead to the generation of free radicals, metabolic dysfunction, protein synthesis inhibition and the activation of proteases, phospholipases, endonucleases and nitric oxide synthase (NOS). The plasma membrane of the neuron is damaged by NOS activation, which can also contribute to seizures (Lorigados Pedre et al., 2013). In PTZ-induced seizures where GABAergic inhibition is blocked, a similar effect is observed (Liu et al., 2012). The theory that REST at low levels binds *Bdnf* but higher REST levels allows additional repression of *GluR2* suggests that REST binds to *Bdnf* with greater strength than to *GluR2*. While it

is shown that REST binding to *GluR2* is weaker than REST binding to the *Scn2a* promoter (Myers et al., 1998), the binding affinities of REST to *GluR2* and *Bdnf* need to be compared.

In summary, REST appears to have an anti-epileptic role in partial epilepsy models such as kindling and 4AP, through direct repression of the epileptogenesis driver *Bdnf*. In contrast, REST takes on a pro-epileptic role in post-SE models, where its repression of *GluR2* and other protective factors contributes to epileptogenesis, seizure and cell death.

1.3 The use of organotypic cultures in epilepsy models

Just as various agents have been used to create epilepsy models *in vivo*, they have also been used to create epilepsy models in organotypic cultures. Organotypic hippocampal slice cultures (OHSCs) are slices of hippocampus which are cultured for a number of weeks or months *in vitro*, allowing ease of manipulation and analysis. They retain much of their synaptic and structural architecture from the donor animal, allowing a realistic platform for monitoring processes involving hippocampal network connections over long time periods. During slicing, afferent and efferent fibers from different brain regions or from the contralateral hippocampus are axotomized, causing some cell death, inflammation and rearrangement of synaptic connections (Grabiec et al., 2017; Li et al., 2016b). During synaptic reorganisation following axotomy in slice cultures, new synaptic connections are made with projections from CA1 to CA3 and dentate gyrus, and axonal sprouting of mossy fibers (Bausch and McNamara, 2000; Gutiérrez and Heinemann, 1999). This reorganisation results in increased excitability of the granule cells (Lindroos et al., 2005). OHSCs have been observed to spontaneously develop epileptiform activity which increases with incubation time, with 50% of cultures at 21 days *in vitro* showing spontaneous ictal activity (Dyhrfjeld-Johnsen et al., 2010). ‘Ictal’ is defined as the period during a seizure, corresponding to repeated frequent bursts of action potentials in neurons in the brain. Seizure-like events (SLEs) involve electrophysiologically monitored epileptiform activity consisting of ictal burst firing in brain slices. They follow the same electrophysiological patterns as seizures *in vivo* and in patients but cannot be fully confirmed to be seizures due to the inability to visualise the behavioural aspects of the seizure. Similar to the process of epileptogenesis, inflammation is also recreated from

the trauma of slicing. Slicing was found to induce interictal and ictal discharges, chronic activation of astrocytes and microglia and release of pro-inflammatory cytokines throughout the 21 day culture period. Cell death peaked immediately after slicing, and later on, coinciding with SLEs. The anticonvulsants phenytoin or kynurenic acid blocked the SLEs but did not affect epileptogenesis progression (Berdichevsky et al., 2012). This highlights the similarities that the organotypic model has with epileptogenesis in patients, with the slicing providing the insult required to trigger the process. The spontaneously developing seizure activity in OHSCs was found not to be dependent on culture medium amino acid composition (Liu et al., 2017). However, it was discovered that cultures gradually deprived of serum in the growth medium developed spontaneous epileptiform activity whereas cultures incubated with serum-containing medium did not (Magalhães et al., 2018). It is important to be aware that organotypic cultures may display some inherent excitability and inflammation compared to an unsliced brain *in vivo*, particularly when grown in culture for long periods of time. As other groups have observed, this can be very useful for studying epileptogenesis and screening new epilepsy drugs (Albus et al., 2012; Berdichevsky et al., 2012; Magalhães et al., 2018)

1.3.1 Types of organotyic epilepsy models

Epileptiform activity has been induced in OHSCs following direct stimulation by various methods. The first of these discussed is when OHSCs are exposed to Mg^{2+}-free ACSF. Similar to the effects of epilepsy observed in patients and animal models, SLEs induced by Mg^{2+} -free ACSF in OHSCs also cause neuronal Ca^{2+} influx, hippocampal cell death, mitochondrial damage and dysfunction, and increased nitric oxide synthase (NOS) and reactive oxygen species (Heinemann et al., 2002a; Heinemann et al., 2002b; Kovács et al., 1999). Anti-epileptic drugs failed to prevent low Mg^{2+}-induced SLEs in over 93% of OHSCs, irrespective of donor age or time in culture (Albus et al., 2008), demonstrating the power of the Mg^{2+} model to replicate drug-resistant epilepsy.

Repetitive electrical stimulation can also be used to trigger epileptiform activity, similar to kindling *in vivo*. It is shown to be associated with a depression of GABA-ergic inhibition (Thompson and Gähwiler, 1989). In contrast to the low Mg^{2+} model, anticonvulsants prevented SLEs following high frequency stimulation. This

demonstrates repetitive stimulation in OHSCs to serve as a suitable model for screening antiepileptic drugs. The reasons for the difference in pharmacoresistance across model types are unknown but are likely due to differences in epileptogenic mechanisms within the cells and network between models (Albus et al., 2012; Berdichevsky et al., 2016; Prasad Tripathi and Ayyannan, 2017; Wahab et al., 2010).

As used commonly *in vivo*, chemoconvulsants can be used *in vitro* through direct exposure of OHSCs to media containing the drug. Pilocarpine induced SLEs and loss of dendritic spines in OHSCs (Müller et al., 1993), but only mild neuronal death (Poulsen et al., 2002; Thomas et al., 2005). Pilocarpine induces mossy fiber sprouting and suppression of excitatory currents in OHSCs through group II metabotropic glutamate receptor subunits (Thomas et al., 2005). BDNF and neuropeptide Y increase is also observed (Poulsen et al., 2002), reflecting observations in epilepsy patients. Similarly, the $GABA_A$ receptor antagonists bicuculline and picrotoxin are often used in epilepsy models, and application to OHSCs leads to interictal bursting, hippocampal degeneration and loss of dendritic spines (Drakew et al., 1996; Scanziani et al., 1994; Thompson, 1993), demonstrating their relevance to epilepsy in the clinic. Kainate is probably the most commonly used chemoconvulsant *in vivo* but is also frequently used to induce SLEs in OHSCs. Reversible epileptiform activity without neuronal damage is observed following 1µM kainate whereas 5µM kainite causes irreversible epileptiform activity with neuronal damage in OHSCs, highlighting the close association between seizure activity and neuron death (Benedikz et al., 1993). Mossy fiber sprouting has also been observed in response to kainate application in OHSCs (Routbort et al., 1999), contributing to hyperexcitability in granule cells (Bausch and McNamara, 2004).

OHSCs are commonly used to model epilepsy through techniques mirroring *in vivo* epilepsy models. High frequency stimulation reflects *in vivo* kindling, while chemoconvulsant applications produce the same physiological responses as injection *in vivo*. The true relevance of culturing in low Mg^{2+} media is unclear as this does not reflect the brain's natural environment. Epilepsy models can also be produced from OHSCs taken from animals which have undergone the kindling process or had SE induced from injected chemoconvulsants. OHSCs provide the advantage of a large number of slices for experiments while minimising animal use, which can be

manipulated in culture with ease. They therefore deliver a convenient experimental platform between cell culture and *in vivo* research.

1.4 Neuronal Kv7 Channels

Two target genes of REST which are particularly relevant for epilepsy are *KCNQ2* and *KCNQ3*, encoding Kv7.2 and Kv7.3 proteins, respectively, which compose the Kv7.2/7.3 tetrameric neuronal 'M channels'. Mutations in the genes *KCNQ2* and *KCNQ3* are associated with Benign Familial Neonatal Convulsions (BFNC) and Epileptic Encephalopathy; epileptic syndromes affecting neonates and infants (Cooper and Jan, 2003). Furthermore, Kv7 channel opening drugs such as Retigabine are powerful antiepileptics. Together this suggests Kv7 channel disregulation could be implicated in general epileptogenic mechanisms.

Kv7 channels are a type of voltage-gated K^+ channel composed of subunits Kv7.1-Kv7.5, with Kv7.2-Kv7.5 expressed in the nervous system (Wang et al., 1998). They are found throughout the central and peripheral nervous systems, including pyramidal neurons in the human cortex and hippocampus (Cooper et al., 2000). Kv7.1 is the only Kv7 channel subunit not expressed in the brain. Kv7.1 is expressed in the heart, where mutations can cause long QT syndrome, affecting heartbeat regulation. Kv7.4 is mostly expressed in sensory cells in the cochlea, with low expression in the brain. Kv7.2 and Kv7.3 subunits are localised to the axon initial segment (AIS) of neurons by the organising scaffold protein ankyrin-G (Cooper, 2011; Devaux et al., 2004; Pan et al., 2006), and their localisation is critical for their function (Shah et al., 2008). The tetrameric subunits composing neuronal Kv7 channels are usually heteromers of Kv7.2 and Kv7.3 (Hadley et al., 2003), though Kv7.2 homomers can also form (Schwarz et al., 2006). Kv7.2 is understood to be the most important for channel function. Knocking out *Kcnq2* from cortical pyramidal neurons in mice abolishes the M-current and causes seizure-like behaviours and early death, whereas *Kcnq3* knockout mice live into adulthood with no signs of seizure activity (Soh et al., 2014). The Kv7 channel is also termed the 'M' channel due to its original discovery as propagating the 'M' current (or Kv7 current), which is suppressed by M1 muscarinic receptor activation. The Kv7 current is a steady outward rectifying current of K^+ ions from the cell, discovered in 1980 by Brown and colleagues (Brown and Adams, 1980; Constanti and Brown, 1981). The Kv7 current is active at subthreshold potentials and

does not inactivate, giving it control over the resting membrane potential and helping to prevent neuronal hyperexcitability. It slowly activates at a threshold near resting membrane potential, and slowly deactivates afterwards. Action potentials cause an enhancement of Kv7 current (Kirkwood and Lisman, 1992).

Each neuronal Kv7 channel subunit has 6 transmembrane domains and a P loop acting as a selectivity filter, as well as intracellular N and C-terminal domains (Figure 1.2). Segments 1-4 (S1-S4) act as a voltage sensing domain, and S5 and S6 create the pore structure which interlocks with the S5 and S6 domains from the other 3 subunits. The long C-terminal is necessary for the localisation of the subunit to the plasma membrane (Schwake et al., 2000), as well as binding of different ligands such as phosphatidylinositol 4,5-bisphosphate (PIP_2), calmodulin and protein kinase C. The voltage sensing domain contains a helix containing basic residues that spans the membrane and shifts position. The S4-S5 linker relays the effects of this conformational change to the pore region. The shift of the S4 segment is stabilised by acidic residues in S1 and S2. Once the pore is open, K^+ ions move through the pore. Oxygen atoms in the carbonyl backbone of glycine residues in the selectivity filter form a 'psuedo-hydration shell' that allows K^+ ions through but not other ions such as Na^+ (Abbott, 2020).

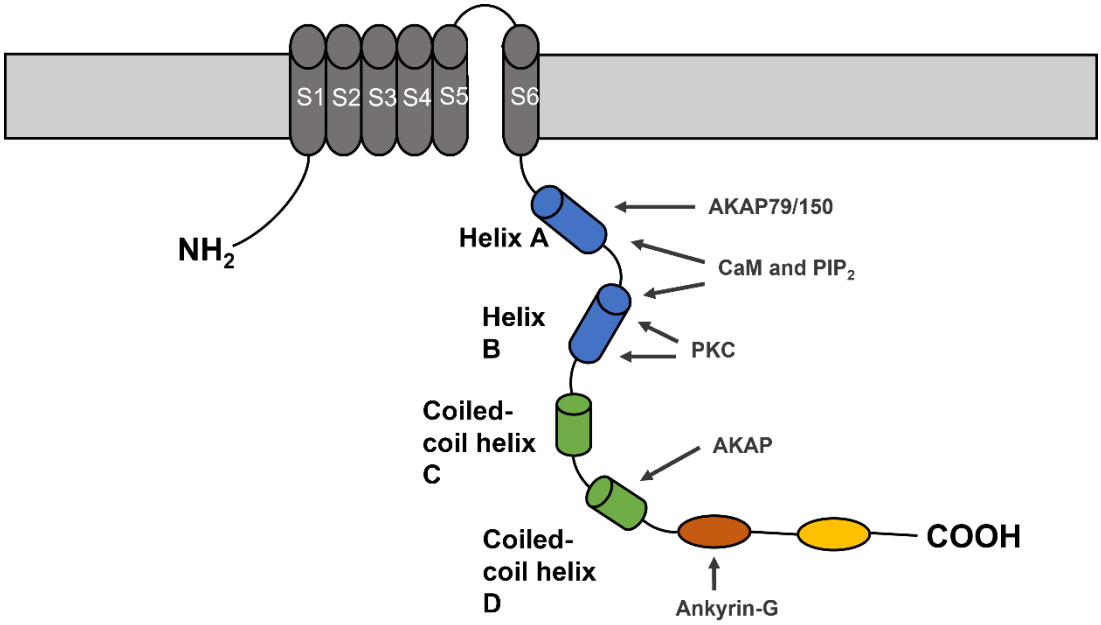

Figure 1.2. Kv7 channel subunit structure and ligand binding sites. Each Kv7 subunit contains 6 transmembrane domains (S1-S6). Between S5 and S6 is a P-loop. The long intracellular C-terminal domain has 2 helix domains and 2 coiled-coil helix domains. AKAP79/150 binds to helix A. Calmodulin (CaM) and PIP_2 bind to helix A and helix B. Protein kinase C (PKC) binds at two different sites on helix B. AKAP binds to coiled-coil helix D, and ankyrin-G binds near the C-terminal region.

1.4.1 Kv7 channels in the hippocampus

Kv7 current was first identified in hippocampal pyramidal neurons in 1982 (Halliwell and Adams, 1982). Kv7.2-7.5 channel subunits are found in the soma and dendrites of CA1 and CA3 hippocampal pyramidal neurons (Hu et al., 2007; Klinger et al., 2011; Shah et al., 2002). Kv7 channels are particularly important for regulating excitability of hippocampal CA1 pyramidal neurons, due to their regulation of resting membrane potential and action potential threshold (Shah et al., 2008). Here they activate during spike afterdepolarisation and prevent the spike from becoming a burst of action potentials (Yue and Yaari, 2004). They have also been shown to regulate the interspike interval in hippocampal interneurons (Lawrence et al., 2006). Interestingly, muscarinic stimulation has been shown to activate two different pathways of modulation for Kv7 in the hippocampus depending on cell type. CA1 pyramidal neurons undergo Kv7 current suppression due to PIP_2 depletion in response to muscarinic stimulation, similar to the mechanism previously outlined in peripheral ganglia. However, in dentate gyrus granule cells, muscarinic stimulation enhanced

Kv7 current due to a PIP_2 increase (Carver and Shapiro, 2019). During seizures, the opioid peptide dynorphin A is released in the dentate gyrus granule cells of the hippocampus where it counteracts hyperexcitability through activation of kappa opioid receptors (Simonato and Romualdi, 1996). This activation of opioid receptors appears to enhance Kv7 current in CA3 pyramidal neurons (Madamba et al., 1999), suggesting a neuroprotective function of Kv7 channels to prevent further hyperexcitability.

1.4.2 Mutations in *KCNQ2* and *KCNQ3* are associated with neonatal and infantile epilepsies

Although the link between *KCNQ* genes and common forms of epilepsy are unclear, *KCNQ2* and *KCNQ3* mutations are known to be responsible for neonatal epilepsies such as BFNC and neonatal-onset developmental and epileptic encephalopathy (DEE). BFNC is a rare autosomal dominant idiopathic neonatal epilepsy syndrome causing spontaneous clonic seizures, occurring between 3 days and 3-10 weeks after birth, followed by remission. It is characterised by brief multifocal seizures involving various body parts. There are around 10 BFNC-causing mutations in *KCNQ2*, and two in *KCNQ3*. *KCNQ2* was first identified as the major gene suffering C-terminal mutations in BFNC (Biervert et al., 1998; Singh et al., 1998). Despite spontaneous remission in most, around thirty-one percent of those with *KCNQ2* mutations continue to have seizures after 6 months of age (Grinton et al., 2015), and 16% of infants with BFNC develop seizures later in life (Ronen et al., 1993). BFNC is associated with around a 25% loss in potassium current (Schroeder et al., 1998), and is genetically heterogeneous (Ryan et al., 1991). BFNC affects only around 1 in 100,000 people. However, having a genetic basis makes them a popular target of research as they could help understanding of idiopathic epilepsies, which account for a large proportion of temporal lobe epilepsy cases. Individuals with a genetic vulnerability to seizures may develop epilepsy after a precipitating environmental trigger such as a brain injury. This could also account for the 16% of BFNC patients who go on to develop adult epilepsy (Rogawski, 2000). BFNC is usually inherited as *KCNQ2* mutations from one of the parents in an autosomal dominant manner. It results in a heterozygous missense or frameshift in random places or deletions of an exon or the whole gene (Goto et al., 2019).

In addition to BFNC, heterozygous mutations in *KCNQ2* and *KCNQ3* can give rise to DEE, which involves developmental delay, intellectual disability and autism. Interestingly, twenty-five to thirty percent of people with an autism spectrum disorder also have epilepsy. DEE occurs between a few weeks after birth and somewhere between 9 months and 4 years old, and involves daily seizures which are pharmacoresistant and associated with developmental impairment. *KCNQ2* mutations are responsible for around 13% of unexplained DEE cases (Weckhuysen et al., 2013). In contrast to BFNC, *KCNQ2* mutations causing DEE are always *de novo* and usually a missense variant occurring in or around the S6 domain, which is essential for channel activity (Goto et al., 2019; Millichap et al., 2016).

Similar to BFNC, loss of function mutations are also commonly responsible for DEE, through various effects. It seems that missense loss of function mutations may cause DEE through a double effect of reducing Kv7.2 expression at the plasma membrane, while also inhibiting Kv7 voltage-sensing ability. (Abidi et al., 2015; Orhan et al., 2014). Frameshift mutations are also capable of causing BFNC and DEE, usually resulting in premature mRNA termination (Goldberg-Stern et al., 2009; Lauritano et al., 2019). The greater effects of frameshift mutations on the mRNA transcript compared to missense mutations can be predicted to lead to an overall loss of expression of *KCNQ2* in most cases.

It has been suggested that remission of *KCNQ*-linked neonatal seizures is linked to reduction of Kv7 channel activity and switching of the GABAergic system from excitatory to inhibitory during development (Okada et al., 2003). The GABAergic switch occurs as the Cl^- ion transporter KCC2 increases in expression (Rivera et al., 1999). Another factor could be that over time in development, other Kv7 subunits compensate for the *KCNQ2* mutations. The mutations in *KCNQ2* cause small reductions in potassium current early in life when *KCNQ2* expression is low, but later in development *KCNQ2* expression in the brain increases, so the child would not be so sensitive to the mutation (Weber et al., 2006). There is also a *KCNQ2* splice variant which is prominent in fetal brain and dampens potassium currents of channels it incorporates into (Smith et al., 2001), which could contribute to neonatal-specific hyperexcitation.

1.4.3 Animal models of epilepsy induced by mutations in *Kcnq2* and *Kcnq3*

To investigate the mechanisms behind BFNC and DEE and elucidate further the roles of *KCNQ2* and *KCNQ3* in epileptic syndromes, research groups have developed animal models studying the effects of *KCNQ2* and *KCNQ3* mutations. Modelling BFNC and DEE, mice with heterozygous *KCNQ2* and *KCNQ3* mutations had increased sensitivity to electrically-induced seizures. Homozygous mice for these mutations had neonatal seizures associated with reduced Kv7 current, neuronal plasticity and increased neuropeptide Y in hippocampal granule cells, but without neuron death or mossy fiber sprouting (Singh et al., 2008). Full homozygous *KCNQ2* knockout mice die due to pulmonary problems, but heterozygous knockouts showed seizures and hypersensitivity to the chemoconvulsant PTZ, associated with reduced *KCNQ2* expression (Tomonoh et al., 2014; Watanabe et al., 2000). Similarly, another group conditionally deleted *KCNQ2* from pyramidal cortical neurons. This led to neuronal hyperexcitability with decreased medium afterhyperpolarisation and a longer afterdepolarisation, and mice showing seizure behaviours and dying at the third week of life. In contrast, mice with *KCNQ3* deletion lived to adulthood, suggesting Kv7.2 to be more critical for pyramidal neuron function than Kv7.3 (Soh et al., 2014). This demonstrates how critical Kv7.2 channels are in stabilising membrane excitability. To block Kv7 function in the brain while avoiding the fatal heart problems in development, mice were created to express conditional dominant negative *KCNQ2* subunits in the brain. These mice showed suppressed Kv7 current, spontaneous seizures and memory deficits with hippocampal changes. Pyramidal neurons showed hyperexcitability, as well as reduced intrinsic subthreshold theta resonance, medium afterhyperpolarisation and spike-frequency adaptation (Peters et al., 2005). Ganglia from *KCNQ2* heterozygous mutant mouse embryos showed a 30% reduction of *KCNQ2* mRNA expression along with 60% reduction of Kv7 current, but also had a 40-50% increase in expression of *KCNQ3* and *KCNQ5* (Robbins et al., 2013). The increase in *KCNQ3* and *KCNQ5* expression may suggest a compensatory mechanism to maintain levels of Kv7 channels at the plasma membrane. However, as current from Kv7.3 and Kv7.5 subunits is lower than Kv7.2 homomers or Kv7.2/7.3 heteromers the current is unable to be compensated with increased expression of these channel subunits. Collective data from these studies demonstrates the clear importance of fully functional neuronal Kv7 channels in preventing hyperexcitability and seizures. The

variations in severity of effects observed in the mice across the different studies may be reflective of the strength of the knockdown method in each case, with the suggestion that no Kv7 current at all could lead to death from excitotoxicity in the brain early in life. Kv7 mutation studies provide understanding about BFNC and DEE, but also highlight that if neuronal Kv7 channels are inhibited or downregulated at any age, this could quickly lead to spontaneous seizures.

1.4.4 Endogenous modulation

In addition to being voltage gated, Kv7 channel function is regulated by intracellular signalling molecules. Ligands which affect Kv7 channel dynamics include PIP_2, calmodulin, A kinase anchoring protein (AKAP) and protein kinase C (PKC). Kv7 channel function is affected by stimulation of receptors by specific hormones and peptides, such as acetylcholine, bradykinin, angiotensin and substance P. All of these share the commonality that they couple to G_q or G_{11} proteins which activate PLCβ, causing hydrolysis of PIP_2 to inositol triphosphate (IP_3) and diacylglycerol (DAG) (Delmas and Brown, 2005; Haley et al., 2000).

1.4.5 Muscarinic suppression of Kv7 current

Kv7 current is suppressed by muscarinic receptor stimulation. This reduction of Kv7 current causes the excitatory effects of acetylcholine on the neuron and increases the likelihood of an action potential (Brown and Adams, 1980; Marrion et al., 1989). Stimulation of muscarinic acetylcholine receptor 1 causes phospholipase C (PLC) hydrolysis of PIP_2 and resulting suppression of Kv7 current in under a minute (Horowitz et al., 2005). Kv7 depends upon PIP_2 binding for channel opening, and PIP_2 dissociation following its hydrolysis causes Kv7 channel closure (Suh et al., 2006). PLC hydrolyses PIP_2 to inositol triphosphate (IP_3) and diacylglycerol (DAG, Figure 1.3). The IP_3 diffuses away from the membrane and the DAG binds and activates a complex of AKAP and PKC, allowing PKC to phosphorylate and further deactivate Kv7 (Suh and Hille, 2007). PKC contributes to but is not essential for muscarinic suppression of Kv7 current (Bosma and Hille, 1989). Activation of PKC causes it to phosphorylate serine residues in Kv7 via the scaffold protein AKAP (Bal et al., 2010; Hoshi et al., 2010; Hoshi et al., 2003). However, AKAP also mediates an increase in KCNQ2 and KCNQ3 mRNA expression in response to acetylcholine-stimulated neuronal activity in DRG neurons (Zhang and Shapiro, 2012), which may work as a

protective mechanism to counteract the reduction in Kv7 function mediated by PLC and PKC.

Interestingly, in addition to its Kv7 deactivation effects, muscarinic stimulation also induces transport of Kv7.2 and Kv7.3 homomers to the surface membrane, through binding of α and β-tubulin and collapsing response mediator protein 2 (CRMP-2) to the translocation domain on the N-terminal of the channel (Jiang et al., 2015). CRMP-2 is reduced in epilepsy, and after neurotoxin exposure *in vitro* and traumatic brain injury in rat hippocampus (Zhang et al., 2007). Furthermore, CRMP-2 knockdown by siRNA decreased viability in neurons (Na et al., 2017). The reduction of cell surface expression of Kv7 could be initiated by glutamate via PKC and Ca^{2+} (Li et al., 2015), as a component of excitotoxicity. This highlights the possibility that in epilepsy patients, there may be a reduced number of Kv7 channels at the surface membrane due to glutamate, but also due to an inability of CRMP-2 to traffic Kv7.2 and Kv7.3 homomers, and this could perpetuate excitotoxicity and contribute to neuronal death. In contrast to reduced surface Kv7 channels, increased expression of muscarinic receptors have been found in the cerebral cortex of the epileptic brain and kindled rats (Anju et al., 2018), suggesting the response to acetylcholine could be further heightened through stronger Kv7 current suppression.

Suppression of Kv7 current has been shown to mediate muscarinic-induced stimulation of glutamatergic transmission along the Schaffer collateral from CA3 to CA1 pyramidal neurons, through depolarisation and activation of voltage gated Ca^{2+} channels (Sun and Kapur, 2012). The Kv7 channel opener NH6 (a novel derivative of N-phenylanthranilic acid) reduced EPSC frequency in CA1 pyramidal neurons while linopiridine increased EPSC frequency, suggesting Kv7 channels inhibit release of glutamate and GABA (Peretz et al., 2007). This demonstrates how increased excitability within a neuron following muscarinic suppression of Kv7 channels can contribute to increased excitability within the hippocampus as a whole.

1.4.6 Bradykinin suppression of Kv7 current

As with muscarinic receptor stimulation, when bradykinin activates the bradykinin receptor, the receptor couples to G_q or G_{11} proteins, causing hydrolysis of PIP_2 to IP_3 and DAG by PLC (Figure 1.3). However, bradykinin receptors are located closer to the IP_3 receptors on the endoplasmic reticulum. This allows activation of the IP_3

receptors by IP_3, which triggers release of Ca^{2+} from the endoplasmic reticulum. The Ca^{2+} binds to calmodulin, which induces closure of the Kv7 channels. Bradykinin also stimulates PIP_2 synthesis by PI_4 kinase so no overall reduction in PIP_2 is observed (Delmas and Brown, 2005). Calmodulin is able to bind to subunits Kv7.2, Kv7.4 and Kv7.5 but not Kv7.1 or Kv7.3 due to the presence or absence of a calmodulin binding site in the C-terminal sequence (Gamper et al., 2005). In contrast to its effects upon Kv7 activity at the plasma membrane, calmodulin is also required for Kv7 trafficking, and stabilising its open state. The initial binding of Kv7.2 to calmodulin in the ER is dependent on Ca^{2+}. Mutations in helix A of Kv7.2 (R353G and L339R) cause BFNC by inhibiting the stability of the 'active' Kv7.2-calmodulin complex. The mutation prevents Kv7.2 from exiting the ER, leading to fewer channels at the plasma membrane (Alaimo et al., 2009; Etxeberria et al., 2008). The L351V, L351F, Y362C and R553Q mutations were also found to cause alterations in calmodulin binding affinities, to varying degrees, and can also cause BFNC (Ambrosino et al., 2015). Therefore calmodulin has a complex role in modulation of Kv7 channels, being necessary for its expression, allowing Kv7 current, but also necessary for its suppression via bradykinin (Zhou et al., 2016).

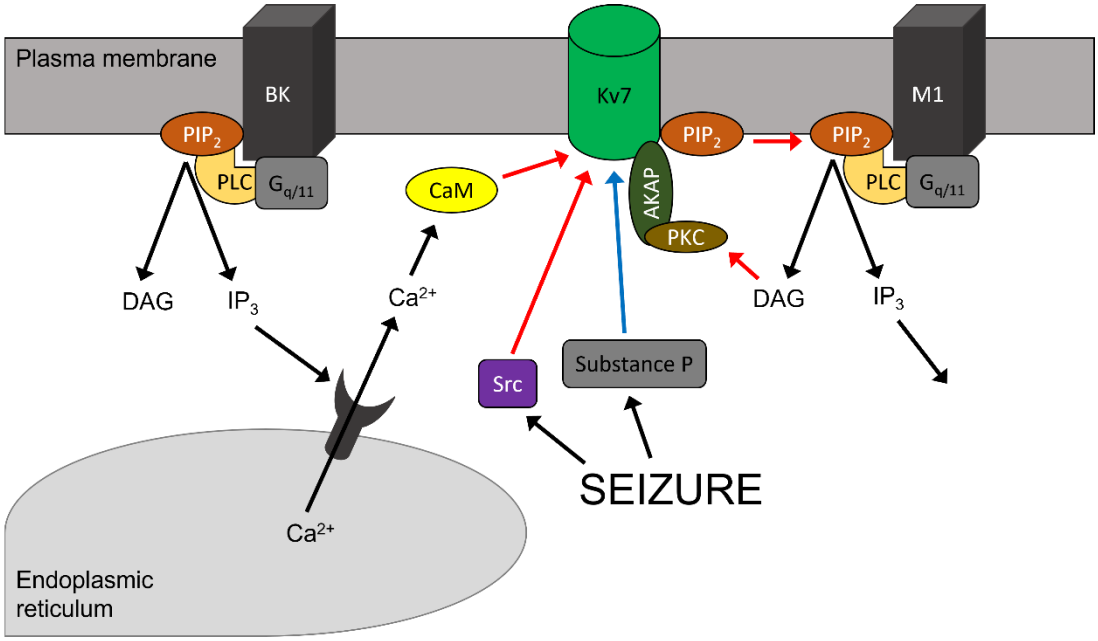

Figure 1.3. Regulation of gating of Kv7 channels. Kv7 channels may be activated (blue arrow) or deactivated (red arrows) by intracellular signalling. Stimulation of muscarinic receptors (M1) or bradykinin receptors (BK) causes phospholipase C (PLC) to hydrolyse PIP_2 into diacylglycerol (DAG) and inositol triphosphate (IP_3). Hydrolysis of PIP_2 by muscarinic receptor stimulation leads to dissociation of DAG and local depletion of PIP_2 near the Kv7 channel, causing PIP_2 to unbind from the Kv7 channel and initiating its closure. DAG binds to a complex of protein kinase C (PKC) and AKAP, which causes Kv7 deactivation. IP_3 produced through bradykinin receptor stimulation activates IP_3 receptors on the endoplasmic reticulum membrane, which then release Ca^{2+}. Ca^{2+} binds to calmodulin (CaM) which causes Kv7 deactivation. Seizures activate Src tyrosine kinase, which cause Kv7 deactivation, and substance P, which causes Kv7 activation.

1.4.7 Other modulators of Kv7 function

In addition to the common muscarinic and bradykinin receptor deactivation of Kv7 channels, other endogenous mechanisms are capable of regulating them directly during seizure. The tyrosine residues in Kv7 channels can be phosphorylated by Src tyrosine kinases which suppress current from Kv7.3, Kv7.4 and Kv7.5 subunits and Kv7.2/7.3 heteromers (Gamper et al., 2003), independently of G-protein modulation pathways (Li et al., 2004b). The function of Kv7 modulation by Src is currently unclear, but Src levels are increased during epileptiform activity in the hippocampus, and epileptiform activity can be prevented by the Src inhibitor 4-amino-5-(4-

chlorophenyl)-7-(*t*-butyl)pyrazolo[3,4-d]pyrimidine (PP2)(Sanna et al., 2000). This suggests Src may be involved in the pathogenesis of epileptogenesis. The neuromodulator substance P is also increased during epilepsy and is believed to contribute to the disorder. Its mechanism of action is not clear, but may involve alterations to NMDA channels and inwardly rectifying K^+ currents (Chi et al., 2018). Unlike Src, substance P enhances Kv7 current (Lin et al., 2012), which may act as a neuroprotective mechanism, contrary to its greater overall pro-epileptic role.

1.4.8 Drugs, metabolites and plants that enhance neuronal Kv7 current

Due to the role of Kv7 channels in regulation of neuronal excitability, Kv7 channel openers have been investigated for their use as anti-epileptic medications. The most well known Kv7 channel opener is retigabine. Retigabine is an antiepileptic medication initially discovered to have strong seizure-suppressant effects in rat and mouse models of seizures induced electrically, and by pentylenetetrazole, picrotoxin and NMDA (Rostock et al., 1996). This effect was found to work through opening Kv7.2/7.3 channels (Rundfeldt and Netzer, 2000; Wickenden et al., 2000). Retigabine significantly reduced seizure frequency in patients who were refractory to treatment (Porter et al., 2007). It negatively shifts the voltage dependence of activation (Main et al., 2000) and increases the mean maximal open probability of Kv7.2/7.3 channels, producing a hyperpolarising shift of voltage dependence (Tatulian and Brown, 2003). Retigabine acts on Kv7.2-5 subunits, but not Kv7.1. Kv7.3 subunits are most sensitive to retigabine, followed by Kv7.2/7.3 heteromers, and then Kv7.2 and Kv7.4 (Tatulian et al., 2001). A conserved Trp residue (W265 in KCNQ3) in the S5 domain was found to be critical for the effects of retigabine (Schenzer et al., 2005). Trp236 in S5 and Gly301 in S6 were also found to be crucial to retigabine's effect (Wuttke et al., 2005). It is understood that Kv7 channel defects only account for certain types of neonatal epilepsies, yet retigabine's anti-seizure activity in the broad spectrum of adult epilepsies occurs through its opening of Kv7 channels. Though it does not treat the underlying cause of the epilepsy, its ability to shift the voltage dependence of activation of Kv7 channels to a more negative potential allows more channels to be open at resting membrane potential. This increases Kv7 current, protecting against hyperexcitability (Brown and Passmore, 2009). However, it does not act directly on the voltage sensing domain; instead it stabilises the S4-S5 link in an open position (Delmas and Brown, 2005). Retigabine has also been shown to be effective in reducing

seizures and cell death after traumatic brain injury (Vigil et al., 2020). However, despite retigabine's potency with opening Kv7 channels and blocking seizure, it had to be removed from the market due to side effects caused by a lack of specificity to neuronal Kv7.2/3 channels. The Trp residue so essential for retigabine binding has also recently been discovered to be the site for binding of endogenous molecules such as γ-aminobutyric acid (GABA), γ-amino-β-hydroxy-butyric acid (GABOB) and β-hydroxybutyric acid (BHB)(Manville et al., 2018, 2020). Although the full implications of GABA and GABA analogues binding to Kv7 channels are not yet fully understood, it highlights the potential for GABA modulation in Kv7 channel opening for therapeutic use in epilepsy.

Due to retigabine's lack of specificity for Kv7.2 and Kv7.3 subunits and its concurrent activation of GABA channels, other compounds have been investigated for their Kv7-opening qualities. ICA-27243 [N-(6-chloro-pyridin-3-yl)-3,4-difluoro-benzamide], ICA-105665, and ICA-069673 are potent and selective Kv7.2/7.3 channel openers which have shown efficacy against induced epileptiform activity *in vivo* (Kasteleijn-Nolst Trenité et al., 2013; Roeloffs et al., 2008; Wang et al., 2017). SCR2682 was recently developed and validated as a potent selective neuronal Kv7 channel opener, acting upon Trp 236 to negatively shift the voltage dependence of activation (Zhang et al., 2019). The antiepileptic drug gabapentin has also recently been shown to activate Kv7.3 homomers and Kv7.2/7.3 heteromers, in addition to its more well known mechanism of inhibition upon voltage gated Ca^{2+} channels (Manville and Abbott, 2018b). Another opener of Kv7 channels is N-ethylmaleimide (NEM); a cysteine-modifying alkene compound (Li et al., 2004a). The antiepileptic drug valproic acid exerts its mechanism of action in a few ways (Rahman and Nguyen, 2021). It has been shown to maintain Kv7 current indirectly, preventing muscarinic-induced Kv7 current suppression by inhibiting palmitoylation of AKAP79/150 (Kay et al., 2015). AKAP which is not palmitoylated will prevent PKC from phosphorylating and deactivating Kv7 following muscarinic receptor stimulation. In a similar method to valproic acid, palmitoylation of AKAP may be prevented by dietary intake of medium chain fatty acids in the ketogenic diet. Therefore inactivation of AKAP-PKC may enhance Kv7 current as a means of stabilising excitability during seizures for people following the ketogenic diet, contributing to its benefits (Hoshi, 2020). Another mechanism of the ketogenic diet may be through creation of β-

hydroxybutyric acid (BHB), which binds to Kv7 channels (Manville et al., 2018, 2020). BHB levels correlated with seizure control in children (Gilbert et al., 2000), so the ketogenic diet may gain some of its antiepileptic effects through BHB enhancement of Kv7.2/7.3 current.

Recently certain plant metabolites have been found to affect Kv7 channels. Cilantro (Coriandrum sativum) extract activated Kv7.2/7.3 channels, negatively shifting their voltage dependence of activation. The cilantro metabolite E-2-dodecenal was discovered to have the same effect when used at 100μM (Manville and Abbott, 2019). In addition to cilantro, mallotoxin and isovaleric acid were found to act synergistically to open Kv7.2/7.3 channels (Manville and Abbott, 2018a). Previously mallotoxin alone was observed to have no effect on Kv7.2/7.3 currents (Matschke et al., 2016), suggesting both compounds are necessary. Furthermore, the combination of mallotoxin and isovaleric acid reduced PTZ-induced seizures in mice, highlighting the potency of these two compounds combined as they are in the *Mallotus oppositifolius* plant. When the two compounds were combined with retigabine, Kv7.2/7.3 channels remained open even at -120mV, suggesting potential for a combined therapy with reduced side effects (Manville and Abbott, 2018a).

Due to the well understood role of neuronal Kv7.2/7.3 channels in excitability and seizure control, many groups are investigating specific channel openers as a new class of antiepileptic drugs. Forty-two compounds were recently tested for efficacy as Kv7 channel activators, compared to retigabine (Ostacolo et al., 2020). Work from the Abbott group highlights the potential of certain plant metabolites in opening Kv7 channels which may have been overlooked so far, and may allow for smaller doses of drugs like retigabine in a combined therapy approach. Certain mutations cause neonatal epilepsies through reducing the transcriptional expression of Kv7.2/7.3 channels or their localization to the plasma membrane. *KCNQ2/3* expression is an area which has lacked investigation compared to the research done on Kv7.2/7.3 channel function and modulation. However, it should not be overlooked, as new types of biotherapeutics such as gene therapy may be better able to target neuronal Kv7.2/7.3 channels, upregulating their expression in specific neuronal types or brain regions, preventing the types of off-target side effects occurring from more traditional Kv7 channel openers such as retigabine. Such biotherapeutics could heal the cause of

neonatal epilepsies, and provide more tolerable and efficacious treatments for a majority of epilepsy sufferers.

1.4.9 Regulation of Kv7 channel expression in epilepsy

While research into neuronal Kv7 channel function has been vast and thorough, far less is known about the mechanisms regulating transcriptional expression levels of Kv7 channels. In pilocarpine and PTZ models of epilepsy, *Kcnq2* but not *Kcnq3* mRNA was found to increase in the CA1 and CA3 pyramidal neurons, but not in dentate gyrus granule cells. Accordingly, Kv7 current amplitude was increased in CA1 pyramidal neurons in brain slices from the epileptic model animals, but remained the same in dentate gyrus granule cells. Furthermore, traumatic brain injury caused an increase in *Kcnq2* expression in the hippocampus ipsilateral to the injury (Carver et al., 2020). In contrast, Maslarova and colleagues observed reduced Kv7.2 and Kv7.3 protein in the entorhinal cortex of rats with pilocarpine-induced seizures (Maslarova et al., 2013). While it seems likely that mRNA and protein expression would follow similar patterns, the observed differences could reflect true differences in sublocations within the hippocampus, or could be affected by timing. The observed differences in Kv7 expression between the dentate gyrus and the CA1 and CA3 regions following pilocarpine (Carver et al., 2020) are likely due to principal neuron type (pyramidal neurons in the CA1 and CA3, and granule cells in the dentate gyrus). The principal cells in the entorhinal cortex are pyramidal neurons and stellate cells, so it is difficult to compare studies. Maslarova and colleagues also prepared brain slices after 3 Racine scale 4-5 seizures, while Carver and colleagues waited 48 hours after seizure to prepare their brain slices. If Carver and colleagues prepared their slices further into the epileptogenic process than Maslarova and colleagues, findings could represent an overall initial decrease followed by an increase in Kv7.2/7.3 in the hippocampus and entorhinal cortex.

In addition to changes in *KCNQ2* and *KCNQ3* gene expression and Kv7.2 and Kv7.3 protein expression following brain insults and seizures, mechanisms controlling expression of *KCNQ2* and *KCNQ3* by transcription factors have been outlined. In 2010 Mucha and colleagues discovered that the *KCNQ2* and *KCNQ3* genes are negatively regulated by the transcription factor REST, and positively regulated by the transcription factor Specificity protein 1 (SP1) (Mucha et al., 2010). A DNase I

hypersensitivity assay identified putative transcription factor binding sites which were proposed through bioinformatic analysis to be binding sites for Sp1 and REST. Binding of Sp1 and REST to the promoters of the *KCNQ2* and *KCNQ3* genes was confirmed by gel mobility shift assays and luciferase assays in SH-SY5Y cells. Luciferase activity was heavily reduced in the presence of the Sp1 binding inhibitor mithramycin A. Mithramycin also blocked *KCNQ2* and *KCNQ3* gene expression by 90% in dorsal root ganglia (DRG) neurons, and reduced Kv7.2 protein expression in SH-SY5Y cells. Kv7 current and Kv7.2 immunoreactivity was also significantly enhanced in DRG neurons transfected with an *Sp1* expression plasmid. Infection of DRG neurons with adenovirus driving *REST* expression induced a repression of *Kcnq2* and *Kcnq3* mRNA expression, compared to no observed effect from adenovirus lacking *REST* modulation. Kv7 current in small TRP1-positive DRG neurons infected with adenovirus driving *REST* overexpression was reduced to 14% that of small TRP1-positive neurons infected with adenovirus lacking *REST* modulation, or non-infected neurons from the same dish, demonstrating REST's repressive effects on *Kcnq2/3* in the DRG. REST overexpressing cells also showed increased likelihood of action potential firing following a 400pA current injection from a -65mV baseline membrane potential, likely as as a result of repressed Kv7 channel function. Kv7 current and Kv7.2 immunoreactivity was also observed to be reduced in DRG neurons grown in inflammatory conditions (Mucha et al., 2010). Repression of *Kcnq2* by upregulated levels of REST was demonstrated in a partial sciatic nerve ligation neuropathic pain model in the DRG (Rose et al., 2011). However, the repression of *KCNQ2* and *KCNQ3* by REST in epilepsy has not been investigated.

The Sp1-mediated enhancement of *KCNQ2* and *KCNQ3* expression and the Kv7 current would be expected to reduce neuronal excitability. Hippocampal Sp1 activity is increased following kainate-induced seizures, but this is proposed to contribute to epileptogenesis through upregulation of the proconvulsive opioid peptide enkephalin (Bing et al., 1997; Feng et al., 1999). Sp1 has also been shown to enhance expression of lncRNA small nucleolar RNA host gene 1 (SNHG1) and P2X purinoceptor 7 (P2RX7), which are both upregulated in epilepsy, driving inflammation and neuronal injury (Engel et al., 2017; Zhao et al., 2020). Sp1-mediated gene activation and REST-mediated repression are demonstrated to act as opposing regulatory forces upon a selection of shared target genes (Formisano et al., 2015b; Paonessa et al., 2013; Yuan

et al., 2013). In addition, REST can bind the Sp1 protein and repress its activity (Plaisance et al., 2005), and Sp1 has been reported to bind to the *Rest* promoter and upregulate it (Formisano et al., 2015a). However, Sp1 also enhances expression of huntingtin (Wang et al., 2012), which is responsible for sequestering REST in the cytoplasm (Zuccato et al., 2003). The close relationship between Sp1 and REST may behave as a self-regulatory negative feedback loop, the balance of which may depend on upstream regulatory factors, and influence expression levels of shared target genes such as *KCNQ2* and *KCNQ3*.

In 2012 Zhang and Shapiro identified another transcription factor regulating *Kcnq2* and *Kcnq3*, which was Nuclear Factor of Activated T-cells (NFAT)(Zhang and Shapiro, 2012). The NFAT transcription factors NFATc1-NFATc4 are regulated by Ca^{2+} signalling, and influence neuronal development and axon growth. They noticed increased mRNA expression of *Kcnq2* and *Kcnq3* in rat superior cervical ganglion (SCG) neurons following stimulation with high K^+ or acetylcholine, and increased Kv7 current amplitudes following 48, 60 or 72 hours of stimulation with high K^+. SCG neurons transfected with a constitutively active NFAT mutant had a greater tonic amplitude than control neurons. SCG neurons transfected with NFATc1 or NFATc2 shRNA knockdown showed a blunted Kv7 current response to high K^+, demonstrating NFAT as critical for the induced Kv7 current increase. Imaging showed high K^+ causing endogenous NFATc1 translocation from the cytoplasm to the nucleus. Blockers of the NFAT pathway including cyclosporin A prevented translocation of NFATc1 to the nucleus and increase in Kv7 current amplitude in response to high K^+. Bioinformatic analysis and luciferase reporter assay in PC12 cells identified two NFAT binding sites in both *Kcnq2* and *Kcnq3*, with luciferase luminescence blocked by cyclosporin A. The mechanism was also shown to be dependent on AKAP79/150 and Ca^{2+} increase through local L-type Ca^{2+} channels, which NFAT relies upon for its activation by calcineurin. *In vivo*, an increase in *Kcnq2* and *Kcnq3* mRNA was observed after pilocarpine or kainate-induced seizures, but this effect was not observed in AKAP knockout mice. They propose a mechanism where AKAP79/150 associates with L-type Ca^{2+} channels and forms a complex with calmodulin, calcineurin and PKA. Influx of Ca^{2+} through the Ca^{2+} channels activates calcineurin, which activates NFAT, triggering its translocation from the cytoplasm to the nucleus, where it enhances transcription of *Kcnq2* and *Kcnq3* and as a negative feedback mechanism,

dampening hyperexcitability in a neuroprotective manner. They note that types of NFAT that translocate are likely cell-type specific, as it is NFATc4 which translocates in hippocampal neurons (Oliveria et al., 2007). In support of this mechanism, AKAP knockout in SCG neurons provides mice with protection from pilocarpine-induced seizures by maintaining Kv7 currents (Tunquist et al., 2008).

In summary, transcriptional expression of *KCNQ2* and *KCNQ3* is shown to be repressed by the transcription factor REST and enhanced by the transcription factor Sp1 in peripheral neurons, and enhanced by the transcription factor NFAT in sympathetic neurons. While REST repression of *KCNQ2* in the periphery was confirmed to play a role in neuropathic pain (Rose et al., 2011), transcription factor modulation of *KCNQ2* and *KCNQ3* in the central nervous system has not been investigated. In parallel to peripheral hyperexcitability contributing to chronic pain states, hyperexcitability in the brain leads to seizure and epilepsy. Findings suggest that changes in *KCNQ2* and *KCNQ3* expression occur during epilepsy in the hippocampus, though the exact nature and relevance of these changes is unclear, and may depend heavily on hippocampal region and possibly stages of epileptogenesis. In addition to changes in Kv7 channel gating and expression during epilepsy, its localisation to the plasma membrane may be affected by factors such as reduced levels of CRMP-2, for example (Zhang et al., 2007).

A)

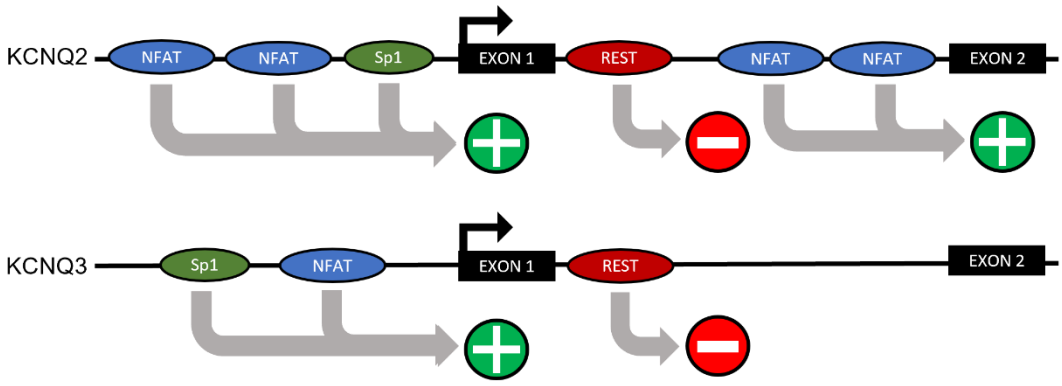

B)

KCNQ2 Sp1 sequence

Human	GGGGCGGGGC
Mouse	CGGGCGGGGC
Rat	CGGGCGTGGG

KCNQ3 Sp1 sequence

Human	GAGGCGGGGC
Mouse	GAGGCGGGGC
Rat	GAGGCGTGGC

KCNQ2 REST sequence

Human	GTCAGGACCATGGCCAG
Mouse	TCCAGGACCATGGTCAG
Rat	TCCAGGACCATGGTCAG

KCNQ3 REST sequence

Human	CTCAGGACCTAGGACAG
Mouse	ATCTGGACCAAGGACAG
Rat	GTCAGGACCTGGGACAG

KCNQ2 NFAT sequence

Rat	AAAGG/CCTTT

KCNQ3 NFAT sequence

Rat	CCTTT

Figure 1.4. Transcription factor binding sites and sequences of the *KCNQ2* and *KCNQ3* genes. ***(A)*** Schematic representations of the promoter and first intron regions of the *KCNQ2* and *KCNQ3* genes. Exons are represented by black boxes and the transcription start site is marked by an arrow. Binding sites for the transcription factors Sp1 (green), NFAT (blue) and REST (red) are represented by elipses. Positions of binding sites are not drawn to scale. ***(B)*** Binding sequences of Sp1, REST and NFAT on the *KCNQ2* and *KCNQ3* genes for human, mouse and rat. NFAT binding sequence for human and mouse *KCNQ2* and *KCNQ3* has not been determined.

1.5 Project aims

While a wealth of data exists on Kv7.2/3 function in control and epileptic models *in vitro* and *in vivo*, understanding of *KCNQ2* and *KCNQ3* gene expression and its regulation is limited. Neuronal Kv7 channels are important for controlling the resting membrane potential and dampening hyperexcitability, and reduced transcriptional expression of Kv7 channels leads to hyperexcitability and seizures (Singh et al., 2008). I have seen that the *Kcnq2* and *Kcnq3* genes are negatively regulated by the transcription factor REST and positively regulated by the transcription factor Sp1 in DRG neurons, and positively regulated by the transcription factor NFAT in SCG neurons. As REST is consistently upregulated following seizures in patients and animal models, this increased REST would be expected to increase repression of *Kcnq2* and *Kcnq3*, as was observed in DRG neurons grown in inflammatory conditions (Mucha et al., 2010). Following seizure, a greater repression of *KCNQ2* and *KCNQ3* would release the brakes on hyperexcitability, potentially contributing to epileptogenesis. Sp1 is upregulated following seizures (Feng et al., 1999) and enhances *Kcnq2* and *Kcnq3* expression, which would dampen hyperexcitability if it were not for the fact that REST represses Sp1 so likely prevents this from happening (Mucha et al., 2010). NFAT upregulates *Kcnq2* and *Kcnq3* in SCG neurons following its translocation from the cytoplasm to the nucleus after Ca^{2+} influx and calcineurin activation of NFAT. This is proposed to act as a negative feedback loop to dampen hyperexcitability and protect against epileptogenesis (Zhang and Shapiro, 2012). Therefore there is evidence of a mechanism for increasing excitability and a mechanism for reducing excitability through transcription factor control of *Kcnq2* and *Kcnq3* in peripheral and sympathetic neurons. An increase in excitability in principal glutamatergic neurons in central brain regions such as the hippocampus would push the networks towards a more epileptic-like state. Therefore it would seem advantageous to investigate the described mechanisms of transcriptional control of *KCNQ2* and *KCNQ3* in the hippocampus for their potential contribution to or protection from epileptogenesis. Epileptogenesis reflects cellular and molecular changes occurring during the 'latent' period in patients between an initial brain insult and the emergence of noticeable seizures. Multifaceted in nature, many components of the process have been identified but details of their interconnectivity and contribution to the whole are yet to be determined. Changes in neuronal transcriptional

expression of *KCNQ2* and *KCNQ3* in response to seizure would be expected to be long-term over days or weeks in animal models or *in vitro*, or months in epilepsy patients, implicating it in the 'latent' phase, contributing to or protecting from epileptogenesis.

In this research I use organotypic hippocampal slice cultures to investigate expression of KCNQ2 and KCNQ3 in normal and epileptic conditions. Whereas previous work has focussed on neuronal cultures, organotypic cultures provide data from living brain tissue. The study begins with development and validation of the organotypic culture system followed by the infection of the organotypic cultures with adenovirus delivering overexpression or functional knockdown of REST, and the observed effects of this upon KCNQ2 and KCNQ3 expression. The levels of KCNQ2 and KCNQ3 are then assessed in epileptic models to enable a deeper understanding of their contribution to epileptogenesis.

Chapter 2

Materials and Methods

2.1 Materials

The Ad-GFP, AdGFP-*REST* and AdGFP-*Rest*-DN viral constructs were previously developed in the Wood lab, University of Leeds (Bruce et al., 2006; Wood et al., 2003). The pcDNA3-GFP-*NFATc3* construct, as well as SH-SY5Y and HEK293 cell lines were provided by the Wood lab. Dr Sylvain Gigout, University of Leeds kindly provided 100mM 4-aminopyridine.

2.2 The previous synthesis and uses of the viral constructs

The adenoviral constructs used in this thesis were synthesised by a modified version of the protocol by He and colleagues and incorporate a GFP marker driven by a CMV promoter to allow analysis of the infectivity of the virus (He et al., 1998). One viral construct contains the GFP marker only, and one contains the gene for the Repressor Element 1-Silencing Transcription factor (*REST*)/Neuron-Restrictive Silencer Factor (NRSF) in addition to the GFP marker. The *REST* sequence is human. The dominant negative *Rest* sequence is mouse and was taken from the Anderson group (Chen et al., 1998). The DN*Rest* construct contains the *Rest* binding domain only, with a myc epitope. This means that it is able to bind to the RE1 site on the target gene, preventing endogenous REST from binding and repressing the gene. Due to its lack of C and N terminal sites the DN*Rest* is unable to recruit the cofactors (see Introduction) necessary to induce transcriptional repression.

2.3 Cell culture

SH-SY5Y cells and HEK293 cells were cultured in 9cm petri dishes (Scientific Labs), with Dulbecco's modified Eagle's medium (DMEM, PAA laboratories) with high glucose (4500mg/L) supplemented with 10% v/v foetal bovine serum (PAA) and 6g/L penicillin and 10g/L streptomycin (Sigma) at 37°C with 5% CO_2. Cells were passaged at 80% confluence: Cells were washed with 5ml sterile PBS (room temperature), then incubated with 1ml of Trypsin-Ethylenediaminetetraacetic acid (EDTA, Sigma) for 3 minutes at 37°C with 5% CO_2. Cells were resuspended in 10ml fresh cell medium (pre-warmed to 37°C) which was split into new culture dishes with fresh medium added up to 10ml total. Cells were grown and used for experiments between passages

P10-P30. All work with cell lines was performed in a Class II tissue culture hood.

2.3.1 Transfection of HEK293 cells with pcDNA3-GFP-*NFATc3* plasmid

HEK293 cells were cultured to approximately 70% confluency prior to transfection, in a 6 well plate. The plasmid pcDNA3-GFP-*NFATc3* (Tomida et al., 2003) plasmid DNA (6µg) was mixed with 300µl DMEM. Lipofectamine (24µl, Invitrogen) was mixed with 300µl Eagle's Modified Eagle's medium (Sigma). Both solutions were mixed together and incubated for 20 minutes at room temperature. Medium was aspirated from cells and they were washed with 1ml of PBS per well. PBS was aspirated and cells were washed with 1ml DMEM per well. DMEM (2.4ml) was added to the solution of plasmid DNA and lipofectamine, and mixed. DMEM was aspirated from cells and 1ml of the plasmid DNA, lipofectamine and DMEM solution was added to each well of cells. Cells were incubated for 4 hours at 37°C with 5% CO_2. Solution was then aspirated from the wells and replaced with regular cell culture media. Transfection efficiency was assessed at 24 hours by visualising GFP expression in the cells with the Evos FL Auto 2 fluorescence microscope.

2.3.2 Viral titrations

To calculate viral titres, SH-SY5Y cells were seeded in 500µl cell medium in a 24 well plate at 60-70% confluency. Twenty-four hours later, the medium was replaced with medium containing AdGFP, AdGFP-*REST* or AdGFP-*Rest*-DN virus and incubated for 24 hours in a humidified 37°C, 5% CO_2 incubator. Wells were infected in triplicate with viral stock solutions of AdGFP, AdGFP-*REST* or AdGFP-*Rest*-DN diluted at $1:10^2$, $1:10^3$, $1:10^4$ or $1:10^5$ in cell medium. Plates were then imaged on the Evos FL Auto 2 fluorescence microscope. Three images were taken at 10x objective in randomly selected locations in each well containing viral particles at a dilution of $1:10^5$, as this dilution gave 20-40% cell infection which is optimal for accurate titre determination. GFP-expressing cells were counted using ImageJ software, and the average taken of the 3 images. Virus titre was calculated by counting number of infected cells per image, and the average calculated for the whole 1.9cm^2 well. This was used to calculate viral particles per volume of virus and infectious particles per ml. For infections with each viral construct, 3 images were taken from each of the 3

wells of cells infected at $1:10^5$. GFP-expressing cells were counted and used to calculate viral particles per ml of virus applied. AdGFP virus was calculated to be $4.9x10^9$vp/ml, AdGFP-*REST* was found to be $4.0x10^9$vp/ml and AdGFP-DN*Rest* was found to be $4.9x10^9$vp/ml.

2.4 Organotypic hippocampal slice culture

All work with animals was carried out in accordance with the UK Animals (Scientific Procedures) Act 1986. Organotypic hippocampal slice cultures were prepared as previously reported (Grabiec et al., 2017). Postnatal day 6-9 (P6-9) Wistar rat pups were anaesthetised with isoflurane and sacrificed by cervical dislocation followed by decapitation as outlined in the Schedule 1 guidelines. The brain was removed and placed into ice-cold artificial cerebrospinal fluid (ACSF containing 124mM NaCl, 26mM $NaHCO_3$, 3mM KCl, 1.25mM NaH_2PO_4, 1.5mM $MgCl_2$, 1.5mM $CaCl_2$, 10mM Glucose) bubbled with carbogen. After removal of one third of the rostral side and 1mm of the caudal edge, the brain was fixed to the vibratome stage using superglue. The brain was sliced into 400µm coronal sections using a Leica VT1200S vibratome (Leica Biosystems, UK) and transferred into freshly made ACSF bubbled with carbogen, using a wide-mouthed pipette. The osmolarity of the ACSF solution was verified as 295-315 using an Osmomat 3000 osmometer (Gonotec). Hippocampal regions were dissected from each slice under sterile conditions and transferred with a wide-mouthed pipette onto semiporous membrane inserts (Falcon) in a 6-well tissue culture plate containing 1ml organotypic medium consisting of 50% Eagle's minimum essential medium, 25% heat-inactivated horse serum, 25% Hank's Balanced Salt Solution (HBSS), 1% 6g/L penicillin and 10g/L streptomycin (all from Sigma), 0.5% B-27 supplement (Gibco) and supplemented with 16.65mM glucose (Fisher Scientific), and 14.69mM HEPES (Melford, pH 7.2). Fresh media was made up once a week and the pH of each batch was verified using a PHM220 Lab pH Meter (Radiometer analytical). Cultures were maintained at 37°C and 5% CO_2, and medium was replaced twice a week thereafter.

2.4.1 Adenoviral infection of organotypic cultures

Virus stocks were diluted in pre-warmed organotypic medium. One hundred microlitres of this solution was placed on top of each slice on a membrane insert in a 6-well plate which was incubated at 37°C with 5% CO_2. Medium was replaced with fresh organotypic medium after 3 days.

2.4.2 Quantification of infection of organotypic cultures with adenovirus

Organotypic cultures were infected with AdGFP at $5x10^6$vp/ml or $5x10^7$vp/ml or AdGFP-*REST* at $2x10^7$vp/ml at 0, 4 or 8 days following plating, and cultured at 37°C with 5% CO_2. After 3 days in culture, slices were fixed in 4% w/v paraformaldehyde (PFA , Sigma) dissolved in PBS for 1 hour at room temperature. The PFA was removed and the cultures washed 3 times with 500µl PBS, exposed to 0.05µg/ml DAPI (Calbiochem) in PBS for 45 seconds and washed 3 more times with PBS. They were mounted onto slides with Fluoromount with DAPI (Sigma), then imaged with an Evos FL Auto 2 fluorescence microscope. Six images were taken per slice (3 images from each region; CA1, CA3, dentate gyrus) at 20X magnification. GFP-expressing and DAPI-positive cells were counted using ImageJ, and infection of organotypic cultures with adenovirus was quantified as percentage of total DAPI-positive cell nuclei which expressed GFP.

2.4.3 Viability staining of organotypic cultures with propidium iodide

Organotypic slices were cut out of membrane inserts and placed in individual wells of a 24 well plate. Propidium iodide solution (MP Biomedicals) in organotypic medium (5µM final concentration) was added to each well and cultures incubated at 37°C with 5% CO_2 for 1 hour. The medium solution was aspirated, the cultures washed 3 times in PBS for 20 minutes each, and 4% w/v paraformaldehyde (PFA) was applied at room temperature for 30 minutes. Cultures were washed 3 times in PBS, exposed to 0.05µg/ml DAPI (Calbiochem) in PBS for 30 seconds, and washed 3 more times with PBS for 5 minutes each time. Cultures were mounted onto slides with Fluoromount with DAPI (Sigma), and imaged with an Evos FL Auto 2 fluorescence microscope, maintaining a constant brightness for the red filter. For cell death count, 3 images were

taken from each of regions; CA1, CA3 and dentate gyrus per slice culture (at 20x magnification). To quantify proportion of propidium iodide-stained cells, number of propidium iodide positive cells and total number of cell nuclei were counted in each 20x image using ImageJ software. Red propidium iodide-stained cells were calculated as a proportion of total cells, and the average of all 3 images per region per slice was recorded. This was used to calculate the average percentage of total cells that were living in each region of each slice. For fluorescence intensity quantification of propidium iodide staining, 3 different areas of each region (CA1, CA3, dentate gyrus) within the same image (4x magnification) were quantified. Background was subtracted from signal value per image, and the mean was taken of the 3 to give a mean value per region per slice. For both analyses, N=3 slices for each timepoint.

2.4.4 Viability staining of organotypic cultures following infection with adenovirus

Organotypic cultures were infected with $1x10^7$vp/ml AdGFP and stained with ethidium homodimer after 3, 6 or 9 days in culture. Cultures were incubated at 37°C with 5% CO_2 for 30 minutes in ethidium homodimer (Invitrogen E1169) in organotypic medium (4µM final concentration), washed in PBS, and fixed in 4% w/v PFA for 30 minutes. They were then washed 3 times in PBS, exposed to 0.05µg/ml DAPI (Calbiochem) for 30 seconds, washed 3 more times in PBS and mounted with Fluoromount with DAPI (Sigma). Slices were imaged with an Evos FL Auto 2 fluorescence microscope, maintaining a constant brightness for the red filter. Three images at 20x magnification were taken from each major region (CA1, CA3 and dentate gyrus) per slice culture, and 2-4 slices per time point were imaged. Ethidium homodimer-stained cells were counted using ImageJ software and the proportion of GFP expressing cells was calculated.

2.5 Chemical treatment of organotypic cultures

2.5.1 Treatment of organotypic cultures with kainate

At 7 days in culture, organotypic medium beneath the membrane insert was replaced with 5µM kainate in pre-warmed medium (10µl of a 500µM solution of kainate in

dH_2O, in organotypic medium up to 1ml total), or with fresh pre-warmed medium for the vehicle-treated group. Cultures were incubated for 18 hours at 37°C with 5% CO_2 before processing for immunohistochemistry, RT-PCR or western blot.

2.5.2 Treatment of organotypic cultures with 4-aminopyridine and/or cyclosporin A

At 14 days in culture, organotypic medium beneath the membrane insert was replaced with 100µM 4-aminopyridine (4AP) in pre-warmed medium (1µl of a 100mM solution of 4AP in dH_2O, in organotypic medium up to 1ml total), or 1µM cyclosporin A, a mixture of both solutions (1µl of a 1mM solution of cyclosporin A in dH_2O, and 10µl of a 100mM solution of 4AP in dH_2O, in organotypic medium up to 1ml total), or with fresh pre-warmed medium for the vehicle-treated group. Organotypic cultures exposed to 4AP and cyclosporin A were incubated for 4 days at 37°C with 5% CO_2. Following incubation, slice cultures were further processed for immunohistochemistry, RT-PCR or western blot.

2.6 RNA extraction and qRT-PCR

2.6.1 RNA extraction from organotypic cultures

Each hippocampal slice culture was scraped from the membrane insert of the 6-well plate and suspended in 300µl of ice-cold Tri Reagent (Invitrogen) in a 1.5ml microcentrifuge tube. It was homogenised with a pestle and vortexed. Chloroform (100µl, Sigma) was added to each sample, which was then vortexed and incubated at 3 minutes at room temperature. Samples were centrifuged for 15 mins at 4°C, 12,000 RPM (13,900 x G) in a Fresco 17 Microcentrifuge (Thermo Scientific). The aqueous layer containing RNA was removed into a new tube with 100µl ice-cold chloroform. This was again vortexed and incubated for 3 minutes at room temperature, followed by further centrifugation for 15 minutes at 4°C, 12,000 RPM (13,900 x G). The aqueous layer was removed into a new tube and mixed with an equivalent volume of isopropanol. The sample was vortexed and incubated at room temperature for 10 minutes to allow precipitation of the RNA. To pellet the precipitated RNA, tubes were centrifuged for 15 minutes at 4°C, 12,000 RPM (13,900 x G), and the supernatant

discarded. Pellets were washed with 500µl of 70% ethanol (Sigma) and centrifuged for 5 minutes at 13,300 RPM (170 x G), and the supernatant removed. The wash step was repeated twice more. Residual ethanol was removed, and the pellet was air-dried for 3 minutes on ice. Twelve microlitres of Tris-EDTA (TE: 10mM Tris, 1mM EDTA) was added to each sample followed by heating at 65°C for 5 minutes to dissolve the RNA. Samples were then chilled on ice for 1 minute and mixed by centrifugation at 6,000 RMP (3300 x G) for 30 seconds in a Genfuge 24D digital microcentrifuge (Progen Scientific). RNA concentrations and purities were determined by spectrometry using a NanoDrop 2000c spectrophotometer (Thermo Scientific) at 260nm and purity checked using the 260nm/280nm ratio

2.6.2 Reverse transcription

To synthesise cDNA, 500ng of extracted RNA with 2µl (100ng) random hexamer primer (Bioline), 0.2µl (100ng) oligo-dT (Eurogentec), and dH_2O to make the reaction volume up to 13.6µl, was incubated at 65°C for 5 minutes to prime the poly(A) 3' ends of the RNA, before placing the samples on ice for 1 minute. To the samples was added 6.4µl of mastermix containing (per reaction): 0.2µl of M-MLV Reverse Transcription (Promega), 4µl M-MLV RT 5X Buffer (Promega), 2µl 20mM dNTPs (Bioline), and 0.2µl RNasin Ribonuclease Inhibitor, to give a final reaction volume of 20µl. The reverse transcription reaction was incubated at 37°C for 1 hour and resulting cDNA was diluted with 80µl of TE (10mM Tris and 2mM EDTA, pH7.4), and stored at -20°C.

2.6.3 Quantitative reverse transcription PCR

Quantitative real-time PCR was performed in duplicate, and negative controls with cDNA replaced with either dH_2O or RNA, were included for each primer pair. Quantitative PCR was performed on a Corbett Rotor Gene 6000 PCR, using the cycle parameters: 95°C for 10 minutes, 40 cycles of 95° for 10 sec, 60° for 15 sec, 72°C for 30 sec and a melt curve ramping 1°C per second from 50°C to 95°C. Each reaction (20µl total) contained 0.6µl of each 10µM primer in water, 5µl cDNA and 10µl 2X SensiMix SYBR Hi-Rox (Bioline). Sequences of primer pairs are detailed in Table 1. Transcript levels were analysed by real time analysis of SYBR Green fluorescent

reporter dye intercalation into amplified double stranded DNA using Rotor Gene 6000 Series software 1.7. Expression of all reference genes remained consistent across experimental groups.

Gene	Sense	Antisense	Amplicon size	Position
Human/ mouse *REST*	CATACAGGAGAACGCC CATA	GCCCATTGTGAACCTGT CCTT	180bp	1028s, 1208a
Rat *Sdha*	TCCTTCCCACTGTGCA TTACAA	CGTACAGACCAGGCAC AATCTG	104bp	1222s, 1326a
Rat cyclophilin A	CCACCGTGTTCTTCGA CATC	TTGCCACCAGTGCCATT ATG	197bp	48s, 245a
Rat *Rest*	ACCTGAGAGCCGGGG ATAAC	TAAGGGCGTTCTCCTGT GTGA	198bp	710s, 908a
Rat *Kcnq2*	TCGGCCGGACACTTGG ATAT	CATCATGCTGGGGTCTT CGG	146bp	1785s, 1931a
Rat *Kcnq3*	CGTCTGATTGCTGCCA CCTT	TCTGACGGTGCTGTTCC TGA	108bp	1417s, 1525a
Rat *Bdnf*	ATCCACTGAGCAAAGC CGAAC	CAGCCTCATGCAACCG AAGTA	197bp	518s, 715a
Rat *Hcn1*	ACTCCCTTTCGGTGGA CAAT	TGATTGGAGGGATCGCT TGT	233bp	1726s, 1959a
Rat *Scg10*	AAGCAGATCAACAAG CGTGC	TCTCCTCCAAAGCCTTC TGG	243bp	251s, 494a
Rat *Scn2a*	ATCAAGTCCCTCCGAA CGTT	GTTGTTGACCACGCTC ACAT	242bp	4113s, 4355a
Rat *Sp1*	CAGCAGGTGGAGAAG AAGGA	AATGGCCTCTCCCCTGT ATG	231bp	1777s, 2008a

Table 2.1. List of RT-PCR primers.

2.6.4 qRT-PCR analysis:

Firstly, the mean Ct value was taken from both technical replicates for each sample with each primer set. For each sample, Ct value of the reference gene is subtracted

from Ct value of the gene of interest to give ΔCt. Then 2 is raised to the power of negative ΔCt to give expression of the gene of interest as a decimal, relative to expression of the reference gene. This number is multiplied by 100 to give expression of gene of interest as % of expression of the reference gene.

ΔCt = Ct (gene of interest) – Ct (reference gene)

Relative expression = $2^{-\Delta Ct}$

Expression as % of reference gene = relative expression x 100

2.6.5 Primer design and validation

Primer pairs were designed using the Primer 3 software (Rozen et al., 2000). All primers were analysed for sequence specificity using a Blast search of the NCBI nucleotide database and confirmed as spanning an intron using UCSC genome browser. The specificity of PCR amplicons for each primer pair was determined using electrophoresis through a 2% agarose gel: 1g agarose (Melford MB1200) in 50ml TAE buffer (40mM Tris base, 20mM acetic acid, 1mM EDTA). Two microlitres of 10x DNA loading buffer [50% glycerol (Sigma) in TE with bromophenol blue (Sigma)] was mixed into each tube of 20µl qPCR product, and 10µl of this was loaded onto the gel, alongside 5µl of 100bp DNA ladder (New England Biolabs N3231). Gels were run in TAE buffer at 70V for 1.5 hours. Only primer pairs producing an amplicon of the correct size, as identified through comparison to the 100bp ladder, and predicted using NCBI Blast were used experimentally. qPCR melt curve analysis was further used to confirm successful amplification. qPCR control using appropriate RNA sample in place of cDNA was used to check for primer pairs amplifying contaminating genomic DNA, which were excluded from experimental work.

2.7 Western blotting

Three organotypic cultures were scraped from the membrane insert into a microcentrifuge tube with 60µl of lysis buffer [50mM Tris-HCl (pH 7.5), 1mM EGTA, 1mM EDTA, 1% w/v Nonidet NP-40, 1mM sodium orthovanadate, 50mM sodium fluoride, 5mM sodium pyrophosphate, 0.27M sucrose, 1mM DTT, and protease

inhibitor tablet (1 per 20ml buffer, Merck)], per sample, on ice. Samples were homogenised with 5 strokes of a pestle and incubated on ice for 10 minutes. Samples were centrifuged at 4°C, 12,000 RPM for 15 minutes and the supernatant was removed into a fresh micro-centrifuge tube. Protein concentrations were analysed using the Pierce 660nm protein assay kit (Thermo Scientific) following the manufacturer's instructions. Ten microlitres of a 1:10 dilution of each sample was prepared in a 96-well plate (Greiner Bio-One) alongside 10µl of each of a set of BSA standards of known concentration. 150µl of Pierce 660nm protein assay reagent was added to each sample in the 96-well plate and mixed. All reactions were performed in triplicate. The OD of the plate at 660nm was then taken using a FLUOstar Omega plate reader (BMG Labtech). Average readings were used to plot absorbance against concentration for the BSA standards. Average readings for absorbance of 1:10 sample dilutions were used to calculate concentration for each sample. Equal amounts of protein were prepared from each sample in an experiment (between 20 and 30µg). To each sample was added 6µl 5x gel loading buffer (10% SDS, 50% glycerol, 0.5% bromophenol blue, 250mM Tris HCl, pH 6.8), 2µl 2M DTT, and dH_2O added up to a total volume of 30µl. Samples underwent sodium dodecyl sulphate-polyacrylamide gel electrophoresis (SDS-PAGE) alongside 5µl prestained protein ladder (Badrilla AccuMark). SDS-PAGE gels of 1.5mm thickness comprised of a 6% stacking gel and 10% resolving gel. Resolving gel was composed of 10% Acrylamide:Bis-acrylamide 37.5:1 (Severn Biotech), 365mM Tris pH 8.8, 0.1% sodium dodecylsulphate (SDS), 0.1% ammonium persulfate (APS, Sigma) and 0.08% Tetramethylethylenediamine (TEMED, Sigma). Stacking gel was composed of 125mM Tris pH 6.8, 6% Acrylamide:Bis-acrylamide 37.5:1, 0.1% SDS, 0.1% APS and 0.1% TEMED. Electrophoresis was performed at 100V through the stacking gel and then 140V through the resolving gel, in electrophoresis buffer [25mM Tris Base (Fisher Scientific), 250mM glycine (Fisher Scientific) and 0.1% w/v SDS and dH_2O]. Gels ran until the ladder bands had separated clearly, and then stacking gels were removed from resolving gels. PVDF membranes (Amersham) were soaked in methanol for 5 minutes followed by soaking in transfer buffer [192mM glycine, 24mM Tris Base, 20% methanol (Fisher Scientific) in dH_2O] for 5 minutes. Wet-transfer was performed at 30V for 1 hour in transfer buffer using an XCell II wet transfer module (Invitrogen). Membranes were blocked with 5% w/v skimmed-milk powder in PBST (PBS with 0.1% v/v Tween 20, Sigma) for 1 hour at room temperature. Membranes were washed in PBS 3 times for 5 minutes each at

room temperature on a rocker. Membranes were cut along ladder bands marking regions between the sizes of the proteins of interest, for parallel blotting with different antibodies. Primary antibody solution was prepared; Anti-β-Tubulin, 1:1000 (Cell Signalling, mouse monoclonal, D3U1W) was dissolved in PBST with 5% w/v skimmed milk powder. Anti-REST, 1:1000 (upstate, rabbit polyclonal, 07-579) and Anti-BDNF, 1:1000 (Abcam, rabbit polyclonal, 108319) were each prepared by dissolving the antibody in PBST with 5% w/v BSA (Thermo Scientific). Membranes were incubated with primary antibodies at 4°C overnight with agitation, before washing 3 times for 5 minutes each with PBST at room temperature. Appropriate secondary antibodies; Anti-rabbit IgG, HRP-linked, 1:1000 dilution (Cell Signalling Technology, 7074); Anti-mouse IgG, HRP-linked, 1:1000 dilution (Cell Signalling Technology, 7076) were diluted in PBST with 5% w/v skimmed-milk powder and were incubated at room temperature for 1.5 hours, followed by washing 3 times for 5 minutes with PBST at room temperature. Bound secondary antibodies were visualised using the Super Signal West Pico Plus Chemiluminescent Substrate kit (ThermoScientific) and an iBright 1500 imager (Invitrogen). Quantification of resulting bands was carried out by densitometry using ImageJ software. All bands were normalised to the β-Tubulin loading control.

2.8 Immunohistochemistry

2.8.1 Cyclosporin treatment and immunofluorescence of cultured HEK293 cells

HEK293 cells that had been transfected with the *NFATc3* plasmid were plated onto cover slips in a 6-well plate and exposed to 1uM cyclosporin A (1ul of 1mM cyclosporin A in 1ml cell medium) for 18 hours. Cells were fixed for 1 hour in 4% w/v PFA and washed with 1ml PBS. To assist antigen retrieval, cells were incubated in trypsin working buffer (0.05% trypsin, 0.1% $CaCl_2$ in dH_2O) for 5 minutes at 37°C. Cells were washed in 1ml PBS and blocked in buffer containing donkey serum [5% donkey serum (Merck D9663), 0.25% Triton X100 and 0.05% Tween20 in PBS] for 2 hours at room temperature. NFAT4 primary antibody (rabbit polyclonal, 4998, Cell signaling) solution was diluted in PBS containing 50mg/ml BSA and was applied to the cells overnight at 4°C with agitation. Cells were washed 3 times for 5 minutes in PBS at room temperature, and then donkey anti-rabbit Alexa Fluor 555 secondary

antibody (used at 1:1000 diluted in PBS containing 50mg/ml BSA) was applied for 1.5 hours. Cells were washed 3 times for 5 minutes at room temperature in PBS and treated with 50ng/ml DAPI in PBS (as 1µl of 500µg stock in 10ml PBS, Calbiochem) where indicated in results, for 45 seconds. They were washed 3 more times at room temperature with PBS and mounted onto slides with Fluoromount with DAPI. Imaging was performed using a Zeiss LSM880 Inverted confocal microscope with 40X objective lens. Images were processed and analysed with Fiji (ImageJ) software.

2.8.2 Immunohistochemistry of organotypic cultures

Organotypic cultures on membrane inserts in 6-well plates were cut from the membrane and placed individually into wells of a 24 well plate. They were fixed for 45 minutes in 500µl 4% w/v PFA at room temperature, and then washed with 500µl PBS. To assist antigen retrieval they were incubated at 37°C for 5 minutes in 500µl trypsin working buffer (0.05% trypsin and 0.1% $CaCl_2$ in dH_2O) and permeabilised overnight at 4°C in 500µl permeabilisation solution (0.1% Triton-X100 in PBS). Cultures were washed in 500µl PBS and blocked for 2 hours at room temperature in buffer containing donkey or goat serum [5% goat serum (Fisher Scientific 10189722), 0.25% Triton X100 and 0.05% Tween20 in PBS]. Primary antibody (diluted in PBS containing 50mg/ml BSA) was applied at 4°C for 4 days. Anti-GFAP (rabbit polyclonal antibody Z0334 from DAKO) was used at 1:300; Anti-REST (rabbit polyclonal antibody 07-579 from Upstate) was used at 1:500; Anti-HUC/D (HuA/B/C/D rabbit polyclonal antibody 13032-1-AP from Proteintech) was used at 1:1000; Anti-β-Tubulin III (mouse monoclonal antibody T8578 from Sigma) was used at 1:1000; Anti-KCNQ2 (mouse monoclonal antibody sc-271852 from Santa Cruz) was used at 1:300; Anti-BDNF (rabbit polyclonal antibody 108319 From Abcam) was used at 1:15; Anti-Iba1 (rabbit polyclonal PA5-27436 from Invitrogen) at 1:300; Anti-oligodendrocyte specific protein antibody (rabbit polyclonal Ab53041 from Abcam) at 1:2000. Cultures were washed 3 times for 5 minutes in PBS at room temperature, and then secondary antibody (used at 1:1000 diluted in PBS containing 50mg/ml BSA) applied at 4°C for 4 days. The following Alexa Fluor secondary antibodies were used; donkey anti-rabbit 555, donkey anti-rabbit 488, donkey anti-mouse 555, goat anti-rabbit 405, donkey anti-mouse 555. Cultures were washed 3 times for 5 minutes at room temperature in PBS and treated with 50ng/ml DAPI in PBS (as 1µl of 500µg

stock in 10ml PBS, Calbiochem) where indicated in results, for 45 seconds. They were washed 3 more times at room temperature with PBS and mounted onto slides with Fluoromount with DAPI. Imaging was performed using a Zeiss LSM880 Inverted confocal microscope with 40X objective lens. Images were processed and analysed with Fiji (ImageJ) software.

2.9 Cell attached patch clamping of organotypic cultures

Glass pipettes (Harvard apparatus, 30-0066) were pulled using a pipette puller and fire polished to give a resistance of 2-3MΩ. Organotypic cultures were used between 12 and 27 days in vitro. The culture was cut out from the membrane insert and placed in the ACSF-filled recording chamber, and a small weight used to anchor the membrane to the chamber surface. The gravity fed perfusion system delivered fresh ACSF to the slice in the recording chamber throughout the experiment. A syringe was used to fill the pipette with 37°C ACSF, and air bubbles tapped out. The fluorescence microscope was used inside a Faraday cage to minimise interference with the signal. The fluorescence microscope was used to focus on the CA1 region of the hippocampal slice and pyramidal neurons were identified by their localisation within the molecular layer. The pipette was lowered onto a pyramidal neuron with a motor-driven manipulator (Luigs & Neumann Feinmechanik and Elektrotechnik Gmbh), and a seal was obtained by applying negative pressure with a syringe. Recordings were made with a EPC10 USB patch clamp amplifier (HEKA elektronik), using PatchMaster software for recording and analysis. Recording of spontaneous action potential currents in voltage-clamp mode was started and continued for 15 minutes, when perfusion was switched to ACSF containing 100µM 4AP (50µl of a 100mM 4AP per 50ml solution). The recording continued for 30 minutes. The first 2 minutes after obtaining a seal were discounted from the analysis as physical interference with the cell membrane by the pipette during patching had been observed to cause a brief destabilisation of tonic action potential firing patterns lasting less than 2 minutes. The first 15 minutes after switching the perfusion to ACSF containing 4AP were also discounted from the analysis drug wash-in time. Action potential spikes were counted manually or using Spyder software, with both systems calibrated to each other. Spikes were counted if they were >20pA. Number of spikes from 15 minutes before 4AP were compared to number of spikes after the wash-in of the 4AP.

2.10 Statistics and data analysis:

For each data set, the Shapiro Wilks test was used to determine whether data were normally distributed. Parametric tests were used for comparisons of means between data sets that were all normally distributed. Non-parametric tests were used for comparisons of means between data sets that were either non-normally distributed or a mixture of groups that are normally and non-normally distributed. For parametric pairwise comparisons of means, Student's t-test was used. One-tailed t-tests were used when the effect was expected to change in one specific direction, predicted from previously published literature. Two-tailed t-tests were used when it was unclear from the literature which direction an effect may change in, if any. For parametric comparisons of means across multiple groups, one-way ANOVA was used. For non-parametric pairwise comparisons of means, the Mann-Whitney U test was used. For non-parametric comparisons of means across multiple groups, the Kruskal-Wallis test was used. If the Kruskal-Wallis test showed a significant difference, the Mann-Whitney U test was used for comparisons between all pairs of groups individually. The use of Student's t-test or ANOVA for analysis implies data are normally distributed, while the use of Mann-Whitney U test or Kruskal-Wallis test implies data are non-normally distributed or a mixture of normal and non-normal data groups.

Standard error of the mean was used in the graphs showing the viability and infection stains as well as qPCR results. This was because the most valuable data in these experiments overall was the comparisons between the means rather than the spread of individual data points. Standard deviation was used in the bar charts showing the western blot quantification in order to show the spread and variability of the data, as these experiments demonstrated high variability in REST and BDNF protein levels across different samples. For immunohistochemistry quantification, either box plots or bar graphs with standard deviation were used to show the spread of the data within each group, as immunohistochemistry can produces high variability of signal intensities.

Chapter 3

Adenoviral expression of REST in organotypic hippocampal slice cultures and its effects on *Kcnq2/3*/Kv7.2/3 expression

3.1 Introduction

Following Mucha and colleagues' discovery that REST represses *KCNQ2* and *KCNQ3* mRNA and Kv7.2/7.3 current in DRG neurons (Mucha et al., 2010), I wanted to investigate whether a similar mechanism exists in the CNS. A suppression of the Kv7 current in the CNS due to reduced expression of *KCNQ2* and *KCNQ3* would be expected to cause increased excitability, potentially causing epilepsy. REST has been shown to be involved in epilepsy, and changes in Kv7 channels' function are linked to neonatal epileptic syndromes and epilepsy medications. The hippocampus is a region highly affected in epilepsy, and is often the site of origin for seizures in temporal lobe epilepsy (Avoli, 2007). Therefore, organotypic hippocampal slice cultures were used to investigate whether REST represses KCNQ2 and KCNQ3 expression in the hippocampus. As REST increases following seizures (Navarrete-Modesto et al., 2019; Palm et al., 1998; Spencer et al., 2006), it was hypothesised that this could contribute to epileptogenesis through repression of *Kcnq2* and *Kcnq3*, causing a reduction in Kv7 current and resulting increase in neuronal excitability. Adenoviral constructs carrying a GFP reporter and either a REST cassette, a dominant negative REST cassette, or no transgene, were used to infect organotypic hippocampal cultures to determine the effects of exogenous REST modulation on *Kcnq2* and *Kcnq3* expression. As REST recruits HDACs to assist in repression of its target genes (Ooi and Wood, 2007), the HDAC inhibitor suberanilohydroxamic acid (SAHA), also known as vorinostat, was used to determine a potential role for histone deacetylation in regulation of *Kcnq2* and *Kcnq3*. SAHA inhibits classes I, II and IV HDACs, which includes the HDACs recruited by REST. HDAC regulation of *KCNQ2* and *KCNQ3* has not been investigated. However, like REST, epigenetic changes in the brain such as histone acetylation are believed to play a role in epileptogenesis, with HDAC inhibitors showing potential as anti-epileptic drugs (Citraro et al., 2017).

There are various techniques available for gene transfer in organotypic cultures, including electroporation, biolistics and viral infection (Murphy and Messer, 2001). Biolistics uses heavy metal particles to shoot the genetic material into the slice, which could disrupt slice integrity (Arnold et al., 1994). Electroporation is up to 80% efficient but targets individual neurons in the culture rather than all cells across the slice (Keener et al., 2020). Gene transfer using viral delivery is likely the most

appropriate and well-established method for widespread transduction of cells throughout a slice culture. However, most groups have previously used microinjections which result in infection of cells localised to the injection site only (Ehrengruber et al., 2001; Ehrengruber et al., 1999). For our purposes of delivering REST and dominant negative REST constructs to allow quantifiable regulation of REST target genes, a much more thorough level of viral infection was required than that reported previously. Gene expression levels were to be quantified from the total cell population using qRT-PCR, due to its high levels of accuracy. Although neuronal gene expression was the primary focus, hippocampal tissue was harvested and processed as containing all cell types for technical simplicity. Adenoviral infection of cell types including neurons would be sufficient for this purpose, but a high proportion of overall cells would need to be infected. The preparation of organotypic cultures with high viability would need a low level of cell death detracting from the amount of transgene expression in adenoviral infected cells. Adenoviral infection of organotypic cultures needed to be improved upon compared to previous groups. In addition, adenoviral infection needed to be characterised to determine whether transgene expression is robust, reliable and targeted to neurons where the *Kcnq2* and *Kcnq3* genes may be affected. Furthermore, in order to modulate expression of the *Kcnq2* and *Kcnq3* genes encoding the Kv7.2 and Kv7.3 subunits, adenoviral delivery of the REST transgenes would need to be confirmed in neurons.

Adenovirus is a DNA virus which is responsible for mild infections of the respiratory tract and gastrointestinal system, and conjunctivitis. Replication-deficient adenovirus is commonly used in the clinic for gene therapy, in addition to its uses for gene delivery in vitro. Continued transgene expression from adenoviral delivery has been observed for weeks in organotypic cultures (Miyaguchi et al., 1999; Teschemacher et al., 2005), demonstrating its potential for the present study. Incubation of 2-3 day old thalamic explants in adenovirus resulted in about 45% of the surface area of the slice expressing the transgene. However, this was accompanied by a loss of structural integrity and necrosis, believed to be due to viral cytotoxicity (Wilkemeyer and Angelides, 1995). It would be advantageous to develop a method to allow a thorough infection of cells across the slice, to avoid the use of microinjections, and avoid viral toxicity. Other groups have previously relied heavily on microinjections throughout the slice, which infect cells around the injection site only, and could cause mild disruption to the tissue.

In this chapter the infection of organotypic hippocampal slice cultures with adenovirus was optimised and characterised. This technique was then used to assess the effects of exogenous adenovirally delivered REST modulation on expression of *Kcnq2, Kcnq3* and the epileptic marker *Bdnf*. The role of HDACs in regulation of *Kcnq2* and *Kcnq3* expression are also investigated. Some of this work has been published (Butler-Ryan and Wood, 2021a).

3.2 An organotypic hippocampal culture model to study epileptogenesis

Many factors have been described as affecting viability of organotypic slice cultures, including donor age and health, preparation time, culture sterility and medium composition (Humpel, 2015). A process of optimisation of development of organotypic hippocampal slice cultures was performed with the goal of obtaining slices with good cell viability that was retained throughout long term culture. Studies show epileptogenesis occurs in cultured hippocampal slices over several weeks (Dyhrfjeld-Johnsen et al., 2010). Propidium iodide and ethidium homodimer staining was used throughout the culture process to label dead cells, allowing assessment of viability levels. Certain steps in the preparation and plating of organotypic hippocampal slice cultures were found to be particularly important in ensuring high levels of cell viability. At the beginning, the slice preparation time from animal sacrifice to incubation of plated slices was taking around 3 hours, which was improved to 45 minutes. It was found to be critical to transfer the brain into ice-cold ACSF bubbled with carbogen immediately upon removal from the skull, limiting exposure time to the open air. Most published slicing protocols instruct to use a McIlwain tissue chopper while a few suggest a vibratome. Both were tried but the slices from the tissue chopper were found to be inconsistently shaped and poor quality, so the vibratome was used. To begin with, the hippocampi were dissected out from the brain and set in agar for vibratome slicing. An improvement on this was discovered from slicing the whole brain and then dissecting the hippocampal section from each slice, as the hippocampal architecture was now visible and cell viability improved for the first few days in culture. A small paintbrush was originally used for slice transfer, but the direct contact with the tissue caused too much damage so a wide-mouthed pipette was used instead. The final improvement was to pre-plate and incubate the growth medium in the 6 well

plates a few hours before slice plating, to ensure thorough oxygenation of the medium ready for the slices. Together these improvements resulted in good lasting viability of the cells in the hippocampal slice cultures. The final optimised procedures are detailed in Methods. To conserve space in this thesis, data from the optimisation procedure is not shown. After completion of the optimisation process, the procedure was used to prepare organotypic slices which were kept in culture until 3, 6, 9, 15, 18 or 21 days, at which point they were stained with propidium iodide and co-stained with the nuclear marker DAPI, and imaged. The propidium iodide staining was used to quantify cell death in each slice through two different approaches: dead cell counts, and propidium iodide stain intensity. In all 3 of the hippocampal regions throughout the whole 21 day process, an average of at least 88% of total DAPI-positive cells were viable (Figure 3.1A). This total included all cell types. In all images, the CA1 region contained between 86% and 100% viable cells, the CA3 region contained between 61% and 100% viable cells, and the dentate gyrus contained between 69% and 100% viable cells. Furthermore, images showed upwards of 96% living cells at most timepoints, demonstrating good lasting viability. No significant changes in living cell proportion were observed over time for any regions imaged, demonstrating the high viability as consistent over time. Non-significant trends show slight reductions in viability to 94-95% at 3 days in culture in the CA3 and dentate gyrus. This may reflect the unavoidable acute cell death occurring as a result of slice preparation, followed by the dead cells being cleared away. Another non-significant reduction in the proportion of living cells was observed at 9 days in culture in the CA3 region, down to an average of 88±4% for this timepoint only. This may be due to secondary damage occurring from slicing in the CA3 region after 9 days in culture, or it may be that the slices stained at 9 days in culture had experienced more damage in preparation than the other slices.

Fluorescence intensity of propidium iodide staining also did not show any significant changes throughout the culture process, but trends were observed. All 3 regions showed a trend of increasing fluorescence up to a maximum at 9 days in culture followed by a reduction to a minimum fluorescence at 15 days in vitro (Figure 3.1B). This is further demonstrated as brighter fluorescence signal from propidium iodide staining in figure 3.1C (9 days in vitro) and reduced fluorescence signal from propidium iodide staining in figure 3.1D (15 days in vitro). The results from both

analyses combined suggests good overall viability throughout the 21 day culture period, with some potential cell death occurring at 9 days in culture, which would likely be due to secondary damage and synaptic reorganisation occurring from tissue slicing during preparation (Mellentin et al., 2006). Cell death is minimal from 15 days onwards, suggesting synaptic reorganisation has finished and the slices are stable in culture by this point. This data demonstrates that overall organotypic viability is sufficient to allow experimental use of cultures at any timepoint in development.

A)

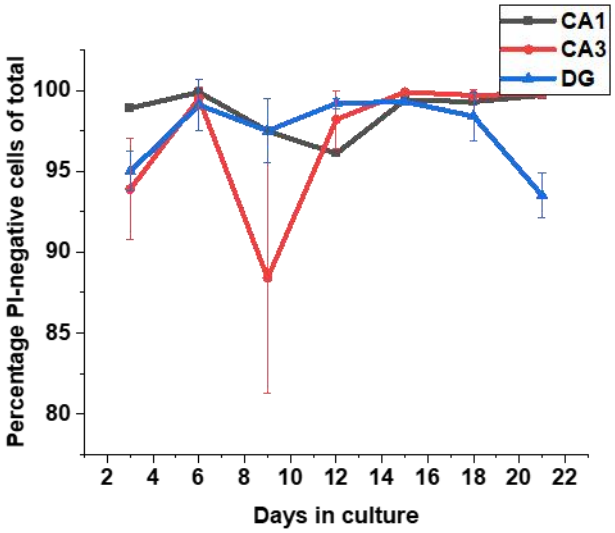
CA1
CA3
DG
Percentage PI-negative cells of total
100
95
90
85
80
2
4
6
8
10
12
14
16
18
20
22
Days in culture

B)

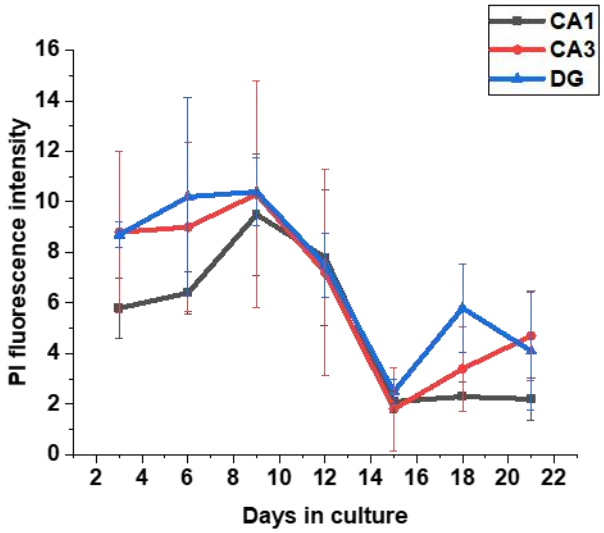
CA1
CA3
DG
PI fluorescence intensity
16
14
12
10
8
6
4
2
0
2
4
6
8
10
12
14
16
18
20
22
Days in culture

C)

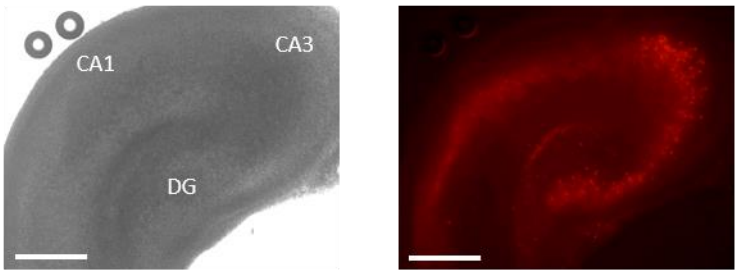
CA1
CA3
DG

D)

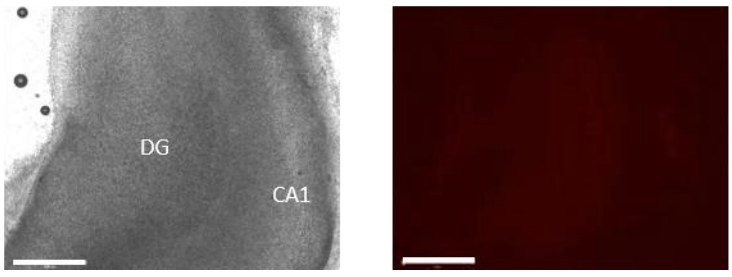
DG
CA1

Figure 3.1. Viability of organotypic hippocampal slice cultures over 21 days in culture. (***A***) Quantification of living cells as a proportion of total DAPI-stained nuclei (calculated as percentage of PI-positive cells subtracted from 100%) in CA1, CA3 and dentate gyrus hippocampal regions in organotypic cultures over 21 days in culture. No significant differences found with individual comparisons using Mann-Whitney U test (mean ± SEM, n = 3). (***B***) Quantification of fluorescence intensity of propidium iodide in CA1, CA3 and dentate gyrus (DG) hippocampal regions in organotypic cultures over 21 days in culture. No significant differences found with ANOVA followed by Tukey's post-hoc test (mean ± SEM, n = 3 slices). (***C***) shows representative fluorescent images of organotypic hippocampal slice cultures stained with propidium iodide (PI) at 9 days in culture. Brightfield (left) and RFP filter (right). Scale bars = 500µm. (***D***) Representative images of cultures stained with propidium iodide at 15 days *in vitro*. Brightfield (left) and RFP filter (right). Scale bars = 500µm.

3.3 Infection of organotypic cultures carrying GFP, *REST* and dominant negative *Rest*

3.3.1 Infection of organotypic cultures is most efficient at 0 days in vitro with high viral titre

The adenoviral constructs were first described by the Wood lab (Wood et al., 2003) and have been used in previous studies (Bingham et al., 2007; Bruce et al., 2004; Bruce et al., 2006; Cheong et al., 2005; Johnson et al., 2006; Mucha et al., 2010).

I wanted to infect organotypic hippocampal slice cultures with the adenoviral constructs to allow REST modulation in cultured hippocampal tissue. However, viral infection efficiency was a common problem in organotypic cultures (Bahr et al., 1994; Casaccia-Bonnefil et al., 1993; Ehrengruber et al., 2001; Ehrengruber et al., 1999). GFP reporter expression following bathing mature organotypic cultures in adenovirus resulted in infection at low levels, but it was noticed that younger slices seemed to take up the virus more readily. To test the effects of time point of infection and viral titre on infection rate, 22 slice cultures were infected on days 0, 4 and 8 of culture with Ad-GFP at $5x10^6$ and $5x10^7$vp/ml, and Ad-GFP-*REST* at $2x10^7$vp/ml. These titres were used to try to optimise infection rate and prevent cytotoxicity. Transgene expression from adenoviral delivery was previously observed to plateau after 2-3 days

(Teschemacher et al., 2005). Therefore, slice cultures in the present study were fixed and imaged after 3 days, and cell nuclei were stained with DAPI. During the first week in culture, slice cultures flatten down to around 150µm thickness (Stoppini et al., 1991), which could increase total cell number per area of tissue. Indeed, number of DAPI-stained cells per image do increase over time, from 95.05±6.45 at 0DIV (days in vitro, n=59), to 126.33±8.49 at 4DIV (n=36), to 149.50±5.13 at 8DIV (n=36), which could be due to flattening of the cultures. This will not affect the data as it is presented as proportion of total DAPI-stained cells. More cells were infected in cultures infected with $5.0x10^7$vp/ml AdGFP at 0 days in culture (41±2%) compared to cultures infected with this titre at 4 days in culture (17±5%, p=0.001) and 8 days in culture (6±1%, p=0.001; Figures 3.2A, 3.2C). Similarly, more cells were infected in cultures infected with $2.0x10^7$vp/ml AdGFP-*REST* at 0 days in culture (41±3%) compared to cultures infected with the same titre viral construct at 4 days in culture (6±2%, p=0.001) or 8 days in culture (13±1%, p=0.001, Figures 3.2B, 3.2C). This shows that infection efficiency is improved when cultures are infected at 0 days in culture rather than 4 or 8 days in culture, with the high titre virus. However, cultures infected with the lower titre $5.0x10^6$vp/ml AdGFP at 0 days (17±1%) did not show any more infected cells than cultures infected with the same titre virus at 4 days (18±4%, p=0.9) or 8 days (6±1%, p=0.087, Figure 3.2C) in culture. This demonstrates that both infection at 0 days in culture, as well as a viral titre of 2-$5x10^7$vp/ml is needed for obtaining optimal viral infection efficiency of hippocampal slice cultures. In addition, more cells were infected in the cultures infected with the higher titre $5.0x10^7$vp/ml AdGFP at 0 days in vitro (41±2%) compared to cultures infected with the lower titre $5.0x10^6$vp/ml AdGFP at 0 days in vitro (16±1%, p=0.001, Figure 3.2C). This further supports the use of a sufficiently high viral titre in combination with infection at day 0 for optimising infection rate. When cultures were infected at later timepoints, we did not observe higher viral titre to result in better infection efficiency. Infection efficiency was not improved in cultures infected at 4 days with $5.0x10^7$vp/ml AdGFP (17±5%) compared to cultures infected with $5.0x10^6$vp/ml AdGFP (18±4%, p=0.9). Furthermore, infection was no different in cultures infected at 8 days with $5.0x10^7$vp/ml AdGFP (6±1%) compared to cultures infected with $5.0x10^6$vp/ml AdGFP (6±1%, p=0.9). This further supports the idea that both a viral titre of 2-$5x10^7$vp/ml combined with infecting the slice cultures on day 0 provides optimal and efficient infection.

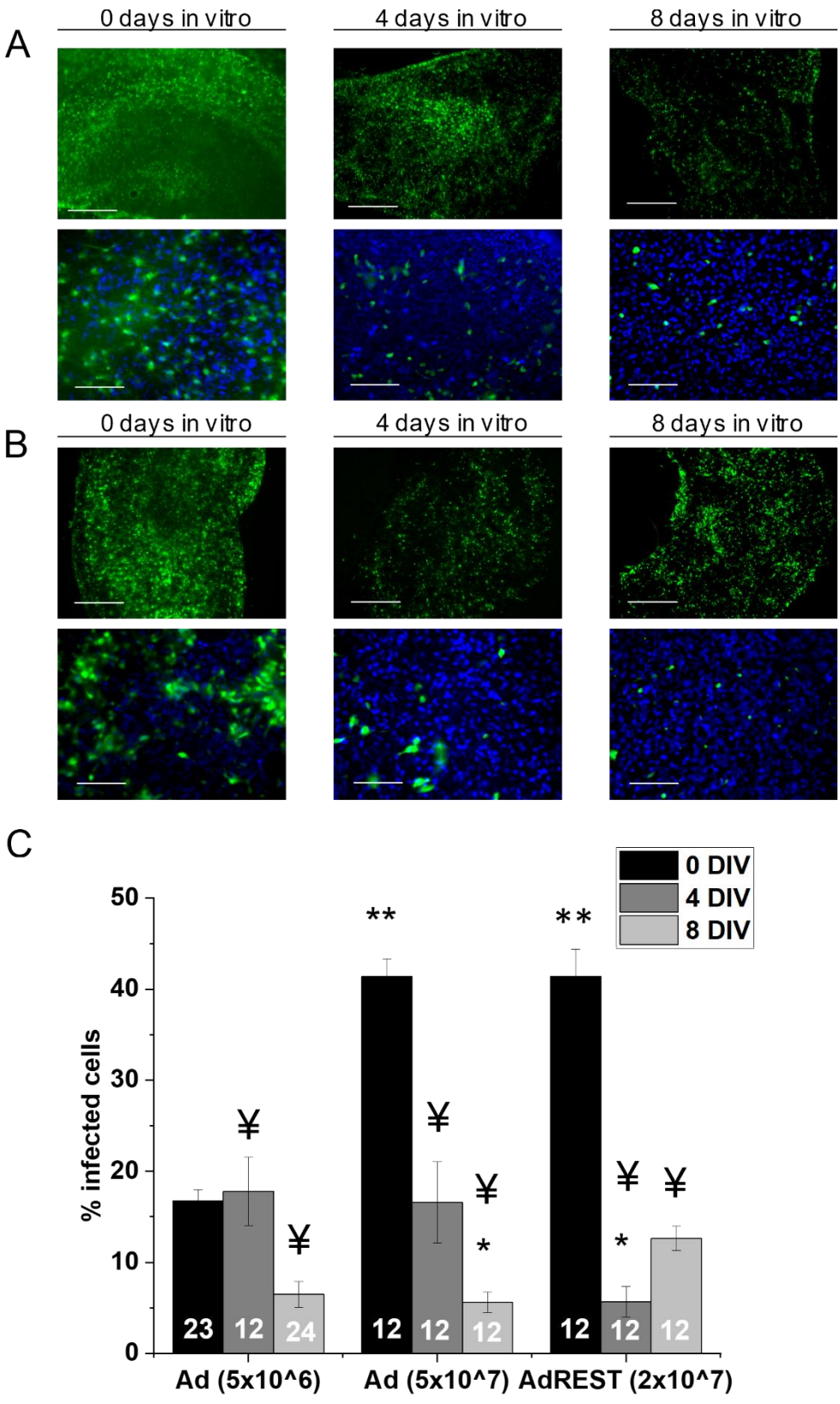

Figure 3.2. Assessment of adenoviral infection efficiency of organotypic hippocampal slice cultures. Organotypic hippocampal slice cultures infected with AdGFP or AdGFP-*REST* at either 0, 4 or 8 days in vitro and co-stained with DAPI.

Figure 3.2 ***continued…*** Top row scale bars = 500µm. Bottom row scale bars = 100µm. (***A***) Representative images of cultures infected with AdGFP ($5x10^7$vp/ml) at 0 days in vitro and imaged after 3 days; whole slice (top row) and CA1 region (bottom row) are presented. (***B***) Representative images of cultures infected with AdGFP-*REST* ($2x10^7$vp/ml) at 0 days in vitro and imaged after 3 days; whole slice (top row) and CA1 region (bottom row) are presented. (***C***) GFP positive cells in AdGFP and AdGFP-*REST* infected cultures were quantified and presented as a proportion of total DAPI-stained nuclei per image. * $p<0.05$ compared to AdGFP ($5.0x10^6$vp/ml) at 0 days in vitro. ** $p<0.01$ compared to AdGFP ($5.0x10^6$vp/ml) at 0 days in vitro. ¥ $p<0.01$ compared to AdGFP ($5.0x10^7$vp/ml) at 0 days in vitro and to AdGFP-*REST* ($2.0x10^7$vp/ml) at 0 days in vitro (mean±SEM). One way anova was used with Tukey's post-hoc test. Two images were taken from each region (CA1, CA3, dentate gyrus) per slice culture. Each condition had 2-4 slices cultures. Images from every region in every slice culture were pooled per condition to give N of 12 to 24 (N numbers written on bars).

3.3.2 Adenovirus infects cells throughout the organotypic hippocampal slice culture, beneath the surface glial layer

The potential mechanism of REST repression of *KCNQ2/3* would be specific to neurons as this is where *KCNQ2* and *KCNQ3* are expressed. However, REST is also expressed in astrocytes (Prada et al., 2011) so its modulation through adenoviral infection of astrocytes should be considered. In addition, the images for quantification of infection only gave 2-dimensional information, and it was important to ascertain whether the virus was penetrating through the slice or simply infecting surface cells. Immunohistochemistry was performed on 5 day old hippocampal slice cultures that had been infected at 0 days in vitro with $2.0x10^7$vp/ml Ad-GFP-*REST*. An anti-GFAP antibody was used to stain astrocytes and DAPI was used to mark all cell nuclei. Five-day old cultures were used so that early effects from slicing such as astrocyte proliferation would have had time to occur. Strong infection by adenovirus can be visualised as bright GFP-expressing cells in the representative Z stack images (Figure 3.3B) of GFP, DAPI and GFAP (red) and 3D reconstruction (Figure 3.3A) of GFP and GFAP (red). These appear to be evenly distributed throughout the imaged region of

the slice culture. The z stack goes all the way through the slice showing full penetration of the virus throughout the tissue. An organotypic hippocampal slice culture is between 150-400µm thick. The z stack is only 16µm deep due to compression of the tissue from the mounting procedure, which the author could not find a way to avoid. The layer of GFAP-positive cells across the top surface of the slice culture is believed to be the 'glial scar' caused by slicing. The GFAP positive cells are not observed to colocalise with GFP expression, suggesting that the virus does not infect astrocytes. GFP-positive areas may appear yellow in the front view 3D image. This is because some of the red GFAP-positive astrocytes occupy the same x/y plane as the GFP-positive cells. However, the GFAP-positive astrocytes occupy a higher z plane than the GFP-positive cells, as can be observed in Figure 3.3B. The even distribution of GFP-expressing cells throughout the full depth of the slice cultures suggests that viral dispersion throughout the slice is likely to occur before reactive gliosis forms the surface glial scar.

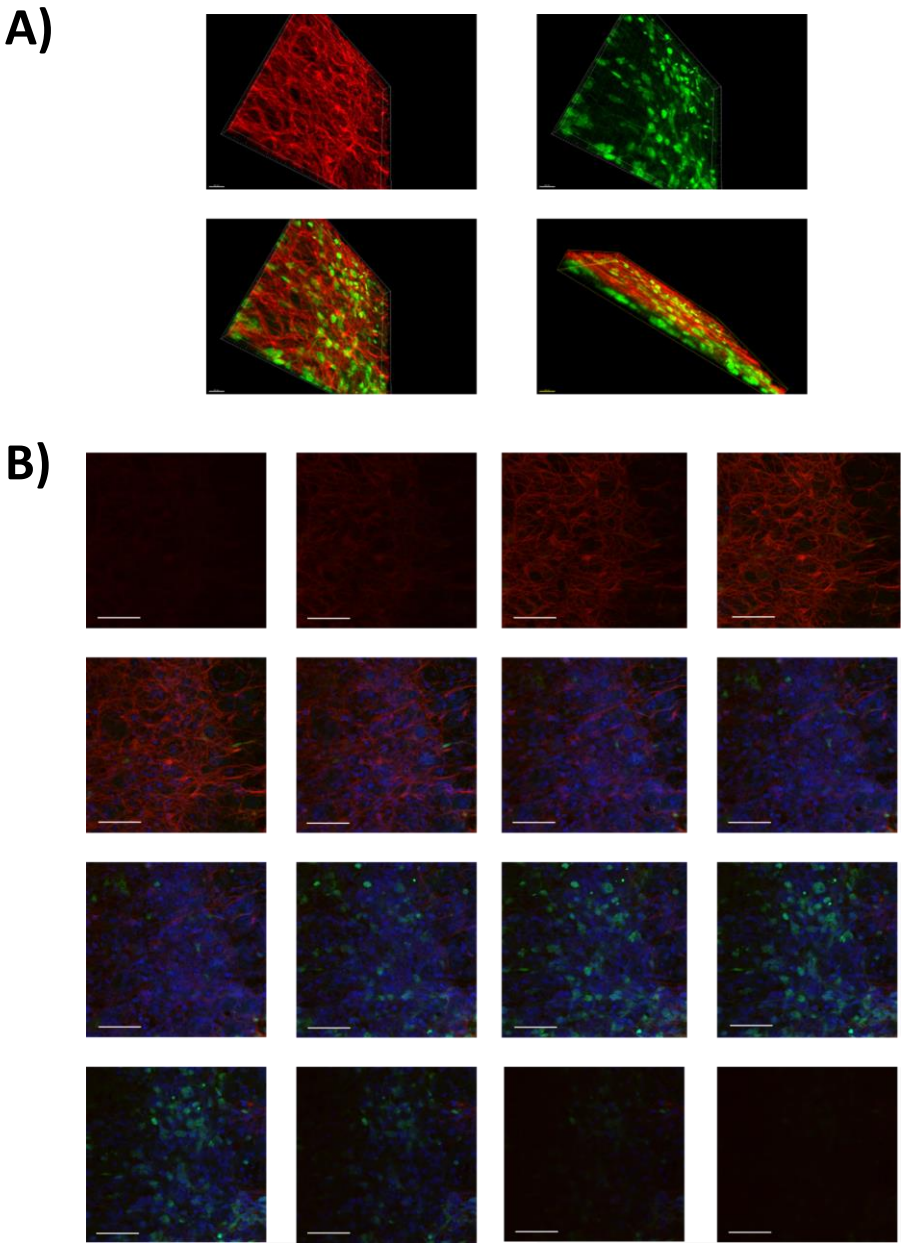

Figure 3.3. Adenovirus infects cells throughout the organotypic hippocampal slice culture, beneath the surface glial layer. Organotypic hippocampal slice cultures infected with AdGFP-*REST* ($2x10^7$vp/ml) and stained with antibodies against astrocytes (GFAP), and co-stained with DAPI. (***A***) 3D reconstruction showing GFP-expressing cells (green) with GFAP-positive cells (red). Scale bars = 20µm. (***B***) A representative z-stack image set top to bottom from CA1 region of an organotypic hippocampal slice culture, merging channels of GFP (green), GFAP (red) and DAPI (blue). Z stack images are 1µm apart on the z axis for a total depth of 16µm. Depth is lower than an organotypic hippocampal slice in culture due to a compression effect from the mounting procedure. Scale bars = 50µm.

3.3.3 GFP positive cells in adenoviral infected organotypic cultures show minimal cell death and continue to express GFP for weeks in culture

Toxicity, cell death and loss of gene expression resulting from viral infection of cells has been previously observed *in vitro* and *in vivo* (Cregan et al., 2000). It was important for us to establish an organotypic system which supports reliable adenoviral transgene expression for weeks in culture without causing significant cytotoxic damage. Therefore, ethidium homodimer was used to quantify cell death in adenoviral-infected GFP-expressing cells. After infection of slice cultures with AdGFP at day 0, they were stained with ethidium homodimer 3, 6 and 9 days later to assess levels of cell death. These time points were chosen to assess cytotoxic responses to viral infection early in the culture process. The slicing of organotypic cultures causes axotomisation and death of some cells, so cells infected with adenovirus and visibly expressing GFP were specifically assessed for cytotoxicity. Representative images of organotypic cultures infected with AdGFP and stained with ethidium homodimer after 3 days in culture are shown (Figure 3.4A). Overall, at 3, 6 and 9 days in culture there was less than 5% colocalisation of GFP expressing cells with ethidium homodimer stained cells (Figure 3.4B). Colocalisation values for each region at each timepoint are shown in Figure 3.4C (n=12 per group). Furthermore, ethidium homodimer staining is no higher in GFP-positive cells than in GFP-negative cells of the adenoviral infected slices. Proportions of red ethidium homodimer staining are 2.19±0.51% in GFP negative and 0.81±0.31% in GFP positive cells at 3DIV (n=36), 5.58±1.39% in GFP negative and 2.11±0.84% in GFP positive cells at 6DIV (n=18), and 0.53±0.12% in GFP negative and 0.41±0.17% in GFP positive cells at 9DIV (n=27, where n = number of images). Non-GFP expressing cells may have a higher likelihood of staining with ethidium homodimer due to many of them being astrocytes. GFP is not observed in astrocytes, but astrocytes may be particularly susceptible to death as a result of slicing. Viability, as proportion of total cells that are ethidium homodimer negative, is no different in AV-treated cultures (99.03±0.24%, n=81) than in non-AV-treated cultures (96.58±0.77%, n=78) across all 3, 6 and 9 DIV cultured slices. This demonstrates minimal toxicity from adenovirus at the titres used. An average of 11.53±0.52% total cells were infected across all conditions in this experiment.

I observed GFP expression in AdGFP-*REST* infected organotypic cultures to still be visible at 2 and 4 weeks in culture, with expression appearing to become slightly fainter over time (Figure 3.4D). This suggests adenoviral infection is stable over weeks in vitro, supporting earlier findings by other groups (Miyaguchi et al., 1999; Teschemacher et al., 2005). This will enable the use of adenoviral infection of hippocampal slice cultures for long-term monitoring of the effects of the REST and dominant negative REST transgenes.

A)

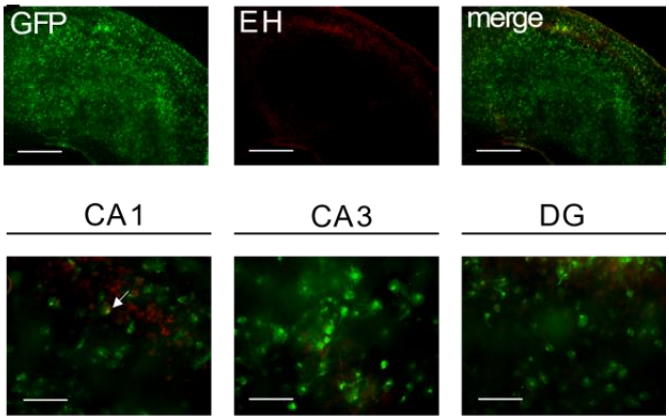

B)

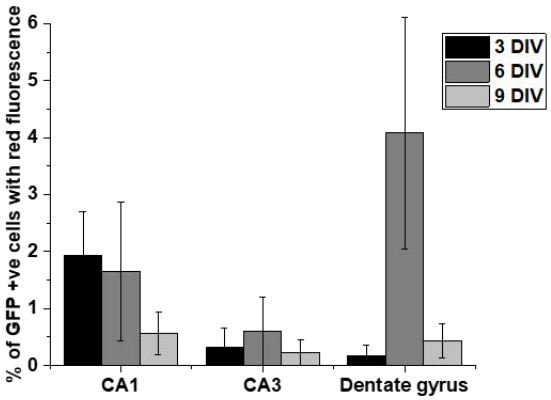

C)

	3 DIV	6 DIV	9 DIV
CA1	1.9±0.8%	1.65±1.2%	0.56±0.4%
CA3	0.33±0.3%	0.60±0.6%	0.23±0.2%
DG	0.18±0.2%	4.08±2.0%	0.44±0.3%

D)

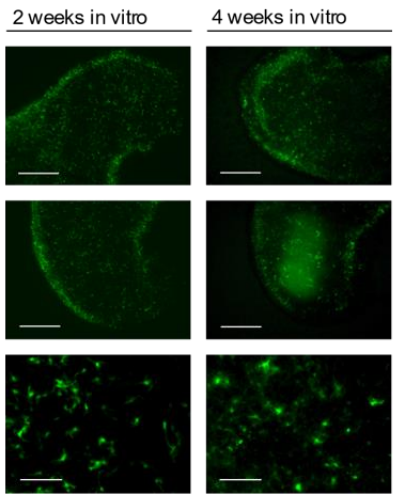

Figure 3.4. GFP positive cells in adenoviral infected organotypic cultures show minimal cell death and continue to express GFP for weeks in culture. ***(A)*** Cultures infected with $1x10^7$vp/ml AdGFP and stained with ethidium homodimer (EH) after 3 days in culture. Top row scale bar = 500µm. Bottom row = 100µm. White arrow shows GFP positive cell stained with ethidium homodimer. ***(B)*** Quantification of proportion of GFP positive cells which also show ethidium homodimer fluorescent signal in the CA1, CA3 and dentate gyrus regions at 3, 6 and 9 days in cultures infected with $1x10^7$vp/ml AdGFP. No significant difference between groups (p=0.0612, Kruskal-Wallis test). Three images taken per region per slice culture, and 2-4 slice cultures per condition. All images were pooled across slice cultures at each timepoint, separated by region, giving N = 6-12 images per region per timepoint. ***(C)*** Numerical values shown. ***(D)*** Images shown from CA3 regions of two independent cultures infected with AdGFP-REST ($2x10^7$vp/ml) and imaged at stated time points. Scale bars for top 2 rows = 500µm. Scale bars for bottom row = 100µm. Mean±SEM.

3.3.4 Adenovirus infects neurons and microglia in organotypic hippocampal slice cultures

Adenovirus was shown to infect cells of the organotypic cultures with high efficiency (Figure 3.2), but it was important to establish that the cell types infected include neurons. Adenoviral GFP reporter expression was not observed in surface astrocytes in organotypic cultures (Figure 3.3). Next, immunohistochemistry of AdGFP-infected organotypic cultures was performed to investigate GFP reporter expression colocalisation with markers for neurons (HUC/D, Figure 3.5A, B, G), microglia (Iba1, Figure 3.5C, D) and oligodendrocytes (OSP: Oligodendrocyte-specific protein, Figure 3.5E, F). GFP expression was observed at either high or low levels in different cells. Some of the cells expressing GFP strongly were colocalised with the HUC/D staining, but some of the cells expressing GFP brightly did not colocalise with HUC/D staining (Figure 3.5G), suggesting the strongly expressing cells were composed of both neuronal and non-neuronal cells. Some of the cells expressing GFP more weakly also colocalised with HUC/D (Figure 3.5A, B), as well as Iba1 (Figure 3.5C, D), and some very weak GFP expression appears to colocalise with OSP (Figure 3.5E, F). This

would suggest that adenovirus can infect neurons, microglia, and oligodendrocytes, respectively. The strength of the GFP signals were quantified for each cell type, and all GFP signals were found to be significantly above background, with background set as the visibly darkest areas within the imaged tissue. A normalised 4.3-fold increase above background of GFP expression was observed in cells showing colocalisation to HUC/D staining (HUC/D-positive=51.21±1.5, n=65; background=11.78±1.5, n=33; $p<0.001$, t-test; Figure 3.5A, B). This demonstrates adenovirus to infect neurons. GFP is also observed to colocalise with Iba1 staining (Figure 3.5C, white arrows mark Iba1-GFP colocalisation) with normalised GFP expression being increased 4.4-fold over background level (Iba1-positive=9.49±3.0, n=20; background=2.15±0.1, n=15; $p<0.001$, t-test; Figure 3.5D). This demonstrates that microglia are infected with adenovirus. Colocalisation of GFP and OSP is barely visible in the images (Figure 3.5E, white arrows mark OSP-GFP colocalization) but normalised GFP expression was increased 2.1-fold above background (OSP=1.84±0.3, n=20; background=0.89±0.3, n=15; $p<0.001$, t-test; Figure 3.5F). Although GFP expression is significantly above background in oligodendrocytes, it is only half as strong compared to background in oligodendrocytes as it is in neurons and microglia. This reflects the weak GFP signal in the OSP-positive cells in the images (Figure 3.5E), and overall suggests that adenoviral transgene expression is less successful in oligodendrocytes than neurons and microglia. This could be because the virus is less effective at infecting oligodendrocytes than neurons and microglia, or it could be that the CMV promoter has a weaker effect in oligodendrocytes. In conclusion, adenovirus infects neurons and microglia reliably, but viral transgene expression in oligodendrocytes is weaker in comparison.

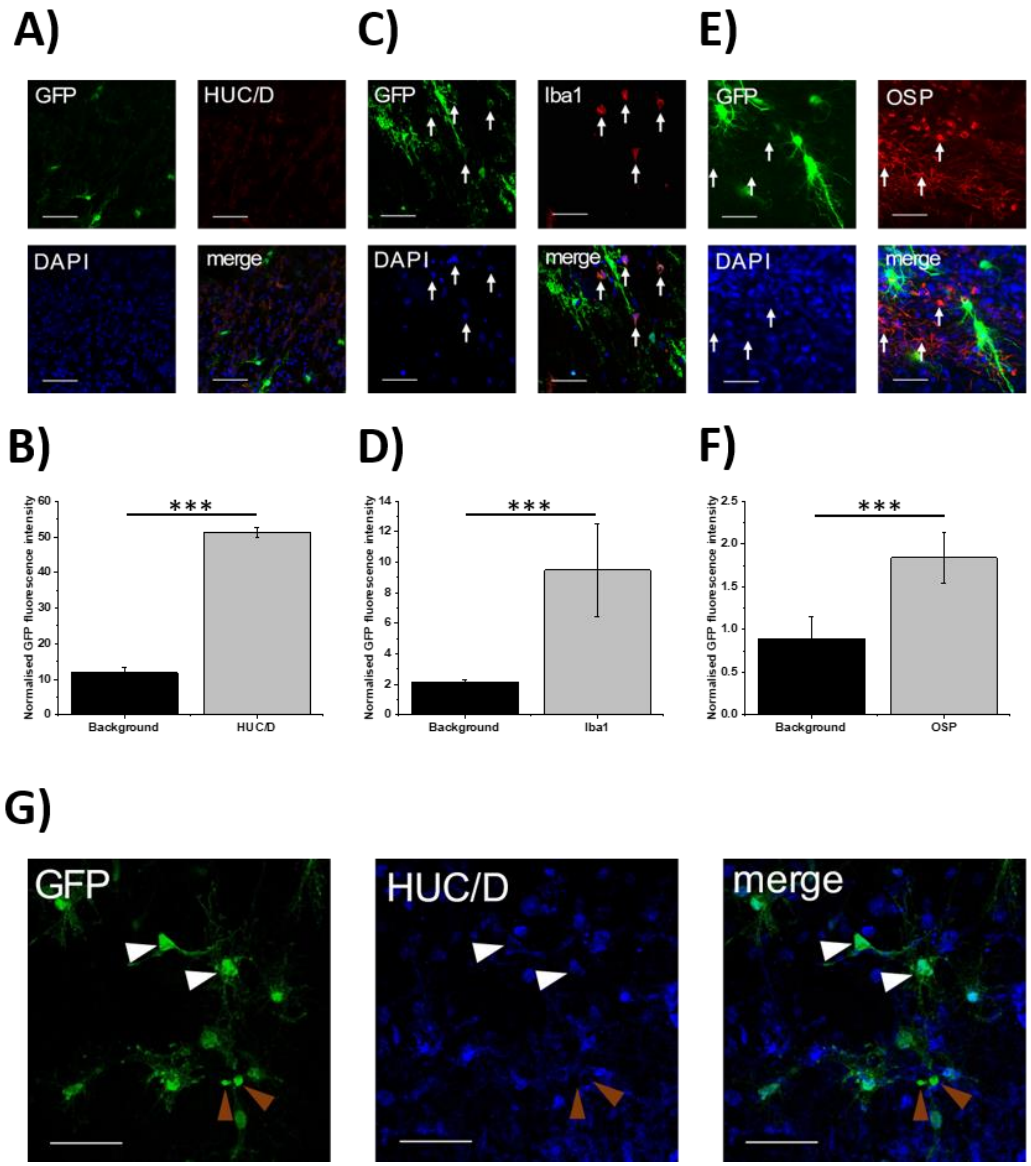

Figure 3.5. Adenovirus infects neurons, microglia and oligodendrocytes in organotypic hippocampal slice cultures. Cultures infected with AdGFP were immunostained with antibodies against neurons (HUC/D), microglia (Iba1) or oligodendrocytes [Oligodendrocyte-specific protein (OSP)]. (***A***) Representative immunohistochemistry images taken in CA1 region from single HUC/D-stained culture, co-stained with DAPI to mark all cell nuclei. (***B***) Quantification of GFP fluorescence intensity in HUC/D positive cells compared to background $p<0.001$, n=33-65 cells per condition (background or HUC/D positive cell). (***C***) Representative immunohistochemistry images taken in CA1 region from single Iba1-stained culture, co-stained with DAPI to mark all cell nuclei. White arrows show Iba1-positive cells. (***D***) Quantification of GFP fluorescence intensity in Iba1 positive cells compared to background $p<0.001$, n=15-20 cells per condition (background or Iba1-positive cell).

Figure 3.5 ***continued…*** (***E***) Representative immunohistochemistry images taken in CA1 region from single OSP-stained culture, co-stained with DAPI to mark all cell nuclei. White arrows show OSP-positive cells. (***F***) Quantification of GFP fluorescence intensity in OSP positive cells compared to background $p<0.001$, n=15-20 cells per condition (background or OSP-positive cell). (***G***) GFP expression and HUC/D staining show colocalisation in some brightly expressing cells (white arrows) but other brightly GFP expressing cells are HUC/D negative (brown arrows). Scale bars are 50µm. Mean±SEM.

3.3.5 Adenoviral infection of organotypic hippocampal slice cultures with Ad-GFP-*REST* causes REST overexpression in infected GFP-expressing cells

As stable adenoviral infection and resulting GFP reporter expression had been confirmed in organotypic neurons, I also wanted to confirm overexpression of the *REST* transgene in infected cells. To demonstrate an upregulation of REST protein, immonhistochemistry was performed on hippocampal slice cultures infected with AdGFP and AdGFP-*REST*, using an antibody against REST, with DAPI co-staining of cell nuclei. Colocalisation between REST and GFP was observed in the culture infected with AdGFP-*REST*, but no REST was observed in the AdGFP infected culture (Figure 3.6A. White arrows show REST positive cells). Quantification of REST signal showed a large increase of REST in GFP-positive cells from the culture infected with AdGFP-*REST* compared to GFP-positive cells from the AdGFP infected culture (Figure 3.6B; AdGFP-REST=20.49±2.8, n=109; AdGFP=2.46±2.1, n=59; $p<0.001$, t-test). In addition, a correlation was observed between REST and GFP signal intensities in GFP-expressing cells of the culture infected with AdGFP-REST (Figure 3.6C; n=109, R=0.55; $p<0.001$, Pearson). There may be variation in the correlation over different cells because of differences in levels of infection, and the antibody penetrating different cell types to different degrees. Regardless, the positive correlation suggests that the increased REST expression is due to the REST from the adenovirus. It is also apparent that the REST expression is occurring in the DAPI-positive cell nuclei (Figure 3.6D; White arrows show REST positive cells).

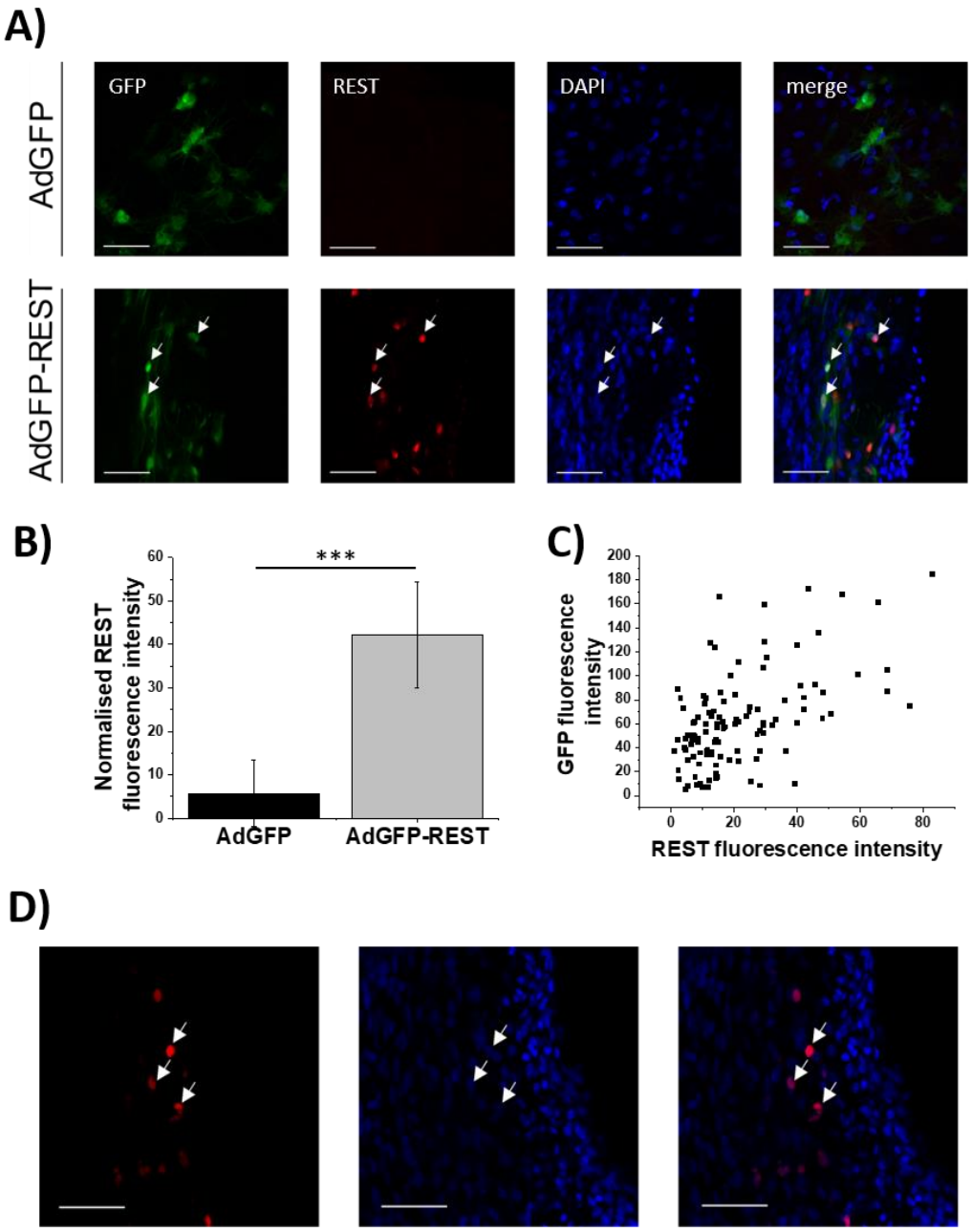

Figure 3.6. Adenoviral infection of organotypic hippocampal slice cultures with Ad-GFP-*REST* causes REST overexpression in infected GFP-expressing cells. Culture infected with AdGFP or AdGFP-*REST* was stained with antibodies against REST, and co-stained with DAPI to mark all cell nuclei. A) Representative immunohistochemistry images are presented. Shade of the colocalisation of red, green and blue may vary due to variations in how strong each colour is. Scale bars are 50µm. B) REST fluorescence intensity with background subtracted, and normalised to GFP fluorescence intensity per cell. C) Signal intensities from REST fluorescence plotted against signal intensities from GFP fluorescence from AdGFP-*REST* infected culture

Figure 3.6 *continued…* (Pearson's correlation, R = 0.55, p<0.001). *p<0.001. D) Representative immunohistochemistry images from an AdGFP-REST infected culture to show localisation of REST expression. White arrows mark 3 cell nuclei across all images to show complete colocalisation of REST expression with DAPI. N=59-109 GFP-positive cells in 1 slice per condition. Scale bars = 50µm. Mean±SEM.

3.4 The effects of adenoviral delivered REST modulation on KCNQ2/3 expression

3.4.1 *Kcnq2/3* expression is upregulated by HDAC inhibition but unaffected by REST modulation in hippocampal slice cultures

The endogenous expression of *Rest, Kcnq2* and *Kcnq3* was monitored over 12 days in culture through reverse-transcription quantitative PCR. All values were normalised to the reference gene Sdha which remained consistent across all sample groups. No significant differences in expression levels were observed between 4, 8 or 12 days in culture for *Rest, Kcnq2* or *Kcnq3* (p=0.0755, Figure 3.7). This suggests that these genes are not directly affected by post-slicing cell death, synaptic reorganisation and slice stabilisation.

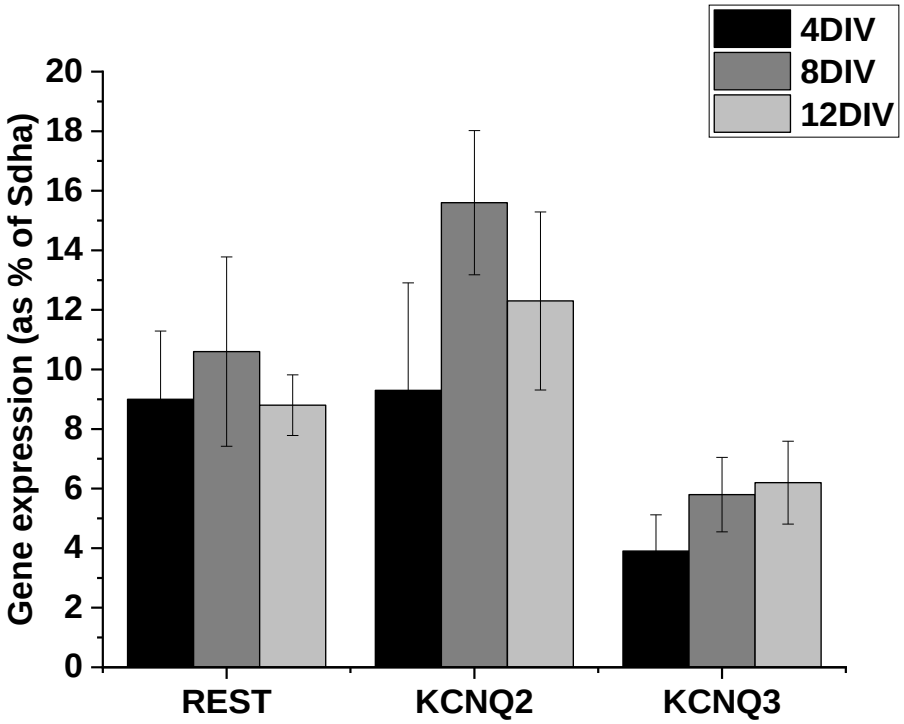

Figure 3.7. No significant changes in endogenous *Rest, Kcnq2* and *Kcnq3* mRNA expression are observed over time in organotypic hippocampal slice cultures. Reverse transcription quantitative PCR analysis of mRNA levels of *Rest, Kcnq2* and *Kcnq3* in organotypic hippocampal slice cultures, harvested for RNA extraction at 4, 8 and 12 days in vitro (DIV). Gene expression is represented as % of *Sdha* reference gene (Mean ± SEM, n = 9-14 samples). No significant differences observed between groups (p=0.0755, Kruskal-Wallis test).

In order to investigate whether REST represses *Kcnq2* and *Kcnq3* in the hippocampus I used qRT-PCR to quantify mRNA levels of these genes following full length and Dominant Negative *Rest* overexpression delivered to organotypic hippocampal cultures by adenoviral infection. Data was normalised to cyclophilin A (*CycA*) reference gene. In addition to *Kcnq2* and *Kcnq3*, I also quantified 3 additional REST target genes; *Sp1*, Superior Cervical Ganglion 10 (*Scg10*), and *Bdnf*. *Bdnf* mRNA levels were also investigated as a marker for epileptogenesis. Organotypic hippocampal cultures were infected with either AdGFP at $4x10^7$vp/ml, AdGFP-*REST* at $4x10^7$vp/ml, or AdGFP-DN*Rest* at $4.9x10^7$vp/ml and cultured for 8 days. Fluorescent images were taken to confirm thorough expression of the GFP reporter

indicating efficient infection (Figure 3.8A), appearing similar to earlier assays (Figure 3.2). SAHA (3μM) or vehicle was applied to the cultures for 48 hours, and cultures were harvested for RNA extraction and qRT-PCR. *REST* mRNA was shown to be 167-fold increased in AdGFP-*REST* infected cultures compared to AdGFP infected cultures ($p=0.011$, Figure 3.8B). DN*Rest* was increased 51-fold in AdGFP-DN*Rest* infected cultures compared to AdGFP infected cultures but this was not significant according to Tukey's post-hoc test due to a large variation. All cultures showed a DN*Rest* increase of at least 15.4-fold. This overexpression of *REST* demonstrates the organotypic cultures are overexpressing the DNA binding region of the human/mouse *REST* sequence to varying degrees. Interestingly, SAHA increased the exogenous *REST* expression even further. Cultures infected with AdGFP-*REST* and exposed to SAHA had 3.2-fold greater *REST* expression than those infected with AdGFP-*REST* without SAHA ($p=0.001$), suggesting HDACs may be regulating the exogenous *REST* and the HDAC inhibition allows a de-repression effect of *REST*. However, this effect was not observed for dominant negative *Rest*. Endogenous *Rest* was also quantified in the cultures and no significant changes were observed between groups, as would be expected (Figure 3.8C).

No effects are observed on *Bdnf* expression by infection of any of the 3 viral constructs alone (Figure 3.8D), which was surprising as *Bdnf* is a target gene of REST. Average *Bdnf* expression in the SAHA-treated groups was not significantly different than in the non SAHA-treated groups, due to a large variation in expression between samples. Expression of one of the SAHA-treated AdGFP infected cultures was 7.8-fold greater than the average of the AdGFP infected cultures without SAHA. The other three SAHA-treated AdGFP infected cultures were no greater than the average of the AdGFP infected cultures without SAHA (0.19±0.17% of CycA). Similarly, one of the SAHA-treated AdGFP-*REST* infected cultures was 17.2-fold greater than the average of the AdGFP-*REST* infected cultures without SAHA (0.025±0.01% of CycA). The other three SAHA-treated AdGFP-*REST* infected cultures were just 2.4-fold, 1.2-fold and 2.4-fold greater than the average of the AdGFP-*REST* infected cultures without SAHA. Finally, *Bdnf* expression in one of the SAHA-treated AdGFP-DN*Rest* infected cultures was 7.2-fold higher than the average of the AdGFP-DN*REST* infected cultures without SAHA. Two of the other cultures were no higher in *Bdnf* than the average of the AdGFP-DN*Rest* infected cultures without SAHA, and one was increased by 81%.

It seems that SAHA caused a large increase in *Bdnf* expression in one of four organotypic cultures in each group, while leaving *Bdnf* expression of the other 3 cultures relatively unchanged. This suggests HDACs do not have an equal amount of regulatory power over *Bdnf* in all cultures. Subtle environmental differences may influence the activity of epigenetic modifiers differently between cultures, and *Bdnf* expression may be particularly sensitive to these variations.

No effects are observed on *Kcnq2* (Figure 3.8E) or *Kcnq3* (Figure 3.8F) expression by infection of any of the 3 viral constructs alone. This suggests that increased REST levels may be insufficient to cause measurable repression of *Kcnq2* or *Kcnq3*, and blocking endogenous REST does not induce a de-repression effect of *Kcnq2* or *Kcnq3*. However, up to 41% of total cells were expected to be infected (Figure 3.2), which could have diluted any effects of the REST modulation, and could also account for the lack of observed changes. HDAC inhibition from SAHA exposure resulted in upregulated *Kcnq2* and *Kcnq3* expression in the AdGFP-infected cultures. SAHA-treated AdGFP-infected cultures showed a 4.7-fold increase in *Kcnq2* compared to their vehicle-treated counterparts ($p=0.009$). Similarly, SAHA-treated AdGFP-infected cultures showed a 2.1-fold increase in *Kcnq3* compared to their vehicle-treated counterparts, but this difference was not significant. No significant differences were observed in the AdGFP-*REST* and AdGFP-DN*Rest* infected cultures treated with SAHA compared to their vehicle-treated counterparts. No effects were observed on expression of the REST target gene *Scg10* from infection with any of the 3 viral constructs or exposure to SAHA (Figure 3.8G). Similarly, no effects were observed on *Sp1* expression from infection with any of the 3 viral constructs or exposure to SAHA (Figure 3.8H). This suggests *Scg10* and *Sp1* are not being repressed by HDACs in the hippocampus under normal conditions. *Scg10* and *Sp1* may not be repressed by REST in the hippocampus, or infection efficiency may have been insufficient to induce effects on REST target genes. The data does not provide information about Sp1 regulation of *Rest, Kcnq2* or *Kcnq3*.

In summary, infection of organotypic hippocampal cultures with AdGFP, AdGFP-*REST* and AdGFP-DN*Rest* caused significant expression of these transgenes in the cultures, but this did not lead to significant changes in expression of endogenous *Rest, Bdnf, Kcnq2, Kcnq3, Scg10* or *Sp1*. Exposure of organotypic cultures to the HDAC

inhibitor SAHA caused a significant upregulation of expression of *Kcnq2*, suggesting HDACs are involved in endogenous repression of *Kcnq2* in normal conditions.

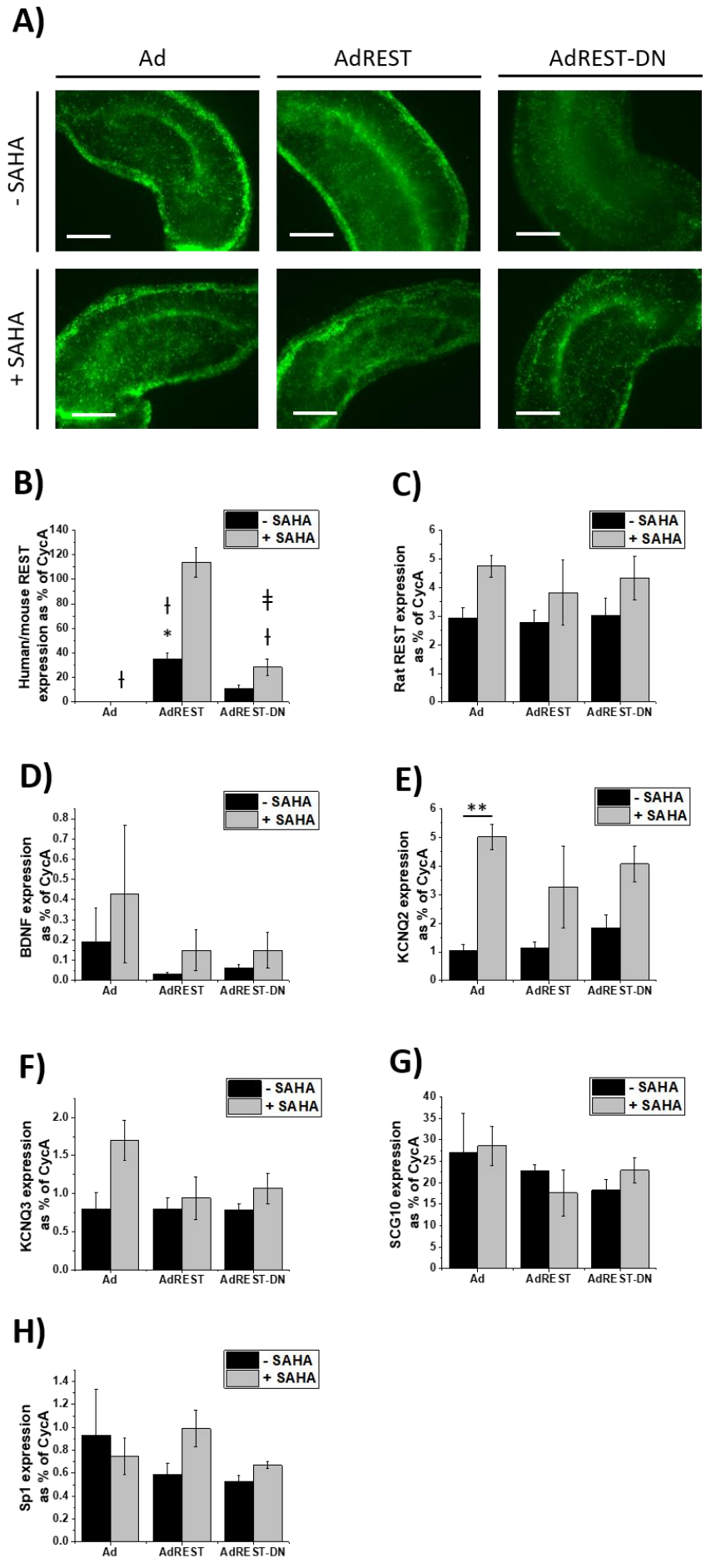
A)
Ad
AdREST
AdREST-DN
- SAHA
+ SAHA
B)
Human/mouse REST expression as % of CycA
C)
Rat REST expression as % of CycA
D)
BDNF expression as % of CycA
E)
KCNQ2 expression as % of CycA
F)
KCNQ3 expression as % of CycA
G)
SCG10 expression as % of CycA
H)
Sp1 expression as % of CycA
- SAHA
+ SAHA
Ad
AdREST
AdREST-DN

Figure 3.8. Changes in mRNA expression in *Bdnf, Rest, Kcnq2, Kcnq3, Scg10* and *Sp1* following infection with adenovirus conferring REST overexpression or functional knockdown, and exposure to SAHA. (***A***) shows representative fluorescent images of organotypic hippocampal slice cultures infected with AdGFP, AdGFP-*REST* or AdGFP-*Rest*-DN. GFP marker (green) indicates infected cells. Scale bars 500µm. (***B-H***) Reverse transcription quantitative PCR analysis of mRNA levels of human/mouse *REST* (***B***), endogenous rat *Rest* (***C***), *Bdnf* (***D***), *Kcnq2* (***E***), *Kcnq3* (***F***), *Scg10* (***G***) and *Sp1* ***(H)*** in organotypic hippocampal slice cultures infected with Ad, Ad*REST* or Ad*Rest*-DN, with or without SAHA exposure. Data are normalised to cyclophilin A (*CycA*) reference gene and expressed relative to Ad – SAHA (mean ± SEM; n = 4 samples; *p < 0.05, **P < 0.01 compared to Ad; ł p < 0.01 compared to AdREST + SAHA; ǂ p < 0.05 compared to Ad + SAHA). All gene data sets analysed by ANOVA with Tukey's post-hoc test except *Bdnf*, which was analysed by Kruskal-Wallis test.

3.4.2 REST overexpression in organotypic cultures does not affect Kv7.2 fluorescence intensity

In order to validate the Kv7.2 antibody used in this thesis work, some experiments were conducted by a colleague, Fred Jones (Ph.D. student) without involvement of myself. The data gathered by him will be described here. Cultured HEK-293 cells were transfected with a *KCNQ2*-YFP plasmid and immunostained with the Kv7.2 antibody, and co-stained with DAPI to mark cell nuclei. Confocal images show complete colocalisation between the YFP signal and the Kv7.2 antibody signal (Figure 3.9A, 4 left images), demonstrating that the Kv7.2 antibody is capable of binding to cells transfected with the *KCNQ2*-YFP plasmid. In addition, brain tissue was taken from a mouse with a *Kcnq2* genetic knockout and immunostained for Kv7.2 and co-stained with DAPI. No Kv7.2 signal was observed in the *Kcnq2* knockout mice (Figure 3.9A, right image). Together this data identifies that the Kv7.2 antibody binds specifically to the Kv7.2 protein.

Following a lack of observed change in *Kcnq2* and *Kcnq3* mRNA in organotypic hippocampal cultures overexpressing REST, I wanted to also examine the levels of Kv7.2 protein expression for changes. I infected the organotypic cultures with either

AdGFP or AdGFP-*REST* and immunostained the cultures with antibodies against neurons (HUC/D) and Kv7.2. An average of 64% of GFP-expressing cells per image were also HUC/D positive, demonstrating these cells as neurons. Representative images of Kv7.2 and HUC/D co-staining following infection with AdGFP or AdGFP-*REST* are shown in figure 3.9B. White arrows show GFP-expressing cells which are HUC/D-positive (neurons) and brown arrows show GFP-expressing cells which are HUC/D-negative (non-neuronal cells). Average Kv7.2 fluorescence intensity was quantified in cells that were positive for both GFP expression and HUC/D staining, defining adenoviral-infected neurons. When Kv7.2 fluorescence intensity from infected cells is normalised to average Kv7.2 fluorescence intensity of uninfected cells from the same image, no difference is observed between average Kv7.2 fluorescence intensity in AdGFP or AdGFP-*REST* infected neurons (Figure 3.9C). This demonstrates that Kv7.2 protein is not observed to be repressed in the hippocampus following adenoviral overexpression of REST. This supports the finding that REST overexpression also did not cause a reduction in *Kcnq2* mRNA (Figure 3.9E), and suggests that in organotypic hippocampal slice cultures overexpression of adenoviral REST does not cause repression of *Kcnq2* mRNA or the Kv7.2 protein it encodes.

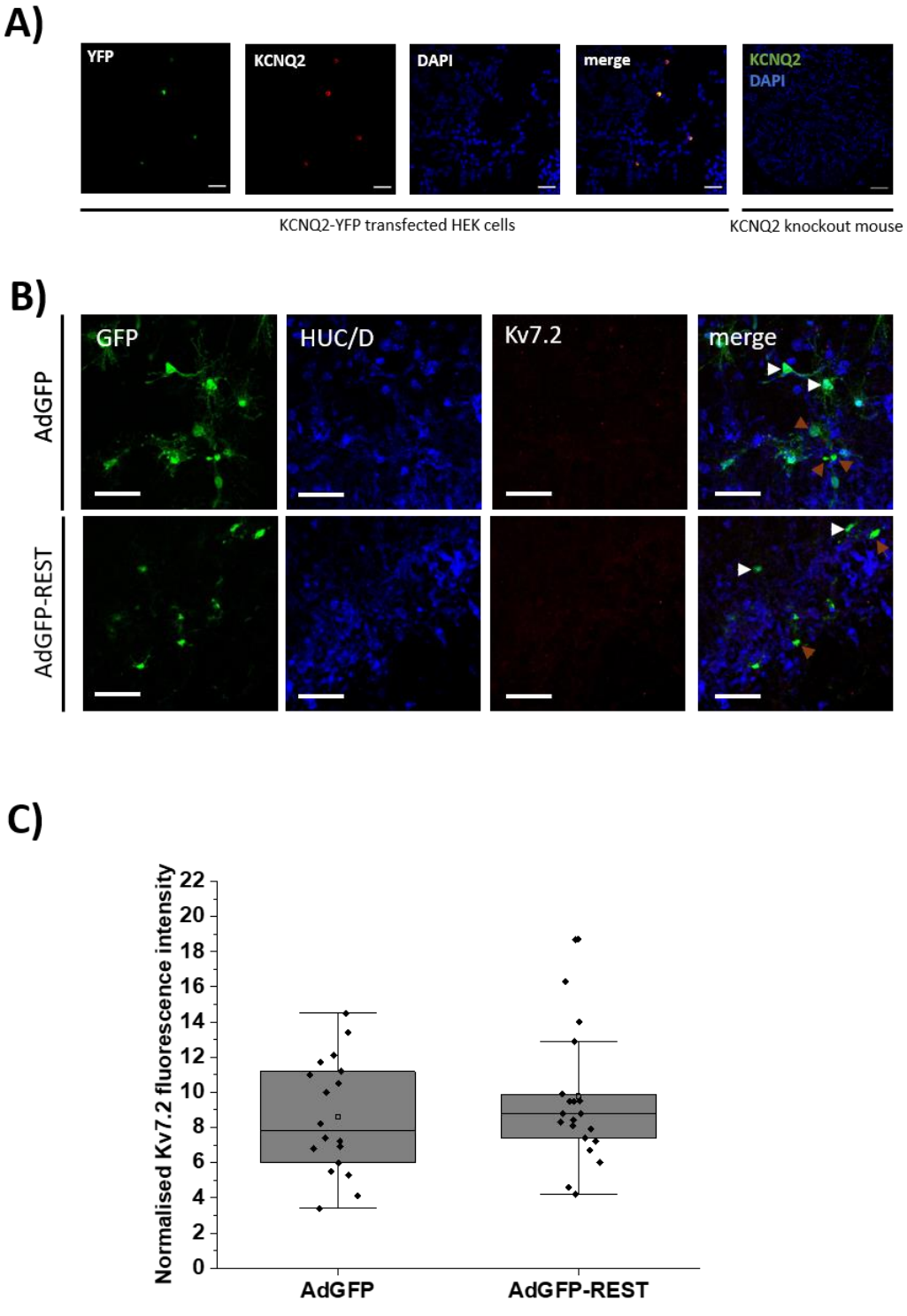

Figure 3.9. REST overexpression in organotypic cultures does not affect Kv7.2 fluorescence intensity. (A) Representative confocal images of cultured DRG neurons transfected with a KCNQ2-YFP plasmid (left 4 images), and DRG from a *Kcnq2* knockout mouse (right image) validate efficacy and specificity of Kv7.2 antibody. Transfected DRG neurons were immunostained with primary antibody against Kv7.2,

Figure 3.9 *continued…* and Alexa Fluor-555 secondary antibody, and co-stained with DAPI. Merged image shows example of colocalisation of Kv7.2 and YFP. DRG from *Kcnq2* knockout mouse (right image) was immunostained with primary antibody against Kv7.2, and Alexa Fluor-488 secondary antibody, and co-stained with DAPI. Images kindly received from Fred Jones of the Gamper Group, University of Leeds. All work conducted for Figure 3.9A conducted by Fred Jones during his Ph.D. **(*B*)** Representative confocal images of hippocampal slice cultures infected with adenovirus carrying a GFP plasmid or a GFP-*REST* plasmid. Infected cells were identified by GFP expression (green). Cultures were immunostained with primary antibodies against Kv7.2 and the neuronal marker HUC/D, and Alexa Fluor-488 (HUC/D) and Alexa Fluor-555 (Kv7.2) secondary antibodies. Merged images show examples of colocalisation of GFP-expressing cells with HUC/D positive neurons (white arrows), and GFP-expressing cells which are HUC/D negative (non-neuronal cells, brown arrows). Scale bars 50µm. (***C***) Box plot shows Kv7.2 fluorescence intensity in GFP-expressing cells from AdGFP and AdGFP-*REST* infected cultures normalised to Kv7.2 intensity from uninfected cells in the same image (n = 18-21 images from 6-8 slice cultures per group. 3-5 cells analysed per image to give an average). No difference observed between groups (p=0.481, Mann-Whitney U test).

3.5 Discussion

3.5.1 Organotypic hippocampal slice cultures are viable over 21 days in culture

In order to use organotypic hippocampal slice cultures in this project to analyse the regulation of KCNQ2 and KCNQ3 by REST in the hippocampus, the viability of the organotypic cultures needed to be optimised. Following the implementation of optimisation steps outlined in Results, cultures showed 88-100% cell viability throughout the 21-day culture period, with at least 98% viability for the majority of the time points. Other groups have similarly found less than 1% cell death in control cultures over 7 days in vitro (Sullivan et al., 2002) and at 15 days in vitro (Simões Pires et al., 2014). The slightly reduced viability I observed at 3 days in vitro was likely to reflect the immediate damage done from slicing. The reduction in viability at 9 (all areas) and 12 (CA1 only) days in vitro could account for a secondary stage of cell loss following synaptic reorganisation within the slice. Caution has been advised when using organotypic cultures for experiments during the first few days (Romero-Leguizamón et al., 2019; Wang and Andreasson, 2010). This is because slicing causes reactive astrogliosis and Ca^{2+} release, and the slices take up to a week to flatten down to the membrane. Axotomy of afferent connections from areas not included in the slice causes cell death and regeneration, though many connections are also believed to be unaffected. The loss of afferent and efferent connections induces a reorganisation of axotomized axons to connect to new fields within the slice (Humpel, 2015). Cell degeneration from slicing is reported to last up until 7 days in vitro, with secondary cell death occurring at 14 days in vitro (particularly in the CA3 region), before reducing by 21 days (Pozzo Miller et al., 1994). In contrast, other groups have observed a reduction in cell death at earlier timepoints. Propidium iodide fluorescence increased from 2 to 6 to 10 days in vitro, but not after 10 days (Paci et al., 2017). It has also been claimed that 6 to 18 days in culture is the ideal time to take cultures for experiments as this is when viability is highest (De Simoni and Yu, 2006). However, my assay showed cell death at 9 days only, with a return to normal 3 days later, which does not fit with previous observations of slicing-induced secondary cell death. As different slice cultures were imaged for each timepoint, this result could be caused by damage done to the slices in that group during preparation, rather than being a true representation of all slices at that timepoint. My results suggest that overall levels of

cell death are low throughout culture, suggesting that this would not significantly interfere with experiments at any timepoint.

3.5.2 Adenoviral infection can efficiently deliver the GFP reporter and transgene *REST* to neurons in organotypic cultures

Most groups previously have used the microinjection method to infect mature organotypic cultures (Wiegert et al., 2017). However, when the infected cells from hippocampal slice cultures infected through the microinjection method were quantified, it showed only around 100 infected cells around the injection site (Ehrengruber et al., 2001). Wanting a more uniform distribution of slice infection, the present study utilizes the droplet method. The bathing of organotypic cultures in virus-medium solution just a few hours after plating was successful in achieving a thorough infection throughout the slice. Other groups have previously tried this method of bathing the slice cultures in viral solution soon after plating, but cell infection was not quantified so efficiency was hard to determine from their results (Avaliani et al., 2016; Avaliani et al., 2014; Schätzle et al., 2016; Selkirk et al., 2005). Images from one group showed what appears to be a good infection coverage, and adeno-associated virus was manipulated to target neurons, astrocytes, microglia or oligodendrocytes specifically, though use of specific promoters (Croft et al., 2019). My results demonstrate that using the droplet method to expose hippocampal slice cultures to adenovirus within a few hours of slice plating allows up to 41% of cells in the slice to be infected. Infecting soon after plating avoids the barrier of the glial scar, which I believe prevents infection in more mature slice cultures. The glial scar forms between day 0 and day 3 of culture in response to the slicing of the tissue, and is associated with an increase in GFAP staining (Gerlach et al., 2016). Glial scars occur due to reactive gliosis which follows CNS trauma (Sofroniew, 2009). The organotypic cultures are infected with virus before the glial scar has a chance to develop, allowing the virus to fully disperse through the slice. In this way, the droplet method is highly efficient and also avoids disruption of the tissue with a micropipette. Furthermore, GFP-expressing cells were observed throughout the full depth of the slice, demonstrating that the droplet method at 0 days in culture is sufficient to allow full viral penetration through the slice.

A thorough infection of cells had been demonstrated but as the cultures were only

stained with DAPI to mark all cell nuclei, this did not differentiate one cell type from another. To allow later investigation into *Kcnq2* and *Kcnq3* expression and their effect on neuronal excitability, it was required to examine whether the adenoviral constructs infect neurons and/or other cell types such as glia. No colocalisation was observed between GFP expression and the GFAP staining of the glial scar on the slice surface. This was unexpected because previously infection of organotypic hippocampal slice cultures with adenovirus has been reported as infecting mainly glial cells (Ehrengruber et al., 2001; Robert et al., 1997), or infection of both neurons and glia (Glover et al., 2002; Miyaguchi et al., 1999). It is possible that the adenovirus did infect astrocytes on the slice surface, which then proliferated during reactive gliosis, diluting the GFP to an undetectable level. However, astrocyte proliferation likely results in a 2-3-fold increase in astrocyte number (Yong, 1992), which would seem insufficient for diluting the GFP to this extent.

Astrocytes would be expected to be present throughout the full depth of the hippocampal slice cultures, but the GFAP staining was only observed at the slice surface. It seems likely that astrocytes were present throughout the slice, but the GFAP antibody did not penetrate through the slice fully to stain them. Therefore, I cannot establish from these results with any certainty whether adenovirus infected astrocytes or not. Adenovirus has been shown to successfully infect primary neuron cultures in vitro (Ehrengruber et al., 1997; Robert et al., 1997). However, as mentioned above, the success of infection of neurons in organotypic hippocampal slice cultures with adenovirus has been mixed (Ehrengruber et al., 2001; Robert et al., 1997). Both neurons and glia were observed to be infected in mature slice cultures (Glover et al., 2002). Another group found it necessary to expose cultures to collagen and the glial cell growth inhibitor cytosine beta D arabinofuranoside hydrochloride (AraC) to achieve infection of both neurons and glial cells in mature slice cultures (Miyaguchi et al., 1999). I observed adenoviral infection of neurons and microglia, with neurons showing a greater GFP reporter fluorescence intensity than microglia. It seems likely that the greater fluorescing cells are infected with more copies of the adenovirus than the lesser fluorescing cells, allowing them to express multiple copies of the GFP transgene. HUC/D colocalisation is observed in cells showing high levels and lower levels of GFP fluorescence, demonstrating neuronal infection. In addition, Iba1 showed colocalisation with cells showing low levels of GFP fluorescence,

demonstrating adenoviral infection and GFP expression in microglia. The lack of observed colocalisation of any cells showing high levels of GFP fluorescence with Iba1, in contrast to HUC/D, supports the finding that adenovirus infects neurons more readily than microglia. The data suggest adenoviral GFP is expressed in oligodendrocytes at very low levels, which could be due to fewer copies of the virus penetrating the cell or could be because the CMV promoter is expressed more weakly in these cells. Adenovirus has previously been observed to infect neurons, microglia, and oligodendrocytes, and my results support these findings (Uchida et al., 2012). The development of a technique for efficient adenoviral infection of neurons will allow the delivery of REST transgenes to test for regulation of neuronal *Kcnq2/3* expression.

A common problem with using adenoviral vectors is toxicity (Cregan et al., 2000) so this was assessed in the organotypic cultures. Ethidium homodimer assays showed less than 5% death in cells of infected organotypic hippocampal slice cultures over 9 days in culture, which was observed to be similar to the rate of cell death in uninfected cultures (results not shown). While some ethidium homodimer-stained dead cells were observed from the images, few were found to colocalise with bright GFP expression, suggesting toxicity to cells was not a concern here. Images were only taken every 3 days. However, when toxicity is observed from viral infection of cells, it is observed to continue 24 and 48 hours later (Sato et al., 2004; Stecher et al., 2001). Another group measured protein synthesis as a marker of Ad5-induced cytotoxicity and saw continued reduction to 90%, 70%, 70% and less than 40% that of control cultures at 3, 5, 7 and 10 days post-infection, respectively (Easton et al., 1998). Together these studies support the idea that toxicity is continuous, and if a burst of cell death occurred in my cultures on an unassessed day it would still have been visible one or two days later when the cultures were stained and imaged. A similar percentage of ethidium homodimer positive cells were observed at 3, 6 and 9 days, suggesting they were not cleared away before re-imaging.

In line with the lack of observed toxicity in the cultures from the adenoviral infections, the GFP expression from adenoviral infected cultures was observed as far as 4 weeks after infection with a gradual diminishment of expression observed over time, supporting previous results (Miyaguchi et al., 1999). This demonstrates adenovirus to be particularly suitable for in vitro gene transfer studies. In comparison, semliki forest

virus showed reporter gene expression for just 1-2 days post-infection before depleting, which was proposed to be due to instability of the semliki forest viral genome. Lentivirus and adeno-associated virus (AAV) gave very low expression for the first few days in culture and then gradually increased from 6-14 days in culture. The delay in expression was believed to reflect the time taken for the AAV single stranded genome to turn into large concatemers of double stranded DNA, and for lentiviral RNA to reverse transcribe and integrate into the host cell genome (Ehrengruber et al., 2001). The continued expression of adenoviral reporter GFP through 2 to 4 weeks in culture suggests that adenovirus is more suitable for in vitro gene delivery than other virus types such as semliki forest virus, AAV or lentivirus.

As the adenoviral infection of the organotypic cultures was demonstrated to be robust, infecting neurons without significant toxicity, evidence of the presence of the delivered *REST* transgene was sought. Infection of the organotypic cultures with adenovirus carrying the transgene *REST* resulted in clear overexpression of REST protein in cell nuclei. However, as cell types were not stained, it is not clear whether the visible REST colocalisation with nuclear DAPI was occurring in neurons or other cell types. The localisation of REST has not been previously examined in organotypic hippocampal slice cultures. However, in postmortem human brain samples, REST was also found in cell nuclei (Kawamura et al., 2019). It is likely that the localisation of REST is quite variable, depending on whether it is needed for repression of its target genes at any time. During ageing, REST levels in the nucleus increase over time which helps to prevent neurodegeneration. Dysfunction of this natural nuclear REST accumulation is implicated in the development of Parkinson's disease, Alzheimer's disease, dementia with Lewy bodies and frontotemporal dementia. On the other hand, too much REST in the nucleus can lead to Huntington's disease. The wild-type huntingtin protein binds to REST and sequesters it in the cytoplasm, but the mutant huntingtin protein present in Huntington's disease is incapable of this, allowing excessive levels of REST to accumulate in the nucleus (Zuccato et al., 2003). The exact mechanism for the translocation of REST from the cytoplasm to the nucleus is not yet known. However, kainate exposure in cultured hippocampal neurons can cause REST to translocate from the cytoplasm to the nucleus (Spencer et al., 2006), suggesting its translocation may be affected in epilepsy pathogenesis, as is its function (see Introduction). Kainate causes an increase in overall REST expression, so the

increased translocation to the nucleus may reflect a general increase in REST production and function in order to repress a large array of target genes during epileptogenesis.

3.5.3 REST overexpression does not induce repression of *Kcnq2*/Kv7.2 in organotypic hippocampal cultures

The promoters of *KCNQ2* and *KCNQ3* were previously shown to be regulated by REST in vitro through luciferase assay, with REST overexpression causing downregulation of *Kcnq2* and *Kcnq3* expression in DRG neurons (Mucha et al., 2010). I aimed to investigate this mechanism in organotypic hippocampal slice cultures to determine if it may be relevant to epileptogenesis. Initially I examined mRNA expression levels of endogenous *Rest, Kcnq2* and *Kcnq3* over time in culture, and saw no significant changes. This suggests that none of the tissue damage incurred by slicing or the resulting synaptic reorganisations affected these genes at an observable level. The endogenous levels of these genes had not been previously measured in organotypic cultures. It is logical that they would be maintained at similar levels in healthy tissue obtained from young rats and cultured in normal conditions. REST is expressed at low levels in the brain post-development (Palm et al., 1998), and as its regulation of its many target genes may depend critically on its cellular levels, its expression is likely to remain stable except when affected by metabolic stress (Butler-Ryan and Wood, 2021b). *Kcnq2* has been shown to express at constant levels in the mouse brain between P7 and P90, while *Kcnq3* was observed to gradually increase over the same time period (Tinel et al., 1998). Similar results were observed in superior cervical ganglion neurons (Hadley et al., 2003). It is likely that my analysis did not extend for long enough to see an increase in *Kcnq3*, if this effect was present. Using quantification from western blot, samples were required from P3 to P90 to observe the increase, and my time period only spanned 4 to 12 days (Tinel et al., 1998).

The same adenoviral construct used by Mucha and colleagues was used in the present study to investigate the effects of REST overexpression on expression of *KCNQ2* and *KCNQ3* in organotypic hippocampal cultures. Infection of organotypic hippocampal cultures with all 3 viral constructs led to a thorough transgene expression, confirmed by visualised GFP reporter and significant increases in mRNA copies of the *REST*

DNA binding domain. However, overexpression of *REST* or dominant negative *Rest* alone had no effect on endogenous *Rest*, or mRNA levels of the REST target genes *Bdnf, Kcnq2, Kcnq3, Scg10* or *Sp1*. The lack of change in *Kcnq2* and *Kcnq3* was surprising, as the same adenoviral REST construct caused around a 20% reduction in *KCNQ2* and 40% reduction in *KCNQ3* mRNA in DRG neurons (Mucha et al., 2010). The lack of effect on *Kcnq2* and *Kcnq3* expression in the present study could be due to the heterogeneous nature of the hippocampal tissue. It is likely that less than half of cells in the organotypic culture are expressing the transgenes, and this will dilute any effects in the quantification. Large overall increases in human/mouse REST mRNA and protein are demonstrated, but infected cell types are a mixture of neuronal and non-neuronal. Colocalisation of the viral GFP reporter with the neuronal marker HUC/D confirms maintenance of REST overexpression in infected neurons. However, only 64% of infected cells were neurons, which provides an additional diluting factor to neuronal REST. As 64% of 41% infected cells equates to 26% of total cells in the organotypic culture being infected neurons, overall neuronal REST overexpression could be insufficient to cause observable change in *Kcnq2/3* expression levels. Alternatively, a lack of change in *Kcnq2* and *Kcnq3* expression could be due to differences in intracellular mechanisms controlling REST regulation of *Kcnq2* and *Kcnq3* between peripheral and central neurons. While little is known about regulation of neuronal *Kcnq2/3* expression, the signalling pathways governing Kv7 channel function have been found to work in very different ways in peripheral neurons, hippocampal pyramidal CA1 neurons and dentate gyrus granule cells (Carver and Shapiro, 2019). Therefore, there is no reason to think such differences could not also occur in regulating the expression of *Kcnq2* and *Kcnq3*. Increased expression of other factors may be required in the hippocampus for REST to bind and repress *Kcnq2* and *Kcnq3*, which are limited in this model. These could include essential REST co-factors such as CoREST or mSin3A. The lack of changes in REST target genes *Bdnf, Scg10* and *Sp1* could be due to insufficient infection as described, or could be because REST is not actively repressing these genes in the hippocampus.

Histone deacetylation was investigated because REST recruits HDACs to repress its target genes (Ooi and Wood, 2007). Inhibition of HDAC activity caused *Kcnq2* expression to increase, suggesting a de-repression effect had occurred. This suggests that *Kcnq2* is being actively repressed by histone deacetylation in the hippocampus.

No investigations of the regulation of *KCNQ2/3* expression by histone deacetylation have been reported in any model. However, the HDAC inhibitor sodium butyrate prevents limbic epileptogenesis in the kindling model (Reddy et al., 2018). Furthermore, the antiepileptic drug valproic acid inhibits HDACs and has been described to lower neuronal excitability by preserving the Kv7 current (Kay et al., 2015). My results suggest that HDACs repress *Kcnq2*. Therefore, in addition to a protection over Kv7 channel function, it is possible that HDAC inhibitors could enhance Kv7 current through upregulation of expression of the KCNQ2 gene, contributing to their antiepileptic properties. HDAC inhibition caused a large increase in *Bdnf* mRNA levels in a quarter of all organotypic cultures exposed, while being relatively unchanged in the rest. HDAC inhibition by SAHA has previously been shown to enhance *Bdnf* expression and neurite outgrowth (Bagheri et al., 2019). As BDNF regulates neuron survival and growth, differences between individual cultures relating to neuron survival and growth could affect differences in the mechanisms regulating *Bdnf* expression.

As REST overexpression caused *Kcnq2* mRNA downregulation in DRG neurons but not organotypic hippocampal cultures, levels of Kv7.2 protein in organotypic cultures were investigated. No difference was seen in fluorescence intensity of Kv7.2 staining in GFP-expressing neurons between the organotypic cultures infected with AdGFP or the cultures infected with AdGFP-*REST*. This could suggest that REST overexpression alone is not sufficient to cause reduction of Kv7.2 protein in the rat hippocampus. This would support the finding that REST overexpression is also insufficient to induce a repression of *Kcnq2* gene expression in organotypic hippocampal cultures, making it likely that *Kcnq2* and Kv7.2 were not downregulated by REST overexpression at any level. Alternatively, the Kv7.2 staining in this experiment may not have produced the required signal strength to observe quantifiable changes. Data from the literature regarding expression changes in *KCNQ2* and *KCNQ3* are limited. Carver and colleagues have reported that *KCNQ2* is upregulated in the CA1 and CA3 regions of the hippocampus 48 hours following chemoconvulsant-induced hyperexcitability, with no changes observed in *KCNQ3* (Carver et al., 2020). This is most likely due to activity-induced activation by the transcription factor NFAT (Zhang and Shapiro, 2012). REST upregulation in the hippocampus occurs during epilepsy and after seizures induced in animal epilepsy models (Navarrete-Modesto et al., 2019; Palm et

al., 1998; Spencer et al., 2006). Evidence also suggests that REST may serve dual roles in epileptogenesis, having the potential to either exacerbate or protect against hyperexcitability (Butler-Ryan and Wood, 2021b). By overexpressing REST, it could be inadvertently enabling a downstream signaling effect that occurs during a seizure, which could indirectly lead to the *KCNQ2* increase seen by Carver and colleagues (Carver et al., 2020). At the same time, the REST overexpression may bind and repress *KCNQ2* directly, as described by Mucha and colleagues (Mucha et al., 2010). If this were the case, the upregulation and downregulation of KCNQ2 could balance out to cause no overall change. However, no change in *KCNQ3* expression in the hippocampus was seen following seizure (Carver et al., 2020), whereas *KCNQ3* was significantly reduced from REST overexpression in DRG neurons (Mucha et al., 2010), so the combination of these forces would likely result in a downregulation of *KCNQ3* in the hippocampus following REST overexpression, which I did not see. Evidence of an indirect mechanism of REST upregulation leading to a compensatory upregulation of *KCNQ2* during seizure in the hippocampus is lacking. Therefore, it seems more likely that the unexpected lack of observed expression changes were due to insufficient infection of the organotypic cultures by the adenovirus and insufficient Kv7.2 immunohistochemical signal.

3.5.4 Conclusion

In this chapter I used adenoviral delivery to modulate the transcription factor REST in organotypic hippocampal cultures to investigate the effects of REST on *Kcnq2/3* and Kv7.2/3 expression. Adenoviral infection of organotypic cultures was optimised to give increased efficiency compared to previous studies, by infecting slice cultures in the acute slice stage, soon after slicing and plating. Adenovirus was found to infect neurons and microglia with minimal oligodendrocyte infection. Cytotoxicity was not observed, and transgene expression continued for weeks in culture. Infection of organotypic cultures with the AdGFP-*REST* construct caused significant *REST* overexpression, but this did not result in an observed repression of *Kcnq* mRNA or Kv7.2 protein, or other REST target genes. However, *Kcnq2* expression was upregulated by HDAC inhibition, implying a de-repression effect and suggesting *Kcnq2* expression is regulated by histone deacetylation in the hippocampus.

Chapter 4

Changes in expression of *Kcnq2*/Kv7.2 and *Kcnq3*/Kv7.2 in organotypic hippocampal epilepsy models

4.1 Introduction

I wanted to examine expression levels of REST, *Kcnq2/*Kv7.2 and *Kcnq3/*Kv7.3 in different epileptic models, to elucidate whether differential *Kcnq2/3* expression may be involved in epileptogenesis, and whether this may be regulated by REST. Endogenous REST is upregulated in epileptic models and epilepsy patients (Brennan et al., 2016; McClelland et al., 2011; Palm et al., 1998). No evidence was found to support the mechanism of REST-mediated repression of *Kcnq2* or *Kcnq3* in the non-epileptic hippocampus (Figures 3.8, 3.9), in contrast to earlier findings in DRG neurons (Mucha et al., 2010). However, REST functions are likely to change in different conditions and across different epileptic models (Butler-Ryan and Wood, 2021b), and REST-mediated repression of *Kcnq2* and *Kcnq3* might only occur to a measurable degree during hyperexcitability.

Due to its regulation of *KCNQ2/3* and regulation by REST, Sp1 was also investigated. The other known regulator of *Kcnq2* and *Kcnq3* expression is NFAT, which causes upregulation of these genes in response to neuronal stimulation, through its translocation to the nucleus (Zhang and Shapiro, 2012). Furthermore, *Kcnq2* and *Kcnq3* mRNA were upregulated in the rat hippocampus 16-20 hours after pilocarpine or kainate injection (Zhang and Shapiro, 2012). The observed upregulation of *Kcnq2* and *Kcnq3* by NFAT in the epileptic models is in direct contrast to the proposed downregulation of *KCNQ2* and *KCNQ3* by REST, demonstrating 2 opposing forces. The Shapiro group later demonstrated through immunostaing that Kv7.2 protein is increased in the CA1 and CA3 hippocampal regions, but not the dentate gyrus, after pilocarpine or PTZ injection (Carver et al., 2020). Maslarova and colleagues observed a reduction in KCNQ2 in all layers of the entorhinal cortex and in the neuropil, and a reduction of KCNQ3 in layers I/II of the entorhinal cortex and the subiculum, in the pilocarpine model (Maslarova et al., 2013). However, the reduction of KCNQ2 in layer III can be atributed to seizure-associated neuronal death (Du et al., 1995).

In order to create models of epilepsy in organotypic hippocampal slice cultures, 2 different convulsants were chosen: Kainate, and 4-aminopyridine. Kainate was chosen due to its ability to create a pathology with high levels of similarity to temporal lobe epilepsy. Kainate, like other chemoconvulsants, triggers epileptogenesis in animal models through its induction of an initial episode of status epilepticus. This leads to

the development of spontaneous seizures, associated with mossy fiber sprouting and hippocampal sclerosis with CA3 neuronal degeneration (Lévesque and Avoli, 2013). While the majority of research using kainate has been done *in vivo*, its effects have also been investigated in organotypic hippocampal slice cultures. Frequent epileptiform spiking was recorded from the granule cell layer of 10-12 day *in vitro* cultures exposed to 6µM kainate, immediately upon exposure, as well as after 24 and 48 hours of exposure. No epileptiform spiking was observed from vehicle-treated cultures. Treatment with kainate over 48 hours also caused significant neuron death and mossy fiber sprouting (Routbort et al., 1999). This supports my choice for kainate as a reliable inducer of seizure-like events in organotypic hippocampal slice cultures for investigation of the genetic changes involved in epileptogenesis.

In addition to kainate, I chose to use 4-aminopyridine (4AP) to induce seizure-like events in the organotypic cultures, as it is commonly used *in vitro*. It enhances release of neurotransmitters including glutamate, and causes depolarisation of neurons (Tapia and Sitges, 1982). It is primarily an inhibitor of Shaker type K^+ channels (McCormack et al., 1994). No effects of 4-aminopyridine are observed on Kv7.1 current, Kv7.2 current, Kv7.3 current, Kv7.2+Kv7.3 current or Kv7.5 current, though it may enhance Kv7.4 current (Khammy et al., 2018; Yang et al., 1998). It has been shown to produce strong epileptiform activity in brain slices (Avoli et al., 1996; Bijak and Misgeld, 1996; Chesnut and Swann, 1990; Motalli et al., 1999) and *in vivo* (Cramer et al., 1994; Fragoso-Veloz and Tapia, 1992; Morales-Villagrán et al., 1996; Yamaguchi and Rogawski, 1992). However, its use in organotypic hippocampal slice cultures has not been validated. The 4AP model is proposed to be useful for investigations of epileptogenesis where GABA signalling is not inhibited (Reddy and Kuruba, 2013).

In this project REST is modulated in hippocampal tissue not only to investigate the potential mechanism of REST repression of *Kcnq2* and *Kcnq3*, but also to recreate the REST upregulation observed after seizure and study the direct effects of this. The gene encoding the neurotrophin BDNF is able to be bound and repressed by REST (Zuccato et al., 2003). However, its expression is also strongly and reliably upregulated in animal epilepsy models (Ernfors et al., 1991; Nibuya et al., 1995) as soon as 100 minutes after seizure (Vezzani et al., 1999). BDNF levels are increased in the hippocampus and neocortex of epileptic patients compared to hippocampal tissue from non-epileptic patients (Hou et al., 2010; Martínez-Levy et al., 2016; Murray et al.,

2000; Takahashi et al., 1999), and is further increased in temporal lobe epilepsy patients with hippocampal sclerosis compared to patients without hippocampal sclerosis (Wang et al., 2011). BDNF is strongly expressed across the hippocampus (Conner et al., 1997). This is why it was chosen for use in this project as a marker for epilepsy in organotypic hippocampal cultures.

In this chapter I investigated expression changes of *Kcnq2/*Kv7.2 and *Kcnq3/*Kv7.2 in 2 different epileptic models in organotypic hippocampal slice cultures. I looked for evidence to support either of the hypotheses regarding transcription factor regulation of *Kcnq2/3* expression. Hippocampal increases in *Kcnq2/3* expression in the epileptic models may be induced by NFAT and would support the findings of the Shapiro group. In contrast, a downregulation of *Kcnq2/3* may be caused by repression from the increased REST levels observed in epilepsy models. The 2 mechanisms may both be active and competing against one another. Using BDNF as an epileptic marker, I used quantitative methods to analyse gene and protein expression to aim to answer the question of what roles these mechanisms play in epilepsy and epileptogenesis.

4.2 The effects of kainate on *Kcnq2/*Kv7.2 and *Kcnq3/*Kv7.3 expression in organotypic hippocampal cultures

4.2.1 Kainate exposure in organotypic cultures increases BDNF protein expression

Using BDNF increase as a marker of epileptogenesis, I wanted to determine whether an 18-hour exposure to 5µM kainate would be adequate to induce an epileptic-like state in the organotypic hippocampal slice cultures at 7 days in culture. This concentration and exposure time were chosen due to being similar to the protocols used by other groups in successfully inducing epileptiform activity in acute or cultured hippocampal slices (Gerace et al., 2017; Routbort et al., 1999). Immunohistochemistry for BDNF protein was used alongside the neuronal marker β-tubulin III following exposure of the organotypic cultures to kainate or vehicle. The majority of the BDNF signal was observed to be not colocalised with the β-tubulin III signal, appearing outside of the neuronal soma, and often most densely around the outer perimeter of the soma, supporting its function as a secreted protein. As BDNF signal was observed to be almost entirely outside of the neurons, BDNF signal intensity was taken from the whole image. The integrated density of BDNF for the image was normalised to the

integrated density of β-tubulin III for the same image. From each slice culture, 2 images were taken from the CA1 region (Figure 4.1A) and 1 image was taken from the dentate gyrus region, reflecting where staining was clearest. The average was taken from all images for quantification. Using this analysis method, a 2-fold increase in BDNF fluorescence intensity was observed in organotypic cultures exposed to kainate (8.48±1.01) compared to vehicle (4.12±0.58), suggesting kainate does cause a significant increase in average BDNF protein levels ($p=0.0006$, Figure 4.1B). There is considerable individual variation in BDNF levels between images and cultures in the same groups. Most of the BDNF protein appears secreted outside of the neurons. This increase in overall BDNF protein suggests that an 18-hour exposure to 5μM kainate is sufficient to create an epileptic-like state in organotypic hippocampal slice cultures.

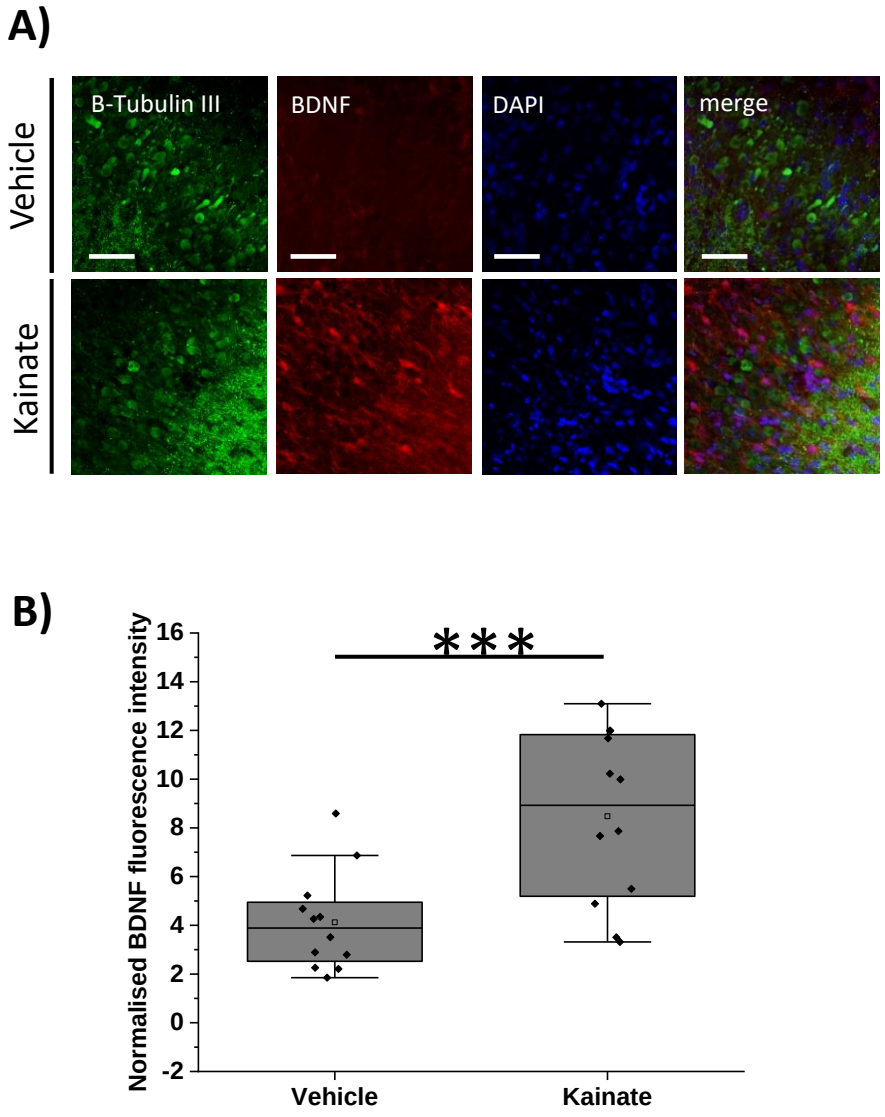

Figure 4.1. Kainate exposure in organotypic cultures increases BDNF protein expression. (***A***) Representative confocal images of CA1 molecular layer in organotypic hippocampal slice cultures exposed to kainate or vehicle and immunostained with primary antibodies against β-Tubulin III and BDNF, and Alexa-Fluor-488 (β-Tubulin III) and Alexa Fluor-555 (BDNF), and co-stained with DAPI. Scale bars 50µm. (***B***) Box plot shows the Integrated Density of fluorescence intensity for BDNF normalised to the Integrated Density of fluorescence intensity of β-Tubulin III of the same image, from CA1 and dentate gyrus in organotypic hippocampal slice cultures exposed to vehicle or kainate (n=12 images from 4 slice cultures; ***P < 0.001, Student's one-tailed t-test).

4.2.2 Changes in mRNA expression following kainate exposure

I hypothesised that changes in the expression of *KCNQ2*/Kv7.2 and *KCNQ3*/Kv7.3 could influence epileptogenesis, by affecting neuronal excitability through destabilising the Kv7 current. Expression of *Kcnq2*/Kv7.2 and *Kcnq3*/Kv7.3 in the kainate epileptic model had not been investigated, so I wanted to examine this in cultured hippocampal tissue. REST expression was examined to investigate whether REST may be involved in *Kcnq2* and *Kcnq3* regulation in the epileptic model. In addition to the main *Rest* isoform, the *Rest* primers are also predicted to bind to rat *Rest1* and rat *Rest5*, but not rat *Rest4*. To gather additional information about REST activity, I wanted to quantify expression levels of some other REST target genes. Hyperpolarisation-activated Cyclic Nucleotide gated potassium channel (*Hcn1*) encodes a potassium channel expressed in hippocampal pyramidal dendrites which is activated by hyperpolarising potentials (Shah, 2012). REST represses *Hcn1* following kainate-induced status epilepticus (McClelland et al., 2011). Expression of the REST target genes *Scg10* (Mori et al., 2002) and Na^+ channel type II, also referred to as the *Scn2A* gene (Lunyak et al., 2002), were quantified. As the 18-hour exposure of cultures at 7 days in vitro to 5µM kainate was shown to be sufficient to increase the epileptic marker BDNF (Figure 4.1), this exposure was used to examine gene expression. Expression was normalised to expression of the Cyclophilin A (*CycA*) reference gene, which remained stable across both conditions, and is represented as percentage of *CycA* expression. A 10.9-fold increase in average *Bdnf* mRNA was observed in the kainate-treated cultures compared to the vehicle-treated cultures ($p=0.0007$, Figure 4.2A), demonstrating that kainate induces strong upregulation of *Bdnf* mRNA expression, supporting the upregulation of BDNF protein (Figure 4.1). No change in *Rest* expression was observed between kainate treated (1.37±0.03% of *CycA*) and vehicle treated cultures (1.30±0.12% of *CycA*, Figure 4.2B). Expression of *Kcnq2* was reduced by 56% in kainate-treated cultures compared to vehicle ($p=0.049$, Figure 4.2C), suggesting kainate causes an overall downregulation of *Kcnq2*. The reduction of *Kcnq3* expression in kainate treated cultures (0.37±0.05% of *CycA*) compared to vehicle (0.58±0.11% of *CycA*, Figure 4.2D) was not significant. An 18% reduction in expression of the REST-target gene *Hcn1* was observed in response to kainate treatment, but this was also not significant (Figure 4.2E). A previous group observed a REST repression of *Hcn1* by 22% after kainate in hippocampal slice cultures, which

matches my findings, but their results were significant due to smaller variation (McClelland et al., 2011). No significant change in expression of the REST target gene *Scg10* was observed in the kainate-treated cultures compared to vehicle (Figure 4.2F). Finally, expression of the REST target gene Na^+ channel type II (*Scn2a*) was reduced by 62% in kainate-exposed cultures compared to vehicle (p=0.03, Figure 4.2G). No difference was observed in expression of *Sp1* between kainate-treated and vehicle-treated cultures (Figure 4.2H), demonstrating that hippocampal *Sp1* expression is not affected in the kainate model. This makes it unlikely that REST is repressing *Sp1* here. Despite no upregulation in REST mRNA at this timepoint, some of the REST target genes (*Kcnq2* and *Scn2a*) were downregulated in response to kainate. Therefore, *Kcnq2* and *Scn2a* could have been repressed by increased activity of REST or a different repressing transcription factor. Alternatively, activity of Sp1, NFAT or other enhancing transcription factors could have been reduced.

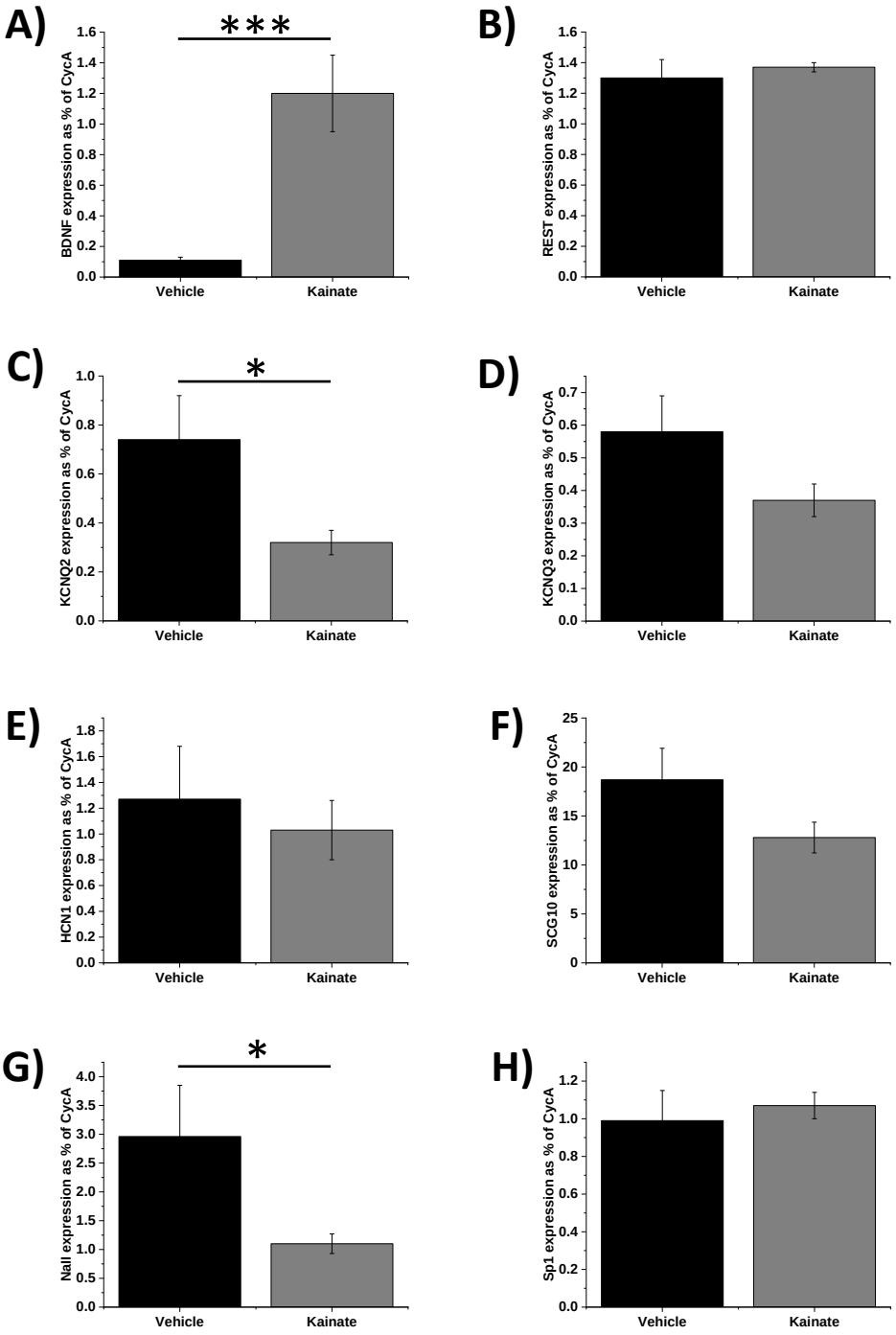

Figure 4.2. Changes in mRNA expression of *Bdnf, Rest,* and REST target genes following kainate exposure. Reverse transcription quantitative PCR analysis of mRNA levels of *Bdnf* (***A***), *Rest* (***B***), *Kcnq2* (***C***), *Kcnq3* (***D***), *Hcn1* (***E***), *Scg10* (***F***) *NaII/Scg10* (***G***) and *Sp1* ***(H)*** in organotypic hippocampal slice cultures exposed to vehicle or kainate. Data (***A-H***) are expressed as % of cyclophilin A reference gene (mean ± SEM; n = 6 samples; *P < 0.05, P*** < 0.001). Student's one-tailed t-test was used for *Bdnf, Rest, Hcn1, Scg10* and *NaII/Scg10* as expression was expected to

Figure 4.2 continued… change in one specific direction for each gene, based on previous literature. Student's two-tailed t-test was used for *Kcnq2* and *Kcnq3* as expectations about gene expression changes were unspecific, based on previous literature.

4.2.3 Kainate has different effects upon Kv7.2 protein expression in different hippocampal regions

Following from the result demonstrating a downregulation of *Kcnq2* mRNA in organotypic hippocampal cultures exposed to kainate compared to vehicle (Figure 4.2C), I wanted to examine whether this downregulation is reflected in Kv7.2 protein levels. Furthermore, immunohistochemistry presents an opportunity to examine Kv7.2 protein changes in different regions of the hippocampus, to determine whether changes occur equally throughout the tissue, or whether different regions are affected differently. Organotypic hippocampal slice cultures were exposed to kainate or vehicle and then fixed and immunostained for Kv7.2, the neuronal marker HUC/D, and co-stained with DAPI. Representative images are shown of the CA1 region (Figure 4.3A) and the dentate gyrus region (Figure 4.3B). Kv7.2 signal intensity within HUC/D-positive neuronal regions was quantified by normalising it to the intensity of the HUC/D signal. In the CA1 region, Kv7.2 fluorescence intensity was reduced by 49% in kainate-treated cultures compared to vehicle ($p=2.7 \times 10^{-4}$, Figure 4.3C). In the CA3 region, no difference was observed in Kv7.2 fluorescence intensity between kainate (7.89±0.49) and vehicle (9.28±0.57, Figure 4.3C) treated cultures. In the dentate gyrus region, Kv7.2 fluorescence intensity was 44% higher in kainate treated cultures than vehicle ($p=0.0378$, Figure 4.3C). When data from all hippocampal regions were pooled, a significant 18% reduction in Kv7.2 fluorescence intensity was observed in the kainate treated cultures compared to vehicle ($p=0.0182$, Figure 4.3D). The overall downregulation of Kv7.2 protein expression in the hippocampus following kainate exposure is consistent with the observed downregulation in *Kcnq2* mRNA harvested from organotypic cultures at the same timepoint (Figure 4.2C). This suggests that the observed change is accurate and both Kv7.2 protein and *Kcnq2* mRNA are downregulated immediately following an 18-hour kainate exposure in the hippocampus overall. The Kv7.2 quantification data from the separate regions provides more detailed information, with expression decreasing in the CA1 region and

increasing in the dentate gyrus following kainate exposure, and no change being observed in the CA3 region. Kv7.2 signal is visibly strong in the images used for this experiment. This and the changes in signal intensities in the CA1 and dentate gyrus suggest that where there are expression changes, the Kv7.2 signal is strong enough to demonstrate these changes quantitatively.

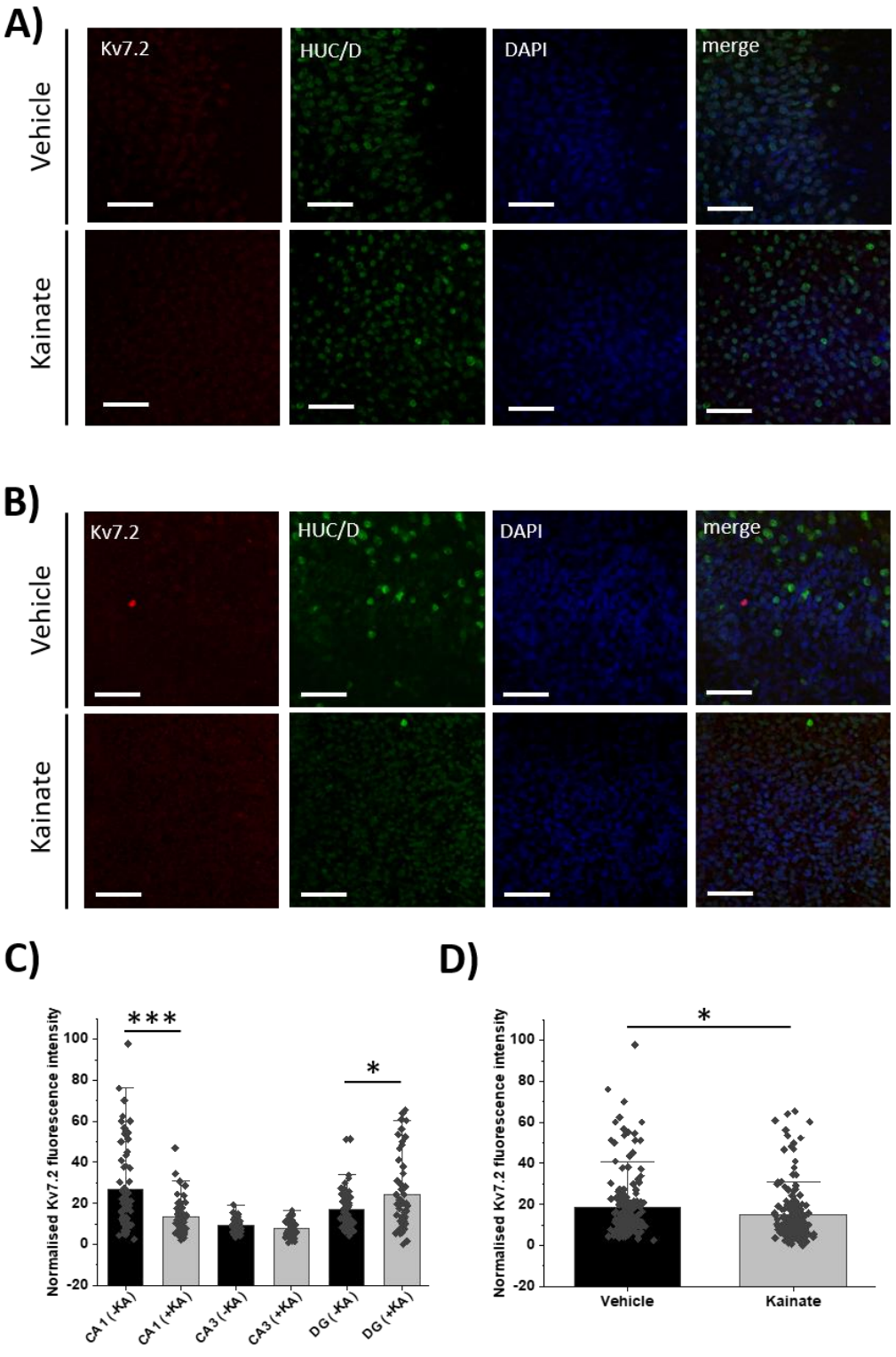

Figure 4.3. Kainate has different effects upon Kv7.2 protein expression in different hippocampal regions. Representative confocal images of hippocampal regions CA1 (***A***) and dentate gyrus (***B***) treated with either vehicle or kainate. Cultures were immunostained with primary antibodies against Kv7.2 and the neuronal marker HUC/D, and Alexa Fluor-488 (HUC/D) and Alexa Fluor-555 (Kv7.2) secondary antibodies, and co-stained with DAPI. Scale bars 50μm. (***C***) Bars show the fluorescence intensity of Kv7.2 normalised to HUC/D fluorescence intensity in each hippocampal region in absence and presence of kainate (mean ± SD; n = 45-60 cells from 4 slice cultures per condition; *P<0.05, ***P < 0.001, Mann-Whitney U test). (***D***) Bars show the fluorescence intensity of Kv7.2 normalised to HUC/D fluorescence intensity in the whole slice overall (mean ± SD; n = 165-175 cells; *P < 0.05, Mann-Whitney U test).

4.2.4 Changes in BDNF and REST protein in organotypic hippocampal slice cultures exposed to kainate

A large increase in *Rest* mRNA and REST protein in the hippocampus following kainate exposure has been described by multiple groups (Brennan et al., 2016; Carminati et al., 2019; McClelland et al., 2011; Palm et al., 1998; Spencer et al., 2006). However, kainate did not cause an upregulation of *Rest* mRNA in the present study (Figure 4.2B). Therefore, it seemed important to quantify the levels of REST protein in organotypic hippocampal cultures following kainate or vehicle exposure, through western blotting. BDNF protein levels were also assessed through western blotting to support previous immunohistochemical evidence of kainate causing an upregulation of BDNF in the hippocampus (Figure 4.1). Three to 5 organotypic hippocampal cultures were homogenised to provide each protein sample. Three samples of vehicle-treated cultures were run on a gel alongside 4 samples of kainate-treated cultures, and each gel was run in duplicate. Bands of REST, BDNF and the β-tubulin loading control from one of these gels is shown in figure 4.4A. REST is observed as a doublet which is most likely due to post-translational modification. REST signal appears consistently weak in all samples of vehicle-treated cultures, while samples of kainate-treated cultures show 2 weak bands and 2 much stronger bands. This suggests that REST increases in some organotypic cultures in response to kainate exposure but does not increase in other cultures. BDNF signal appeared more consistent across the 2 groups.

The average β-tubulin signal intensity does not change in kainate compared to vehicle conditions. REST and BDNF proteins were quantified by normalising band signal intensity to signal of the loading control and is shown as fold change. No significant differences were observed in average BDNF (Figure 4.4B) or REST (Figure 4.4C) in response to kainate compared to vehicle, but this could be due to the small sample number. BDNF is observed to be greater in some of the kainate-exposed samples (2.17, 2.42) while remaining around control vehicle levels in other kainate samples (0.93, 1.16), which can be observed as individual points in figure 4.4C. This is reflective of the BDNF protein increases seen in most, but not all, of the images taken of kainate-treated cultures (Figure 4.1) and may reflect some variability of kainate to induce epileptogenesis in hippocampal slice cultures. Similarly, REST is greater in some of the kainate-exposed samples (3.25, 5.00) while REST remains around control vehicle levels in other kainate samples (0.30, 0.95). The increase in REST protein in half of the kainate-treated samples is sufficient to cause a non-significant 2.3-fold increase in the average REST level. One of the samples showing increased REST also shows increased BDNF, and the other shows low BDNF. The other high BDNF sample shows low REST. This highlights that while BDNF protein increase and REST protein increase can occur together following kainate exposure, each one is also able to upregulate individually while the other remains at a control level. Therefore, the relationship between REST and BDNF appears to vary across different slice cultures.

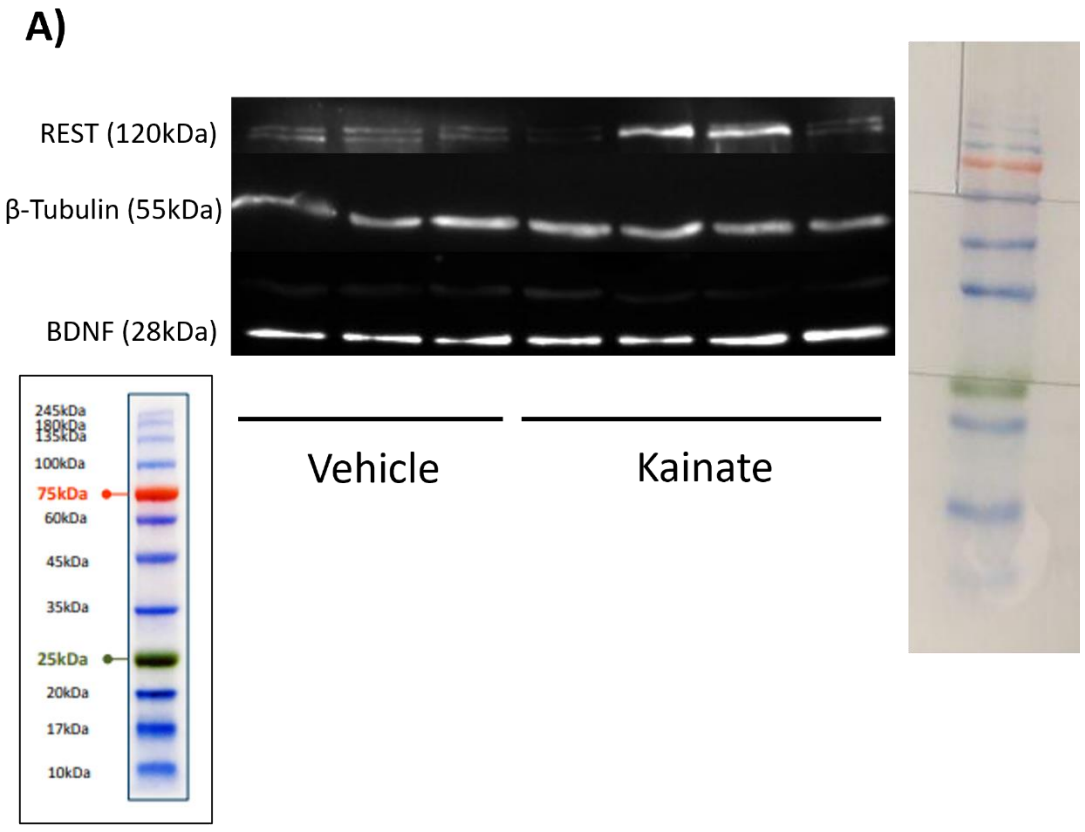

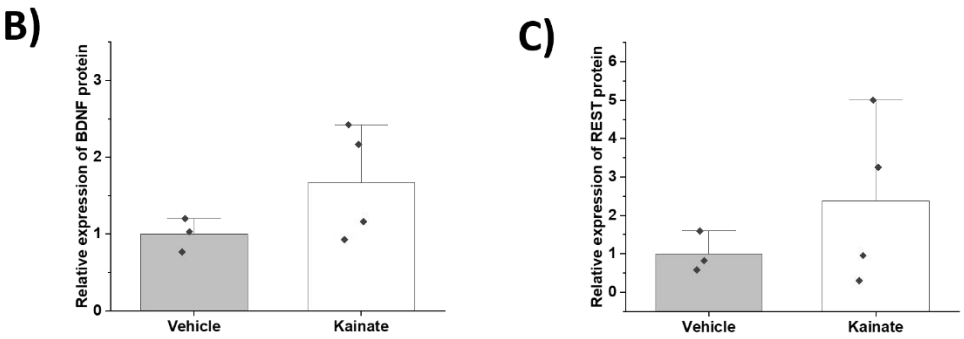

Figure 4.4. Changes in BDNF and REST protein in organotypic hippocampal slice cultures exposed to kainate. (*A*) Western blot of REST and BDNF proteins with β-tubulin loading control taken from cultures exposed to vehicle or kainate, with molecular weight of proteins and molecular weight markers shown. (***B, C***) A non-significant upward trend in average expression of BDNF and REST proteins from cultures exposed to kainate, compared to vehicle (mean ± SD, n=3-4 samples, each sample taken from 3-5 cultures, Student's one-tailed t-test).

4.2.5 The effects of REST modulation on gene expression in the kainate model

I reported that overexpression of REST or dominant negative REST had no observed effects on expression of *Kcnq2* or *Kcnq3* mRNA in organotypic hippocampal cultures (Figure 3.9). As that experiment was not performed under any epileptic conditions, it represented the effects of REST modulation in normal healthy hippocampal tissue. In the kainate epileptic model, *Kcnq2* mRNA levels were reduced (Figure 4.2). To help determine whether *Kcnq2* downregulation was a result of REST-mediated repression in the kainate model, adenoviral REST modulation was applied in the presence of kainate or vehicle. In addition to *Kcnq2* and *Kcnq3*, expression of *Bdnf* was quantified as a REST target gene and marker of epileptogenesis. The homologous DNA binding region found in the *REST* and dominant negative *Rest* constructs was also quantified to confirm transgene expression.

Organotypic hippocampal cultures were infected with adenovirus carrying GFP, GFP-*REST* or GFP-DN*Rest*, and then each one was imaged immediately prior to kainate exposure. The GFP transgene in all 3 viral constructs was visible across each slice, demonstrating thorough infection and transgene expression (Figure 4.5A). In support of this, expression of the viral *REST*/DN*Rest* constructs were also increased, confirming their expression in the cultures (Figure 4.5B). DN*Rest* was 41-fold higher in AdGFP-DN*Rest* infected vehicle-exposed cultures compared to control ($p=0.029$). *REST* expression was 161-fold higher in AdGFP-*REST* infected vehicle-exposed cultures than control, though this difference was not statistically significant according to Mann-Whitney U test. All samples showed at least 43-fold upregulation of *REST* compared to control, making it likely that the presence of REST would be sufficient to interfere with endogenous REST function. Similarly, *REST* was 33-fold higher in AdGFP-*REST* infected kainite-exposed cultures compared to AdGFP infected kainite-exposed cultures ($p=0.00794$). Furthermore, DN*Rest* was 21-fold higher in AdGFP-DN*Rest* infected kainite-exposed cultures compared to AdGFP infected kainite-exposed cultures ($p=0.00433$), demonstrating that the slice cultures were overexpressing *REST* and DN*Rest*.

Bdnf is increased 2.6-fold in AdGFP-DN*Rest* infected vehicle-exposed cultures compared to AdGFP infected vehicle-exposed cultures ($p=0.0286$), while *Bdnf* is unchanged from control in AdGFP-*REST* infected cultures (Figure 4.5C). A 19-fold

non-significant increase in *Bdnf* is observed in kainate-exposed AdGFP infected cultures compared to vehicle-exposed AdGFP infected cultures. This is likely to be non-significant due to the large variation between samples and small sample sizes. I saw previously that kainate causes an increase in BDNF protein expression in most, but not all, cultures (Figures 4.1 and 4.4). In this experiment the *Bdnf* mRNA expression seems to reflect the wide variation in individual protein levels. In some cultures, kainate caused a large increase in *Bdnf* mRNA (1.1%, 1.23% of *CycA*) compared to vehicle (0.03±0.00% of *CycA*). These high *Bdnf* samples also showed increases in *Kcnq2* (0.55, 0.45% of *CycA*) compared to vehicle (0.25±0.06% of *CycA*), suggesting a positive association between the 2 genes. In other cultures, kainate caused only a minimal *Bdnf* increase (0.05, 0.08% of *CycA*), and these were associated with no change in *Kcnq2* (0.21, 0.22% of *CycA*). This supports the idea that kainate causes an upregulation of BDNF protein and *Bdnf* mRNA in most cultures, but not all. Some cultures may have not responded to kainate due to lack of cell viability. The presence of kainite compared to vehicle led to a 53-fold *Bdnf* increase in AdGFP-*REST* infected cultures ($p=0.0357$), and a 9-fold *Bdnf* increase in AdGFP-DN*Rest* infected cultures ($p=0.0476$). The fact that kainate caused a significant *Bdnf* increase in the REST overexpressing cultures but not the AdGFP infected cultures suggests that REST overexpression in the kainate epileptic model causes *Bdnf* to increase further than it would from kainate alone, so REST may exhibit pro-epileptogenic qualities in this model. A 76% reduction of *Bdnf* in kainate-exposed AdGFP-DN*Rest* infected cultures is observed compared to in kainate-exposed AdGFP-*REST* infected cultures ($p=0.0130$). This may suggest that blocking endogenous REST with DNREST in the kainate model results in *Bdnf* downregulation, which would again support the idea of REST being pro-epileptic in the kainate model.

No effects on *Kcnq2* expression were observed from adenoviral REST overexpression in vehicle-exposed cultures (Figure 4.5D). This supports my previous findings that REST overexpression had no effect on *Kcnq2* or *Kcnq3* expression in non-epileptic slice cultures (Figures 3.9E, 3.9F, respectively). However, I previously observed a reduction in *Kcnq2* mRNA expression after kainate exposure (Figure 4.2C). The lack of kainate-induced reduction of *Kcnq2* in this experiment could be due to the presence of the adenovirus in the slices, or could be related to the differences in *Bdnf* upregulation between the 2 experiments. In the current experiment, kainate induced

an average *Bdnf* upregulation of 22-fold (Figure 4.5C), whereas in uninfected slices kainate induced an average *Bdnf* upregulation of 10-fold (Figure 4.2A). This difference could underpin variations in epileptogenesis-related changes.

In the kainate exposed culures, *Kcnq2* expression was lower in AdGFP-DN*Rest* infected cultures than in AdGFP infected cultures (p=0.00433) or AdGFP-*REST* infected cultures (p=0.0173, Figure 4.5D). A similar non-significant trend was observed for *Kcnq3* (Figure 4.5E). Therefore, there appear to be differences in REST regulation of *Kcnq2* between the vehicle and kainate conditions. No significant changes in *Kcnq3* expression were observed across any of the groups (Figure 4.5E).

Sp1 follows a similar expression pattern as *Kcnq2*. *Sp1* expression in kainate-exposed DN*Rest* overexpressing cultures was 71% lower than in vehicle-exposed DN*REST* overexpressing cultures (p=0.004). However, neither showed significantly different *Sp1* levels from their corresponding AdGFP infected cultures. The differences here between the vehicle and kainate conditions may also be due to differential modulation across the 2 conditions.

Expression data of human/mouse *REST* suggests the transgenes for REST modulation are overexpressed. However, the effect may be too small to produce changes in *Kcnq2* and *Sp1* in REST and DNREST overexpressing cultures compared to AdGFP infected cultures. This could be due to adenovirus infecting no more than 41% of total cells (Figure 3.2). This would also explain the lack of effects on *Kcnq2* observed previously (Figure 3.8). In addition, the lack of expected downregulation of *Kcnq2* by kainate in the AdGFP infected cultures was contrary to what was seen earlier in uninfected cultures (Figure 4.2). The lack of *Kcnq2* downregulation here may be due to interference by the adenovirus, or due to different degrees of epileptogenesis being achieved, as suggested by the different levels of *Bdnf* upregulation across experiments.

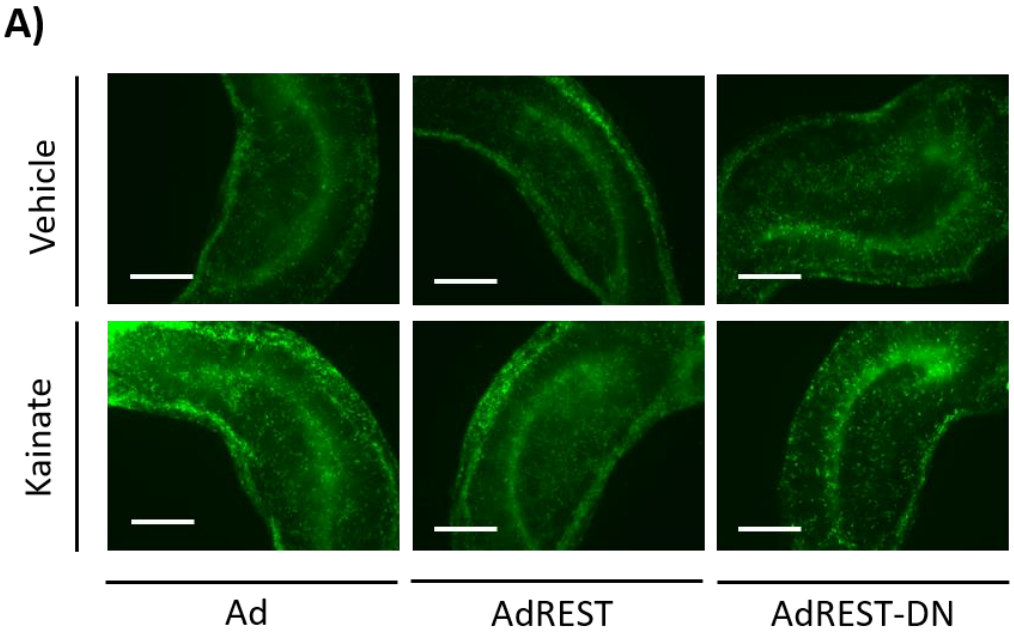
A)
Vehicle
Kainate
Ad
AdREST
AdREST-DN

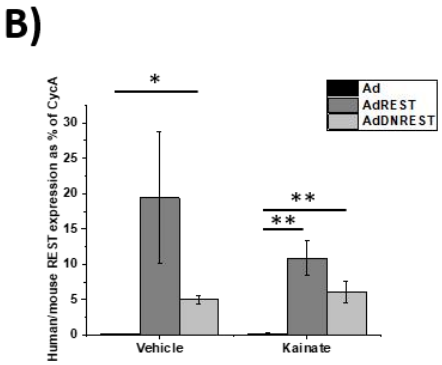
B)
Human/mouse REST expression as % of CycA
Ad
AdREST
AdDNREST
Vehicle
Kainate

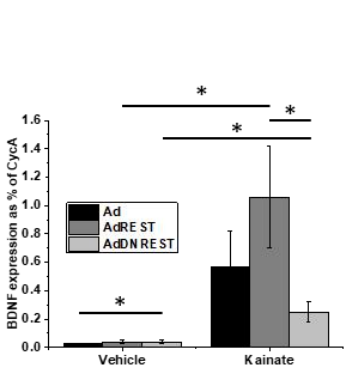
C)
BDNF expression as % of CycA
Ad
AdREST
AdDNREST
Vehicle
Kainate

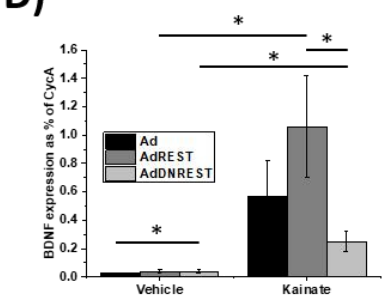
D)
BDNF expression as % of CycA
Ad
AdREST
AdDNREST
Vehicle
Kainate

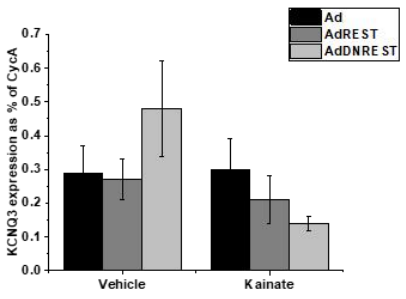
E)
KCNQ3 expression as % of CycA
Ad
AdREST
AdDNREST
Vehicle
Kainate

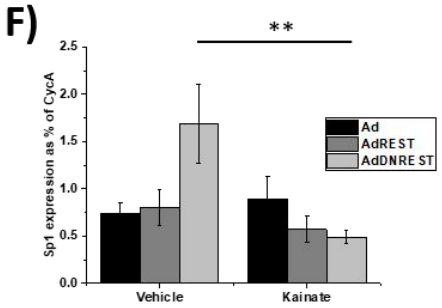
F)
Sp1 expression as % of CycA
Ad
AdREST
AdDNREST
Vehicle
Kainate

Figure 4.5. Changes in mRNA expression in *Bdnf, Rest, Kcnq2, Kcnq3* and *Sp1* following infection with adenovirus delivering REST modulation and exposure to kainate. (***A***) shows representative fluorescent images of organotypic hippocampal slice cultures infected with AdGFP, AdGFP-*REST* or AdGFP-*Rest*-DN prior to exposure with kainate (KA) or vehicle (Veh). GFP marker (green) indicates infected cells. Scale bars 500µm. (***B-F***) Reverse transcription quantitative PCR analysis of mRNA levels of human/mouse *REST* (***B***), *Bdnf* (***C***), *Kcnq2* (***D***), *Kcnq3* (***E***) and *Sp1* ***(F)*** in organotypic hippocampal slice cultures infected with Ad, Ad*REST* or Ad*Rest*-DN and exposed to SAHA or vehicle, and kainate or vehicle (* $p < 0.05$, ** $p < 0.01$). Data are represented as % of cyclophilin A (*CycA*) reference gene (mean ± SEM; n = 3-6 samples). Data sets of *Rest, Bdnf, Kcnq2* and *Kcnq3* expression were analysed by Kruskal-Wallis followed by Mann-Whitney U tests for pairwise comparisons. *Sp1* data set was analysed by ANOVA followed by Tukey's post-hoc test.

4.3 The effects of 4-aminopyridine on *Kcnq2*/Kv7.2 and *Kcnq3*/Kv7.3 expression in organotypic hippocampal cultures

4.3.1 4-aminopyridine increases action potential firing frequency in organotypic hippocampal slice cultures

I was interested in using the convulsant 4-aminopyridine in organotypic hippocampal slice cultures as a second type of epileptic model. Unlike kainate, data from previous studies regarding 4AP use in organotypic cultures was lacking, so the effects on neuronal excitability needed clarification. To confirm its pro-convulsant effects, cell-attached patch clamp recordings were taken in organotypic cultures perfused with 4-aminopyridine in ACSF. Cultures grown in normal medium were taken at 12 to 27 days in vitro and perfused with warm ACSF, and a pipette seal (tight or loose) was made to a cell in the molecular layer of the CA1 hippocampal region of each slice culture. It was observed over many experiments that the action potential spikes were recorded clearly with both tight and loose pipette seals, and seal tightness would not be expected to interfere with spiking frequency, so both were accepted. Seal tightness ranged between 75MΩ and 2.5GΩ. Extracellular cell-attached recordings were taken from each cell perfused in ACSF and then recorded again after wash-in of perfusion containing 100µM 4AP in the ACSF. Representative traces of one of the cells before

4AP wash-in is shown in figure 4.6B, and after 4AP wash in (Figure 4.6C). Firing frequency was observed to increase after 4AP in all slice cultures, with ictal and inter-ictal spiking observed in some post-4AP recordings but not all. Average action potential firing frequency was quantified for the before and after 4AP recordings (Figure 4.6A) and was found to significantly increase in the cells after 4AP perfusion (65.74±24.46 spikes per 10 minutes) compared to before 4AP perfusion (13.34±6.01 spikes per 10 minutes, $p=0.0175$). This suggests 4AP is capable of causing hyperexcitability and epileptiform activity in CA1 pyramidal neurons of organotypic hippocampal cultures, as it does in acute slices (Avoli et al., 1996; Bijak and Misgeld, 1996; Chesnut and Swann, 1990; Motalli et al., 1999), and supports the use of 4AP as an epileptic model.

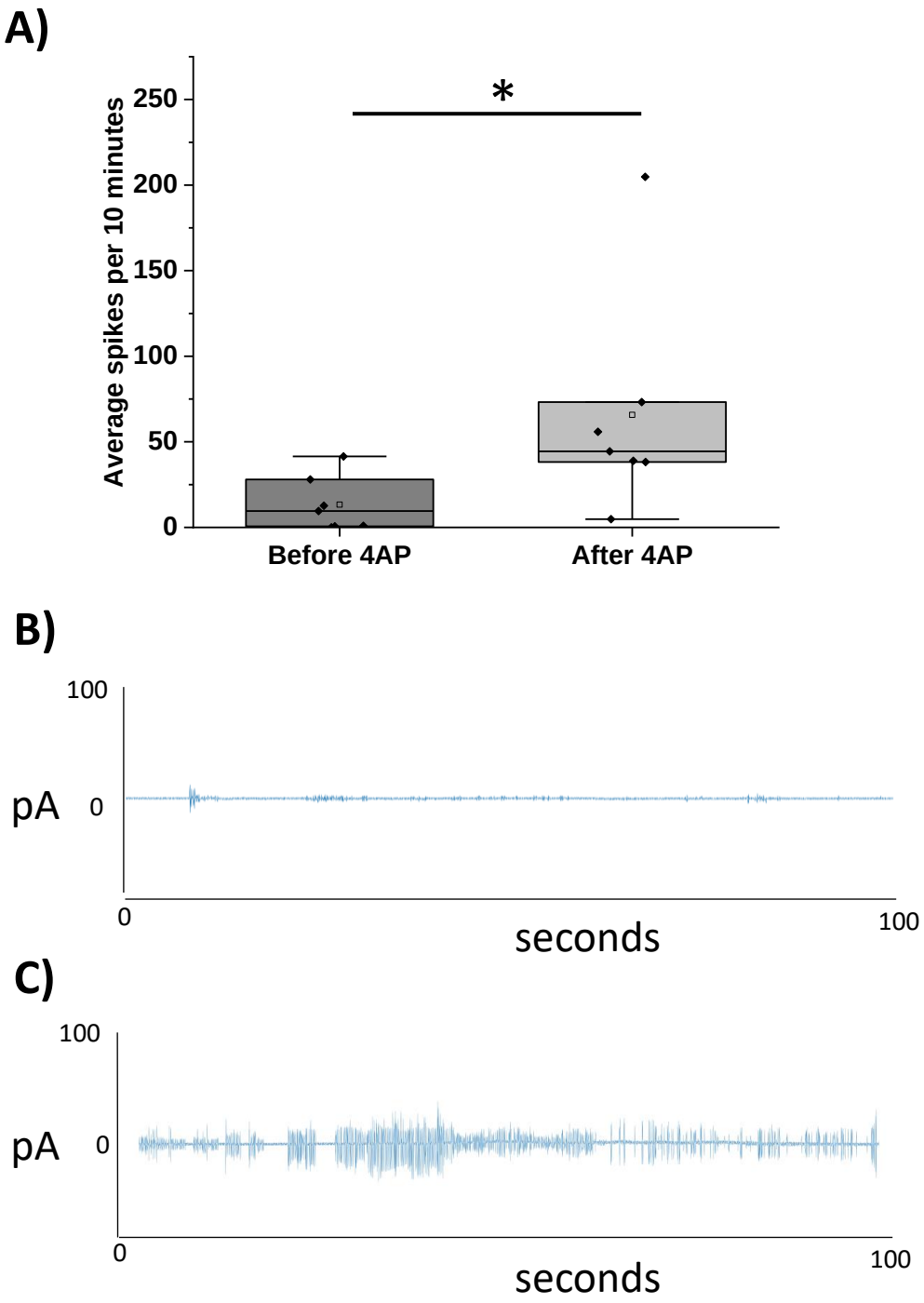

Figure 4.6. Action potential firing frequency is increased by 4-aminopyridine in organotypic hippocampal slice cultures. Cell-attached patch clamping was used to record spontaneous action potentials from pyramidal neurons in the CA1 region, before and during exposure to 4AP. ***(A)*** Average number of action potential spikes every 10 minutes increased following addition of 4AP. *, $P<0.05$, Mann-Whitney U test, n = 7 slice cultures. ***(B)*** Representative traces of spontaneous action potentials before ***(B)*** and during ***(C)*** 4AP exposure.

4.3.2 Exposure of organotypic cultures to 4-aminopyridine increases BDNF protein expression.

Organotypic cultures were exposed to 4AP at 14 days in culture. Cultures were exposed to 100μM 4AP in growth medium for 4 days. This concentration and exposure time were chosen based on the Baldelli group that showed an increase in *Rest* mRNA compared to control (Pozzi et al., 2013). To determine whether this exposure caused a visible increase in BDNF protein expression, organotypic cultures treated with 4AP or vehicle were immunostained for BDNF and the neuronal marker β-tubulin III, and co-stained with DAPI. As with BDNF staining in figure 4.1, BDNF signal (red) here is observed to be mostly outside of the β-tubulin III-positive neuronal soma, and often strongest in regions surrounding the neuron soma (Figure 4.7A),. The integrated density of BDNF was normalised to the integrated density of β-tubulin III per image to calculate BDNF fluorescence intensity values. BDNF fluorescence intensity (Figure 4.7A) was found to be over 3.8-fold higher in 4AP treated cultures than vehicle treated cultures ($p=0.0000005$, Figure 4.7B). As with the results following kainate exposure, there was some overlap in staining intensity between a few of the images from the 4AP (0.85, 1.38, 0.98) and the vehicle treated cultures (1.17). Overall, as with kainate, exposure of organotypic hippocampal cultures to 4AP does induce a significant increase in BDNF protein. This implies some intracellular changes indicative of epileptogenesis have occurred, which is supported by the hyperactivity observed from 4AP exposure in figure 4.7.

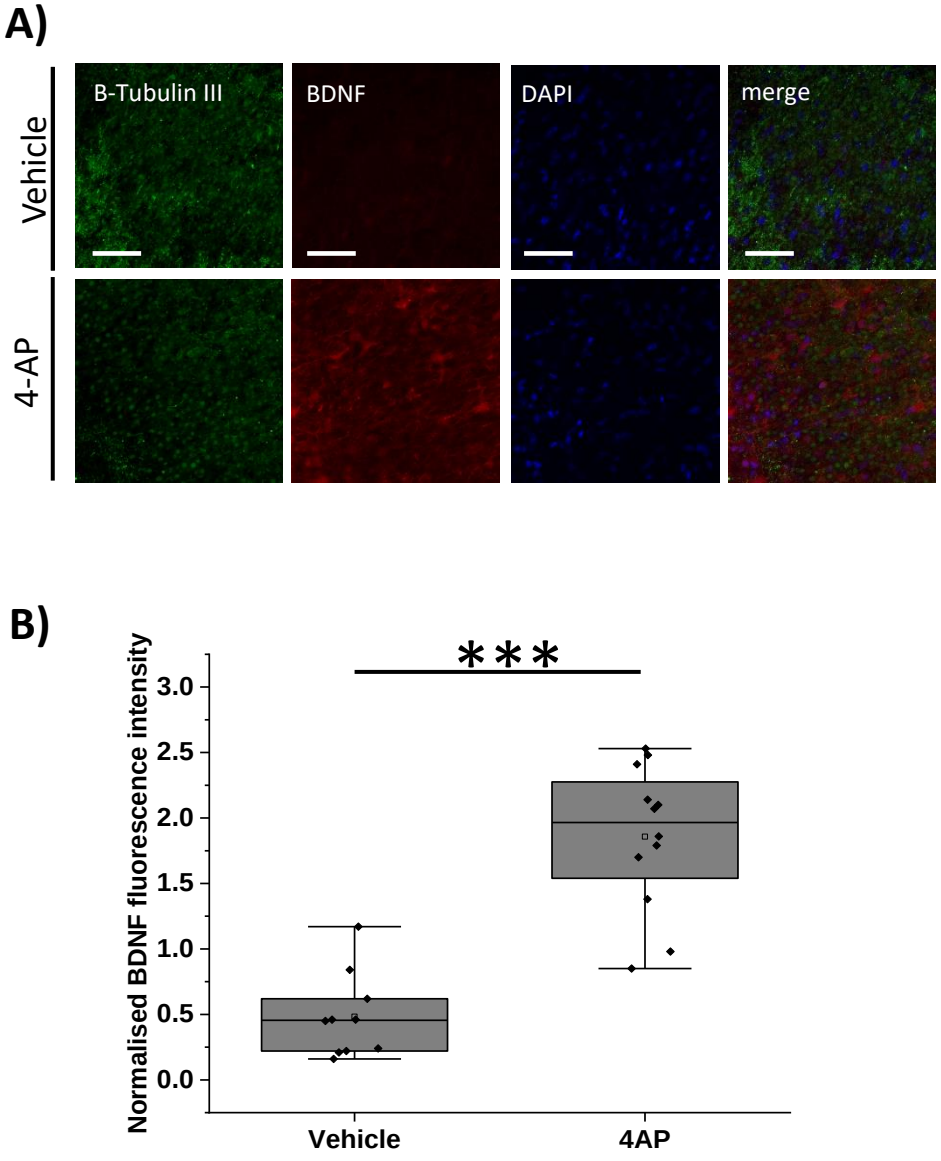

Figure 4.7. Exposure of organotypic cultures to 4-aminopyridine increases BDNF protein expression. (*A*) Representative confocal images of CA1 molecular layer in organotypic hippocampal slice cultures exposed to 4-aminopyridine (4AP) or vehicle and immunostained with primary antibodies against β-Tubulin III and BDNF, and Alexa-Fluor-488 (β-Tubulin III) and Alexa Fluor-555 (BDNF), and co-stained with DAPI. Scale bars 50μm. (***B***) Box plot shows the Integrated Density of fluorescence intensity for BDNF normalised to the Integrated Density of fluorescence intensity of β-Tubulin III of the same image, from CA1 and dentate gyrus in organotypic hippocampal slice cultures exposed to vehicle or 4AP (n=10-12 images from 4 slice cultures; ***$P < 0.001$, Student's one-tailed t-test).

4.3.3 Cyclosporin A reduces nuclear localisation of NFATc3 in HEK cells

Expression of *Kcnq2/3* is enhanced by binding of the transcription factor NFAT in DRG neurons, in response to enhanced neuronal activity (Zhang and Shapiro, 2012). Following Ca^{2+} influx into the neuron, calcineurin activates NFAT, inducing its dissociation from the AKAP complex and translocation into the nucleus, where it is able to upregulate *Kcnq2/3*. Calcineurin function is blocked by the peptide cyclosporin A (See Introduction). I wanted to use cyclosporin A to investigate whether NFAT is functioning to activate *Kcnq2/3* transcription in the hippocampus. Initially it was important to confirm that cyclosporin A was capable of preventing the translocation of NFAT from the cytoplasm to the nucleus. I chose to investigate the translocation of NFATc3 as it is highly prevalent in the hippocampus (Ulrich et al., 2012). HEK293 cells were transfected with the pcDNA3-GFP-NFATc3 plasmid and then exposed to cyclosporin A or vehicle. They were then immunostained for NFATc3 and co-stained with DAPI. Successful transfection is observed by the expression of GFP (Figure 4.8A). The clear colocalisation of the NFAT signal and the GFP signal observed in the confocal images confirms that the NFAT antibody was binding to the NFAT-GFP protein. The pattern of NFAT signal and GFP expression can be observed to differ between the vehicle-treated and cyclosporin A-treated cells. NFATc3 and GFP appear mainly in the nucleus and soma in the vehicle treated cells (see merged image), but in the cyclosporin treated cells NFATc3 and GFP appear to be localised towards more distal projections. The fluorescence intensity of the NFATc3 signal in the cell nuclei was quantified and expressed relative to the upper threshold of NFATc3 signal in the image. Average nuclear NFATc3 fluorescence intensity was found to be 64% lower in cells treated with cyclosporin than cells treated with vehicle ($p=2.03x10^{-8}$, Figure 4.8B). This demonstrates that 1µM cyclosporin A is sufficient to prevent nuclear localisation of NFATc3 in HEK cells. An 18-hour exposure of 1µM cyclosporin A was therefore appropriate for use in further experiments to prevent NFAT binding to *Kcnq2* and *Kcnq3* in the nucleus.

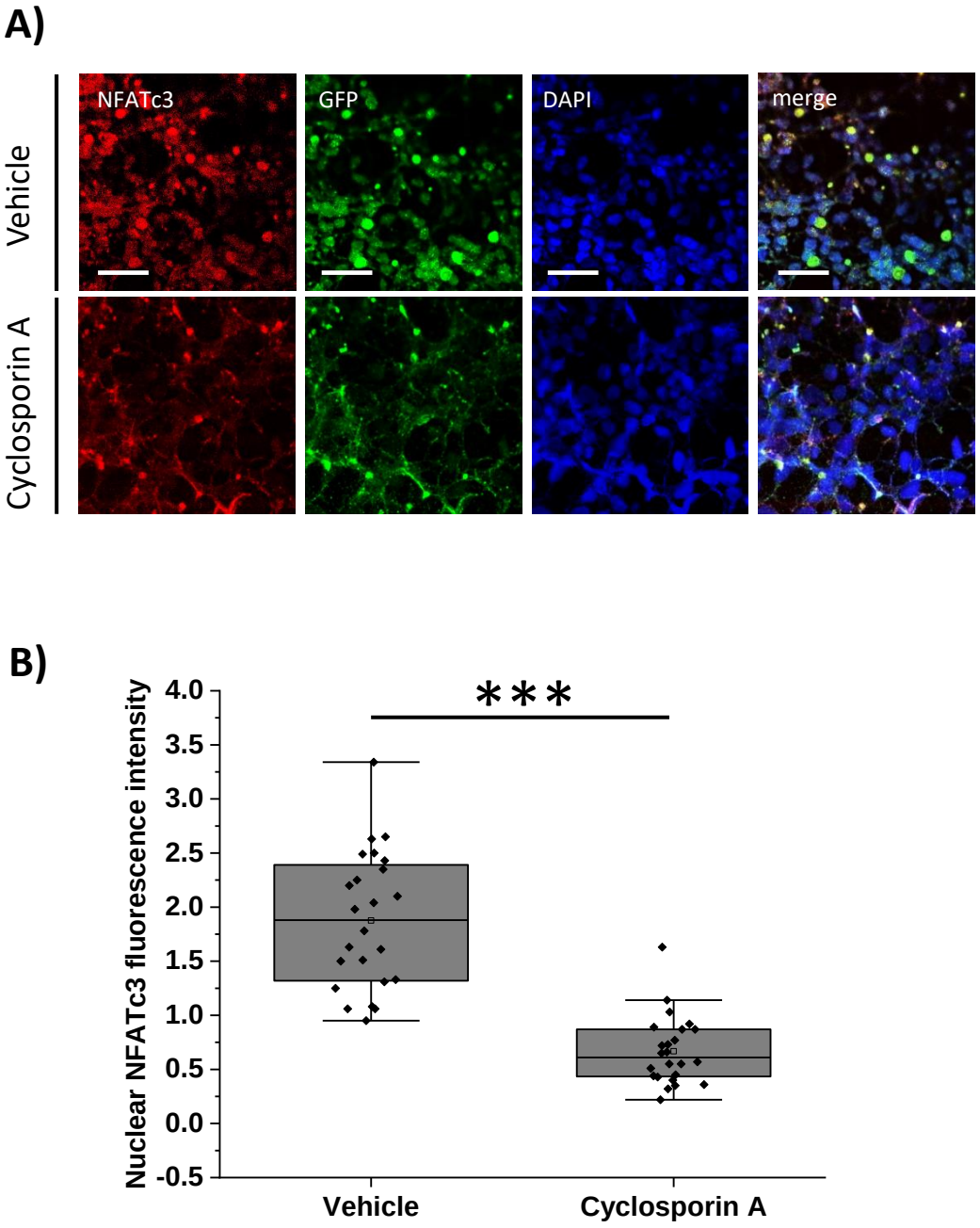

Figure 4.8. Cyclosporin A reduces nuclear localisation of NFATc3 in HEK cells. (***A***) Representative confocal images of HEK cells transfected with NFAT-GFP plasmid and immunostained with primary antibody against NFATc3, and Alexa Fluor-555, and co-stained with DAPI. Scale bars 50µm. (***B***) Box plots show the fluorescence intensity of NFATc3 normalised as a proportion of strongest NFATc3 signal in the same image, in HEK cells cultured with and without cyclosporin A exposure (N=24 cells; ***P < 0.001, Mann-Whitney U test).

4.3.4 Changes in mRNA expression following exposure to 4AP and cyclosporin A

To investigate the expression of *Kcnq2* and *Kcnq3* in epilepsy, I wanted to quantify expression changes in organotypic cultures exposed to 4AP. As with the 4AP exposure for the BDNF immunohistochemistry (Figure 4.7), cultures were exposed at 14 days in vitro for 4 days, to minimise interference from post-slicing effects, and to attempt to recreate the REST increase observed by the Baldelli group (Pozzi et al., 2013). This exposure had also been confirmed to cause an upregulation in protein of the epileptic marker BDNF (Figure 4.7). Furthermore, 4AP had also been shown to induce hyperexcitability in organotypic hippocampal slice cultures (Figure 4.6). In addition to 4AP, cultures were exposed to cyclosporin A to examine whether NFAT was activating transcription of *Kcnq2* and *Kcnq3* in normal or hyperexcitable conditions. Cyclosporin (1µM) was added to the vehicle or 4AP medium towards the end of the incubation, before harvesting for RNA extraction and qRT-PCR. Expression of the REST target gene *Scg10* was quantified to provide more information about potential REST function. All data are normalised to expression of the Sdha reference gene, which remained stable across all groups.

A large increase in average *Bdnf* was observed in cultures treated with 4AP (44.89±8.94% of *Sdha*) compared to vehicle (4.40±0.25% of *Sdha*, $p=2.64x10^{-5}$), cyclosporin (6.12±1.12% of *Sdha*, $p=2.40x10^{-5}$) or cyclosporin with 4AP (14.28±6.52% of *Sdha*, p=0.002, Figure 4.9A). The increase in *Bdnf* mRNA following 4AP exposure is consistent with the observed increase in average BDNF protein (Figure 4.7) and the presence of epileptogenic changes occurring in the cultures, associated with observed hyperexcitability (Figure 4.6). Interestingly, cyclosporin A treatment prevented the upregulation of *Bdnf* caused by 4-AP. This had not been predicted as the combined effects had not previously been investigated.

A 35% reduction in endogenous *Rest* mRNA levels was observed in cyclosporin treated cultures compared to vehicle (p=0.001, Figure 4.9B). Similarly, *Rest* expression in cultures treated with 4AP and cyclosporin (41.56±4.99% of *Sdha*) was lower than *Rest* in vehicle (85.65±6.16% of *Sdha*, p=0.001) or 4AP treated cultures (75.48±4.18% of *Sdha*, p=0.001). This suggests cyclosporin A causes a downregulation of endogenous *Rest* expression, in both normal and hyperexcitable conditions.

No change was observed in average *Kcnq2* expression in 4AP-exposed cultures (38.32±9.47% of *Sdha*) compared to vehicle (43.61±8.90% of *Sdha*), demonstrating that unlike in the kainate model (Figure 4.2C), average *Kcnq2* expression is unaffected in the 4AP epilepsy model. However, *Kcnq2* mRNA was reduced following cyclosporin A (9.22±1.62% of *Sdha* compared to 43.61±8.90% of *Sdha* for vehicle, $p=5.90x10^{-5}$, Figure 4.9C). Similarly, *Kcnq2* mRNA was reduced in cultures exposed to 4AP with cyclosporin A (6.07±1.57% of *Sdha* compared to 43.61±8.90% of *Sdha* for vehicle, $p=9.14x10^{-5}$). In contrast to the lack of effect of 4AP on *Kcnq2* expression, 4AP caused a 26% significant reduction in *Kcnq3* compared to vehicle (p=0.035, Figure 4.9D). Similar to *Kcnq2*, cyclosporin treated cultures showed a 69% reduction in *Kcnq3* expression compared to vehicle (p=0.001). *Kcnq3* in cultures treated with cyclosporin and 4AP (6.76±0.71% of *Sdha*) was also reduced compared to vehicle (35.57±3.87% of *Sdha*, p=0.001) or 4AP (26.10±2.71% of *Sdha*, p=0.001). This suggests cyclosporin causes a downregulation of *Kcnq3*, whether in the presence or absence of 4AP.

Exposure to 4AP (29.23±1.97% of *Sdha*) did not cause any change in expression of *Sp1* compared to vehicle (26.75±1.46% of *Sdha*, Figure 4.9E). Cyclosporin caused a 39% reduction in *Sp1* expression compared to vehicle (p=0.001). Similarly, the combination of cyclosporin and 4AP (18.40±1.05% of *Sdha*) also caused a reduction in *Sp1* expression compared to vehicle (26.75±1.46% of *Sdha*, p=0.001) and 4AP (29.23±1.97% of *Sdha*, p=0.001). This demonstrates that 4AP has no effect on *Sp1* mRNA expression, and that cyclosporin A causes *Sp1* downregulation independently of 4AP. *Scg10* mRNA levels were reduced by 26.5% after 4AP treatment (p=0.0212, Figure 4.9F), suggesting REST may have been repressing *Scg10* in this model.

Bdnf mRNA showed a large variation in degree of expression increase from 4AP exposure in individual samples, reflecting what was observed from the BDNF protein (Figure 4.7). It was noticed that in the samples with the greater *Bdnf* increases, *Kcnq2* and *Kcnq3* also increased. Values for fold changes in gene expression in treatment groups compared to vehicle control were correlated for each sample to examine whether changes in different genes were associated. In cultures exposed to 4AP, *Bdnf* changes were positively correlated to *Kcnq2* (R=0.66, p=0.029, Pearson's, Figure 4.9G) and *Kcnq3* levels (R=0.81, p=0.003, Pearson's, Figure 4.9H). As *Bdnf* is an epileptic marker associated with epilepsy severity (Wang et al., 2011), a greater *Bdnf*

level may suggest an organotypic culture with a greater degree of epileptogenic qualities. Thus, in more strongly epileptic-like cultures, *Kcnq2* and *Kcnq3* levels tend to be higher, whereas in cultures less affected by the 4AP (less than a 5-fold *Bdnf* increase), *Kcnq2* and *Kcnq3* actually decrease (Figures 4.9G, 4.9H). A strong positive correlation was also observed between changes in *Kcnq2* and *Kcnq3* following 4AP exposure (R=0.82, p=0.002, Pearson's, Figure 4.9I), which would be expected. In cultures exposed to cyclosporin A with 4AP, there was a positive correlation between *Rest* and *Kcnq3* (R=0.64, p=0.046, Pearson's, Figure 4.9J), as well as *Bdnf* and *Kcnq2* (R=0.90, p=0.0005, Pearson's, Figure 4.9K), and *Kcnq2* and *Kcnq3* (R=0.79, p=0.006, Pearson's, Figure 4.9K). This suggests the association between *Bdnf* and *Kcnq2* remains when cyclosporin is added to the 4AP, but the association is lost somewhat for *Bdnf* and *Kcnq3* (R=0.54) in this condition. The positive association between *Rest* and *Kcnq2* is also novel and was not present in 4AP conditions alone. As cyclosporin causes a reduction in *Rest* and *Kcnq2*, it appears that the samples with the greater *Rest* reductions are the samples with the greater *Kcnq2* reductions, so cyclosporin has a similar effect on both genes. In cultures treated with cyclosporin only, the only significant correlation was between *Kcnq2* and *Kcnq3* (R=0.60, p=0.030, Pearson's, Figure 4.9N). *Kcnq2* and *Kcnq3* expression is correlated across all conditions suggesting that there is an association between them. No significant correlations were found between *Sp1* and any of the other genes across any of the conditions, which decreases the likelihood that *Sp1* is being regulated by REST or is regulating the expression of *Kcnq2* or *Kcnq3* to any significant degree.

In summary, 4AP exposure causes an increase in *Bdnf* mRNA expression. Cyclosporin A exposure causes a reduction in expression of not only *Kcnq2* and *Kcnq3*, but also *Rest*, and it prevents the *Bdnf* increase triggered by 4AP. The reasons for the downregulation of *Rest* in cyclosporin conditions are unclear. The block of *Bdnf* increase suggests hyperexcitability-associated *Bdnf* upregulation is in some way dependent on calcineurin or its downstream signalling molecules. Though 4AP causes only a small overall downregulation of *Kcnq3* and no effect on *Kcnq2*, 2-fold reductions in *Kcnq2* and *Kcnq3* are observed in cultures with the smallest *Bdnf* increases (less than 5-fold). This suggests expression of *Bdnf* and *Kcnq2/3* are associated in 4AP conditions, while no correlation between *Bdnf* and *Kcnq2/3* is observed in cyclosporin only conditions.

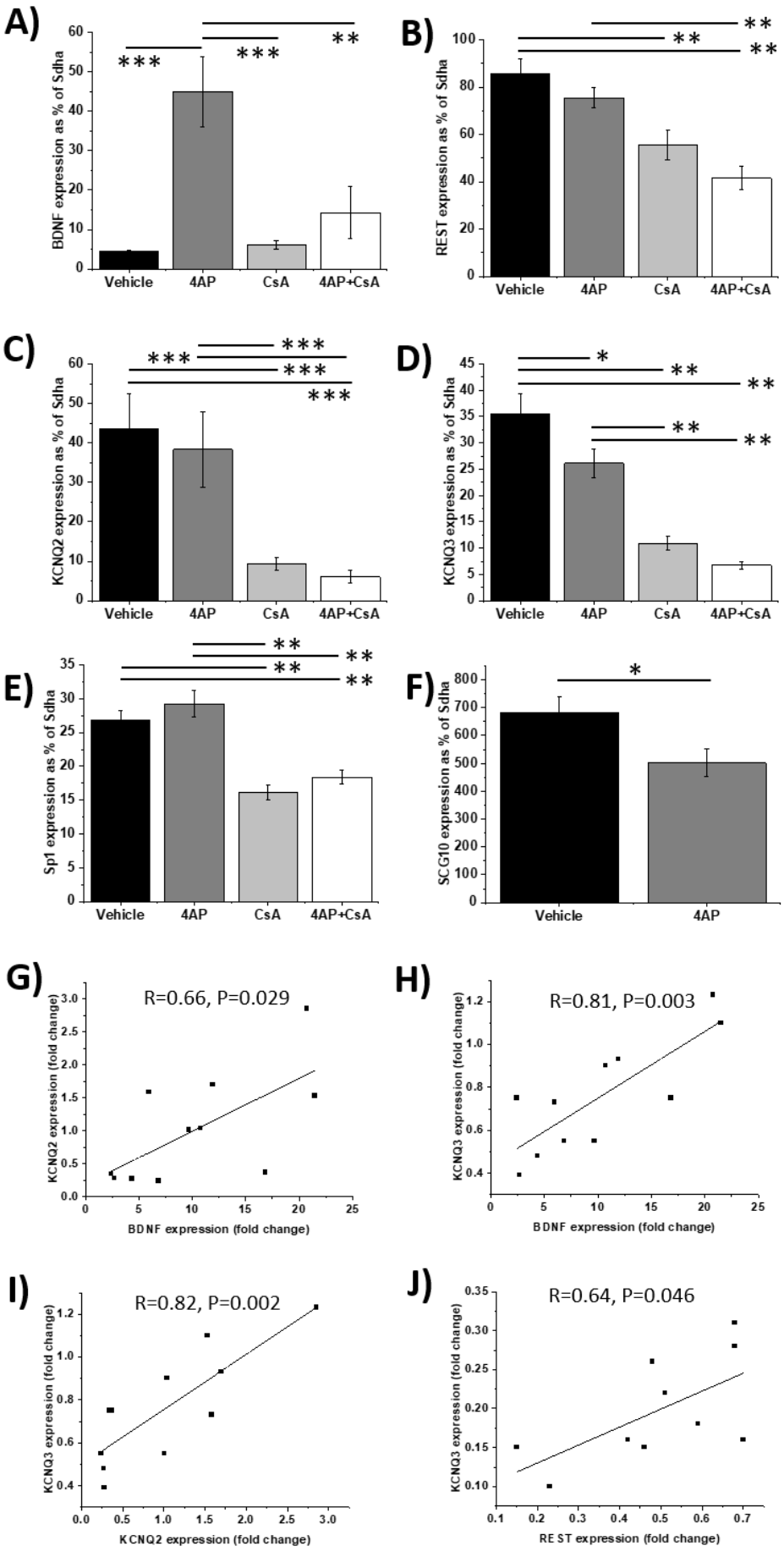
A)
BDNF expression as % of Sdha
Vehicle
4AP
CsA
4AP+CsA
B)
REST expression as % of Sdha
C)
KCNQ2 expression as % of Sdha
D)
KCNQ3 expression as % of Sdha
E)
Sp1 expression as % of Sdha
F)
SCG10 expression as % of Sdha
G)
R=0.66, P=0.029
KCNQ2 expression (fold change)
BDNF expression (fold change)
H)
R=0.81, P=0.003
KCNQ3 expression (fold change)
I)
R=0.82, P=0.002
KCNQ3 expression (fold change)
KCNQ2 expression (fold change)
J)
R=0.64, P=0.046
KCNQ3 expression (fold change)
REST expression (fold change)

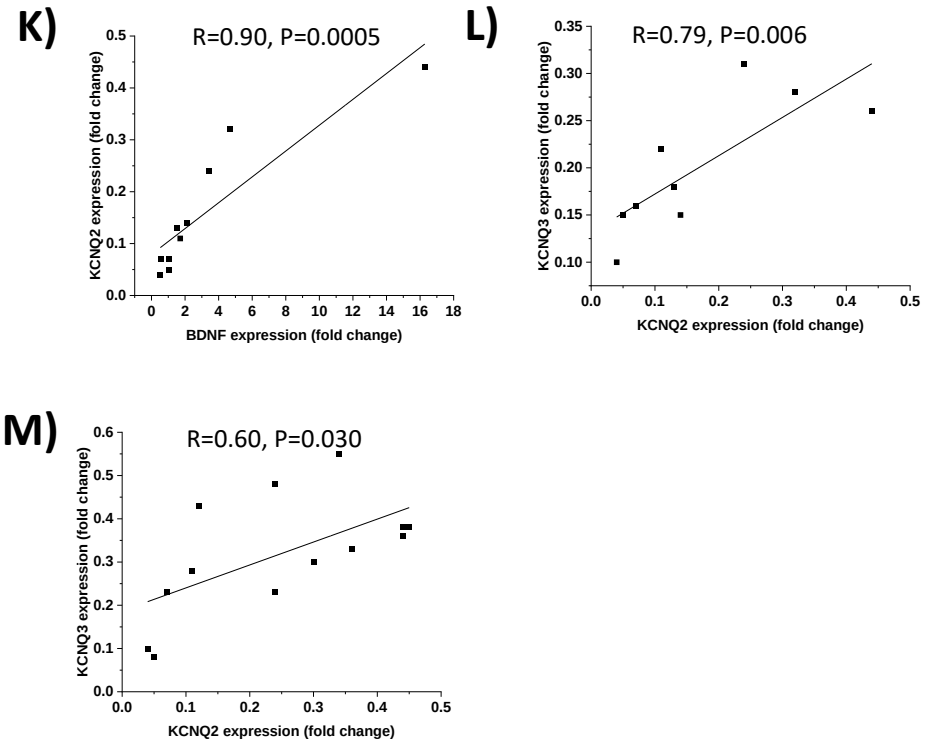

Figure 4.9. Changes in mRNA expression in *Bdnf, Rest, KCNQ2, Kcnq3, Scg10* and *Sp1* following exposure to 4AP, or 4AP with cyclosporin A. Reverse transcription quantitative PCR analysis of mRNA levels of *Bdnf* (***A***), *Rest* (***B***), *Kcnq2* (***C***) *Kcnq3* (***D***) and *Sp1* **(E)** in organotypic hippocampal slice cultures exposed to vehicle, 4AP, cyclosporin A (*CsA*), or 4AP with cyclosporin A (* $p < 0.05$, ** $p < 0.01$). *Bdnf* and *Kcnq2* analysed by Kruskal-Wallis followed by Mann-Whitney U tests for pairwise comparisons. *Rest, Kcnq3, Sp1* and *Scg10* analysed by ANOVA followed by Tukey's post-hoc test. (***A-E***) are expressed as % of *Sdha* reference gene (mean ± SEM; n = 8-13 samples). (***F***) Reverse transcription quantitative PCR analysis of *Scg10* expressed as % of cyclophilin A reference gene. (***G-I***) Significant positive correlations between fold changes in expression of genes comparing vehicle and 4AP groups. (***J-L***) Significant positive correlations between fold changes in expression of genes comparing vehicle and 4AP+CsA groups. (***M***) Significant positive correlations between fold changes in expression of genes comparing vehicle and *CsA* groups.

4.3.5 Changes in BDNF and REST protein in organotypic hippocampal slice cultures exposed to 4AP

Exposure of organotypic hippocampal slice cultures to 100µM 4AP for 4 days caused an increase in *Bdnf* mRNA but no observed difference in *Rest* mRNA levels (Figure 4.9B). To further confirm the BDNF upregulation and to further examine REST expression, I wanted to quantify the protein levels of both through western blotting after the same 4AP exposure. Samples were collected from 3 homogenised organotypic cultures each. Three samples from vehicle-exposed cultures and 3 samples from 4AP-exposed cultures were used, each sample being run on duplicate gels. BDNF and REST bands from one of the gels are shown in figure 4.10A alongside bands for the β-tubulin loading control, which remained the same on average between conditions. Density of the bands was normalised to density of the loading control and data is represented in relation to vehicle. Average BDNF protein showed a slight non-significant raise after 4AP exposure (1.34±0.24, n=3, Figure 4.10B). The quantification suggests that for both BDNF and REST, some samples show increased protein in response to 4AP while others do not increase. However, this is less clear from the visualisation of the individual bands. It appears that REST may have increased in all 4AP samples and one of the vehicle samples, but no distinction can be made with BDNF. Western blotting may lack the sensitivity required to discern subtle upregulations in BDNF and REST protein. However, BDNF upregulation was confirmed through immunohistochemistry (Figure 4.7). In contrast, no evidence of REST upregulation in organotypic hippocampal slice cultures after 4AP exposure has been observed in this project.

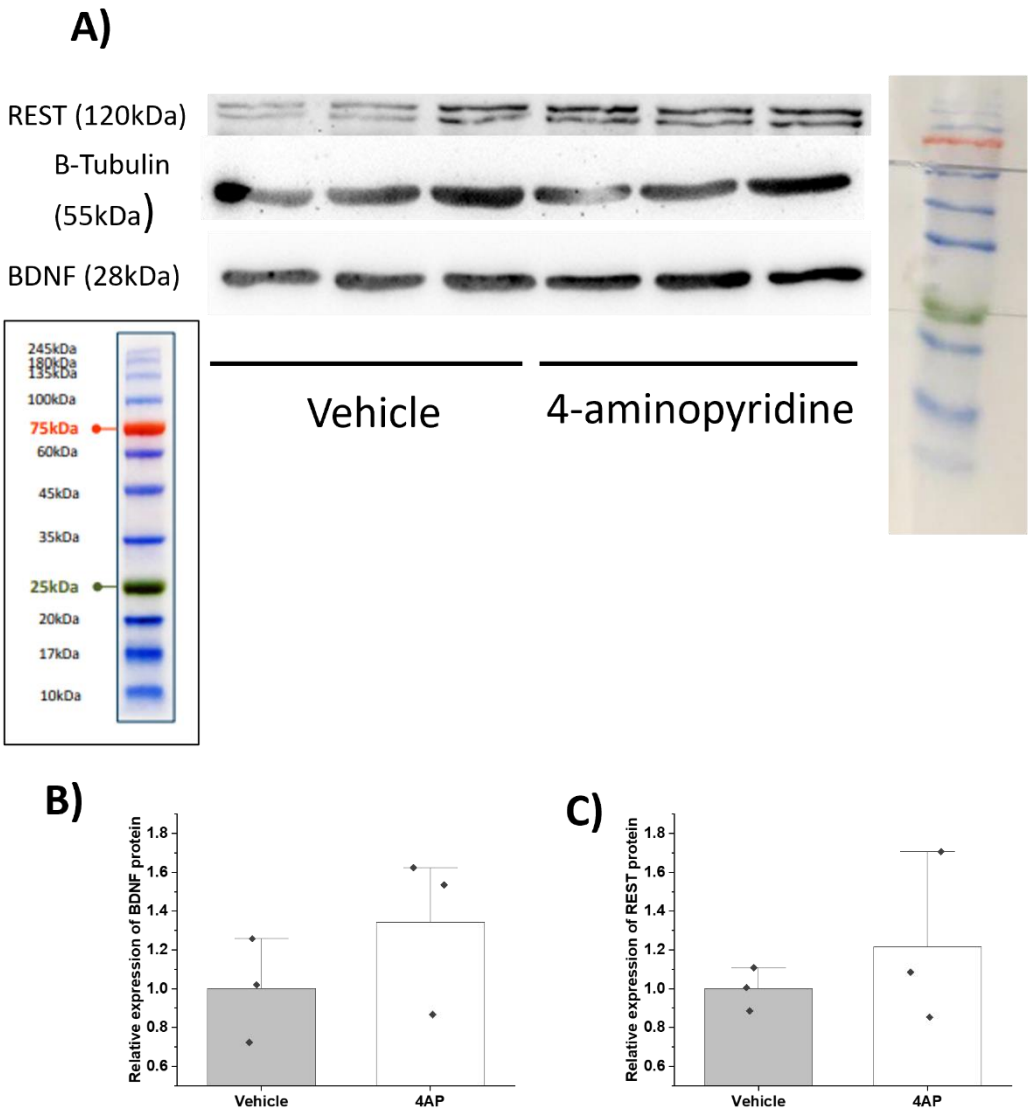

Figure 4.10. Changes in BDNF and REST protein in organotypic hippocampal slice cultures exposed to 4-aminopyridine. (*A*) Western blot of REST and BDNF proteins with tubulin loading control taken from cultures exposed to vehicle or 4-aminopyridine, with molecular weight of proteins and molecular weight markers shown. (***B, C***) No changes in average expression of BDNF and REST proteins from cultures exposed to kainite, compared to vehicle (mean ± SD, n=3 samples, each sample taken from 3 cultures).

4.4 Discussion

4.4.1 The effects of kainate on *Kcnq2*/Kv7.2 and *Kcnq3*/Kv7.3 expression in organotypic hippocampal cultures

Changes in BDNF were used to signify that changes indicative of epileptogenesis had been induced in the organotypic hippocampal slice cultures in response to kainate. Hippocampal *Bdnf* mRNA and BDNF protein is shown to be increased in response to kainate *in vivo* (Ballarín et al., 1991; Wetmore et al., 1994), through increased intracellular calcium (Saarelainen et al., 2001). I observed that BDNF protein increases in most, but not all, organotypic hippocampal slice cultures exposed to kainate, through immunohistochemistry and western blotting. The individual variation may be specific to organotypic cultures. As BDNF regulates neuronal survival and development, variations in treatments between separate cultures during the preparation and culture process may affect BDNF activity, causing the observed differences in expression. In response to kainate, average *Bdnf* mRNA was increased 10-fold in uninfected cultures and 20-fold in infected cultures, suggesting the infected cultures may have been more epileptic-like, on average. REST overexpression and functional knockdown had no effect on *Bdnf* in vehicle-treated cultures. REST binds and directly represses *Bdnf* expression (Tabuchi et al., 2002; Zuccato et al., 2003). REST overexpression was reported to reduce BDNF expression (Hara et al., 2009), and attenuation of REST binding rescued BDNF expression (Zuccato et al., 2007). Furthermore, REST-mediated repression of *Bdnf* has been shown to prevent kindling (Garriga-Canut et al., 2006). In contrast, my results suggest that REST has no effect on *Bdnf* in non-epileptic hippocampal tissue, but that REST upregulates *Bdnf* in the kainate epileptic model. This is likely to be an indirect mechanism.

Kainate has been previously shown to increase hippocampal REST (Brennan et al., 2016; McClelland et al., 2011; Palm et al., 1998). In contrast, no changes in *Rest* mRNA were observed in slice cultures in response to kainate in the present study. However, the REST target genes *Kcnq2* and *NaII/Scn2a* showed reduced mRNA in response to kainate, suggesting REST-mediated repression was likely. Despite a lack of observed *Rest* mRNA increase, REST protein activity could have been enhanced to induce REST-mediated repression of its target genes. REST protein levels were increased in the western blots of some cultures but not others. Chmielewska and

colleagues also saw variation in REST levels after PTZ kindling, with increased REST found in animals resistant to PTZ kindling, and no change in REST found in animals susceptible to kindling (Chmielewska et al., 2020). Therefore, the individual variations in REST protein observed in the current study could reflect individual susceptibility or resistance to epileptogenesis.

Following kainate exposure in uninfected cultures, *Kcnq2* mRNA in organotypic hippocampal slice cultures was reduced. In support of my findings, I also observed that overall Kv7.2 protein was reduced after kainate exposure. Kv7.2 was reduced in the CA1 hippocampal region, while remaining the same as control in the CA3 region and being increased in the dentate gyrus. The differences could reflect cell type-specific effects. The lack of change in the CA3 region was unexpected, as this region is the most highly affected by kainate (Castillo et al., 1997). Indeed, the CA3 region has been described as suffering from severe cell death from kainate compared to other regions, due to the high number of kainate receptors in this region (Ben-Ari and Cossart, 2000; Monaghan and Cotman, 1982; Petralia et al., 1994). Massive kainate-induced neurodegeneration in the CA3 region could blunt any changes in Kv7.2 expression observed from the immunohistochemical staining. The reduction of Kv7.2 protein seen in the CA1 region could reflect a downregulation in pyramidal neurons, while the increase in the dentate gyrus could reflect an upregulation of Kv7.2 in granule cells. The dentate gyrus is the gatekeeper of the hippocampus, receiving afferent fibers from other regions, and the upregulation of Kv7.2 here could imply a neuroprotective mechanism to prevent seizure activity from other brain regions from reaching the hippocampus. It is likely that the overall downregulation of *Kcnq2*/Kv7.2 in the hippocampal slice cultures is from the pyramidal neurons which are prevalent in the molecular layer throughout most of the hippocampus, including the CA1 region. This downregulation would be expected to decrease the Kv7 current and contribute to epileptogenesis.

In contrast to in uninfected cultures, in infected cultures *Kcnq2* was not reduced in response to kainate. The only differences between the 2 experiments were the presence of adenoviral infection in all infected cultures, and an observed higher average *Bdnf* level increase in the infected cultures. It is likely that when *Bdnf* is increased 20-fold, as observed in the infected cultures, the cultures are more strongly epileptic than when *Bdnf* is only increased 10-fold. This greater increase could result in the activation of a

neuroprotective mechanism resulting in the upregulation of *Kcnq2*, balancing out the downregulation caused by kainate, observed in the uninfected cultures. Others have reported neuroprotective effects of BDNF in addition to its pro-epileptogenic ones. Chmielewska and colleagues found that animals resistant to PTZ kindling showed increased levels of BDNF, while kindling-susceptible animals had unchanged BDNF levels (Chmielewska et al., 2020). My data suggests this could involve *Kcnq2* regulation and could be very sensitive to levels of BDNF increase. The wide variation I have observed in BDNF protein increases could reflect the differential ability of individuals to resist epileptogenesis.

No effects were observed on *Kcnq2/3* expression when REST or DNREST were overexpressed in vehicle-treated cultures. In the presence of kainate, *Kcnq2* levels were lower in cultures infected with DN*Rest* than control or REST overexpressing cultures. When *Bdnf* is increased to a large degree (20-fold average) by epileptic conditions, it appears that it may induce a neuroprotective mechanism to upregulate *Kcnq2* and *Kcnq3* in opposition to an unidentified downregulating force, resulting in no overall change in *Kcnq2/3* levels. The DN*Rest* appears to prevent *Bdnf* from upregulating fully from kainate exposure, leading to only a 10-fold average *Bdnf* increase. This 10-fold average *Bdnf* increase in the DN*Rest* kainate cultures is similar to what was observed in the uninfected cultures. This was associated with an overall kainate-induced downregulation from control of *Kcnq2* in the uninfected cultures, as well as in the DN*Rest* kainate cultures. Though not confirmed, this downregulation of *Kcnq2* may be due to REST repression of *Kcnq2*, through increased activity or reduced degradation of the REST protein.

Although the contribution of Sp1 towards epileptogenesis has been described by a few groups (see Introduction), the expression levels of Sp1 have not been previously examined. Sp1 DNA binding affinity was shown to be increased in response to kainate, through an electrophoresis mobility shift-assay (Feng et al., 1999). However, increased binding affinity signifies increased activity but not overall expression level. Binding affinities of Sp1 are affected by post-translational modifications such as phosphorylation, acetylation, sumoylation, ubiquitylation and glycosylation (Tan and Khachigian, 2009). I observed that *Sp1* mRNA levels were unchanged in response to kainate in uninfected cultures. Therefore, it seems likely that in epileptic conditions, *Sp1* transcriptional expression levels remain steady, but Sp1 activity is mainly

regulated by these post-translational modifications. This may also be the case when REST is overexpressed, in both vehicle and kainate-treated cultures, as *Sp1* expression levels remain the same as in control cultures in these conditions. However, when REST function is blocked, *Sp1* expression is higher in vehicle than kainate conditions. This follows a similar expression pattern to *Kcnq2*. *Sp1* levels are likely to be high in the DN*Rest* vehicle cultures because the DN*Rest* blocks endogenous REST function, and REST represses Sp1. Therefore, DN*Rest* is likely to cause a de-repression effect of *Sp1*. Sp1 may also be positively regulating *Kcnq2* (Mucha et al., 2010). The reasons for the reduction in *Sp1* expression in DN*Rest* kainate cultures are more difficult to explain. Though in this experiment the *Sp1* expression pattern is similar to that of *Kcnq2*, in uninfected cultures kainate caused a downregulation of *Kcnq2* while *Sp1* remained the same. Therefore, the level of *Bdnf* increase does not explain the downregulation of *Sp1* in DN*Rest* kainate cultures. Kainate or DN*Rest* alone caused no change in *Sp1* expression, but combined they cause *Sp1* downregulation. This suggests the involvement of another factor which represses *Sp1* and is activated by kainate but repressed by REST. Nuclear Factor kappa B (NF kappaB) and p53 are both identified to inhibit Sp1. NF kappa B is also well characterised as being activated by kainate through calcium influx (Cruise et al., 2000; Li et al., 2010; Miller et al., 2014; Ruan et al., 2019), though evidence of its repression by REST is lacking. NF kappa B activation by kainate may be inhibited by endogenous REST, leading to no overall change in *Sp1* level from kainate alone. Tonic levels of NF kappa B in non-epileptic tissue may not be repressed by REST. However, when kainate activates NF kappa B and endogenous REST is blocked, allowing a de-repression of NF kappa B, this could lead to a noticeable increase in active NF kappa B, which would be enough to cause a significant downregulation of *Sp1*, as is observed.

In summary, exposure of organotypic hippocampal slice cultures to kainate caused an mRNA and protein upregulation of *Bdnf. Rest* mRNA was not observed to change, but the REST target genes *Kcnq2* and *NaII/Scn2a* were downregulated, suggesting REST-mediated repression was likely, though not evident. *Kcnq2* was downregulated by kainate in uninfected slices but unchanged in slices infected with adenovirus, where *Bdnf* levels were higher. This could suggest *Kcnq2* is downregulated when kainate causes around a 10-fold *Bdnf* increase, but that they are maintained at stable levels when kainate causes around a 20-fold *Bdnf* increase, pointing to a BDNF-mediated

neuroprotective mechanism. An increase in REST protein activity may be responsible for the downregulatory force upon *Kcnq2* and *Kcnq3* but this is not confirmed. Kainate-exposed DNREST expressing cultures showed low levels of *Kcnq2* and *Sp1*, alluding to altered signalling in this condition.

4.4.2 The effects of 4-aminopyridine on *Kcnq2*/Kv7.2 and *Kcnq3*/Kv7.3 expression in organotypic hippocampal cultures

In the organotypic hippocampal slice cultures 4AP exposure was observed to cause significantly increased action potential frequency and ictal and interictal activity in many, but not all, of the cultures. This reflects the epileptiform activity that has been seen previously in acute brain slices in response to 4AP exposure (Avoli et al., 1996; Bijak and Misgeld, 1996; Chesnut and Swann, 1990; Motalli et al., 1999) and suggests that 4AP is a suitable convulsant for use as an epileptic model in organotypic hippocampal cultures.

Cyclosporin A is a potent immunosuppressive drug that was used in the current study to block nuclear translocation of the NFAT isoforms in neurons, preventing their enhancement of *Kcnq2/3* transcription (Zhang and Shapiro, 2012). The isoforms of NFAT are NFATc1, NFATc2, NFATc3, NFATc4 and NFAT5, and cyclosporin inhibits the activation of all of these (Li et al., 2016a). I confirmed with immunohistochemistry that cyclosporin prevents nuclear translocation of NFATc3 in HEK cells. Interestingly, traumatic brain injury caused a reduction of NFATc3 in both the nuclear and cytosolic fractions of hippocampal homogenates. It also caused an increase of NFATc4 in the cytosolic fraction and decrease in the nuclear fraction. Further investigation revealed NFATc3 was found mainly in astrocytes and NFATc4 was found mainly in neurons (Yan et al., 2014). NFATc3 was shown to be activated in reactive astrocytes, but not neurons, around damaged neurons in the hippocampal CA1 and CA3 regions in response to kainate injection (Serrano-Pérez et al., 2011). However, a different group saw that NFATc3 underwent rapid dephosphorylation and translocation from the cytoplasm to the nucleus in hippocampal neurons in response to intracellular Ca^{2+} influx. In contrast, NFATc4 remained mostly phosphorylated in the cytoplasm for much longer, relying on suppression of GSK3β for its translocation. Most importantly, NFATc3 knockdown resulted in reduced NFAT-mediated transcription, while knocking down NFATc4 did not (Ulrich et al., 2012). Therefore,

despite NFATc3 being less prevalent in neurons than NFATc4, it seems to be more critical for NFAT-mediated regulation of target genes. The evidence that cyclosporin inhibits NFATc3 translocation in HEK cells suggests it is very likely that cyclosporin inhibits the activation of NFAT target genes such as KCNQ2/3 in hippocampal neurons.

While the upregulation of BDNF in epilepsy patients and in other seizure models is well established (Ernfors et al., 1991; Hou et al., 2010; Martínez-Levy et al., 2016; Murray et al., 2000; Nibuya et al., 1995; Takahashi et al., 1999; Vezzani et al., 1999), BDNF expression had not been investigated in the 4AP epilepsy model. My results showed that BDNF protein was increased in most but not all cultures exposed to 4AP, suggesting the cultures with the increased BDNF had achieved an epileptic-like state. Average *Bdnf* mRNA level was significantly increased by around 10-fold. Interestingly, this 4AP-induced *Bdnf* mRNA increase was prevented by cyclosporin, while *Bdnf* expression was not affected by cyclosporin alone. The previously reported effects of cyclosporin A on *Bdnf* are mixed. Cyclosporin A administration for 30 days caused downregulation of BDNF and its receptor trkB in the hippocampus and midbrain (Chen et al., 2010). Furthermore, cyclosporin A was found to decrease neurogenesis and cognition through downregulation of the interferon-gamma-Shh-BDNF pathway (Wang et al., 2021). In contrast, other groups have observed an increase in hippocampal *Bdnf* mRNA and protein caused by cyclosporin treatment through induction of pCREB (Gabryel and Bernacki, 2009; Miyata et al., 2001). The fact that I saw no difference in *Bdnf* expression from cyclosporin alone was not unexpected and could be the combined result of these pathways. More notably, cyclosporin A was shown to reduce the number of spontaneous recurrent seizures induced by kainate, and prevented epileptiform activity in 4AP-treated hippocampal slices (Jung et al., 2012). It also suppressed epileptogenesis in the rat pilocarpine model (Setkowicz and Ciarach, 2007). It similarly provides neuroprotection in models of traumatic brain injury and stroke (Albensi et al., 2000; Borlongan et al., 2005; Domañska-Janik et al., 2004; Okonkwo and Povlishock, 1999). Therefore, its anti-epileptogenic properties are likely to be the reason why cyclosporin prevented 4AP-induced *Bdnf* upregulation. This suggests that the 4AP exposure was largely inducing an epileptic-like state in the organotypic hippocampal cultures, and the cyclosporin exposure was sufficient to affect downstream pathways.

It had previously been shown that the same 96-hour 4AP exposure used in the current project applied to cultured hippocampal neurons resulted in significant upregulation of REST protein. *Rest* mRNA was increased between 8-48 hours and had reduced to levels not significantly different from control by 96 hours (Pozzi et al., 2013). By choosing an exposure known to result in increased REST protein levels, I hoped to maximise observed responses from REST target genes. It was unclear from western blot whether 4AP caused an increase in REST protein in organotypic hippocampal cultures at this timepoint or not. *Rest* mRNA was unchanged from the 4AP exposure, which was expected and in line with the findings from Pozzi and colleagues. Expression of the REST target gene *Scg10* was reduced by 4AP, which may support the idea of an increased activity of REST, in spite of a lack of *Rest* mRNA increase. Therefore, it is not possible to conclude whether an increase of *Rest* mRNA or REST protein had occurred at any timepoint in response to the 4AP treatment in organotypic hippocampal slice cultures. The effects of cyclosporin on REST had not been investigated, but my results showed that *Rest* was downregulated by cyclosporin, independently of 4AP, which was surprising. The reason for this is unknown as calcineurin has not been previously linked to REST.

The effects of 4AP on *Kcnq2* expression or function have not been previously investigated. On average, *Kcnq2* levels are unaffected by 4AP exposure in organotypic hippocampal slice cultures, suggesting that changes in *Kcnq2* expression are not a central factor in driving or preventing epileptogenesis in the 4AP model. There is also no suggestion of direct *Kcnq2/3* regulation by REST or Sp1 in the 4AP model. However, *Bdnf* and *Kcnq2* expression are positively correlated. In cultures with lower (less than 5-fold) *Bdnf* increases, *Kcnq2* is downregulated by more than 2-fold, and in cultures with higher (more than 20-fold) *Bdnf* increases, *Kcnq2* is upregulated by 1.5-3-fold. This could suggest that the 4AP-induced *Bdnf* increase induces a neuroprotective mechanism which helps towards maintaining *Kcnq2* levels during neuronal hyperexcitability, thus helping to stabilise the anti-excitatory Kv7 current. This BDNF-mediated upregulation may be working in opposition to forces promoting a downregulation of *Kcnq2*, allowing *Kcnq2* expression to remain constant overall. The correlation between *Bdnf* and *Kcnq2* in 4AP conditions becomes even more pronounced when cyclosporin is added, and this is most likely because cyclosporin prevents *Bdnf* upregulation through its anti-epileptogenic properties (Jung et al., 2012;

Setkowicz and Ciarach, 2007). *Kcnq2* expression is reduced by cyclosporin, but in a 4AP-independent manner. The effects of cyclosporin on *Kcnq2* have not been previously reported. NFAT is reported to enhance *Kcnq2* transcription in conditions of increased excitability and seizure (Zhang and Shapiro, 2012), so the fact that cyclosporin is able to modulate *Kcnq2* in a 4AP-independent way may suggest NFAT inhibition is not responsible for this effect. However, in keratinocytes, calcineurin was shown to activate the association of NFAT1/2 with Sp1 to activate transcription of the Sp1 target gene *p21*. Cyclosporin A treatment alone downregulated expression of *p21* through this mechanism (Santini et al., 2001). This suggests that either NFAT1/2 is not a limiting factor or may not be involved in calcineurin activation of *Sp1* in the non-epileptic hippocampus. If a similar mechanism exists in the hippocampus, cyclosporin could block tonic levels of calcineurin in non-epileptic conditions, resulting in reduced Sp1-mediated gene transcription. As *Kcnq2* is a target gene of Sp1, this would be expected to result in reduced *Kcnq2* expression in response to cyclosporin, which is what is observed.

In contrast to the lack of change of *Kcnq2*, *Kcnq3* is reduced by 4AP by a significant 24%. This could be a sign that the mechanism of BDNF-mediated upregulation described for *Kcnq2* also occurs in *Kcnq3*, but to a lesser degree. Therefore, the forces working in opposition to this, causing downregulation of *Kcnq2/3*, have an overall greater effect on *Kcnq3* than *Kcnq2*, inducing an observed downregulation overall. As with *Kcnq2* and *Bdnf*, there was a positive correlation between *Kcnq3* and *Bdnf* in 4AP conditions, with *Kcnq3* expression reduced by at least 20% in all cultures with lower (less than 10-fold) increases in *Bdnf* expression. This supports the idea of greater *Bdnf* increases to be necessary for maintaining *Kcnq2/3* expression at a constant level, and that in cultures where *Bdnf* increase is smaller, this neuroprotective mechanism cannot occur. This would result in reduced Kv7 current and increased overall neuronal excitability. The downregulation of *Kcnq3* is also reduced further by cyclosporin in a 4AP-independent manner, as was seen with *Kcnq2*. Again, this could be explained by the mechanism found in keratinocytes, where tonic levels of calcineurin are required for transcription of Sp1 target genes in non-epileptic conditions, possibly with interaction from NFAT (Santini et al., 2001). This would allow cyclosporin A to cause a reduction in *Kcnq3*, as, like *Kcnq2*, it is also a target gene of Sp1.

As was observed in response to kainate, *Sp1* expression was also unaffected by 4AP exposure. As Sp1 activity has been noted to increase in epileptic conditions (Feng et al., 1999) but its expression does not seem to change, this is more likely to occur due to post-translational modifications such as phosphorylation (Tan and Khachigian, 2009). Interestingly, *Sp1* was reduced by cyclosporin in a 4AP-independent manner. This was similar to the observed effects of cyclosporin on *Kcnq2* and *Kcnq3* expression and would support the idea that calcineurin may be necessary in non-epileptic cells to maintain tonic levels of Sp1 activity to regulate the Sp1 target genes *Kcnq2* and *Kcnq3*. Furthermore, it would suggest that calcineurin's regulation of Sp1 activity may be mediated by changes in *Sp1* transcriptional expression, presumably through another unknown transcription factor. Little is known about the transcriptional regulation of *Sp1*. However, CDK4, SKP2, Rad51, BRCA2 and p21 have been shown to activate the *Sp1* promoter (Tapias et al., 2008), and CDK4 activity is regulated by calcineurin (Chow et al., 2007). This could explain why *Sp1*, *Kcnq2* and *Kcnq3* expression are all downregulated by cyclosporin, independently of the presence of 4AP.

In summary, 4AP exposure caused epileptiform activity in organotyic hippocampal cultures. A 96-hour exposure to 4AP caused mRNA and protein upregulation of the epileptic marker BDNF in most slice cultures. *Rest* mRNA and REST protein and *Sp1* mRNA levels were generally unchanged. Overall *Kcnq2* and *Kcnq3* mRNA expression levels were not affected, though correlations between *Bdnf* and *Kcnq2/3* suggest a potential neuroprotective mechanism to maintain *Kcnq2/3* expression at stable levels in the 4AP model. Reduced Scg10 expression following 4AP exposure may suggest REST-mediated repression but this is uncomfirmed. Cyclosporin treatment suggested no clear evidence of involvement from NFAT, though its prevention of 4AP-induced *Bdnf* upregulation may allude to its documented anti-epileptogenic properties.

Chapter 5

General Discussion

My results showed an overall hippocampal *Kcnq2* downregulation associated with a 10-fold *Bdnf* upregulation in response to kainate. The same kainate exposure also caused an overall hippocampal decrease in Kv7.2 protein, with a decrease in the CA1 and an increase in the dentate gyrus. Kainate exposure that induced a 20-fold *Bdnf* increase, or 96-hour 4AP exposure, resulted in no overall hippocampal change in *Kcnq2* expression. *Kcnq3* was mildly reduced following 96-hour 4AP exposure, but changes following kainate exposure were not significant. I observed indications that *Kcnq2* is repressed by HDACs in healthy conditions. In epileptic conditions, REST appears to feed into epileptogenic mechanisms, indirectly contributing to *Bdnf* upregulation, which supports maintenance of *Kcnq2/3* expression. Here I will discuss these ideas in further detail.

5.1 Kainate can cause downregulation of *Kcnq2*/Kv7.2

My results in hippocampal slice cultures showed that when kainate induced epileptogenic changes marked by *Bdnf* increases of around 10-fold, this caused a downregulation of overall hippocampal *Kcnq2* mRNA after 18 hours. This insult also caused a reduction in Kv7.2 protein in the CA1 region of the hippocampus. As pyramidal neurons are the principal neuron type in the CA1 region, the decrease in Kv7.2 protein in this location is likely to be occurring mostly in the pyramidal neurons. The lack of change in the CA3 region is most likely due to it being particularly sensitive to neuron loss from kainate-induced damage (Holopainen et al., 2004). There was also an increase in Kv7.2 protein in the dentate gyrus at this point, which is indicative of a protective mechanism in this region. This matches some of the findings from the Shapiro lab. When SE was induced in rats with 300mg/kg pilocarpine, an upregulation of *KCNQ2* was observed in the dentate gyrus and a downregulation was observed in the hippocampal CA1 and CA3 regions after 48 hours (Carver et al., 2020). This result was in stark contrast to the main conclusion of the paper, which reported increased levels of *KCNQ2* (but not *KCNQ3*) in the CA1 and CA3 hippocampal regions 48 hours following injection with 60mg/kg PTZ or 230mg/kg pilocarpine, with no changes observed in the dentate gyrus. The lower 230mg/kg pilocarpine dose, and 60mg/kg PTZ, were adequate to cause hyperexcitability but not SE. The authors reasoned that the reduction of *KCNQ2* in CA1/CA3 after the 300mg/kg higher dose of pilocarpine was an error caused by cytotoxicity. In contrast, they reasoned that *KCNQ2* upregulation in the dentate gyrus at this dosage was correct,

as the dentate gyrus has more protection from cell death. This assumption was based on an image of MAP2 staining appearing fainter after the higher dosage. However, this image does not give evidence of preserved MAP2 staining in the dentate gyrus. It seems more likely that the deterioration in MAP2 staining was an artifact of a poor stain, and that the *KCNQ2* changes reported were accurate for all regions at all doses. Cytotoxicity does occur as a result of pilocarpine-induced SE, typically required by the higher (eg. 300mg/kg) doses, but the resulting neuron death occurs in the hilus of the dentate gyrus as well as the CA1 and CA3 hippocampal regions (Borges et al., 2003; Gröticke et al., 2007; Kow et al., 2014; Rangel et al., 2005). At lower pilocarpine doses that cause hyperexcitability without achieving SE, cell death is not observed in any region (Borges et al., 2003; Kow et al., 2014). Therefore, as the Shapiro group observed an increase in *KCNQ2* in the dentate gyrus after SE induced by high-dose pilocarpine, this suggests cell death was not preventing signal measurements, and so the observed CA1/CA3 *KCNQ2* downregulation must have been equally as valid (Carver et al., 2020). The author of this thesis believes that if cell death interfered with accuracy of imaging analysis, it would result in the blunting of all signals to show no changes, as I observed in the CA3 region after kainate exposure in slice cultures.

The Shapiro group had previously found increased levels of hippocampal *Kcnq2* and *Kcnq3* mRNA at 16-20 hours after injections with 280mg/kg pilocarpine or 10mg/kg kainate (Zhang and Shapiro, 2012). However, their mice were included based on clonic seizures and "flag-pole tail" only, which does not meet the definition of full SE, and a large proportion of the mice may have experienced hyperexcitability only. This would fit with their other results that suggest *KCNQ2* is above control levels during pyramidal neuron sub-SE hyperexcitability but below control levels following SE. The Shapiro group's 2012 paper did not examine specific hippocampal regions, but I observed the overall hippocampal expression changes to be reflective of the combined cornu ammonis regions, with changes in the dentate gyrus likely to contribute to overall hippocampal changes to a smaller degree.

Pilocarpine-induced SE has been observed to cause a 1-5-fold *Bdnf* increase *in vivo* (Sun et al., 2013; Thomas et al., 2016), associated with a reduction of *Kcnq2* in the hippocampal pyramidal neurons (Carver et al., 2020). This reflects a similar strength of epileptic insult to my experiments where kainate induced a 10-fold increase in *Bdnf* and a reduction in *Kcnq2*/Kv7.2 in hippocampal pyramidal neurons. At lower

pilocarpine doses which are able to induce hyperexcitability but not SE, hippocampal *KCNQ2* is increased overall and in the pyramidal neurons (Carver et al., 2020; Zhang and Shapiro, 2012). These lower pilocarpine doses would be presumed to cause less *Bdnf* upregulation than the higher doses. In contrast, in one of my experiments kainate induced a 20-fold increase in *Bdnf*, associated with no significant change in *Kcnq2*. I have observed positive associations between *Bdnf* and *Kcnq2* in my experiments, and it may be that the extremely large *Bdnf* upregulation provided an upregulatory force on *Kcnq2* in this case to prevent the downregulation observed when *Bdnf* is increased only 1-10-fold (see Figure 5.1A). In most cases *in vivo* and *in vitro*, SE seems to cause an overall downregulation of hippocampal *Kcnq2*, with *Kcnq3* often following a similar but non-significant trend. In support of this, Maslarova and colleagues reported reduced levels of Kv7.2 and Kv7.3 in the entorhinal cortex adjacent to the hippocampus 2-3 months after SE induced by 340mg/kg pilocarpine (Maslarova et al., 2013), suggesting post-SE *Kcnq2/3* downregulation in pyramidal neurons may persist for some time.

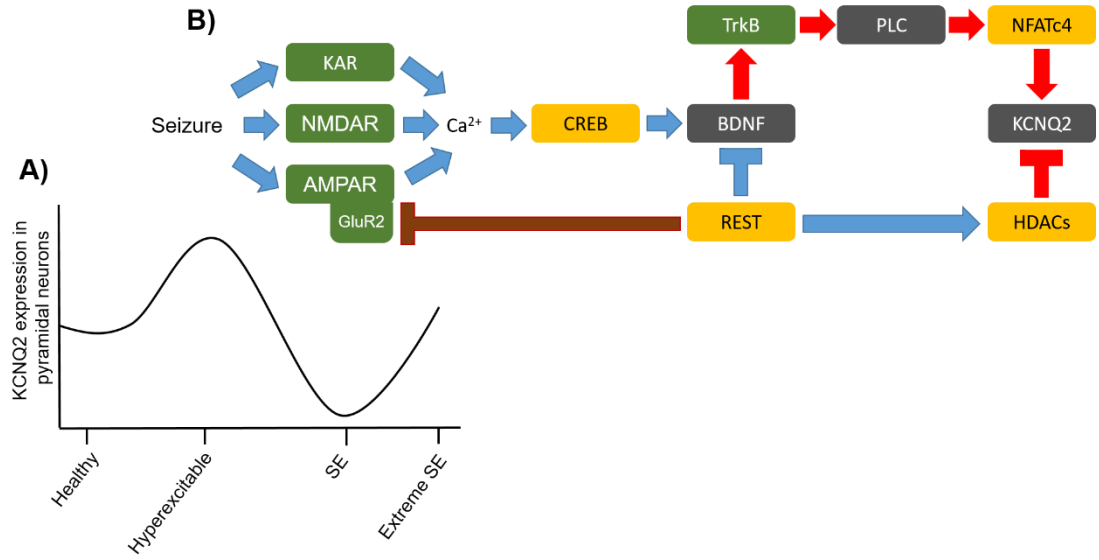

Figure 5.1. Working hypothesis summarising the proposed interactions between REST, BDNF and *Kcnq2*/Kv7.2 in hippocampal pyramidal neurons during seizure and *Kcnq2* expression at varying seizure intensities. ***A)*** When status epilepticus is triggered, NMDA receptors (NMDAR) and AMPA receptors (AMPAR) are activated. If kainate is used to trigger status epilepticus, this also activates kainic acid receptors (KAR). Activation of these receptors initiates a large influx of Ca^{2+} into the neuron, which activates the transcription factor CREB through phosphorylation.

CREB is responsible for the large upregulation of BDNF during seizure. It has widely understood that the transcription factor REST directly represses expression of the *Bdnf* gene. REST is also known to recruit histone deacetylases (HDACs) to enable repression of its target genes. Results from this thesis demonstrated that HDACs are involved in repression of the *Kcnq2* gene. Previous work showed that REST directly represses *KCNQ2* in DRG neurons. REST is also shown by many groups to be upregulated in seizure. Though this REST upregulation was not confirmed in this thesis, results suggested REST protein activity may be enhanced, which could imply REST is responsible for the downregulation of *Kcnq2* I observed in SE-type conditions. Results in this thesis also indicate that in extreme SE-like conditions, REST appears to upregulate *Bdnf,* in contrast to its direct repression of *Bdnf.* This is most likely due to REST's established repression of *GluR2* in seizure, which leads to GluR2-lacking AMPA receptors which have increased Ca^{2+} permeability, causing greater CREB activation and *Bdnf* upregulation. This effect has not been observed in normal SE conditions and may be relevant to extreme SE only. Results from this thesis also demonstrate a correlation between *Bdnf* and *Kcnq2* expression, with BDNF appearing to provide an upregulatory force on *Kcnq2*. BDNF activates its receptor TrkB, which recruits PLC, and PLC can initiate the translocation of NFATc4 from the cytoplasm to the nucleus. NFAT was previously shown to upregulate *Kcnq2*, so greater BDNF upregulation may provide maintenance of *Kcnq2* at normal levels during SE, in opposition to a downregulatory force, which may be caused by REST. ***B)*** The results from this thesis in combination with the literature suggest that *Kcnq2* expression in hippocampal pyramidal neurons changes depending on the strength of the epileptic insult, which can be measured as *Bdnf* increase and*, in vivo*, behavioural signs of seizure. From a baseline of *Kcnq2* expression in healthy pyramidal neurons, sub-SE hyperexcitability was shown by the Shapiro group to increase levels of *Kcnq2*. Work from their group combined with this thesis suggest that *Kcnq2* is reduced from normal levels during SE and SE-like conditions. Finally, a key experiment in this thesis created conditions that can be described as 'extreme SE' with 20-fold *Bdnf* upregulation. Here, *Kcnq2* levels were similar to control conditions, which may be due to the very high levels of BDNF causing an upregulatory force on *Kcnq2*, in opposition to the downregulatory force already present during SE-level conditions.

No changes in *Kcnq2*, and only a mild downregulation in *Kcnq3*, were observed from 4AP exposure, despite this producing a 10-fold upregulation in *Bdnf*. Hyperexcitability, but not SE, can be achieved from 4AP. Therefore, 4AP may represent an intermediary between SE-inducing 1-10-fold *Bdnf* increases that result in *Kcnq2* downregulation, and sub-SE convulsant doses which produce *Kcnq2* upregulation (Carver et al., 2020; Zhang and Shapiro, 2012), balancing out to no change overall (see Figure 5.1A).

In contrast to the downregulated *Kcnq2*/Kv7.2 in the pyramidal neurons after SE, *Kcnq2*/Kv7.2 is upregulated in the dentate gyrus, which would be expected to limit excitotoxic damage. Interestingly, the Shapiro lab recently found that Kv7 channels in these different hippocampal regions respond in opposite ways to muscarinic signalling. While Kv7 current in hippocampal pyramidal neurons is suppressed by muscarinic receptor stimulation, as is famously the case with peripheral neurons, Kv7 current in dentate gyrus granule cells is enhanced by muscarinic stimulation (Carver and Shapiro, 2019). Muscarinic receptors are shown to be active in seizure models (Potier and Psarropoulou, 2001). Therefore, it is possible that this differential Kv7 channel regulation by muscarinic signalling may influence their differential transcriptional expression in hyperexcitability and epilepsy.

The downregulation of other types of potassium channels has also been observed in epileptogenesis (Pacheco Otalora et al., 2008; Sosanya et al., 2015; Whitmire et al., 2017), which may support the idea that *Kcnq2/3* expression is also more likely to decrease than increase. In addition, Kv7.5 levels were reduced in the sclerotic areas of the hippocampus from epilepsy patients (Yus-Nájera et al., 2003). This suggests that when Kv7.2 subunits are lost from pyramidal neurons in epileptic conditions, as myself and others have observed, they are unlikely to be replaced with Kv7.5 subunits. Furthermore, I have not observed any compensatory upregulation of Kv7.3. This makes it highly likely that the overall Kv7 current in hippocampal pyramidal neurons is reduced during epilepsy. This would be expected to reduce the action potential threshold and increase neuronal excitability, exacerbating seizure and contributing to epileptogenesis. However, the variability in expression changes across different insult types requires deeper investigation, and the role of Kv7.2/3 in human epilepsy should be elucidated.

5.2 *Bdnf* upregulation is influenced by REST and maintains *Kcnq2/3* expression in seizure

I observed that overexpressing REST in cultures exposed to kainate caused a huge 40-fold increase in *Bdnf*. This was initially a surprise as REST is known to directly repress *Bdnf* (Tabuchi et al., 2002). Furthermore, *Bdnf* upregulation in response to kainate injection *in vivo* was shown to be suppressed by REST at 3 and 6 hours following injection. *Bdnf* expression was then shown to return to baseline by 24 hours (Timmusk et al., 1999). In the experiments presented in this thesis, *Bdnf* remains at high levels when the hippocampal slice cultures have been exposed to kainate for 18 hours, and this is likely due to the continued exposure, in contrast to the single injection used by Timmusk and colleagues. A continued exposure to kainate would be expected to induce greater epileptogenic changes than a single injection, and this is supported by the 20-40-fold increase in *Bdnf* observed in my experiment compared to the 4-15-fold *Bdnf* increase observed by Timmusk and colleagues at 3 and 6 hours. While REST would also be repressing *Bdnf* directly in the slice cultures, the greater and more prolonged epileptogenic changes resulting from continued kainate exposure would have the greater force, driving *Bdnf* levels up. Unlike *in vivo*, in slice cultures REST appears to be contributing to this *Bdnf* upregulation more than it is contributing to its repression. Overexpressed REST would be expected to cause *Bdnf* upregulation indirectly, through its exacerbating effects on kainate-induced hyperexcitability. REST represses expression of the *GluR2* gene, which leads to an abundance of AMPA receptors lacking the GluR2 subunit, making them highly permeable to Ca^{2+} (Calderone et al., 2003; Pellegrini-Giampietro et al., 1992; Sanchez et al., 2001). Membrane depolarisation causes phosphorylation and activation of CREB, which upregulates *Bdnf* (Finkbeiner et al., 1997). Longer stimulations lead to greater levels of CREB phosphorylation and greater upregulation of BDNF exon III, specifically (Tao et al., 1998). Because of more prolonged exposure to kainate in the slice cultures compared to a single injection, the associated Ca^{2+} influx would be expected to sustain greater CREB phosphorylation and *Bdnf* upregulation (see Figure 5.1B). Therefore, it seems most likely that in hippocampal slice cultures treated directly with kainate, the indirect upregulatory force of REST on *Bdnf* would have become greater than the direct repressive force of REST on *Bdnf* described by Timmusk and colleagues (Timmusk et al., 1999).

I also showed evidence suggesting that *Bdnf* upregulation in epilepsy models is associated with upregulations of *Kcnq2/3*. Intriguingly, in cultured hippocampal CA1-CA3 neurons, BDNF was shown to activate the translocation of NFATc4 from the cytoplasm to the nucleus and NFAT-mediated gene transcription. This occurred through activation of the BDNF receptor TrkB followed by PLC activation (Groth and Mermelstein, 2003). As I have discussed, NFAT translocates to the nucleus in times of neuronal stimulation and seizure, where it enhances the expression of *Kcnq2* and *Kcnq3* (Zhang and Shapiro, 2012). Therefore, BDNF upregulation is likely to cause an upregulatory force on *Kcnq2* and *Kcnq3* via NFAT activation (see Figure 5.1B).

5.3 Is REST upregulated in epileptic conditions and does REST repress *Kcnq2/3*?

The upregulation of *Rest* mRNA and REST protein in response to seizure is well documented in animal models and epilepsy patients (Brennan et al., 2016; McClelland et al., 2011; Palm et al., 1998). I observed increased REST protein levels in half of the samples after an 18-hour kainate exposure, associated with downregulation of the REST target genes *Kcnq2* and *NaII/Scn2a*. However, *Rest* mRNA levels were unchanged, and no significant negative correlations were observed between *Rest* and *Kcnq2* or *Kcnq3* in any of the experiments in this thesis. This could mean that *Kcnq2* and *NaII/Scn2a* were downregulated by a different transcription factor. Alternatively, their downregulation could have resulted from increased activity of the REST protein without changes in mRNA expression, for example from reduced REST protein degradation. No significant changes in REST target genes were observed in response to REST modulation compared to control. However, this was most likely because under 41% of the cells in each slice culture were expressing REST modulation, which would have likely been insufficient to observe a quantifiable change in expression of REST target genes.

The reduced expression levels of *Kcnq2* and *Sp1* in cultures expressing dominant negative REST in the presence of kainate suggests that REST was having some influence over these genes. This was likely due to an indirect mechanism. I have described the indirect contribution of REST to the upregulation of *Bdnf* in epileptic conditions, and of BDNF leading to a maintenance of *Kcnq2* expression in epileptic conditions. Therefore, blocking REST in epileptic conditions would be expected to

lead to a downregulation of *Kcnq2* through these same mechanisms (see Figure 5.1B). This theory is supported by the relatively low rate of *Bdnf* increase in this condition.

5.4 *Kcnq2/3* expression is regulated by HDACs

I observed a de-repression of *Kcnq2* when HDACs were inhibited by SAHA in hippocampal slice cultures, suggesting HDACs regulate *Kcnq2* in the hippocampus. The observed upregulation in *Kcnq2* would increase the overall Kv7 current, stabilising the resting membrane potential and preventing neuronal hyperexcitability. This suggests HDAC inhibitors such as SAHA have potential as anti-epileptic drugs. SAHA, also known as Vorinostat, is an inhibitor of all types of class I and class II HDACs. It is currently licensed as a treatment for refractory or relapsed cutaneous T-cell lymphoma, as it inhibits cancer cell survival. Kainate caused enhancement of the TLR4/MYD88 signalling pathway which leads to microglial activation and neuron death. SAHA pre-treatment suppressed this kainate-mediated enhancement of TLR4/MYD88, as well as reducing seizure scores and increasing seizure latency (Hu and Mao, 2016). The suppression of kainate-induced seizure activity by SAHA would fit with the upregulation of *Kcnq2* I observed from SAHA application, suggesting its seizure-suppressing effects may be partially due to its upregulation of the Kv7 current. When combined with diazepam, increased neuroprotective effects were exerted by SAHA or the HDAC inhibitor valproic acid compared to diazepam alone, following status epilepticus. In addition, increased anticonvulsive effects were observed from valproic acid (Rossetti et al., 2012).

Valproic acid inhibits HDAC classes I and IIa and is commonly prescribed for generalised and partial seizures. It exhibits protective effects against hyperexcitability and neuronal damage in epilepsy (Brandt et al., 2006), most likely by enhancing expression of the anticonvulsive Neuropeptide Y (Brill et al., 2006; Szot et al., 2005). In addition, the class I and II HDAC inhibitor sodium butyrate has shown promise for its anti-epileptic effects. It reduced seizure intensity and increased seizure latency in the PTZ-kindling model, as well as protecting against neuron death (Li et al., 2021). Similarly, daily treatment with sodium butyrate suppressed epileptogenesis and mossy fiber sprouting in the hippocampus in the kindling model (Reddy et al., 2018). These studies support the idea that HDAC inhibitors such as SAHA, valproic acid and sodium butyrate can be potent anti-epileptogenic compounds. However, they can also

change the DNA methylation status of genes, causing side effects (Milutinovic et al., 2007). Therefore, development of more specific treatments would be advantageous.

5.5 Challenges for the future

5.5.1 Unravelling the mechanisms behind *Kcnq2/3* and Kv7.2/3 expression changes in epilepsy and epileptogenesis

Rest mRNA and REST protein has been consistently observed to increase in seizure models by other groups (Brennan et al., 2016; McClelland et al., 2011; Palm et al., 1998). However, in this project I did not observe a *Rest* mRNA increase in hippocampal slice cultures in response to kainate or 4AP, though REST protein was increased in half of the samples. *Rest* qPCR primers had been designed to anneal to rat *Rest*, and were validated as amplifying the correct sized product with robust amplification levels and no observed amplification of contaminating genomic DNA from the RNA sample. The antibody was verified through observation of the correct sized band on western blot, and production of an immunohistochemistry signal in REST-overexpressing cells only. Therefore, *Rest* mRNA and REST protein measurements are expected to be accurate. In addition to the increased REST protein levels in some samples, the REST target genes *Kcnq2* and *NaII/Scn2a* were downregulated in response to kainate. This suggests that REST protein levels may have been increased in response to kainate, without associated mRNA increase. This could occur through a reduction in REST protein degradation. Initially, more data is needed to give a full picture of *Rest* mRNA and REST protein levels throughout the epileptogenesis process. Pulse-chase analysis could be used to follow the degradation of radioactively labelled REST protein after convulsant exposure and elucidate whether REST protein degradation rate is reduced.

It remains uncertain whether the transcription factors REST, Sp1 and NFAT bind and regulate *Kcnq2* and *Kcnq3* in the rat hippocampus. To answer this question, chromatin immunoprecipitation could be used. Antibodies against REST, Sp1 and NFAT would pull down the DNA sequences bound to those transcription factors from rat hippocampal extracts. qPCR would then be used to quantify *Kcnq2* and *Kcnq3* to determine binding. This experiment could compare healthy rat hippocampus with hippocampus from epileptic rats, to establish whether these interactions are altered in epileptic conditions. If REST is not observed to bind to the RE1 sites in *Kcnq2* and

Kcnq3 in epileptic conditions, that would suggest the *Kcnq2* and *Sp1* downregulation I observed in this project is being induced by an alternative transcriptional repressor. Novel binding sites can be identified bioinformatically. Following this, multiplexed competitor EMSA could be used to assess binding of *Kcnq2/3* by a wide selection of around 70 common transcription factors (Smith and Humphries, 2009). This would provide further details of transcription factors which regulate hippocampal *Kcnq2* and *Kcnq3* in epilepsy models.

The experiments in this thesis suggested that convulsant-induced *Bdnf* upregulation causes an upregulatory force on *Kcnq2* and *Kcnq3*. This would protect neurons from hyperexcitability by maintaining the Kv7 current in the face of one or more downregulatory forces. *Kcnq2/3* expression could be quantified in the kainate model in *Bdnf* knockout mice (Lindholm and Castrén, 2014) to determine the contribution of BDNF to *Kcnq2/3* maintenance. Alternatively, a recombinant human TrkB-Fc chimera could be used to block BDNF-TrkB signalling in rats *in vivo* (Li et al., 2019). If experiments show that BDNF does upregulate *Kcnq2/3*, the stearated, membrane-permeable NFAT-blocking peptide St-VIVIT (Zhang and Shapiro, 2012) could be used to assess whether this effect is mediated by NFAT in epileptic conditions. The protection from hyperexcitability conferred by maintaining *Kcnq2/3* expression could provide further evidence supporting the idea of *Bdnf* gene therapy in chronically epileptic patients (Simonato, 2014).

Kv4.2 was reduced in animal epilepsy models but was unchanged in epilepsy patients (Aronica et al., 2009; Monaghan et al., 2008; Su et al., 2008). This highlights the importance of confirming that the expression changes observed in animal models also translate to the human condition. Hippocampal biopsy tissue taken from epilepsy patients at different stages throughout the epileptogenic process should be collected from epilepsy surgeries. This could be used to confirm whether the changes in expression of *Kcnq2* and *Kcnq3* observed in this project and by other groups also occurs in humans. However, as epilepsy surgery is only performed in the most serious of cases this would only give information about *Kcnq2/3* and Kv7.2/7.3 expression in chronic severe epilepsy and would not elucidate expression changes during the latent phase.

The Kv7 channel opener retigabine was withdrawn from clinical use in 2017 due to discolouration of the skin and eyes, vision changes and urinary retention. These side effects are likely to be caused by a combination of accumulating retigabine metabolites, non-specificity of subunit targeting, and effects upon peripheral nerves in addition to the brain (Groseclose and Castellino, 2019; Larsson et al., 2020; Padilla et al., 2009; Rode et al., 2010). By developing a gene therapy for overexpression of *Kcnq2/3* that targets pyramidal neurons, ideally in the hippocampus only, this would be expected to eliminate many of the side effects associated with retigabine. *Kcnq2/3* overexpression would increase the seizure threshold, conferring protection to vulnerable individuals. This could be achieved with the use of specific viral promoters. Work is also underway to increase transduction efficacy. Once achieved, gene therapy could provide a less invasive alternative to surgical resection for patients with partial epilepsies (Simonato, 2014), providing a similarly potent anti-epileptic effect to retigabine without the side-effects.

5.5.2 Final conclusion

Neuronal Kv7.2 and Kv7.3 are known for their importance in regulating the resting membrane potential and limiting hyperexcitability through the Kv7 current. Research from another group previously showed that the transcriptional expression of *Kcnq2* and *Kcnq3* was increased in response to activity and seizure, mediated by the transcription factor NFAT. However, the transcription factor REST is upregulated following seizure, and REST was shown to repress *KCNQ2* and *KCNQ3*. The data presented in this thesis shows that *Kcnq2* mRNA and Kv7.2 protein can be downregulated overall in organotypic hippocampal slice cultures in response to kainate, but there was no evidence of any upregulation in any epileptic model. While an upregulation of *Rest* mRNA was not observed, REST protein was increased in some cultures. Furthermore, some of REST's target genes were downregulated. In addition, *Kcnq2* expression was shown to be regulated by HDACs. The data presented here also suggests that during epileptic conditions REST increase contributes indirectly to *Bdnf* upregulation. In addition, *Bdnf* upregulation in epileptic conditions appears to enable the maintenance of *Kcnq2* and *Kcnq3* expression, possibly through NFAT, as a neuroprotective mechanism against hyperexcitability. This seems to be in balance with a downregulatory force upon *Kcnq2* and *Kcnq3*, which may or may not be due to repression by REST. These conclusions suggest that downregulation of *Kcnq2/3* expression could contribute to epileptogenesis, but the observed changes need to be confirmed in human epilepsy. The conclusions from this thesis support the use of BDNF as an anti-epileptic gene therapy in patients with chronic epilepsy (Simonato, 2014), as BDNF appears to maintain *Kcnq2/3* expression levels and should therefore stabilise the protective Kv7 current. Further work is needed to confirm these theories about the regulation and role of *Kcnq2/3* expression in epilepsy. With advances in gene therapy to penetrate the blood brain barrier and target specific brain areas, *Kcnq2/3* gene modulation could provide anti-epileptic therapy to vulnerable individuals.

Bibliography

- Abbott, G.W. (2020). KCNQs: Ligand- and Voltage-Gated Potassium Channels. Front Physiol *11*, 583.
- Abidi, A., Devaux, J.J., Molinari, F., Alcaraz, G., Michon, F.X., Sutera-Sardo, J., Becq, H., Lacoste, C., Altuzarra, C., Afenjar, A., *et al.* (2015). A recurrent KCNQ2 pore mutation causing early onset epileptic encephalopathy has a moderate effect on M current but alters subcellular localization of Kv7 channels. Neurobiol Dis *80*, 80-92.
- Alaimo, A., Gómez-Posada, J.C., Aivar, P., Etxeberría, A., Rodriguez-Alfaro, J.A., Areso, P., and Villarroel, A. (2009). Calmodulin activation limits the rate of KCNQ2 K+ channel exit from the endoplasmic reticulum. J Biol Chem *284*, 20668-20675.
- Albensi, B.C., Sullivan, P.G., Thompson, M.B., Scheff, S.W., and Mattson, M.P. (2000). Cyclosporin ameliorates traumatic brain-injury-induced alterations of hippocampal synaptic plasticity. Exp Neurol *162*, 385-389.
- Albus, K., Wahab, A., and Heinemann, U. (2008). Standard antiepileptic drugs fail to block epileptiform activity in rat organotypic hippocampal slice cultures. Br J Pharmacol *154*, 709-724.
- Albus, K., Wahab, A., and Heinemann, U. (2012). Primary afterdischarge in organotypic hippocampal slice cultures: effects of standard antiepileptic drugs. Epilepsia *53*, 1928-1936.
- Ambrosino, P., Alaimo, A., Bartollino, S., Manocchio, L., De Maria, M., Mosca, I., Gomis-Perez, C., Alberdi, A., Scambia, G., Lesca, G., *et al.* (2015). Epilepsy-causing mutations in Kv7.2 C-terminus affect binding and functional modulation by calmodulin. Biochim Biophys Acta *1852*, 1856-1866.
- Andrés, M.E., Burger, C., Peral-Rubio, M.J., Battaglioli, E., Anderson, M.E., Grimes, J., Dallman, J., Ballas, N., and Mandel, G. (1999). CoREST: a functional corepressor required for regulation of neural-specific gene expression. Proc Natl Acad Sci U S A *96*, 9873-9878.
- Anju, T.R., Smijin, S., Jobin, M., and Paulose, C.S. (2018). Altered muscarinic receptor expression in the cerebral cortex of epileptic rats: restorative role of Withania somnifera. Biochem Cell Biol *96*, 433-440.

- Arnold, D., Feng, L., Kim, J., and Heintz, N. (1994). A strategy for the analysis of gene expression during neural development. Proc Natl Acad Sci U S A *91*, 9970-9974.
- Aronica, E., Boer, K., Doorn, K.J., Zurolo, E., Spliet, W.G., van Rijen, P.C., Baayen, J.C., Gorter, J.A., and Jeromin, A. (2009). Expression and localization of voltage dependent potassium channel Kv4.2 in epilepsy associated focal lesions. Neurobiol Dis *36*, 81-95.
- Avaliani, N., Andersson, M., Runegaard, A.H., Woldbye, D., and Kokaia, M. (2016). DREADDs suppress seizure-like activity in a mouse model of pharmacoresistant epileptic brain tissue. Gene Ther *23*, 760-766.
- Avaliani, N., Sørensen, A.T., Ledri, M., Bengzon, J., Koch, P., Brüstle, O., Deisseroth, K., Andersson, M., and Kokaia, M. (2014). Optogenetics reveal delayed afferent synaptogenesis on grafted human-induced pluripotent stem cell-derived neural progenitors. Stem Cells *32*, 3088-3098.
- Avoli, M. (2007). The epileptic hippocampus revisited: back to the future. Epilepsy Curr *7*, 116-118.
- Avoli, M., Barbarosie, M., Lücke, A., Nagao, T., Lopantsev, V., and Köhling, R. (1996). Synchronous GABA-mediated potentials and epileptiform discharges in the rat limbic system in vitro. J Neurosci *16*, 3912-3924.
- Bagheri, A., Habibzadeh, P., Razavipour, S.F., Volmar, C.H., Chee, N.T., Brothers, S.P., Wahlestedt, C., Mowla, S.J., and Faghihi, M.A. (2019). HDAC Inhibitors Induce. Int J Mol Sci *20*.
- Bahr, B.A., Neve, R.L., Sharp, J., Geller, A.I., and Lynch, G. (1994). Rapid and stable gene expression in hippocampal slice cultures from a defective HSV-1 vector. Brain Res Mol Brain Res *26*, 277-285.
- Bal, M., Zhang, J., Hernandez, C.C., Zaika, O., and Shapiro, M.S. (2010). Ca2+/calmodulin disrupts AKAP79/150 interactions with KCNQ (M-Type) K+ channels. J Neurosci *30*, 2311-2323.
- Ballarín, M., Ernfors, P., Lindefors, N., and Persson, H. (1991). Hippocampal damage and kainic acid injection induce a rapid increase in mRNA for BDNF and NGF in the rat brain. Exp Neurol *114*, 35-43.

- Ballas, N., Grunseich, C., Lu, D.D., Speh, J.C., and Mandel, G. (2005). REST and its corepressors mediate plasticity of neuronal gene chromatin throughout neurogenesis. Cell *121*, 645-657.
- Bausch, S.B., and McNamara, J.O. (2000). Synaptic connections from multiple subfields contribute to granule cell hyperexcitability in hippocampal slice cultures. J Neurophysiol *84*, 2918-2932.
- Bausch, S.B., and McNamara, J.O. (2004). Contributions of mossy fiber and CA1 pyramidal cell sprouting to dentate granule cell hyperexcitability in kainic acid-treated hippocampal slice cultures. J Neurophysiol *92*, 3582-3595.
- Beaumont, T.L., Yao, B., Shah, A., Kapatos, G., and Loeb, J.A. (2012). Layer-specific CREB target gene induction in human neocortical epilepsy. J Neurosci *32*, 14389-14401.
- Becker, A.J. (2018). Review: Animal models of acquired epilepsy: insights into mechanisms of human epileptogenesis. Neuropathol Appl Neurobiol *44*, 112-129.
- Ben-Ari, Y., and Cossart, R. (2000). Kainate, a double agent that generates seizures: two decades of progress. Trends Neurosci *23*, 580-587.
- Benedikz, E., Casaccia-Bonnefil, P., Stelzer, A., and Bergold, P.J. (1993). Hyperexcitability and cell loss in kainate-treated hippocampal slice cultures. Neuroreport *5*, 90-92.
- Berdichevsky, Y., Dzhala, V., Mail, M., and Staley, K.J. (2012). Interictal spikes, seizures and ictal cell death are not necessary for post-traumatic epileptogenesis in vitro. Neurobiol Dis *45*, 774-785.
- Berdichevsky, Y., Saponjian, Y., Park, K.I., Roach, B., Pouliot, W., Lu, K., Swiercz, W., Dudek, F.E., and Staley, K.J. (2016). Staged anticonvulsant screening for chronic epilepsy. Ann Clin Transl Neurol *3*, 908-923.
- Biervert, C., Schroeder, B.C., Kubisch, C., Berkovic, S.F., Propping, P., Jentsch, T.J., and Steinlein, O.K. (1998). A potassium channel mutation in neonatal human epilepsy. Science *279*, 403-406.
- Bijak, M., and Misgeld, U. (1996). Suppression by GABAB receptors of 4-aminopyridine-induced hyperactivity in guinea-pig dentate neurons. Neurosci Lett *205*, 49-52.

- Binder, D.K., Routbort, M.J., and McNamara, J.O. (1999a). Immunohistochemical evidence of seizure-induced activation of trk receptors in the mossy fiber pathway of adult rat hippocampus. J Neurosci *19*, 4616-4626.
- Binder, D.K., Routbort, M.J., Ryan, T.E., Yancopoulos, G.D., and McNamara, J.O. (1999b). Selective inhibition of kindling development by intraventricular administration of TrkB receptor body. J Neurosci *19*, 1424-1436.
- Bing, G., Wilson, B., Hudson, P., Jin, L., Feng, Z., Zhang, W., Bing, R., and Hong, J.S. (1997). A single dose of kainic acid elevates the levels of enkephalins and activator protein-1 transcription factors in the hippocampus for up to 1 year. Proc Natl Acad Sci U S A *94*, 9422-9427.
- Bingham, A.J., Ooi, L., Kozera, L., White, E., and Wood, I.C. (2007). The repressor element 1-silencing transcription factor regulates heart-specific gene expression using multiple chromatin-modifying complexes. Mol Cell Biol *27*, 4082-4092.
- Blümcke, I., Thom, M., Aronica, E., Armstrong, D.D., Bartolomei, F., Bernasconi, A., Bernasconi, N., Bien, C.G., Cendes, F., Coras, R., *et al.* (2013). International consensus classification of hippocampal sclerosis in temporal lobe epilepsy: a Task Force report from the ILAE Commission on Diagnostic Methods. Epilepsia *54*, 1315-1329.
- Boison, D. (2017). New insights into the mechanisms of the ketogenic diet. Curr Opin Neurol *30*, 187-192.
- Borges, K., Gearing, M., McDermott, D.L., Smith, A.B., Almonte, A.G., Wainer, B.H., and Dingledine, R. (2003). Neuronal and glial pathological changes during epileptogenesis in the mouse pilocarpine model. Exp Neurol *182*, 21-34.
- Borlongan, C.V., Yu, G., Matsukawa, N., Xu, L., Hess, D.C., Sanberg, P.R., and Wang, Y. (2005). Acute functional effects of cyclosporine-A and methylprednisolone treatment in adult rats exposed to transient ischemic stroke. Life Sci *76*, 1503-1512.

- Bosma, M.M., and Hille, B. (1989). Protein kinase C is not necessary for peptide-induced suppression of M current or for desensitization of the peptide receptors. Proc Natl Acad Sci U S A *86*, 2943-2947.
- Brandt, C., Gastens, A.M., Sun, M., Hausknecht, M., and Löscher, W. (2006). Treatment with valproate after status epilepticus: effect on neuronal damage, epileptogenesis, and behavioral alterations in rats. Neuropharmacology *51*, 789-804.
- Brennan, G.P., Dey, D., Chen, Y., Patterson, K.P., Magnetta, E.J., Hall, A.M., Dube, C.M., Mei, Y.T., and Baram, T.Z. (2016). Dual and Opposing Roles of MicroRNA-124 in Epilepsy Are Mediated through Inflammatory and NRSF-Dependent Gene Networks. Cell Rep *14*, 2402-2412.
- Brill, J., Lee, M., Zhao, S., Fernald, R.D., and Huguenard, J.R. (2006). Chronic valproic acid treatment triggers increased neuropeptide y expression and signaling in rat nucleus reticularis thalami. J Neurosci *26*, 6813-6822.
- Brooks-Kayal, A.R., and Russek, S.J. (2012). Regulation of GABAA Receptor Gene Expression and Epilepsy. In Jasper's Basic Mechanisms of the Epilepsies, th, J.L. Noebels, M. Avoli, M.A. Rogawski, R.W. Olsen, and A.V. Delgado-Escueta, eds. (Bethesda (MD)).
- Brown, D.A., and Adams, P.R. (1980). Muscarinic suppression of a novel voltage-sensitive K+ current in a vertebrate neurone. Nature *283*, 673-676.
- Brown, D.A., and Passmore, G.M. (2009). Neural KCNQ (Kv7) channels. Br J Pharmacol *156*, 1185-1195.
- Bruce, A.W., Donaldson, I.J., Wood, I.C., Yerbury, S.A., Sadowski, M.I., Chapman, M., Göttgens, B., and Buckley, N.J. (2004). Genome-wide analysis of repressor element 1 silencing transcription factor/neuron-restrictive silencing factor (REST/NRSF) target genes. Proc Natl Acad Sci U S A *101*, 10458-10463.
- Bruce, A.W., Krejcí, A., Ooi, L., Deuchars, J., Wood, I.C., Dolezal, V., and Buckley, N.J. (2006). The transcriptional repressor REST is a critical regulator of the neurosecretory phenotype. J Neurochem *98*, 1828-1840.
- Buckmaster, P.S., Ingram, E.A., and Wen, X. (2009). Inhibition of the mammalian target of rapamycin signaling pathway suppresses dentate

granule cell axon sprouting in a rodent model of temporal lobe epilepsy. J Neurosci *29*, 8259-8269.

- Butler-Ryan, R., and Wood, I.C. (2021a). Efficient infection of organotypic hippocampal slice cultures with adenovirus carrying the transgene REST/NRSF. J Neurosci Methods *356*, 109147.
- Butler-Ryan, R., and Wood, I.C. (2021b). The functions of repressor element 1-silencing transcription factor in models of epileptogenesis and post-ischemia. Metab Brain Dis.
- Butler, L.S., Silva, A.J., Abeliovich, A., Watanabe, Y., Tonegawa, S., and McNamara, J.O. (1995). Limbic epilepsy in transgenic mice carrying a Ca2+/calmodulin-dependent kinase II alpha-subunit mutation. Proc Natl Acad Sci U S A *92*, 6852-6855.
- Cacheaux, L.P., Ivens, S., David, Y., Lakhter, A.J., Bar-Klein, G., Shapira, M., Heinemann, U., Friedman, A., and Kaufer, D. (2009). Transcriptome profiling reveals TGF-beta signaling involvement in epileptogenesis. J Neurosci *29*, 8927-8935.
- Calderone, A., Jover, T., Noh, K.M., Tanaka, H., Yokota, H., Lin, Y., Grooms, S.Y., Regis, R., Bennett, M.V., and Zukin, R.S. (2003). Ischemic insults derepress the gene silencer REST in neurons destined to die. J Neurosci *23*, 2112-2121.
- Carminati, E., Buffolo, F., Rocchi, A., Michetti, C., Cesca, F., and Benfenati, F. (2019). Mild Inactivation of RE-1 Silencing Transcription Factor (REST) Reduces Susceptibility to Kainic Acid-Induced Seizures. Front Cell Neurosci *13*, 580.
- Carver, C.M., Hastings, S.D., Cook, M.E., and Shapiro, M.S. (2020). Functional responses of the hippocampus to hyperexcitability depend on directed, neuron-specific KCNQ2 K. Hippocampus *30*, 435-455.
- Carver, C.M., and Shapiro, M.S. (2019). Gq-Coupled Muscarinic Receptor Enhancement of KCNQ2/3 Channels and Activation of TRPC Channels in Multimodal Control of Excitability in Dentate Gyrus Granule Cells. J Neurosci *39*, 1566-1587.
- Casaccia-Bonnefil, P., Benedikz, E., Shen, H., Stelzer, A., Edelstein, D., Geschwind, M., Brownlee, M., Federoff, H.J., and Bergold, P.J. (1993).

Localized gene transfer into organotypic hippocampal slice cultures and acute hippocampal slices. J Neurosci Methods *50*, 341-351.

- Castillo, P.E., Malenka, R.C., and Nicoll, R.A. (1997). Kainate receptors mediate a slow postsynaptic current in hippocampal CA3 neurons. Nature *388*, 182-186.
- Chen, C.C., Hsu, L.W., Huang, L.T., and Huang, T.L. (2010). Chronic administration of cyclosporine A changes expression of BDNF and TrkB in rat hippocampus and midbrain. Neurochem Res *35*, 1098-1104.
- Chen, Y., Xie, Y., Wang, H., and Chen, Y. (2013). [SIRT1 expression and activity are up-regulated in the brain tissue of epileptic patients and rat models]. Nan Fang Yi Ke Da Xue Xue Bao *33*, 528-532.
- Chen, Z.F., Paquette, A.J., and Anderson, D.J. (1998). NRSF/REST is required in vivo for repression of multiple neuronal target genes during embryogenesis. Nat Genet *20*, 136-142.
- Cheong, A., Bingham, A.J., Li, J., Kumar, B., Sukumar, P., Munsch, C., Buckley, N.J., Neylon, C.B., Porter, K.E., Beech, D.J., *et al.* (2005). Downregulated REST transcription factor is a switch enabling critical potassium channel expression and cell proliferation. Mol Cell *20*, 45-52.
- Chesnut, T.J., and Swann, J.W. (1990). Suppression of 4-aminopyridine-induced epileptogenesis by the GABAA agonist muscimol. Epilepsy Res *5*, 8-17.
- Chi, G., Huang, Z., Li, X., Zhang, K., and Li, G. (2018). Substance P Regulation in Epilepsy. Curr Neuropharmacol *16*, 43-50.
- Chmielewska, N., Wawer, A., Maciejak, P., Turzyńska, D., Sobolewska, A., Skórzewska, A., Osuch, B., Płaźnik, A., and Szyndler, J. (2020). The role of REST/NRSF, TrkB and BDNF in neurobiological mechanisms of different susceptibility to seizure in a PTZ model of epilepsy. Brain Res Bull *158*, 108-115.
- Chong, J.A., Tapia-Ramírez, J., Kim, S., Toledo-Aral, J.J., Zheng, Y., Boutros, M.C., Altshuller, Y.M., Frohman, M.A., Kraner, S.D., and Mandel, G. (1995). REST: a mammalian silencer protein that restricts sodium channel gene expression to neurons. Cell *80*, 949-957.

- Chow, R., Olesen, J., Onyskiw, C., and Baksh, S. (2007). Mitotic regulation of CDK4 by the serine/threonine phosphatase, calcineurin. Biochem Biophys Res Commun *363*, 506-512.
- Churn, S.B., Sombati, S., Jakoi, E.R., Severt, L., DeLorenzo, R.J., and Sievert, L. (2000). Inhibition of calcium/calmodulin kinase II alpha subunit expression results in epileptiform activity in cultured hippocampal neurons. Proc Natl Acad Sci U S A *97*, 5604-5609.
- Citraro, R., Leo, A., Santoro, M., D'agostino, G., Constanti, A., and Russo, E. (2017). Role of Histone Deacetylases (HDACs) in Epilepsy and Epileptogenesis. Curr Pharm Des *23*, 5546-5562.
- Conforti, P., Zuccato, C., Gaudenzi, G., Ieraci, A., Camnasio, S., Buckley, N.J., Mutti, C., Cotelli, F., Contini, A., and Cattaneo, E. (2013). Binding of the repressor complex REST-mSIN3b by small molecules restores neuronal gene transcription in Huntington's disease models. J Neurochem *127*, 22-35.
- shah, J.M., Lauterborn, J.C., Yan, Q., Gall, C.M., and Varon, S. (1997). Distribution of brain-derived neurotrophic factor (BDNF) protein and mRNA in the normal adult rat CNS: evidence for anterograde axonal transport. J Neurosci *17*, 2295-2313.
- Constanti, A., and Brown, D.A. (1981). M-Currents in voltage-clamped mammalian sympathetic neurones. Neurosci Lett *24*, 289-294.
- Cooper, E.C. (2011). Made for "anchorin": Kv7.2/7.3 (KCNQ2/KCNQ3) channels and the modulation of neuronal excitability in vertebrate axons. Semin Cell Dev Biol *22*, 185-192.
- Cooper, E.C., Aldape, K.D., Abosch, A., Barbaro, N.M., Berger, M.S., Peacock, W.S., Jan, Y.N., and Jan, L.Y. (2000). Colocalization and coassembly of two human brain M-type potassium channel subunits that are mutated in epilepsy. Proc Natl Acad Sci U S A *97*, 4914-4919.
- Cooper, E.C., and Jan, L.Y. (2003). M-channels: neurological diseases, neuromodulation, and drug development. Arch Neurol *60*, 496-500.
- Cramer, C.L., Stagnitto, M.L., Knowles, M.A., and Palmer, G.C. (1994). Kainic acid and 4-aminopyridine seizure models in mice: evaluation of efficacy of anti-epileptic agents and calcium antagonists. Life Sci *54*, PL271-275.

- Cregan, S.P., MacLaurin, J., Gendron, T.F., Callaghan, S.M., Park, D.S., Parks, R.J., Graham, F.L., Morley, P., and Slack, R.S. (2000). Helper-dependent adenovirus vectors: their use as a gene delivery system to neurons. Gene Ther *7*, 1200-1209.
- Croft, C.L., Cruz, P.E., Ryu, D.H., Ceballos-Diaz, C., Strang, K.H., Woody, B.M., Lin, W.L., Deture, M., Rodríguez-Lebrón, E., Dickson, D.W., *et al.* (2019). rAAV-based brain slice culture models of Alzheimer's and Parkinson's disease inclusion pathologies. J Exp Med *216*, 539-555.
- Cruise, L., Ho, L.K., Veitch, K., Fuller, G., and Morris, B.J. (2000). Kainate receptors activate NF-kappaB via MAP kinase in striatal neurones. Neuroreport *11*, 395-398.
- de Montigny, C., and Tardif, D. (1981). Differential excitatory effects of kainic acid on CA3 and CA1 hippocampal pyramidal neurons: further evidence for the excitotoxic hypothesis and for a receptor-mediated action. Life Sci *29*, 2103-2111.
- De Simoni, A., and Yu, L.M. (2006). Preparation of organotypic hippocampal slice cultures: interface method. Nat Protoc *1*, 1439-1445.
- Delmas, P., and Brown, D.A. (2005). Pathways modulating neural KCNQ/M (Kv7) potassium channels. Nat Rev Neurosci *6*, 850-862.
- Devaux, J.J., Kleopa, K.A., Cooper, E.C., and Scherer, S.S. (2004). KCNQ2 is a nodal K+ channel. J Neurosci *24*, 1236-1244.
- Dickson, J.M., Jacques, R., Reuber, M., Hick, J., Campbell, M.J., Morley, R., and Grünewald, R.A. (2018). Emergency hospital care for adults with suspected seizures in the NHS in England 2007-2013: a cross-sectional study. BMJ Open *8*, e023352.
- Dinocourt, C., Gallagher, S.E., and Thompson, S.M. (2006). Injury-induced axonal sprouting in the hippocampus is initiated by activation of trkB receptors. Eur J Neurosci *24*, 1857-1866.
- Domañska-Janik, K., Buzañska, L., Dłuzniewska, J., Kozłowska, H., Sarnowska, A., and Zabłocka, B. (2004). Neuroprotection by cyclosporin A following transient brain ischemia correlates with the inhibition of the early efflux of cytochrome C to cytoplasm. Brain Res Mol Brain Res *121*, 50-59.

- Drakew, A., Müller, M., Gähwiler, B.H., Thompson, S.M., and Frotscher, M. (1996). Spine loss in experimental epilepsy: quantitative light and electron microscopic analysis of intracellularly stained CA3 pyramidal cells in hippocampal slice cultures. Neuroscience *70*, 31-45.
- Du, F., Eid, T., Lothman, E.W., Köhler, C., and Schwarcz, R. (1995). Preferential neuronal loss in layer III of the medial entorhinal cortex in rat models of temporal lobe epilepsy. J Neurosci *15*, 6301-6313.
- Dyhrfjeld-Johnsen, J., Berdichevsky, Y., Swiercz, W., Sabolek, H., and Staley, K.J. (2010). Interictal spikes precede ictal discharges in an organotypic hippocampal slice culture model of epileptogenesis. J Clin Neurophysiol *27*, 418-424.
- Easton, R.M., Johnson, E.M., and Creedon, D.J. (1998). Analysis of events leading to neuronal death after infection with E1-deficient adenoviral vectors. Mol Cell Neurosci *11*, 334-347.
- Ehrengruber, M.U., Doupnik, C.A., Xu, Y., Garvey, J., Jasek, M.C., Lester, H.A., and Davidson, N. (1997). Activation of heteromeric G protein-gated inward rectifier K+ channels overexpressed by adenovirus gene transfer inhibits the excitability of hippocampal neurons. Proc Natl Acad Sci U S A *94*, 7070-7075.
- Ehrengruber, M.U., Hennou, S., Büeler, H., Naim, H.Y., Déglon, N., and Lundstrom, K. (2001). Gene transfer into neurons from hippocampal slices: comparison of recombinant Semliki Forest Virus, adenovirus, adeno-associated virus, lentivirus, and measles virus. Mol Cell Neurosci *17*, 855-871.
- Ehrengruber, M.U., Lundstrom, K., Schweitzer, C., Heuss, C., Schlesinger, S., and Gähwiler, B.H. (1999). Recombinant Semliki Forest virus and Sindbis virus efficiently infect neurons in hippocampal slice cultures. Proc Natl Acad Sci U S A *96*, 7041-7046.
- Engel, T., Brennan, G.P., Sanz-Rodriguez, A., Alves, M., Beamer, E., Watters, O., Henshall, D.C., and Jimenez-Mateos, E.M. (2017). A calcium-sensitive feed-forward loop regulating the expression of the ATP-gated purinergic P2X7 receptor via specificity protein 1 and microRNA-22. Biochim Biophys Acta Mol Cell Res *1864*, 255-266.

- Ernfors, P., Bengzon, J., Kokaia, Z., Persson, H., and Lindvall, O. (1991). Increased levels of messenger RNAs for neurotrophic factors in the brain during kindling epileptogenesis. Neuron *7*, 165-176.
- Etxeberria, A., Aivar, P., Rodriguez-Alfaro, J.A., Alaimo, A., Villacé, P., Gómez-Posada, J.C., Areso, P., and Villarroel, A. (2008). Calmodulin regulates the trafficking of KCNQ2 potassium channels. FASEB J *22*, 1135-1143.
- Feng, Z., Chang, R.C., Bing, G., Hudson, P., Tiao, N., Jin, L., and Hong, J.S. (1999). Long-term increase of Sp-1 transcription factors in the hippocampus after kainic acid treatment. Brain Res Mol Brain Res *69*, 144-148.
- Finkbeiner, S., Tavazoie, S.F., Maloratsky, A., Jacobs, K.M., Harris, K.M., and Greenberg, M.E. (1997). CREB: a major mediator of neuronal neurotrophin responses. Neuron *19*, 1031-1047.
- Formisano, L., Guida, N., Laudati, G., Boscia, F., Esposito, A., Secondo, A., Di Renzo, G., and Canzoniero, L.M. (2015a). Extracellular signal-related kinase 2/specificity protein 1/specificity protein 3/repressor element-1 silencing transcription factor pathway is involved in Aroclor 1254-induced toxicity in SH-SY5Y neuronal cells. J Neurosci Res *93*, 167-177.
- Formisano, L., Guida, N., Valsecchi, V., Cantile, M., Cuomo, O., Vinciguerra, A., Laudati, G., Pignataro, G., Sirabella, R., Di Renzo, G., *et al.* (2015b). Sp3/REST/HDAC1/HDAC2 Complex Represses and Sp1/HIF-1/p300 Complex Activates ncx1 Gene Transcription, in Brain Ischemia and in Ischemic Brain Preconditioning, by Epigenetic Mechanism. J Neurosci *35*, 7332-7348.
- Fragoso-Veloz, J., and Tapia, R. (1992). NMDA receptor antagonists protect against seizures and wet-dog shakes induced by 4-aminopyridine. Eur J Pharmacol *221*, 275-280.
- Fritschy, J.M., Kiener, T., Bouilleret, V., and Loup, F. (1999). GABAergic neurons and GABA(A)-receptors in temporal lobe epilepsy. Neurochem Int *34*, 435-445.
- Gabryel, B., and Bernacki, J. (2009). Effect of FK506 and cyclosporine A on the expression of BDNF, tyrosine kinase B and p75 neurotrophin receptors in astrocytes exposed to simulated ischemia in vitro. Cell Biol Int *33*, 739-748.

- Gamper, N., Li, Y., and Shapiro, M.S. (2005). Structural requirements for differential sensitivity of KCNQ K+ channels to modulation by Ca2+/calmodulin. Mol Biol Cell *16*, 3538-3551.
- Gamper, N., Stockand, J.D., and Shapiro, M.S. (2003). Subunit-specific modulation of KCNQ potassium channels by Src tyrosine kinase. J Neurosci *23*, 84-95.
- Garriga-Canut, M., Schoenike, B., Qazi, R., Bergendahl, K., Daley, T.J., Pfender, R.M., Morrison, J.F., Ockuly, J., Stafstrom, C., Sutula, T., *et al.* (2006). 2-Deoxy-D-glucose reduces epilepsy progression by NRSF-CtBP-dependent metabolic regulation of chromatin structure. Nat Neurosci *9*, 1382-1387.
- Gerace, E., Resta, F., Landucci, E., Renzi, D., Masi, A., Pellegrini-Giampietro, D.E., Calabrò, A., and Mannaioni, G. (2017). The gliadin peptide 31-43 exacerbates kainate neurotoxicity in epilepsy models. Sci Rep *7*, 15146.
- Gerlach, J., Donkels, C., Münzner, G., and Haas, C.A. (2016). Persistent Gliosis Interferes with Neurogenesis in Organotypic Hippocampal Slice Cultures. Front Cell Neurosci *10*, 131.
- Gilbert, D.L., Pyzik, P.L., and Freeman, J.M. (2000). The ketogenic diet: seizure control correlates better with serum beta-hydroxybutyrate than with urine ketones. J Child Neurol *15*, 787-790.
- Glover, C.P., Bienemann, A.S., Heywood, D.J., Cosgrave, A.S., and Uney, J.B. (2002). Adenoviral-mediated, high-level, cell-specific transgene expression: a SYN1-WPRE cassette mediates increased transgene expression with no loss of neuron specificity. Mol Ther *5*, 509-516.
- Goldberg-Stern, H., Kaufmann, R., Kivity, S., Afawi, Z., and Heron, S.E. (2009). Novel mutation in KCNQ2 causing benign familial neonatal seizures. Pediatr Neurol *41*, 367-370.
- Goodkin, H.P., Yeh, J.L., and Kapur, J. (2005). Status epilepticus increases the intracellular accumulation of GABAA receptors. J Neurosci *25*, 5511-5520.
- Goto, A., Ishii, A., Shibata, M., Ihara, Y., Cooper, E.C., and Hirose, S. (2019). Characteristics of KCNQ2 variants causing either benign neonatal

epilepsy or developmental and epileptic encephalopathy. Epilepsia *60*, 1870-1880.

- Grabiec, U., Hohmann, T., Hammer, N., and Dehghani, F. (2017). Organotypic Hippocampal Slice Cultures As a Model to Study Neuroprotection and Invasiveness of Tumor Cells. J Vis Exp.
- Grimes, J.A., Nielsen, S.J., Battaglioli, E., Miska, E.A., Speh, J.C., Berry, D.L., Atouf, F., Holdener, B.C., Mandel, G., and Kouzarides, T. (2000). The co-repressor mSin3A is a functional component of the REST-CoREST repressor complex. J Biol Chem *275*, 9461-9467.
- Grinton, B.E., Heron, S.E., Pelekanos, J.T., Zuberi, S.M., Kivity, S., Afawi, Z., Williams, T.C., Casalaz, D.M., Yendle, S., Linder, I., *et al.* (2015). Familial neonatal seizures in 36 families: Clinical and genetic features correlate with outcome. Epilepsia *56*, 1071-1080.
- Grooms, S.Y., Opitz, T., Bennett, M.V., and Zukin, R.S. (2000). Status epilepticus decreases glutamate receptor 2 mRNA and protein expression in hippocampal pyramidal cells before neuronal death. Proc Natl Acad Sci U S A *97*, 3631-3636.
- Groseclose, M.R., and Castellino, S. (2019). An Investigation into Retigabine (Ezogabine) Associated Dyspigmentation in Rat Eyes by MALDI Imaging Mass Spectrometry. Chem Res Toxicol *32*, 294-303.
- Groth, R.D., and Mermelstein, P.G. (2003). Brain-derived neurotrophic factor activation of NFAT (nuclear factor of activated T-cells)-dependent transcription: a role for the transcription factor NFATc4 in neurotrophin-mediated gene expression. J Neurosci *23*, 8125-8134.
- Gröticke, I., Hoffmann, K., and Löscher, W. (2007). Behavioral alterations in the pilocarpine model of temporal lobe epilepsy in mice. Exp Neurol *207*, 329-349.
- Gu, B., Huang, Y.Z., He, X.P., Joshi, R.B., Jang, W., and McNamara, J.O. (2015). A Peptide Uncoupling BDNF Receptor TrkB from Phospholipase Cγ1 Prevents Epilepsy Induced by Status Epilepticus. Neuron *88*, 484-491.
- Gutiérrez, R., and Heinemann, U. (1999). Synaptic reorganization in explanted cultures of rat hippocampus. Brain Res *815*, 304-316.

- Hadley, J.K., Passmore, G.M., Tatulian, L., Al-Qatari, M., Ye, F., Wickenden, A.D., and Brown, D.A. (2003). Stoichiometry of expressed KCNQ2/KCNQ3 potassium channels and subunit composition of native ganglionic M channels deduced from block by tetraethylammonium. J Neurosci *23*, 5012-5019.
- Haley, J.E., Delmas, P., Offermanns, S., Abogadie, F.C., Simon, M.I., Buckley, N.J., and Brown, D.A. (2000). Muscarinic inhibition of calcium current and M current in Galpha q-deficient mice. J Neurosci *20*, 3973-3979.
- Hall, A.M., Brennan, G.P., Nguyen, T.M., Singh-Taylor, A., Mun, H.S., Sargious, M.J., and Baram, T.Z. (2017). The Role of Sirt1 in Epileptogenesis. eNeuro *4*.
- Halliwell, J.V., and Adams, P.R. (1982). Voltage-clamp analysis of muscarinic excitation in hippocampal neurons. Brain Res *250*, 71-92.
- Hara, D., Fukuchi, M., Miyashita, T., Tabuchi, A., Takasaki, I., Naruse, Y., Mori, N., Kondo, T., and Tsuda, M. (2009). Remote control of activity-dependent BDNF gene promoter-I transcription mediated by REST/NRSF. Biochem Biophys Res Commun *384*, 506-511.
- He, T.C., Zhou, S., da Costa, L.T., Yu, J., Kinzler, K.W., and Vogelstein, B. (1998). A simplified system for generating recombinant adenoviruses. Proc Natl Acad Sci U S A *95*, 2509-2514.
- He, X.P., Kotloski, R., Nef, S., Luikart, B.W., Parada, L.F., and McNamara, J.O. (2004). Conditional deletion of TrkB but not BDNF prevents epileptogenesis in the kindling model. Neuron *43*, 31-42.
- He, X.P., Pan, E., Sciarretta, C., Minichiello, L., and McNamara, J.O. (2010). Disruption of TrkB-mediated phospholipase Cgamma signaling inhibits limbic epileptogenesis. J Neurosci *30*, 6188-6196.
- Heinemann, U., Buchheim, K., Gabriel, S., Kann, O., Kovacs, R., and Schuchmann, S. (2002a). Cell death and metabolic activity during epileptiform discharges and status epilepticus in the hippocampus. Prog Brain Res *135*, 197-210.
- Heinemann, U., Buchheim, K., Gabriel, S., Kann, O., Kovács, R., and Schuchmann, S. (2002b). Coupling of electrical and metabolic activity during epileptiform discharges. Epilepsia *43 Suppl 5*, 168-173.

- Holmes, K.H., Bilkey, D.K., Laverty, R., and Goddard, G.V. (1990). The N-methyl-D-aspartate antagonists aminophosphonovalerate and carboxypiperazinephosphonate retard the development and expression of kindled seizures. Brain Res *506*, 227-235.
- Holopainen, I.E., Järvelä, J., Lopez-Picon, F.R., Pelliniemi, L.J., and Kukko-Lukjanov, T.K. (2004). Mechanisms of kainate-induced region-specific neuronal death in immature organotypic hippocampal slice cultures. Neurochem Int *45*, 1-10.
- Horowitz, L.F., Hirdes, W., Suh, B.C., Hilgemann, D.W., Mackie, K., and Hille, B. (2005). Phospholipase C in living cells: activation, inhibition, Ca2+ requirement, and regulation of M current. J Gen Physiol *126*, 243-262.
- Hoshi, N. (2020). M-Current Suppression, Seizures and Lipid Metabolism: A Potential Link Between Neuronal Kv7 Channel Regulation and Dietary Therapies for Epilepsy. Front Physiol *11*, 513.
- Hoshi, N., Langeberg, L.K., Gould, C.M., Newton, A.C., and Scott, J.D. (2010). Interaction with AKAP79 modifies the cellular pharmacology of PKC. Mol Cell *37*, 541-550.
- Hoshi, N., Zhang, J.S., Omaki, M., Takeuchi, T., Yokoyama, S., Wanaverbecq, N., Langeberg, L.K., Yoneda, Y., Scott, J.D., Brown, D.A., *et al.* (2003). AKAP150 signaling complex promotes suppression of the M-current by muscarinic agonists. Nat Neurosci *6*, 564-571.
- Hou, X., Wang, X., and Zhang, L. (2010). Conditional downregulation of brain- derived neurotrophic factor and tyrosine kinase receptor B blocks epileptogenesis in the human temporal lobe epilepsy hippocampus. Neurol India *58*, 29-34.
- Hu, H., Vervaeke, K., and Storm, J.F. (2007). M-channels (Kv7/KCNQ channels) that regulate synaptic integration, excitability, and spike pattern of CA1 pyramidal cells are located in the perisomatic region. J Neurosci *27*, 1853-1867.
- Hu, Q.P., and Mao, D.A. (2016). Histone deacetylase inhibitor SAHA attenuates post-seizure hippocampal microglia TLR4/MYD88 signaling and inhibits TLR4 gene expression via histone acetylation. BMC Neurosci *17*, 22.

- Hu, X.L., Cheng, X., Cai, L., Tan, G.H., Xu, L., Feng, X.Y., Lu, T.J., Xiong, H., Fei, J., and Xiong, Z.Q. (2011a). Conditional deletion of NRSF in forebrain neurons accelerates epileptogenesis in the kindling model. Cereb Cortex *21*, 2158-2165.
- Hu, X.L., Cheng, X., Fei, J., and Xiong, Z.Q. (2011b). Neuron-restrictive silencer factor is not required for the antiepileptic effect of the ketogenic diet. Epilepsia *52*, 1609-1616.
- Huang, X., Zhang, H., Yang, J., Wu, J., McMahon, J., Lin, Y., Cao, Z., Gruenthal, M., and Huang, Y. (2010). Pharmacological inhibition of the mammalian target of rapamycin pathway suppresses acquired epilepsy. Neurobiol Dis *40*, 193-199.
- Huang, Y., Myers, S.J., and Dingledine, R. (1999). Transcriptional repression by REST: recruitment of Sin3A and histone deacetylase to neuronal genes. Nat Neurosci *2*, 867-872.
- Humpel, C. (2015). Organotypic brain slice cultures: A review. Neuroscience *305*, 86-98.
- Iihara, K., Joo, D.T., Henderson, J., Sattler, R., Taverna, F.A., Lourensen, S., Orser, B.A., Roder, J.C., and Tymianski, M. (2001). The influence of glutamate receptor 2 expression on excitotoxicity in Glur2 null mutant mice. J Neurosci *21*, 2224-2239.
- Isackson, P.J., Huntsman, M.M., Murray, K.D., and Gall, C.M. (1991). BDNF mRNA expression is increased in adult rat forebrain after limbic seizures: temporal patterns of induction distinct from NGF. Neuron *6*, 937-948.
- Jiang, L., Kosenko, A., Yu, C., Huang, L., Li, X., and Hoshi, N. (2015). Activation of m1 muscarinic acetylcholine receptor induces surface transport of KCNQ channels through a CRMP-2-mediated pathway. J Cell Sci *128*, 4235-4245.
- Johnson, D.S., Mortazavi, A., Myers, R.M., and Wold, B. (2007). Genome-wide mapping of in vivo protein-DNA interactions. Science *316*, 1497-1502.
- Johnson, R., Gamblin, R.J., Ooi, L., Bruce, A.W., Donaldson, I.J., Westhead, D.R., Wood, I.C., Jackson, R.M., and Buckley, N.J. (2006). Identification of

the REST regulon reveals extensive transposable element-mediated binding site duplication. Nucleic Acids Res *34*, 3862-3877.

- Johnson, R., Samuel, J., Ng, C.K., Jauch, R., Stanton, L.W., and Wood, I.C. (2009). Evolution of the vertebrate gene regulatory network controlled by the transcriptional repressor REST. Mol Biol Evol *26*, 1491-1507.
- Jung, S., Yang, H., Kim, B.S., Chu, K., Lee, S.K., and Jeon, D. (2012). The immunosuppressant cyclosporin A inhibits recurrent seizures in an experimental model of temporal lobe epilepsy. Neurosci Lett *529*, 133-138.
- Kang, S.K., Johnston, M.V., and Kadam, S.D. (2015). Acute TrkB inhibition rescues phenobarbital-resistant seizures in a mouse model of neonatal ischemia. Eur J Neurosci *42*, 2792-2804.
- Kasteleijn-Nolst Trenité, D.G., Biton, V., French, J.A., Abou-Khalil, B., Rosenfeld, W.E., Diventura, B., Moore, E.L., Hetherington, S.V., and Rigdon, G.C. (2013). Kv7 potassium channel activation with ICA-105665 reduces photoparoxysmal EEG responses in patients with epilepsy. Epilepsia *54*, 1437-1443.
- Kawamura, M., Sato, S., Matsumoto, G., Fukuda, T., Shiba-Fukushima, K., Noda, S., Takanashi, M., Mori, N., and Hattori, N. (2019). Loss of nuclear REST/NRSF in aged-dopaminergic neurons in Parkinson's disease patients. Neurosci Lett *699*, 59-63.
- Kay, H.Y., Greene, D.L., Kang, S., Kosenko, A., and Hoshi, N. (2015). M-current preservation contributes to anticonvulsant effects of valproic acid. J Clin Invest *125*, 3904-3914.
- Keener, D.G., Cheung, A., and Futai, K. (2020). A highly efficient method for single-cell electroporation in mouse organotypic hippocampal slice culture. J Neurosci Methods *337*, 108632.
- Keezer, M.R., Sisodiya, S.M., and Sander, J.W. (2016). Comorbidities of epilepsy: current concepts and future perspectives. Lancet Neurol *15*, 106-115.
- Khammy, M.M., Kim, S., Bentzen, B.H., Lee, S., Choi, I., Aalkjaer, C., and Jepps, T.A. (2018). 4-Aminopyridine: a pan voltage-gated potassium channel inhibitor that enhances K. Br J Pharmacol *175*, 501-516.

- Kirkwood, A., and Lisman, J.E. (1992). Action potentials produce a long-term enhancement of M-current in frog sympathetic ganglion. Brain Res *580*, 281-287.
- Kjeldsen, M.J., Kyvik, K.O., Christensen, K., and Friis, M.L. (2001). Genetic and environmental factors in epilepsy: a population-based study of 11900 Danish twin pairs. Epilepsy Res *44*, 167-178.
- Klinger, F., Gould, G., Boehm, S., and Shapiro, M.S. (2011). Distribution of M-channel subunits KCNQ2 and KCNQ3 in rat hippocampus. Neuroimage *58*, 761-769.
- Kobow, K., Auvin, S., Jensen, F., Löscher, W., Mody, I., Potschka, H., Prince, D., Sierra, A., Simonato, M., Pitkänen, A., *et al.* (2012). Finding a better drug for epilepsy: antiepileptogenesis targets. Epilepsia *53*, 1868-1876.
- Kochan, L.D., Churn, S.B., Omojokun, O., Rice, A., and DeLorenzo, R.J. (2000). Status epilepticus results in an N-methyl-D-aspartate receptor-dependent inhibition of Ca2+/calmodulin-dependent kinase II activity in the rat. Neuroscience *95*, 735-743.
- Kokaia, M., Ernfors, P., Kokaia, Z., Elmér, E., Jaenisch, R., and Lindvall, O. (1995). Suppressed epileptogenesis in BDNF mutant mice. Exp Neurol *133*, 215-224.
- Kovács, R., Gutiérrez, R., Kivi, A., Schuchmann, S., Gabriel, S., and Heinemann, U. (1999). Acute cell damage after low Mg2+-induced epileptiform activity in organotypic hippocampal slice cultures. Neuroreport *10*, 207-213.
- Kow, R.L., Jiang, K., Naydenov, A.V., Le, J.H., Stella, N., and Nathanson, N.M. (2014). Modulation of pilocarpine-induced seizures by cannabinoid receptor 1. PLoS One *9*, e95922.
- Lähteinen, S., Pitkänen, A., Saarelainen, T., Nissinen, J., Koponen, E., and Castrén, E. (2002). Decreased BDNF signalling in transgenic mice reduces epileptogenesis. Eur J Neurosci *15*, 721-734.
- Larsson, J.E., Karlsson, U., Wu, X., and Liin, S.I. (2020). Combining endocannabinoids with retigabine for enhanced M-channel effect and improved KV7 subtype selectivity. J Gen Physiol *152*.

- Lauritano, A., Moutton, S., Longobardi, E., Tran Mau-Them, F., Laudati, G., Nappi, P., Soldovieri, M.V., Ambrosino, P., Cataldi, M., Jouan, T., *et al.* (2019). A novel homozygous KCNQ3 loss-of-function variant causes non-syndromic intellectual disability and neonatal-onset pharmacodependent epilepsy. Epilepsia Open *4*, 464-475.
- Lawrence, J.J., Saraga, F., Churchill, J.F., Statland, J.M., Travis, K.E., Skinner, F.K., and McBain, C.J. (2006). Somatodendritic Kv7/KCNQ/M channels control interspike interval in hippocampal interneurons. J Neurosci *26*, 12325-12338.
- Leite, J.P., Babb, T.L., Pretorius, J.K., Kuhlman, P.A., Yeoman, K.M., and Mathern, G.W. (1996). Neuron loss, mossy fiber sprouting, and interictal spikes after intrahippocampal kainate in developing rats. Epilepsy Res *26*, 219-231.
- Lévesque, M., and Avoli, M. (2013). The kainic acid model of temporal lobe epilepsy. Neurosci Biobehav Rev *37*, 2887-2899.
- Li, C., Lu, Q., Huang, P., Fu, T., Guo, L., and Xu, X. (2015). Activity-dependent downregulation of M-Type (Kv7) K^+ channels surface expression requires the activation of iGluRs/Ca^{2+}/PKC signaling pathway in hippocampal neuron. Neuropharmacology *95*, 154-167.
- Li, D., Bai, X., Jiang, Y., and Cheng, Y. (2021). Butyrate alleviates PTZ-induced mitochondrial dysfunction, oxidative stress and neuron apoptosis in mice via Keap1/Nrf2/HO-1 pathway. Brain Res Bull *168*, 25-35.
- Li, M., He, H.P., Gong, H.Q., Zhang, J., Ma, W.J., Zhou, H., Cao, D.S., Wang, N., and Zhang, T.C. (2016a). NFATc4 and myocardin synergistically up-regulate the expression of LTCC α1C in ET-1-induced cardiomyocyte hypertrophy. Life Sci *155*, 11-20.
- Li, Q., Han, X., and Wang, J. (2016b). Organotypic Hippocampal Slices as Models for Stroke and Traumatic Brain Injury. Mol Neurobiol *53*, 4226-4237.
- Li, S.Y., Sun, W.G., Jia, Y.H., Wu, G.S., An, G.S., Ni, J.H., and Jia, H.T. (2010). Calcium signal-initiated early activation of NF-kappaB in neurons is a neuroprotective event in response to kainic acid-induced excitotoxicity. Biochemistry (Mosc) *75*, 101-109.

- Li, X., Wu, Q., Xie, C., Wang, C., Wang, Q., Dong, C., Fang, L., Ding, J., and Wang, T. (2019). Blocking of BDNF-TrkB signaling inhibits the promotion effect of neurological function recovery after treadmill training in rats with spinal cord injury. Spinal Cord *57*, 65-74.
- Li, Y., Gamper, N., and Shapiro, M.S. (2004a). Single-channel analysis of KCNQ K+ channels reveals the mechanism of augmentation by a cysteine-modifying reagent. J Neurosci *24*, 5079-5090.
- Li, Y., Langlais, P., Gamper, N., Liu, F., and Shapiro, M.S. (2004b). Dual phosphorylations underlie modulation of unitary KCNQ K(+) channels by Src tyrosine kinase. J Biol Chem *279*, 45399-45407.
- Lin, C.C., Chen, W.N., Chen, C.J., Lin, Y.W., Zimmer, A., and Chen, C.C. (2012). An antinociceptive role for substance P in acid-induced chronic muscle pain. Proc Natl Acad Sci U S A *109*, E76-83.
- Lindholm, J.S., and Castrén, E. (2014). Mice with altered BDNF signaling as models for mood disorders and antidepressant effects. Front Behav Neurosci *8*, 143.
- Lindroos, M.M., Soini, S.L., Kukko-Lukjanov, T.K., Korpi, E.R., Lovinger, D., and Holopainen, I.E. (2005). Maturation of cultured hippocampal slices results in increased excitability in granule cells. Int J Dev Neurosci *23*, 65-73.
- Liu, J., Saponjian, Y., Mahoney, M.M., Staley, K.J., and Berdichevsky, Y. (2017). Epileptogenesis in organotypic hippocampal cultures has limited dependence on culture medium composition. PLoS One *12*, e0172677.
- Liu, M., Sheng, Z., Cai, L., Zhao, K., Tian, Y., and Fei, J. (2012). Neuronal conditional knockout of NRSF decreases vulnerability to seizures induced by pentylenetetrazol in mice. Acta Biochim Biophys Sin (Shanghai) *44*, 476-482.
- Liu, X., Feng, Z., Du, L., Huang, Y., Ge, J., Deng, Y., and Mei, Z. (2019). The Potential Role of MicroRNA-124 in Cerebral Ischemia Injury. Int J Mol Sci *21*.
- Lorigados Pedre, L., Morales Chacon, L.M., Orozco Suarez, S., Pavon Fuentes, N., Estupinan Diaz, B., Serrano Sanchez, T., Garcia Maeso, I., and Rocha Arrieta, L. (2013). Inflammatory mediators in epilepsy. Curr Pharm Des *19*, 6766-6772.

- Loup, F., Wieser, H.G., Yonekawa, Y., Aguzzi, A., and Fritschy, J.M. (2000). Selective alterations in GABAA receptor subtypes in human temporal lobe epilepsy. J Neurosci *20*, 5401-5419.
- Lu, T., Aron, L., Zullo, J., Pan, Y., Kim, H., Chen, Y., Yang, T.H., Kim, H.M., Drake, D., Liu, X.S., *et al.* (2014). REST and stress resistance in ageing and Alzheimer's disease. Nature *507*, 448-454.
- Lunyak, V.V., Burgess, R., Prefontaine, G.G., Nelson, C., Sze, S.H., Chenoweth, J., Schwartz, P., Pevzner, P.A., Glass, C., Mandel, G., *et al.* (2002). Corepressor-dependent silencing of chromosomal regions encoding neuronal genes. Science *298*, 1747-1752.
- Madamba, S.G., Schweitzer, P., and Siggins, G.R. (1999). Dynorphin selectively augments the M-current in hippocampal CA1 neurons by an opiate receptor mechanism. J Neurophysiol *82*, 1768-1775.
- Magalhães, D.M., Pereira, N., Rombo, D.M., Beltrão-Cavacas, C., Sebastião, A.M., and Valente, C.A. (2018). Ex vivo model of epilepsy in organotypic slices-a new tool for drug screening. J Neuroinflammation *15*, 203.
- Main, M.J., Cryan, J.E., Dupere, J.R., Cox, B., Clare, J.J., and Burbidge, S.A. (2000). Modulation of KCNQ2/3 potassium channels by the novel anticonvulsant retigabine. Mol Pharmacol *58*, 253-262.
- Manville, R.W., and Abbott, G.W. (2018a). Ancient and modern anticonvulsants act synergistically in a KCNQ potassium channel binding pocket. Nat Commun *9*, 3845.
- Manville, R.W., and Abbott, G.W. (2018b). Gabapentin Is a Potent Activator of KCNQ3 and KCNQ5 Potassium Channels. Mol Pharmacol *94*, 1155-1163.
- Manville, R.W., and Abbott, G.W. (2019). Cilantro leaf harbors a potent potassium channel-activating anticonvulsant. FASEB J *33*, 11349-11363.
- Manville, R.W., Papanikolaou, M., and Abbott, G.W. (2018). Direct neurotransmitter activation of voltage-gated potassium channels. Nat Commun *9*, 1847.
- Manville, R.W., Papanikolaou, M., and Abbott, G.W. (2020). M-Channel Activation Contributes to the Anticonvulsant Action of the Ketone Body. J Pharmacol Exp Ther *372*, 148-156.

- Marrion, N.V., Smart, T.G., Marsh, S.J., and Brown, D.A. (1989). Muscarinic suppression of the M-current in the rat sympathetic ganglion is mediated by receptors of the M1-subtype. Br J Pharmacol *98*, 557-573.
- Martínez-Levy, G.A., Rocha, L., Lubin, F.D., Alonso-Vanegas, M.A., Nani, A., Buentello-García, R.M., Pérez-Molina, R., Briones-Velasco, M., Recillas-Targa, F., Pérez-Molina, A., *et al.* (2016). Increased expression of BDNF transcript with exon VI in hippocampi of patients with pharmaco-resistant temporal lobe epilepsy. Neuroscience *314*, 12-21.
- Maslarova, A., Salar, S., Lapilover, E., Friedman, A., Veh, R.W., and Heinemann, U. (2013). Increased susceptibility to acetylcholine in the entorhinal cortex of pilocarpine-treated rats involves alterations in KCNQ channels. Neurobiol Dis *56*, 14-24.
- Matschke, V., Piccini, I., Schubert, J., Wrobel, E., Lang, F., Matschke, J., Amedonu, E., Meuth, S.G., Strünker, T., Strutz-Seebohm, N., *et al.* (2016). The Natural Plant Product Rottlerin Activates Kv7.1/KCNE1 Channels. Cell Physiol Biochem *40*, 1549-1558.
- McClelland, S., Flynn, C., Dubé, C., Richichi, C., Zha, Q., Ghestem, A., Esclapez, M., Bernard, C., and Baram, T.Z. (2011). Neuron-restrictive silencer factor-mediated hyperpolarization-activated cyclic nucleotide gated channelopathy in experimental temporal lobe epilepsy. Ann Neurol *70*, 454-464.
- McCormack, K., Joiner, W.J., and Heinemann, S.H. (1994). A characterization of the activating structural rearrangements in voltage-dependent Shaker K+ channels. Neuron *12*, 301-315.
- McNamara, J.O., Huang, Y.Z., and Leonard, A.S. (2006). Molecular signaling mechanisms underlying epileptogenesis. Sci STKE *2006*, re12.
- McNamara, R.K., and Routtenberg, A. (1995). NMDA receptor blockade prevents kainate induction of protein F1/GAP-43 mRNA in hippocampal granule cells and subsequent mossy fiber sprouting in the rat. Brain Res Mol Brain Res *33*, 22-28.
- Mellentin, C., Møller, M., and Jahnsen, H. (2006). Properties of long-term synaptic plasticity and metaplasticity in organotypic slice cultures of rat hippocampus. Exp Brain Res *170*, 522-531.

- Michalakis, M., Holsinger, D., Ikeda-Douglas, C., Cammisuli, S., Ferbinteanu, J., DeSouza, C., DeSouza, S., Fecteau, J., Racine, R.J., and Milgram, N.W. (1998). Development of spontaneous seizures over extended electrical kindling. I. Electrographic, behavioral, and transfer kindling correlates. Brain Res *793*, 197-211.
- Miller, J.A., Kirkley, K.A., Padmanabhan, R., Liang, L.P., Raol, Y.H., Patel, M., Bialecki, R.A., and Tjalkens, R.B. (2014). Repeated exposure to low doses of kainic acid activates nuclear factor kappa B (NF-κB) prior to seizure in transgenic NF-κB/EGFP reporter mice. Neurotoxicology *44*, 39-47.
- Millichap, J.J., Park, K.L., Tsuchida, T., Ben-Zeev, B., Carmant, L., Flamini, R., Joshi, N., Levisohn, P.M., Marsh, E., Nangia, S., *et al.* (2016). KCNQ2 encephalopathy: Features, mutational hot spots, and ezogabine treatment of 11 patients. Neurol Genet *2*, e96.
- Milutinovic, S., D'Alessio, A.C., Detich, N., and Szyf, M. (2007). Valproate induces widespread epigenetic reprogramming which involves demethylation of specific genes. Carcinogenesis *28*, 560-571.
- Miyaguchi, K., Maeda, Y., Kojima, T., Setoguchi, Y., and Mori, N. (1999). Neuron-targeted gene transfer by adenovirus carrying neural-restrictive silencer element. Neuroreport *10*, 2349-2353.
- Miyata, K., Omori, N., Uchino, H., Yamaguchi, T., Isshiki, A., and Shibasaki, F. (2001). Involvement of the brain-derived neurotrophic factor/TrkB pathway in neuroprotecive effect of cyclosporin A in forebrain ischemia. Neuroscience *105*, 571-578.
- Moia, L.J., Matsui, H., de Barros, G.A., Tomizawa, K., Miyamoto, K., Kuwata, Y., Tokuda, M., Itano, T., and Hatase, O. (1994). Immunosuppressants and calcineurin inhibitors, cyclosporin A and FK506, reversibly inhibit epileptogenesis in amygdaloid kindled rat. Brain Res *648*, 337-341.
- Monaghan, D.T., and Cotman, C.W. (1982). The distribution of [3H]kainic acid binding sites in rat CNS as determined by autoradiography. Brain Res *252*, 91-100.
- Monaghan, M.M., Menegola, M., Vacher, H., Rhodes, K.J., and Trimmer, J.S. (2008). Altered expression and localization of hippocampal A-type

potassium channel subunits in the pilocarpine-induced model of temporal lobe epilepsy. Neuroscience *156*, 550-562.

- Morales-Villagrán, A., Ureña-Guerrero, M.E., and Tapia, R. (1996). Protection by NMDA receptor antagonists against seizures induced by intracerebral administration of 4-aminopyridine. Eur J Pharmacol *305*, 87-93.
- Mori, N., Mizuno, T., Murai, K., Nakano, I., and Yamashita, H. (2002). Effect of age on the gene expression of neural-restrictive silencing factor NRSF/REST. Neurobiol Aging *23*, 255-262.
- Moriwaki, A., Lu, Y.F., Hayashi, Y., Tomizawa, K., Tokuda, M., Itano, T., Hatase, O., and Matsui, H. (1996). Immunosuppressant FK506 prevents mossy fiber sprouting induced by kindling stimulation. Neurosci Res *25*, 191-194.
- Motalli, R., Louvel, J., Tancredi, V., Kurcewicz, I., Wan-Chow-Wah, D., Pumain, R., and Avoli, M. (1999). GABA(B) receptor activation promotes seizure activity in the juvenile rat hippocampus. J Neurophysiol *82*, 638-647.
- Mucha, M., Ooi, L., Linley, J.E., Mordaka, P., Dalle, C., Robertson, B., Gamper, N., and Wood, I.C. (2010). Transcriptional control of KCNQ channel genes and the regulation of neuronal excitability. J Neurosci *30*, 13235-13245.
- Müller, M., Gähwiler, B.H., Rietschin, L., and Thompson, S.M. (1993). Reversible loss of dendritic spines and altered excitability after chronic epilepsy in hippocampal slice cultures. Proc Natl Acad Sci U S A *90*, 257-261.
- Murphy, R.C., and Messer, A. (2001). Gene transfer methods for CNS organotypic cultures: a comparison of three nonviral methods. Mol Ther *3*, 113-121.
- Murray, K.D., Isackson, P.J., Eskin, T.A., King, M.A., Montesinos, S.P., Abraham, L.A., and Roper, S.N. (2000). Altered mRNA expression for brain-derived neurotrophic factor and type II calcium/calmodulin-dependent protein kinase in the hippocampus of patients with intractable temporal lobe epilepsy. J Comp Neurol *418*, 411-422.
- Myers, S.J., Peters, J., Huang, Y., Comer, M.B., Barthel, F., and Dingledine, R. (1998). Transcriptional regulation of the GluR2 gene: neural-specific

expression, multiple promoters, and regulatory elements. J Neurosci *18*, 6723-6739.

- Na, E.J., Nam, H.Y., Park, J., Chung, M.A., Woo, H.A., and Kim, H.J. (2017). PI3K-mTOR-S6K Signaling Mediates Neuronal Viability via Collapsin Response Mediator Protein-2 Expression. Front Mol Neurosci *10*, 288.
- Naruse, Y., Aoki, T., Kojima, T., and Mori, N. (1999). Neural restrictive silencer factor recruits mSin3 and histone deacetylase complex to repress neuron-specific target genes. Proc Natl Acad Sci U S A *96*, 13691-13696.
- Navarrete-Modesto, V., Orozco-Suárez, S., Alonso-Vanegas, M., Feria-Romero, I.A., and Rocha, L. (2019). REST/NRSF transcription factor is overexpressed in hippocampus of patients with drug-resistant mesial temporal lobe epilepsy. Epilepsy Behav *94*, 118-123.
- Nibuya, M., Morinobu, S., and Duman, R.S. (1995). Regulation of BDNF and trkB mRNA in rat brain by chronic electroconvulsive seizure and antidepressant drug treatments. J Neurosci *15*, 7539-7547.
- Okada, M., Zhu, G., Hirose, S., Ito, K.I., Murakami, T., Wakui, M., and Kaneko, S. (2003). Age-dependent modulation of hippocampal excitability by KCNQ-channels. Epilepsy Res *53*, 81-94.
- Okonkwo, D.O., and Povlishock, J.T. (1999). An intrathecal bolus of cyclosporin A before injury preserves mitochondrial integrity and attenuates axonal disruption in traumatic brain injury. J Cereb Blood Flow Metab *19*, 443-451.
- Oliveria, S.F., Dell'Acqua, M.L., and Sather, W.A. (2007). AKAP79/150 anchoring of calcineurin controls neuronal L-type Ca2+ channel activity and nuclear signaling. Neuron *55*, 261-275.
- Ontario, H.Q. (2012). Epilepsy surgery: an evidence summary. Ont Health Technol Assess Ser *12*, 1-28.
- Ooi, L., Belyaev, N.D., Miyake, K., Wood, I.C., and Buckley, N.J. (2006). BRG1 chromatin remodeling activity is required for efficient chromatin binding by repressor element 1-silencing transcription factor (REST) and facilitates REST-mediated repression. J Biol Chem *281*, 38974-38980.

- Ooi, L., and Wood, I.C. (2007). Chromatin crosstalk in development and disease: lessons from REST. Nat Rev Genet *8*, 544-554.
- Orhan, G., Bock, M., Schepers, D., Ilina, E.I., Reichel, S.N., Loffler, H., Jezutkovic, N., Weckhuysen, S., Mandelstam, S., Suls, A., *et al.* (2014). Dominant-negative effects of KCNQ2 mutations are associated with epileptic encephalopathy. Ann Neurol *75*, 382-394.
- Ostacolo, C., Miceli, F., Di Sarno, V., Nappi, P., Iraci, N., Soldovieri, M.V., Ciaglia, T., Ambrosino, P., Vestuto, V., Lauritano, A., *et al.* (2020). Synthesis and Pharmacological Characterization of Conformationally Restricted Retigabine Analogues as Novel Neuronal Kv7 Channel Activators. J Med Chem *63*, 163-185.
- Pacheco Otalora, L.F., Hernandez, E.F., Arshadmansab, M.F., Francisco, S., Willis, M., Ermolinsky, B., Zarei, M., Knaus, H.G., and Garrido-Sanabria, E.R. (2008). Down-regulation of BK channel expression in the pilocarpine model of temporal lobe epilepsy. Brain Res *1200*, 116-131.
- Paci, P., Gabriele, S., and Ris, L. (2017). A new method allowing long-term potentiation recordings in hippocampal organotypic slices. Brain Behav *7*, e00692.
- Padilla, K., Wickenden, A.D., Gerlach, A.C., and McCormack, K. (2009). The KCNQ2/3 selective channel opener ICA-27243 binds to a novel voltage-sensor domain site. Neurosci Lett *465*, 138-142.
- Palm, K., Belluardo, N., Metsis, M., and Timmusk, T. (1998). Neuronal expression of zinc finger transcription factor REST/NRSF/XBR gene. J Neurosci *18*, 1280-1296.
- Pan, Z., Kao, T., Horvath, Z., Lemos, J., Sul, J.Y., Cranstoun, S.D., Bennett, V., Scherer, S.S., and Cooper, E.C. (2006). A common ankyrin-G-based mechanism retains KCNQ and NaV channels at electrically active domains of the axon. J Neurosci *26*, 2599-2613.
- Paonessa, F., Latifi, S., Scarongella, H., Cesca, F., and Benfenati, F. (2013). Specificity protein 1 (Sp1)-dependent activation of the synapsin I gene (SYN1) is modulated by RE1-silencing transcription factor (REST) and 5'-cytosine-phosphoguanine (CpG) methylation. J Biol Chem *288*, 3227-3239.

- Parent, J.M., Yu, T.W., Leibowitz, R.T., Geschwind, D.H., Sloviter, R.S., and Lowenstein, D.H. (1997). Dentate granule cell neurogenesis is increased by seizures and contributes to aberrant network reorganization in the adult rat hippocampus. J Neurosci *17*, 3727-3738.
- Pecoraro-Bisogni, F., Lignani, G., Contestabile, A., Castroflorio, E., Pozzi, D., Rocchi, A., Prestigio, C., Orlando, M., Valente, P., Massacesi, M., *et al.* (2018). REST-Dependent Presynaptic Homeostasis Induced by Chronic Neuronal Hyperactivity. Mol Neurobiol *55*, 4959-4972.
- Pellegrini-Giampietro, D.E., Zukin, R.S., Bennett, M.V., Cho, S., and Pulsinelli, W.A. (1992). Switch in glutamate receptor subunit gene expression in CA1 subfield of hippocampus following global ischemia in rats. Proc Natl Acad Sci U S A *89*, 10499-10503.
- Peretz, A., Sheinin, A., Yue, C., Degani-Katzav, N., Gibor, G., Nachman, R., Gopin, A., Tam, E., Shabat, D., Yaari, Y., *et al.* (2007). Pre- and postsynaptic activation of M-channels by a novel opener dampens neuronal firing and transmitter release. J Neurophysiol *97*, 283-295.
- Peters, H.C., Hu, H., Pongs, O., Storm, J.F., and Isbrandt, D. (2005). Conditional transgenic suppression of M channels in mouse brain reveals functions in neuronal excitability, resonance and behavior. Nat Neurosci *8*, 51-60.
- Petralia, R.S., Wang, Y.X., and Wenthold, R.J. (1994). Histological and ultrastructural localization of the kainate receptor subunits, KA2 and GluR6/7, in the rat nervous system using selective antipeptide antibodies. J Comp Neurol *349*, 85-110.
- Pitkänen, A., Lukasiuk, K., Dudek, F.E., and Staley, K.J. (2015). Epileptogenesis. Cold Spring Harb Perspect Med *5*.
- Plaisance, V., Niederhauser, G., Azzouz, F., Lenain, V., Haefliger, J.A., Waeber, G., and Abderrahmani, A. (2005). The repressor element silencing transcription factor (REST)-mediated transcriptional repression requires the inhibition of Sp1. J Biol Chem *280*, 401-407.
- Porter, R.J., Partiot, A., Sachdeo, R., Nohria, V., Alves, W.M., and Group, S. (2007). Randomized, multicenter, dose-ranging trial of retigabine for partial-onset seizures. Neurology *68*, 1197-1204.

- Potier, S., and Psarropoulou, C. (2001). Endogenous acetylcholine facilitates epileptogenesis in immature rat neocortex. Neurosci Lett *302*, 25-28.
- Potter, W.B., O'Riordan, K.J., Barnett, D., Osting, S.M., Wagoner, M., Burger, C., and Roopra, A. (2010). Metabolic regulation of neuronal plasticity by the energy sensor AMPK. PLoS One *5*, e8996.
- Poulsen, F.R., Jahnsen, H., Blaabjerg, M., and Zimmer, J. (2002). Pilocarpine-induced seizure-like activity with increased BNDF and neuropeptide Y expression in organotypic hippocampal slice cultures. Brain Res *950*, 103-118.
- Pozzi, D., Lignani, G., Ferrea, E., Contestabile, A., Paonessa, F., D'Alessandro, R., Lippiello, P., Boido, D., Fassio, A., Meldolesi, J., *et al.* (2013). REST/NRSF-mediated intrinsic homeostasis protects neuronal networks from hyperexcitability. EMBO J *32*, 2994-3007.
- Pozzo Miller, L.D., Mahanty, N.K., Connor, J.A., and Landis, D.M. (1994). Spontaneous pyramidal cell death in organotypic slice cultures from rat hippocampus is prevented by glutamate receptor antagonists. Neuroscience *63*, 471-487.
- Prada, I., Marchaland, J., Podini, P., Magrassi, L., D'Alessandro, R., Bezzi, P., and Meldolesi, J. (2011). REST/NRSF governs the expression of dense-core vesicle gliosecretion in astrocytes. J Cell Biol *193*, 537-549.
- Prasad Tripathi, R.K., and Ayyannan, S.R. (2017). Anticonvulsant activity, organotypic hippocampal neuroprotection assay and in-silico sodium channel blocking potential of 2-amino-6-nitrobenzothiazole derived semicarbazones. Biomed Pharmacother *95*, 1451-1460.
- Prince, H.K., Conn, P.J., Blackstone, C.D., Huganir, R.L., and Levey, A.I. (1995). Down-regulation of AMPA receptor subunit GluR2 in amygdaloid kindling. J Neurochem *64*, 462-465.
- Rahman, M., and Nguyen, H. (2021). Valproic Acid. In StatPearls (Treasure Island (FL)).
- Rakhade, S.N., Yao, B., Ahmed, S., Asano, E., Beaumont, T.L., Shah, A.K., Draghici, S., Krauss, R., Chugani, H.T., Sood, S., *et al.* (2005). A common pattern of persistent gene activation in human neocortical epileptic foci. Ann Neurol *58*, 736-747.

- Rangel, P., Cysneiros, R.M., Arida, R.M., de Albuquerque, M., Colugnati, D.B., Scorza, C.A., Cavalheiro, E.A., and Scorza, F.A. (2005). Lovastatin reduces neuronal cell death in hippocampal CA1 subfield after pilocarpine-induced status epilepticus: preliminary results. Arq Neuropsiquiatr *63*, 972-976.
- Reddy, D.S., and Kuruba, R. (2013). Experimental models of status epilepticus and neuronal injury for evaluation of therapeutic interventions. Int J Mol Sci *14*, 18284-18318.
- Reddy, S.D., Clossen, B.L., and Reddy, D.S. (2018). Epigenetic Histone Deacetylation Inhibition Prevents the Development and Persistence of Temporal Lobe Epilepsy. J Pharmacol Exp Ther *364*, 97-109.
- Rivera, C., Voipio, J., Payne, J.A., Ruusuvuori, E., Lahtinen, H., Lamsa, K., Pirvola, U., Saarma, M., and Kaila, K. (1999). The K+/Cl- co-transporter KCC2 renders GABA hyperpolarizing during neuronal maturation. Nature *397*, 251-255.
- Rivera, C., Voipio, J., Thomas-Crusells, J., Li, H., Emri, Z., Sipilä, S., Payne, J.A., Minichiello, L., Saarma, M., and Kaila, K. (2004). Mechanism of activity-dependent downregulation of the neuron-specific K-Cl cotransporter KCC2. J Neurosci *24*, 4683-4691.
- Robbins, J., Passmore, G.M., Abogadie, F.C., Reilly, J.M., and Brown, D.A. (2013). Effects of KCNQ2 gene truncation on M-type Kv7 potassium currents. PLoS One *8*, e71809.
- Robert, J.J., Bouilleret, V., Ridoux, V., Valin, A., Geoffroy, M.C., Mallet, J., and Le Gal La Salle, G. (1997). Adenovirus-mediated transfer of a functional GAD gene into nerve cells: potential for the treatment of neurological diseases. Gene Ther *4*, 1237-1245.
- Rode, F., Svalø, J., Sheykhzade, M., and Rønn, L.C. (2010). Functional effects of the KCNQ modulators retigabine and XE991 in the rat urinary bladder. Eur J Pharmacol *638*, 121-127.
- Roeloffs, R., Wickenden, A.D., Crean, C., Werness, S., McNaughton-Smith, G., Stables, J., McNamara, J.O., Ghodadra, N., and Rigdon, G.C. (2008). In vivo profile of ICA-27243 [N-(6-chloro-pyridin-3-yl)-3,4-difluoro-

benzamide], a potent and selective KCNQ2/Q3 (Kv7.2/Kv7.3) activator in rodent anticonvulsant models. J Pharmacol Exp Ther *326*, 818-828.

- Rogawski, M.A. (2000). KCNQ2/KCNQ3 K+ channels and the molecular pathogenesis of epilepsy: implications for therapy. Trends Neurosci *23*, 393-398.
- Rogawski, M.A., and Donevan, S.D. (1999). AMPA receptors in epilepsy and as targets for antiepileptic drugs. Adv Neurol *79*, 947-963.
- Rojas, A., Jiang, J., Ganesh, T., Yang, M.S., Lelutiu, N., Gueorguieva, P., and Dingledine, R. (2014). Cyclooxygenase-2 in epilepsy. Epilepsia *55*, 17-25.
- Romero-Leguizamón, C.R., Elnagar, M.R., Kristiansen, U., and Kohlmeier, K.A. (2019). Increasing cellular lifespan with a flow system in organotypic culture of the Laterodorsal Tegmentum (LDT). Sci Rep *9*, 1486.
- Ronen, G.M., Rosales, T.O., Connolly, M., Anderson, V.E., and Leppert, M. (1993). Seizure characteristics in chromosome 20 benign familial neonatal convulsions. Neurology *43*, 1355-1360.
- Roopra, A., Qazi, R., Schoenike, B., Daley, T.J., and Morrison, J.F. (2004). Localized domains of G9a-mediated histone methylation are required for silencing of neuronal genes. Mol Cell *14*, 727-738.
- Roopra, A., Sharling, L., Wood, I.C., Briggs, T., Bachfischer, U., Paquette, A.J., and Buckley, N.J. (2000). Transcriptional repression by neuron-restrictive silencer factor is mediated via the Sin3-histone deacetylase complex. Mol Cell Biol *20*, 2147-2157.
- Rose, K., Ooi, L., Dalle, C., Robertson, B., Wood, I.C., and Gamper, N. (2011). Transcriptional repression of the M channel subunit Kv7.2 in chronic nerve injury. Pain *152*, 742-754.
- Roseti, C., van Vliet, E.A., Cifelli, P., Ruffolo, G., Baayen, J.C., Di Castro, M.A., Bertollini, C., Limatola, C., Aronica, E., Vezzani, A., *et al.* (2015). GABAA currents are decreased by IL-1β in epileptogenic tissue of patients with temporal lobe epilepsy: implications for ictogenesis. Neurobiol Dis *82*, 311-320.
- Rossetti, F., de Araujo Furtado, M., Pak, T., Bailey, K., Shields, M., Chanda, S., Addis, M., Robertson, B.D., Moffett, M., Lumley, L.A., *et al.* (2012).

Combined diazepam and HDAC inhibitor treatment protects against seizures and neuronal damage caused by soman exposure. Neurotoxicology *33*, 500-511.

- Rostock, A., Tober, C., Rundfeldt, C., Bartsch, R., Engel, J., Polymeropoulos, E.E., Kutscher, B., Löscher, W., Hönack, D., White, H.S., *et al.* (1996). D-23129: a new anticonvulsant with a broad spectrum activity in animal models of epileptic seizures. Epilepsy Res *23*, 211-223.
- Routbort, M.J., Bausch, S.B., and McNamara, J.O. (1999). Seizures, cell death, and mossy fiber sprouting in kainic acid-treated organotypic hippocampal cultures. Neuroscience *94*, 755-765.
- Ruan, Y., Qiu, X., Lv, Y.D., Dong, D., Wu, X.J., Zhu, J., and Zheng, X.Y. (2019). Kainic acid Induces production and aggregation of amyloid β-protein and memory deficits by activating inflammasomes in NLRP3- and NF-κB-stimulated pathways. Aging (Albany NY) *11*, 3795-3810.
- Rundfeldt, C., and Netzer, R. (2000). The novel anticonvulsant retigabine activates M-currents in Chinese hamster ovary-cells tranfected with human KCNQ2/3 subunits. Neurosci Lett *282*, 73-76.
- Ryan, S.G., Wiznitzer, M., Hollman, C., Torres, M.C., Szekeresova, M., and Schneider, S. (1991). Benign familial neonatal convulsions: evidence for clinical and genetic heterogeneity. Ann Neurol *29*, 469-473.
- Saarelainen, T., Vaittinen, S., and Castrén, E. (2001). trkB-receptor activation contributes to the kainate-induced increase in BDNF mRNA synthesis. Cell Mol Neurobiol *21*, 429-435.
- Sanchez, R.M., Koh, S., Rio, C., Wang, C., Lamperti, E.D., Sharma, D., Corfas, G., and Jensen, F.E. (2001). Decreased glutamate receptor 2 expression and enhanced epileptogenesis in immature rat hippocampus after perinatal hypoxia-induced seizures. J Neurosci *21*, 8154-8163.
- Sanna, P.P., Berton, F., Cammalleri, M., Tallent, M.K., Siggins, G.R., Bloom, F.E., and Francesconi, W. (2000). A role for Src kinase in spontaneous epileptiform activity in the CA3 region of the hippocampus. Proc Natl Acad Sci U S A *97*, 8653-8657.
- Santini, M.P., Talora, C., Seki, T., Bolgan, L., and Dotto, G.P. (2001). Cross talk among calcineurin, Sp1/Sp3, and NFAT in control of p21(WAF1/CIP1)

expression in keratinocyte differentiation. Proc Natl Acad Sci U S A *98*, 9575-9580.

- Santoro, B., Lee, J.Y., Englot, D.J., Gildersleeve, S., Piskorowski, R.A., Siegelbaum, S.A., Winawer, M.R., and Blumenfeld, H. (2010). Increased seizure severity and seizure-related death in mice lacking HCN1 channels. Epilepsia *51*, 1624-1627.
- Sato, M., Racine, R.J., and McIntyre, D.C. (1990). Kindling: basic mechanisms and clinical validity. Electroencephalogr Clin Neurophysiol *76*, 459-472.
- Sato, Y., Shiraishi, Y., and Furuichi, T. (2004). Cell specificity and efficiency of the Semliki forest virus vector- and adenovirus vector-mediated gene expression in mouse cerebellum. J Neurosci Methods *137*, 111-121.
- Scanziani, M., Debanne, D., Müller, M., Gähwiler, B.H., and Thompson, S.M. (1994). Role of excitatory amino acid and GABAB receptors in the generation of epileptiform activity in disinhibited hippocampal slice cultures. Neuroscience *61*, 823-832.
- Scharfman, H.E., Goodman, J.H., Sollas, A.L., and Croll, S.D. (2002). Spontaneous limbic seizures after intrahippocampal infusion of brain-derived neurotrophic factor. Exp Neurol *174*, 201-214.
- Schätzle, P., Kapitein, L.C., and Hoogenraad, C.C. (2016). Live imaging of microtubule dynamics in organotypic hippocampal slice cultures. Methods Cell Biol *131*, 107-126.
- Schenzer, A., Friedrich, T., Pusch, M., Saftig, P., Jentsch, T.J., Grötzinger, J., and Schwake, M. (2005). Molecular determinants of KCNQ (Kv7) K+ channel sensitivity to the anticonvulsant retigabine. J Neurosci *25*, 5051-5060.
- Schoenherr, C.J., Paquette, A.J., and Anderson, D.J. (1996). Identification of potential target genes for the neuron-restrictive silencer factor. Proc Natl Acad Sci U S A *93*, 9881-9886.
- Schouten, M., Fratantoni, S.A., Hubens, C.J., Piersma, S.R., Pham, T.V., Bielefeld, P., Voskuyl, R.A., Lucassen, P.J., Jimenez, C.R., and Fitzsimons, C.P. (2015). MicroRNA-124 and -137 cooperativity controls caspase-3

activity through BCL2L13 in hippocampal neural stem cells. Sci Rep *5*, 12448.

- Schroeder, B.C., Kubisch, C., Stein, V., and Jentsch, T.J. (1998). Moderate loss of function of cyclic-AMP-modulated KCNQ2/KCNQ3 K+ channels causes epilepsy. Nature *396*, 687-690.
- Schwake, M., Pusch, M., Kharkovets, T., and Jentsch, T.J. (2000). Surface expression and single channel properties of KCNQ2/KCNQ3, M-type K+ channels involved in epilepsy. J Biol Chem *275*, 13343-13348.
- Schwarz, J.R., Glassmeier, G., Cooper, E.C., Kao, T.C., Nodera, H., Tabuena, D., Kaji, R., and Bostock, H. (2006). KCNQ channels mediate IKs, a slow K+ current regulating excitability in the rat node of Ranvier. J Physiol *573*, 17-34.
- Selkirk, J.V., Stiefel, T.H., Stone, I.M., Naeve, G.S., Foster, A.C., and Poulsen, D.J. (2005). Over-expression of the human EAAT2 glutamate transporter within neurons of mouse organotypic hippocampal slice cultures leads to increased vulnerability of CA1 pyramidal cells. Eur J Neurosci *21*, 2291-2296.
- Serrano-Pérez, M.C., Martín, E.D., Vaquero, C.F., Azcoitia, I., Calvo, S., Cano, E., and Tranque, P. (2011). Response of transcription factor NFATc3 to excitotoxic and traumatic brain insults: identification of a subpopulation of reactive astrocytes. Glia *59*, 94-107.
- Setkowicz, Z., and Ciarach, M. (2007). Neuroprotectants FK-506 and cyclosporin A ameliorate the course of pilocarpine-induced seizures. Epilepsy Res *73*, 151-155.
- Shah, M., Mistry, M., Marsh, S.J., Brown, D.A., and Delmas, P. (2002). Molecular correlates of the M-current in cultured rat hippocampal neurons. J Physiol *544*, 29-37.
- Shah, M.M. (2012). HCN1 channels: a new therapeutic target for depressive disorders? Sci Signal *5*, pe44.
- Shah, M.M., Migliore, M., Valencia, I., Cooper, E.C., and Brown, D.A. (2008). Functional significance of axonal Kv7 channels in hippocampal pyramidal neurons. Proc Natl Acad Sci U S A *105*, 7869-7874.

- Shi, Y., Lan, F., Matson, C., Mulligan, P., Whetstine, J.R., Cole, P.A., and Casero, R.A. (2004). Histone demethylation mediated by the nuclear amine oxidase homolog LSD1. Cell *119*, 941-953.
- Simões Pires, E.N., Frozza, R.L., Hoppe, J.B., Menezes, B.e.M., and Salbego, C.G. (2014). Berberine was neuroprotective against an in vitro model of brain ischemia: survival and apoptosis pathways involved. Brain Res *1557*, 26-33.
- Simonato, M. (2014). Gene therapy for epilepsy. Epilepsy Behav *38*, 125-130.
- Simonato, M., and Romualdi, P. (1996). Dynorphin and epilepsy. Prog Neurobiol *50*, 557-583.
- Singh, N.A., Charlier, C., Stauffer, D., DuPont, B.R., Leach, R.J., Melis, R., Ronen, G.M., Bjerre, I., Quattlebaum, T., Murphy, J.V., *et al.* (1998). A novel potassium channel gene, KCNQ2, is mutated in an inherited epilepsy of newborns. Nat Genet *18*, 25-29.
- Singh, N.A., Otto, J.F., Dahle, E.J., Pappas, C., Leslie, J.D., Vilaythong, A., Noebels, J.L., White, H.S., Wilcox, K.S., and Leppert, M.F. (2008). Mouse models of human KCNQ2 and KCNQ3 mutations for benign familial neonatal convulsions show seizures and neuronal plasticity without synaptic reorganization. J Physiol *586*, 3405-3423.
- Sloviter, R.S. (2017). Epileptogenesis meets Occam's Razor. Curr Opin Pharmacol *35*, 105-110.
- Smith, A.J., and Humphries, S.E. (2009). Characterization of DNA-binding proteins using multiplexed competitor EMSA. J Mol Biol *385*, 714-717.
- Smith, J.S., Iannotti, C.A., Dargis, P., Christian, E.P., and Aiyar, J. (2001). Differential expression of kcnq2 splice variants: implications to m current function during neuronal development. J Neurosci *21*, 1096-1103.
- Sofroniew, M.V. (2009). Molecular dissection of reactive astrogliosis and glial scar formation. Trends Neurosci *32*, 638-647.
- Soh, H., Pant, R., LoTurco, J.J., and Tzingounis, A.V. (2014). Conditional deletions of epilepsy-associated KCNQ2 and KCNQ3 channels from cerebral cortex cause differential effects on neuronal excitability. J Neurosci *34*, 5311-5321.

- Sosanya, N.M., Brager, D.H., Wolfe, S., Niere, F., and Raab-Graham, K.F. (2015). Rapamycin reveals an mTOR-independent repression of Kv1.1 expression during epileptogenesis. Neurobiol Dis *73*, 96-105.
- Spencer, E.M., Chandler, K.E., Haddley, K., Howard, M.R., Hughes, D., Belyaev, N.D., Coulson, J.M., Stewart, J.P., Buckley, N.J., Kipar, A., *et al.* (2006). Regulation and role of REST and REST4 variants in modulation of gene expression in in vivo and in vitro in epilepsy models. Neurobiol Dis *24*, 41-52.
- Stecher, H., Shayakhmetov, D.M., Stamatoyannopoulos, G., and Lieber, A. (2001). A capsid-modified adenovirus vector devoid of all viral genes: assessment of transduction and toxicity in human hematopoietic cells. Mol Ther *4*, 36-44.
- Stellwagen, D., Beattie, E.C., Seo, J.Y., and Malenka, R.C. (2005). Differential regulation of AMPA receptor and GABA receptor trafficking by tumor necrosis factor-alpha. J Neurosci *25*, 3219-3228.
- Stelzer, A., Slater, N.T., and ten Bruggencate, G. (1987). Activation of NMDA receptors blocks GABAergic inhibition in an in vitro model of epilepsy. Nature *326*, 698-701.
- Stoppini, L., Buchs, P.A., and Muller, D. (1991). A simple method for organotypic cultures of nervous tissue. J Neurosci Methods *37*, 173-182.
- Su, T., Cong, W.D., Long, Y.S., Luo, A.H., Sun, W.W., Deng, W.Y., and Liao, W.P. (2008). Altered expression of voltage-gated potassium channel 4.2 and voltage-gated potassium channel 4-interacting protein, and changes in intracellular calcium levels following lithium-pilocarpine-induced status epilepticus. Neuroscience *157*, 566-576.
- Suh, B.C., and Hille, B. (2007). Regulation of KCNQ channels by manipulation of phosphoinositides. J Physiol *582*, 911-916.
- Suh, B.C., Inoue, T., Meyer, T., and Hille, B. (2006). Rapid chemically induced changes of PtdIns(4,5)P2 gate KCNQ ion channels. Science *314*, 1454-1457.
- Sullivan, B.L., Leu, D., Taylor, D.M., Fahlman, C.S., and Bickler, P.E. (2002). Isoflurane prevents delayed cell death in an organotypic slice culture model of cerebral ischemia. Anesthesiology *96*, 189-195.

- Sun, J., and Kapur, J. (2012). M-type potassium channels modulate Schaffer collateral-CA1 glutamatergic synaptic transmission. J Physiol *590*, 3953-3964.
- Sun, Y., Jia, Z., Liu, G., Zhou, L., Liu, M., Yang, B., and Yang, T. (2013). PPARγ Agonist Rosiglitazone Suppresses Renal mPGES-1/PGE2 Pathway in db/db Mice. PPAR Res *2013*, 612971.
- Sutula, T., He, X.X., Cavazos, J., and Scott, G. (1988). Synaptic reorganization in the hippocampus induced by abnormal functional activity. Science *239*, 1147-1150.
- Sutula, T., Koch, J., Golarai, G., Watanabe, Y., and McNamara, J.O. (1996). NMDA receptor dependence of kindling and mossy fiber sprouting: evidence that the NMDA receptor regulates patterning of hippocampal circuits in the adult brain. J Neurosci *16*, 7398-7406.
- Szot, P., White, S.S., Shen, D.D., and Anderson, G.D. (2005). Valproic acid, but not lamotrigine, suppresses seizure-induced c-fos and c-Jun mRNA expression. Brain Res Mol Brain Res *135*, 285-289.
- Tabuchi, A., Yamada, T., Sasagawa, S., Naruse, Y., Mori, N., and Tsuda, M. (2002). REST4-mediated modulation of REST/NRSF-silencing function during BDNF gene promoter activation. Biochem Biophys Res Commun *290*, 415-420.
- Takahashi, M., Hayashi, S., Kakita, A., Wakabayashi, K., Fukuda, M., Kameyama, S., Tanaka, R., Takahashi, H., and Nawa, H. (1999). Patients with temporal lobe epilepsy show an increase in brain-derived neurotrophic factor protein and its correlation with neuropeptide Y. Brain Res *818*, 579-582.
- Tan, N.Y., and Khachigian, L.M. (2009). Sp1 phosphorylation and its regulation of gene transcription. Mol Cell Biol *29*, 2483-2488.
- Tao, X., Finkbeiner, S., Arnold, D.B., Shaywitz, A.J., and Greenberg, M.E. (1998). Ca2+ influx regulates BDNF transcription by a CREB family transcription factor-dependent mechanism. Neuron *20*, 709-726.
- Tapia, R., and Sitges, M. (1982). Effect of 4-aminopyridine on transmitter release in synaptosomes. Brain Res *250*, 291-299.

- Tapias, A., Ciudad, C.J., Roninson, I.B., and Noé, V. (2008). Regulation of Sp1 by cell cycle related proteins. Cell Cycle *7*, 2856-2867.
- Tatulian, L., and Brown, D.A. (2003). Effect of the KCNQ potassium channel opener retigabine on single KCNQ2/3 channels expressed in CHO cells. J Physiol *549*, 57-63.
- Tatulian, L., Delmas, P., Abogadie, F.C., and Brown, D.A. (2001). Activation of expressed KCNQ potassium currents and native neuronal M-type potassium currents by the anti-convulsant drug retigabine. J Neurosci *21*, 5535-5545.
- Teschemacher, A.G., Wang, S., Lonergan, T., Duale, H., Waki, H., Paton, J.F., and Kasparov, S. (2005). Targeting specific neuronal populations using adeno- and lentiviral vectors: applications for imaging and studies of cell function. Exp Physiol *90*, 61-69.
- Thomas, A.M., Corona-Morales, A.A., Ferraguti, F., and Capogna, M. (2005). Sprouting of mossy fibers and presynaptic inhibition by group II metabotropic glutamate receptors in pilocarpine-treated rat hippocampal slice cultures. Neuroscience *131*, 303-320.
- Thomas, A.X., Cruz Del Angel, Y., Gonzalez, M.I., Carrel, A.J., Carlsen, J., Lam, P.M., Hempstead, B.L., Russek, S.J., and Brooks-Kayal, A.R. (2016). Rapid Increases in proBDNF after Pilocarpine-Induced Status Epilepticus in Mice Are Associated with Reduced proBDNF Cleavage Machinery. eNeuro *3*.
- Thompson, S.M. (1993). Consequence of epileptic activity in vitro. Brain Pathol *3*, 413-419.
- Thompson, S.M., and Gähwiler, B.H. (1989). Activity-dependent disinhibition. III. Desensitization and GABAB receptor-mediated presynaptic inhibition in the hippocampus in vitro. J Neurophysiol *61*, 524-533.
- Tian, F.F., Zeng, C., Guo, T.H., Chen, Y., Chen, J.M., Ma, Y.F., Fang, J., Cai, X.F., Li, F.R., Wang, X.H., *et al.* (2009). Mossy fiber sprouting, hippocampal damage and spontaneous recurrent seizures in pentylenetetrazole kindling rat model. Acta Neurol Belg *109*, 298-304.

- Timmusk, T., Palm, K., Lendahl, U., and Metsis, M. (1999). Brain-derived neurotrophic factor expression in vivo is under the control of neuron-restrictive silencer element. J Biol Chem *274*, 1078-1084.
- Tinel, N., Lauritzen, I., Chouabe, C., Lazdunski, M., and Borsotto, M. (1998). The KCNQ2 potassium channel: splice variants, functional and developmental expression. Brain localization and comparison with KCNQ3. FEBS Lett *438*, 171-176.
- Tomida, T., Hirose, K., Takizawa, A., Shibasaki, F., and Iino, M. (2003). NFAT functions as a working memory of Ca2+ signals in decoding Ca2+ oscillation. EMBO J *22*, 3825-3832.
- Tomonoh, Y., Deshimaru, M., Araki, K., Miyazaki, Y., Arasaki, T., Tanaka, Y., Kitamura, H., Mori, F., Wakabayashi, K., Yamashita, S., *et al.* (2014). The kick-in system: a novel rapid knock-in strategy. PLoS One *9*, e88549.
- Tunquist, B.J., Hoshi, N., Guire, E.S., Zhang, F., Mullendorff, K., Langeberg, L.K., Raber, J., and Scott, J.D. (2008). Loss of AKAP150 perturbs distinct neuronal processes in mice. Proc Natl Acad Sci U S A *105*, 12557-12562.
- Uchida, K., Nakajima, H., Hirai, T., Yayama, T., Chen, K., Guerrero, A.R., Johnson, W.E., and Baba, H. (2012). The retrograde delivery of adenovirus vector carrying the gene for brain-derived neurotrophic factor protects neurons and oligodendrocytes from apoptosis in the chronically compressed spinal cord of twy/twy mice. Spine (Phila Pa 1976) *37*, 2125-2135.
- Ulrich, J.D., Kim, M.S., Houlihan, P.R., Shutov, L.P., Mohapatra, D.P., Strack, S., and Usachev, Y.M. (2012). Distinct activation properties of the nuclear factor of activated T-cells (NFAT) isoforms NFATc3 and NFATc4 in neurons. J Biol Chem *287*, 37594-37609.
- Uludag, I.F., Duksal, T., Tiftikcioglu, B.I., Zorlu, Y., Ozkaya, F., and Kirkali, G. (2015). IL-1β, IL-6 and IL1Ra levels in temporal lobe epilepsy. Seizure *26*, 22-25.
- Uzüm, G., Sarper Diler, A., Bahçekapili, N., and Ziya Ziylan, Y. (2006). Erythropoietin prevents the increase in blood-brain barrier permeability during pentylentetrazol induced seizures. Life Sci *78*, 2571-2576.

- Vasil'ev, D.S., Tumanova, N.L., Lavrent'eva, V.V., Starshinova, L.A., Zhabko, E.P., Lukomskaia, N.I.a., Zhuravin, I.A., and Magazanik, L.G. (2013). [The ability of NMDA glutamate receptor blockers to prevent a pentylenetetrazole kindling in mice and morphological changes in the hippocampus]. Ross Fiziol Zh Im I M Sechenova *99*, 1023-1035.
- Vezzani, A., Ravizza, T., Moneta, D., Conti, M., Borroni, A., Rizzi, M., Samanin, R., and Maj, R. (1999). Brain-derived neurotrophic factor immunoreactivity in the limbic system of rats after acute seizures and during spontaneous convulsions: temporal evolution of changes as compared to neuropeptide Y. Neuroscience *90*, 1445-1461.
- Vigil, F.A., Bozdemir, E., Bugay, V., Chun, S.H., Hobbs, M., Sanchez, I., Hastings, S.D., Veraza, R.J., Holstein, D.M., Sprague, S.M., *et al.* (2020). Prevention of brain damage after traumatic brain injury by pharmacological enhancement of KCNQ (Kv7, "M-type") K. J Cereb Blood Flow Metab *40*, 1256-1273.
- Viviani, B., Bartesaghi, S., Gardoni, F., Vezzani, A., Behrens, M.M., Bartfai, T., Binaglia, M., Corsini, E., Di Luca, M., Galli, C.L., *et al.* (2003). Interleukin-1beta enhances NMDA receptor-mediated intracellular calcium increase through activation of the Src family of kinases. J Neurosci *23*, 8692-8700.
- Wahab, A., Albus, K., and Heinemann, U. (2010). Drug refractoriness of epileptiform activity in organotypic hippocampal slice cultures depends on the mode of provocation. Epilepsy Res *90*, 304-308.
- Wang, A.W., Yang, R., and Kurata, H.T. (2017). Sequence determinants of subtype-specific actions of KCNQ channel openers. J Physiol *595*, 663-676.
- Wang, F.J., Li, C.M., Hou, X.H., Wang, X.R., and Zhang, L.M. (2011). Selective upregulation of brain-derived neurotrophic factor (BDNF) transcripts and BDNF direct induction of activity independent N-methyl-D-aspartate currents in temporal lobe epilepsy patients with hippocampal sclerosis. J Int Med Res *39*, 1358-1368.
- Wang, G., Zhang, H., Sun, J., Zhang, Y., He, F., and Zou, J. (2021). Cyclosporin A impairs neurogenesis and cognitive abilities in brain

development via the IFN-γ-Shh-BDNF pathway. Int Immunopharmacol *96*, 107744.

- Wang, H.S., Pan, Z., Shi, W., Brown, B.S., Wymore, R.S., Cohen, I.S., Dixon, J.E., and McKinnon, D. (1998). KCNQ2 and KCNQ3 potassium channel subunits: molecular correlates of the M-channel. Science *282*, 1890-1893.
- Wang, Q., and Andreasson, K. (2010). The organotypic hippocampal slice culture model for examining neuronal injury. J Vis Exp.
- Wang, R., Luo, Y., Ly, P.T., Cai, F., Zhou, W., Zou, H., and Song, W. (2012). Sp1 regulates human huntingtin gene expression. J Mol Neurosci *47*, 311-321.
- Wang, W., Wang, X., Chen, L., Zhang, Y., Xu, Z., Liu, J., Jiang, G., Li, J., Zhang, X., Wang, K., *et al.* (2016). The microRNA miR-124 suppresses seizure activity and regulates CREB1 activity. Expert Rev Mol Med *18*, e4.
- Watanabe, H., Nagata, E., Kosakai, A., Nakamura, M., Yokoyama, M., Tanaka, K., and Sasai, H. (2000). Disruption of the epilepsy KCNQ2 gene results in neural hyperexcitability. J Neurochem *75*, 28-33.
- Weber, Y.G., Geiger, J., Kämpchen, K., Landwehrmeyer, B., Sommer, C., and Lerche, H. (2006). Immunohistochemical analysis of KCNQ2 potassium channels in adult and developing mouse brain. Brain Res *1077*, 1-6.
- Weckhuysen, S., Ivanovic, V., Hendrickx, R., Van Coster, R., Hjalgrim, H., Møller, R.S., Grønborg, S., Schoonjans, A.S., Ceulemans, B., Heavin, S.B., *et al.* (2013). Extending the KCNQ2 encephalopathy spectrum: clinical and neuroimaging findings in 17 patients. Neurology *81*, 1697-1703.
- Weissberg, I., Wood, L., Kamintsky, L., Vazquez, O., Milikovsky, D.Z., Alexander, A., Oppenheim, H., Ardizzone, C., Becker, A., Frigerio, F., *et al.* (2015). Albumin induces excitatory synaptogenesis through astrocytic TGF-β/ALK5 signaling in a model of acquired epilepsy following blood-brain barrier dysfunction. Neurobiol Dis *78*, 115-125.
- Wetmore, C., Olson, L., and Bean, A.J. (1994). Regulation of brain-derived neurotrophic factor (BDNF) expression and release from hippocampal neurons is mediated by non-NMDA type glutamate receptors. J Neurosci *14*, 1688-1700.

- Whitmire, L.E., Ling, L., Bugay, V., Carver, C.M., Timilsina, S., Chuang, H.H., Jaffe, D.B., Shapiro, M.S., Cavazos, J.E., and Brenner, R. (2017). Downregulation of KCNMB4 expression and changes in BK channel subtype in hippocampal granule neurons following seizure activity. PLoS One *12*, e0188064.
- Wickenden, A.D., Yu, W., Zou, A., Jegla, T., and Wagoner, P.K. (2000). Retigabine, a novel anti-convulsant, enhances activation of KCNQ2/Q3 potassium channels. Mol Pharmacol *58*, 591-600.
- Wiebe, S., Blume, W.T., Girvin, J.P., Eliasziw, M., and Group, E.a.E.o.S.f.T.L.E.S. (2001). A randomized, controlled trial of surgery for temporal-lobe epilepsy. N Engl J Med *345*, 311-318.
- Wiegert, J.S., Gee, C.E., and Oertner, T.G. (2017). Viral Vector-Based Transduction of Slice Cultures. Cold Spring Harb Protoc *2017*.
- Wilkemeyer, M.F., and Angelides, K.J. (1995). Adenovirus-mediated expression of a reporter gene in thalamocortical cocultures. Brain Res *703*, 129-138.
- Wood, I.C., Belyaev, N.D., Bruce, A.W., Jones, C., Mistry, M., Roopra, A., and Buckley, N.J. (2003). Interaction of the repressor element 1-silencing transcription factor (REST) with target genes. J Mol Biol *334*, 863-874.
- Wuttke, T.V., Seebohm, G., Bail, S., Maljevic, S., and Lerche, H. (2005). The new anticonvulsant retigabine favors voltage-dependent opening of the Kv7.2 (KCNQ2) channel by binding to its activation gate. Mol Pharmacol *67*, 1009-1017.
- Yamaguchi, S., and Rogawski, M.A. (1992). Effects of anticonvulsant drugs on 4-aminopyridine-induced seizures in mice. Epilepsy Res *11*, 9-16.
- Yan, H.Q., Shin, S.S., Ma, X., Li, Y., and Dixon, C.E. (2014). Differential effect of traumatic brain injury on the nuclear factor of activated T Cells C3 and C4 isoforms in the rat hippocampus. Brain Res *1548*, 63-72.
- Yang, W.P., Levesque, P.C., Little, W.A., Conder, M.L., Ramakrishnan, P., Neubauer, M.G., and Blanar, M.A. (1998). Functional expression of two KvLQT1-related potassium channels responsible for an inherited idiopathic epilepsy. J Biol Chem *273*, 19419-19423.

- Yonekawa, W.D., Kupferberg, H.J., and Woodbury, D.M. (1980). Relationship between pentylenetetrazol-induced seizures and brain pentylenetetrazol levels in mice. J Pharmacol Exp Ther *214*, 589-593.
- Yong, V.W. (1992). Proliferation of human and mouse astrocytes in vitro: signalling through the protein kinase C pathway. J Neurol Sci *111*, 92-103.
- Yu, Y., and Jiang, J. (2020). COX-2/PGE. Epilepsia Open *5*, 418-431.
- Yuan, Y., Chow, B.K., Lee, V.H., and Lee, L.T. (2013). Neuron-restrictive silencer factor functions to suppress Sp1-mediated transactivation of human secretin receptor gene. Biochim Biophys Acta *1829*, 231-238.
- Yue, C., and Yaari, Y. (2004). KCNQ/M channels control spike afterdepolarization and burst generation in hippocampal neurons. J Neurosci *24*, 4614-4624.
- Yus-Nájera, E., Muñoz, A., Salvador, N., Jensen, B.S., Rasmussen, H.B., Defelipe, J., and Villarroel, A. (2003). Localization of KCNQ5 in the normal and epileptic human temporal neocortex and hippocampal formation. Neuroscience *120*, 353-364.
- Zattoni, M., Mura, M.L., Deprez, F., Schwendener, R.A., Engelhardt, B., Frei, K., and Fritschy, J.M. (2011). Brain infiltration of leukocytes contributes to the pathophysiology of temporal lobe epilepsy. J Neurosci *31*, 4037-4050.
- Zeng, L.H., Rensing, N.R., and Wong, M. (2009). The mammalian target of rapamycin signaling pathway mediates epileptogenesis in a model of temporal lobe epilepsy. J Neurosci *29*, 6964-6972.
- Zhang, F., Liu, Y., Tang, F., Liang, B., Chen, H., Zhang, H., and Wang, K. (2019). Electrophysiological and pharmacological characterization of a novel and potent neuronal Kv7 channel opener SCR2682 for antiepilepsy. FASEB J *33*, 9154-9166.
- Zhang, J., and Shapiro, M.S. (2012). Activity-dependent transcriptional regulation of M-Type (Kv7) K(+) channels by AKAP79/150-mediated NFAT actions. Neuron *76*, 1133-1146.
- Zhang, Z., Ottens, A.K., Sadasivan, S., Kobeissy, F.H., Fang, T., Hayes, R.L., and Wang, K.K. (2007). Calpain-mediated collapsin response mediator

protein-1, -2, and -4 proteolysis after neurotoxic and traumatic brain injury. J Neurotrauma *24*, 460-472.

- Zhao, M.W., Qiu, W.J., and Yang, P. (2020). SP1 activated-lncRNA SNHG1 mediates the development of epilepsy via miR-154-5p/TLR5 axis. Epilepsy Res *168*, 106476.
- Zhou, X., Zhuang, F., Li, H., Zheng, K., Hong, Z., Feng, W., Zhou, W., and Chen, J. (2016). Calmodulin regulates KCNQ2 function in epilepsy. Am J Transl Res *8*, 5610-5618.
- Zhu, X., Dong, J., Shen, K., Bai, Y., Zhang, Y., Lv, X., Chao, J., and Yao, H. (2015). NMDA receptor NR2B subunits contribute to PTZ-kindling-induced hippocampal astrocytosis and oxidative stress. Brain Res Bull *114*, 70-78.
- Zhu, X., Han, X., Blendy, J.A., and Porter, B.E. (2012). Decreased CREB levels suppress epilepsy. Neurobiol Dis *45*, 253-263.
- Zuccato, C., Belyaev, N., Conforti, P., Ooi, L., Tartari, M., Papadimou, E., MacDonald, M., Fossale, E., Zeitlin, S., Buckley, N., *et al.* (2007). Widespread disruption of repressor element-1 silencing transcription factor/neuron-restrictive silencer factor occupancy at its target genes in Huntington's disease. J Neurosci *27*, 6972-6983.
- Zuccato, C., Tartari, M., Crotti, A., Goffredo, D., Valenza, M., Conti, L., Cataudella, T., Leavitt, B.R., Hayden, M.R., Timmusk, T., *et al.* (2003). Huntingtin interacts with REST/NRSF to modulate the transcription of NRSE-controlled neuronal genes. Nat Genet *35*, 76-83.
- Zucker, D.K., Wooten, G.F., and Lothman, E.W. (1983). Blood-brain barrier changes with kainic acid-induced limbic seizures. Exp Neurol *79*, 422-433.
- Zullo, J.M., Drake, D., Aron, L., O'Hern, P., Dhamne, S.C., Davidsohn, N., Mao, C.A., Klein, W.H., Rotenberg, A., Bennett, D.A., *et al.* (2019). Regulation of lifespan by neural excitation and REST. Nature *574*, 359-364.